Modeling of Inter-Vehicular Gaps and Driver Behavior in Heterogeneous Traffic Stream with Weak Lane Discipline

Thesis submitted to the

Indian Institute of Technology Guwahati

For the fulfilment of the degree of

Doctor of Philosophy (Ph.D.)
in
Civil Engineering
by

Anuj Kishor Budhkar
(Roll no. 136104015)

Thesis supervisor
Dr Akhilesh Kumar Maurya

Department of Civil Engineering,
Indian Institute of Technology Guwahati,
Guwahati, Assam, India-781039
October, 2017

Indian Institute of Technology Guwahati,
Guwahati, Assam-781039, INDIA

Certificate

This is to certify that thesis entitled '**Modeling of Inter-Vehicular Gaps and Driver Behavior in Heterogeneous Traffic Stream with Weak Lane Discipline**', submitted by Anuj Kishor Budhkar (Roll no. 136104015) to the Indian Institute of Technology Guwahati, for the award of degree of Doctor of Philosophy in Civil Engineering is a record of bonafide research work carried out by him under my supervision and guidance. In my opinion the thesis work has reached the requisite standard fulfilling the requirement for the degree of Doctor of Philosophy in Civil Engineering.

The results contained in this thesis have not been submitted in part or full to any other University or Institute for award of any degree or diploma.

(Dr. Akhilesh Kumar Maurya)
Thesis Supervisor
Associate Professor
Department of Civil Engineering
Indian Institute of Technology Guwahati,
Guwahati, Assam, India-781039.

October, 2017

Statement

I do hereby declare that the matter embodied in this thesis is the result of investigations carried out by me in the Department of Civil Engineering, Indian Institute of Technology Guwahati, Guwahati, Assam, India.

In keeping with the general practice of reporting scientific observations, due acknowledgements have been made wherever the work is based on the findings of other investigators.

(Anuj Kishor Budhkar)
Department of Civil Engineering
Indian Institute of Technology Guwahati,
Guwahati, Assam, India-781039

October, 2017

Acknowledgements

The challenging research work of modeling a complex traffic stream in developing countries was impossible without the assistance and inputs from people belonging to diverse fields and expertise. I take this opportunity to acknowledge each one of them.

My thesis supervisor Dr. Akhilesh Kumar Maurya, Associate Professor, Department of Civil Engineering, IIT Guwahati, is really a source of inspiration for me. Putting my heartfelt gratitude towards him is beyond the limit of words. His constant assistance, encouragement, meticulous guidance and thoughtful involvement right from the inception stage of this thesis to completion has helped me achieve the desired objectives of this thesis. I remain indebted to him. I extend my sincere thanks to Dr. S. Velmurugan, Senior Principal Scientist, CSIR-CRRI and external examiner of this thesis, Dr. Sreedeep S., Professor, Department of Civil Engineering and Chairman, Doctoral Committee for this thesis work, Dr. R. Choudhary, Associate Professor, Department of Civil Engineering and Member, Doctoral Committee for this thesis work, and Dr. R. Sinha, Professor, Department of Electronics and Electrical Engineering and Member, Doctoral Committee for this thesis work, for their constructive suggestions and timely criticism, which helped me achieve the goals of my research work.

I also thank Dr. P. Chakroborty, Professor, Department of Civil Engineering, IIT Kanpur, Dr. G. Barua, Professor, and Dr. C. Mallikarjuna, Associate Professor, Department of Civil Engineering, IIT Guwahati, for their valuable suggestions for improvement of this work.

I owe a lot to the students of Transportation Systems Engineering, Department of Civil Engineering, IIT Guwahati. I express my sincere thanks to Geetimukta Mahapatra (Research Scholar), Sibaji Gaj (Research Scholar, Department of Computer Sciences and Engineering), Pankil Khandelwal (M.Tech student), B.Tech students – Pratik Raj and Keshav Kothari for their valuable assistance in various stages of data-collection. Further, I thank Nilanjan Adhikary (M.Tech student), and summer internship students (Wasim, Ankita, Shubham, Hariom and Tanushree) for their painstaking efforts in assisting me with traffic data extraction. I also thank Vishal Kumar (M.Tech student) and Sanhita Das, Suresh Nama and Arunabha Banerjee (Research Scholars) for their help at various stages in my research work.

I thank my friends in IIT Guwahati – Mr. Nilesh Patil, Mr. Vasudevan Matampu and Mr. Biplab Ghosh (Research Scholars), and the staff of IIT Guwahati (notably, Mr. Rajib Gogoi and Mr. Narayan Kalita) who have made my stay here a wonderful experience.

My parents, wife, daughter and elder brother deserve special mention. I cannot put in words the immense support and encouragement they have given me for my research. I also express my gratitude to all others who have indirectly contributed to development of this thesis work.

Anuj Kishor Budhkar.

Abstract

The traffic stream of developing countries like India is different than that of the developed world, due to two peculiar phenomena- (i) Weak lane-discipline (random placement of vehicles over entire width of the road) and (ii) Presence of heterogeneous or mixed traffic; or large number of vehicle types. In such traffic conditions, reaction of drivers is not just in the form of acceleration or deceleration but also simultaneous veering or lateral movement. Drivers maintain certain lateral clearance between vehicles for their safety, which depends on speed and type of their vehicles. Thus, lateral and longitudinal gap-maintaining become important parameters in such traffic stream. Therefore, a simulation model developed for such traffic stream must model longitudinal and lateral gap-maintaining behavior of different vehicles. Previous studies on such traffic have not incorporated the lateral and longitudinal gap-maintenance behavior in their proposed simulation models extensively. The studies on gap-maintenance need to incorporate (i) weak lane-discipline, (ii) vehicle variability; and (iii) driver variability. The previously developed comprehensive simulation models have poorly addressed these characteristics, which are one of the basic features of vehicular interaction in Indian traffic stream. Therefore, a comprehensive simulation model incorporating the realistic lateral and longitudinal gap-maintaining behavior of heterogeneous traffic is required.

Thus, the goal of this work is to develop a simulation model, which can replicate real world traffic conditions in heterogeneous urban, mid-block traffic stream, incorporating the models of inter-vehicular gaps and driver behavior of such a stream. To achieve this goal, initially, there should be a detailed analysis of lateral and longitudinal gaps and their relationship with speeds and vehicle types. Moreover, factors affecting the decision to overtake also needs detailed investigation. Thereafter, these developed models can be incorporated in the developed simulation model, in addition to set of algorithms governing driver behavior in mixed traffic stream. For this purpose, an accurate data-collection is also required for development of inter-vehicular gap-maintaining models.

The lateral gap-maintaining behavior needs accurate estimation of lateral gap between vehicles and their speed during overtaking. An instrumented vehicle equipped with ultrasonic sensors (on its both sides) and high accuracy GPS along with a camera is developed to measure lateral clearances and vehicle speeds. More than 6,000 lateral interactions are observed across six different cities with different instrumented vehicle types. On the other hand, study of longitudinal gap-maintaining behavior requires variation of longitudinal gap with speeds and staggering (centerline separation). For this purpose, a semi-manual, video image-based camera calibration program is developed, which is used to extract trajectories of LV and FV in mixed traffic stream. Based on trajectories, the longitudinal gaps, staggering and vehicle speeds are obtained. More than 14,000 interactions are observed for mixed traffic stream across 12 different sections located in different cities of India.

On the analysis of these collected data, inter-vehicular lateral and longitudinal gaps are observed to increase with speed, while longitudinal gaps are observed to decrease with increase in

staggering. The variation of lateral clearance with speeds is modeled as a linear regression equation (deterministic part) with positive slope, and Beta-distributed homoscedastic residuals (stochastic part). The variation is different for different vehicle pairs, and it is observed that similar vehicle pairs maintain lesser lateral clearance than dissimilar pairs. Similarly, the variation of longitudinal gaps with speed and centerline separation consists of single degree regression equations (deterministic part) having positive slope with speed and negative slope with centerline separation, and Burr-distributed heteroskedastic residuals (stochastic part). Further, when vehicle interacts (either laterally or longitudinally) with multiple vehicles simultaneously, it is observed that there is significant compromise in gap-maintaining behavior, especially at higher speeds. A categorical model for decision of overtaking in mixed traffic conditions is developed (using logistic regression), which is used for prediction of overtaking decision, if inter-vehicular gaps and speeds are known.

A rule-based simulation model is developed incorporating lateral and longitudinal gap-maintaining models and overtaking behavioral model, in addition to free-flowing and vehicle following behavioral model. The stochastic nature of various inter-vehicular gap-maintaining relationships is assimilated into the model by means of a risk factor, which is considered as a measure of driver aggressiveness. All vehicle positions are updated simultaneously at discrete intervals of time, using different models mentioned above. Developed model is well-calibrated using genetic algorithms, validated with field conditions, and compared with the commercial simulation software VISSIM (calibrated in the similar way). The validation is conducted for macroscopic properties (speed-flow relationship) and microscopic properties (time headway distribution, speed distribution, average lateral shifts, lateral and longitudinal gap-maintaining behavior, etc). It is observed that for most cases, the developed model can perform better than VISSIM. The developed model is also used for generating specific cases to test its applicability. The capacity of simulated road section can be estimated based on fitting of a generalized model for speed-density relationship. This capacity is observed to increase with increase in desired speed and road width, but capacity per unit road width decreases with increase in road width. The simulation model is also used to study the impact of segregation of buses from other vehicles.

Thus, the simulation model developed on the basis of inter-vehicular gaps can have large contribution to the traffic engineering community, especially for designing road capacity at given desired speeds, widths and compositions; effect of traffic segregation, safety analysis, development of simulators, etc.

Contents

List of Tables

List of Figures

Glossary of terms

Abbreviations

2W	Motorized two wheelers
3W	Motorized three wheelers
BRT	Bus Rapid Transit System
CS	Centerline separation
FV	Following vehicle
GA	Genetic Algorithms
GPS	Global Positioning System
IV	Interacting vehicle
IR	Interaction range ahead of vehicle
LC	Lateral clearance between adjacent vehicle edges
LCV	Light Commercial Vehicles
LG	Longitudinal gap between leading and following vehicles
LV	Leading vehicle
K-S	Kolmogorov-Smirnov test
TV	Test vehicle
$\bar{v}$	Average speed
$v_{LV\|FV}$	Relative speed
φ	The residual term about best fit regression equation.

Units

km/h	kilometers per hour
cm	centimeters
m	meters
veh/h	vehicles per hour
x	Longitudinal position of vehicle on road
y	Lateral position of vehicle on road
t	time interval
T	Driver reaction time in seconds

CHAPTER 1

Introduction

1.1 Overview

In developing countries like India, Nepal, Vietnam, Bangladesh, congestion problems are prevalent, affecting the road users due to increase in a number of vehicles. To combat the traffic congestion problem, an extensive understanding and analysis of the traffic stream behavior are necessary. Study of various traffic characteristics is necessary for planning, designing and operation of roadway facilities, in addition to regulation and control of traffic.

Traffic stream behavior is an outcome of the human driving process, which is a natural phenomenon. Thus, this behavior is complex. Moreover, one cannot perform experiments in the real-world traffic stream to understand or improve the traffic movement patterns. The situations that are of interest to traffic engineers cannot be reproduced in the laboratory (road, drivers and vehicles). Traffic simulation is a powerful and cost-efficient tool for road design and evaluation of traffic management methods. Simulating means imitating the roadway and traffic conditions planned or present in the real world. A simulation framework is essential to evaluate the detailed traffic performance at different roadway sections, implement the models of different driver behaviors and hence simulate large-scale real-world traffic situations in detail. The simulation approaches can be broadly classified as microscopic – defining vehicle-wise movements, and macroscopic – considering movement of entire traffic streams. Modelling the driver behavior requires a detailed understanding of the vehicular interactions with the surrounding traffic using gaps maintained between vehicles, governing speeds in various traffic situations, reactions in the form of acceleration or deceleration or veering, or a combination of these behaviors. Hence microscopic modelling of traffic flow can well represent the dynamics of vehicular movements and its lateral and longitudinal interactions within a traffic stream.

The traffic in developing countries is chaotic and does not move in well-defined channels thus increasing interactions between vehicles. To analyze such a stream, a study of the effect of adjacent and leading vehicles on behavior of a driver in the traffic stream is necessary. This effect causes drivers to maintain certain longitudinal and lateral gaps within traffic stream. Each driver will respond to particular situations of traffic stream, differently based on his/her perception capability and aggressiveness. Simultaneous lateral and longitudinal interactions make the system complex. This complexity of micro-level interactions needs addressed while developing a traffic simulation model for such traffic stream. A model which involves modeling of all drivers’ behavior can be used for simulating traffic behavior, thus effective solutions of traffic problems can be addressed.

1.2 Traffic stream in developing countries

The traffic stream in developing countries is more complex to analyze than developed countries due to some of its peculiar features such as heterogeneous nature of vehicles and no lane discipline and. They are described below in detail.

1.2.1 Heterogeneous or mixed traffic

A large number of vehicle types are generally observed on roads in developing countries which vary significantly in their sizes and operating characteristics. Variability in their sizes and operating characteristics complicate the analysis of such traffic stream. These different motorized vehicles are generally classified in the following classes by the Indian Roads Congress (IRC- 106: 1990), for in urban areas.

- Two-wheelers, motor cycle or scooter etc., (hereafter, referred as motorized two wheelers and abbreviated as 2W)
- Passenger car or pick-up van (hereafter referred as 'car')
- Auto-rickshaw or motorized three wheelers (hereafter, referred as motorized three wheelers and abbreviated as 3W)
- Light Commercial Vehicle (hereafter referred as 'LCV')
- Truck or Bus (They are classified as heavy vehicles hereafter. There is less difference in operating characteristics of these vehicles on urban roads with flat terrain).
- Agricultural Tractor Trailer (They are not commonly found in urban traffic conditions and not considered in analysis in this thesis).

1.2.2 Weak or no lane discipline

Due to a high variability of vehicle sizes and operating characteristics, vehicles interact two dimensionally with their neighboring vehicles and exhibit no (or weak) lane discipline (i.e., vehicles do not move in lanes). Due to this feature, following behavior is observed-

- Vehicles do not follow demarcated paths but occupy any available space.
- They overtake other vehicles as and when a sufficient gap is available.
- They also follow each other in a staggered manner to perceive the traffic scenario in front of leading vehicle. A person driving a vehicle following another vehicle in a staggered manner can keep less distance between its own vehicle and leading vehicle.
- The reaction of drivers is in the form of not just acceleration or deceleration but also a simultaneous veering or lateral movement.

Fig. 1.1 shows the comparison of lane-following traffic in developed countries with the traffic of no lane discipline in Mumbai.

Fig 1.1 Traffic stream in (a) developed countries and (b) developing countries. *Source*- (a): I-80 Eastshore freeway in Berkeley, USA. (*https://en.wikipedia.org/wiki/Interstate_80_in_California*); and (b) Western Express Highway in Mumbai, India. (*images.mid-day.com/2012/nov/Kalanager.jpg*).

Due to variability in their sizes and maneuvering capabilities, individual vehicle types need to be separately assessed for their properties influencing the macroscopic traffic parameters. Moreover, weak lane discipline ensures that there are a large number of lateral interactions along with the longitudinal car-following interactions (common in developed countries). Vehicles in such traffic stream are spread over the entire width of the road and do not move in well-demarcated paths (i.e., lanes).

Vehicles frequently veer during overtaking other vehicles to maximize their speed. Drivers maintain certain lateral clearance between vehicles for their safety while veering, which depends on speed and type of their vehicles. Vehicles of smaller dimensions are observed to move parallel to each other, and also create situations when there are multiple leader/follower vehicles for a single follower/leader vehicle. Due to this behavior, various phenomena are observed such as staggered following, maintaining a shorter headway while following in a staggered manner, attempting to overtake between diagonal space between vehicles, moving abreast, and travelling as per the dynamic lanes of different widths formed by the vehicles. Thus, lateral and longitudinal gap-maintaining between vehicles become important parameters in such traffic stream.

Therefore, a simulation model developed for such traffic stream must model longitudinal and lateral gap-maintaining behavior in addition to the decision to overtake for different vehicles. Western traffic planning methodologies broadly address the problems of homogeneous traffic and thereby prove inadequate to solve problems involving non-homogeneous traffic conditions with weak lane discipline (Tiwari *et al.* 2003). Some of the car-following models can be modified to accommodate the heterogeneity. But, incorporating the weak or no lane discipline is not possible.

1.3 Problem statement

Various car-following and lane-changing models are devised in the developed world separately, which can be valid for vehicles maintaining strict lane discipline. Interactions between vehicles, in heterogeneous and weak lane discipline traffic stream, takes place not just between leading and following vehicles, but also between neighboring vehicles. Classic models (May, 1959; Gunay, 2003) described lateral friction between vehicles moving side-by-side. This was showcased further by various researchers (Mallikarjuna, *et al.*, 2013; Dimayacyac and Palmiano, 2016; Bangarraju, *et al.*, 2016), but not modeled considering different vehicle types and an introduction of term focusing variability in driver behavior. There were piecemeal models which addressed few characteristics of traffic in developing countries individually, such as vehicle-following in mixed traffic (Ravishankar and Mathew, 2009), maintaining of weak lane discipline (Gunay, 2007). Further, drivers' decision to overtake is not influenced only by occupancy in neighboring lanes, but also on the basis of inter-vehicular gaps and speed of leading vehicle. Literature does not yield any study in the aspect of overtaking decision modeling for weak lane discipline traffic. Therefore, a precise measurement of inter-vehicular gaps is needed for such traffic stream. Previous data collection methods for measuring inter-vehicular gaps (Nagraj, 1990; Pal and Mallikarjuna, 2013) suffered from some accuracy issues.

Based on these traffic characteristics, development of a comprehensive simulation model is necessary, which takes into account the inter-vehicular characteristics such as maintaining lateral gaps, vehicle-following behavior, overtaking or veering decisions, etc. Comprehensive models incorporating lateral and longitudinal interactions of vehicles were developed previously for these traffic streams (Arasan and Koshy, 2005; Maurya, 2007; Mallikarjuna and Rao, 2009; etc.). However, most of these models were not precisely calibrated for various field conditions and some of them were not computationally efficient. Therefore, a comprehensive model is required which inculcates the gap-maintaining behavior of drivers including its variability across different drivers and vehicle types, overtaking decision (depending on inter-vehicular gap-perception), and overtaking rules (based on available road space for overtaking rather than occupancy of neighboring lanes). Further, the developed model should be calibrated, and validated at both microscopic and macroscopic levels.

1.4 Objectives of the study

The goal of this work is to develop a simulation model, which can replicate real-world traffic conditions in heterogeneous urban, mid-block traffic stream with weak lane discipline, depending upon modeling the inter-vehicular gap-maintenance and driver behavior in such a stream. This broad objective can be classified into following two research objectives-

Research Objective-1: Analysis and modeling of inter-vehicular longitudinal and lateral spacing with speeds for heterogeneous traffic with weak lane discipline.

- Modeling the lateral gap-maintaining behavior between vehicles during overtaking and its relationship with speeds for different vehicle types.

- Modeling the longitudinal gap-maintaining behavior between vehicles during following, and its relationship with the staggering and speeds of vehicles for different vehicle types.
- Modeling overtaking decision of a following driver, depending upon inter-vehicular gaps.

Research Objective-2: Development of a comprehensive driver behavior model incorporating inter-vehicular gap features and relationships

- Development of a driver behavior model in heterogeneous, weak lane discipline traffic conditions incorporating the lateral and longitudinal interactions.
- Calibration and validation of the developed model and its comparison with popular commercial simulation software.
- Generation of various hypothetical scenarios to test the applicability of the developed model.

1.5 Scope of the research work

The proposed research work consists of the development of a comprehensive driver behavior model in mixed traffic stream having no lane discipline as observed in developing countries. It includes incorporation of inter-vehicular gap-maintaining features and their relationships with vehicle speeds, variation across different vehicle types and variability in their driver behavior. The study scope includes mid-block sections in urban locations in developing countries like India. Essentially, the developed model does not incorporate the influence of any external characteristics such as intersecting or merging traffic, pedestrians and other road hindrances, gradient, horizontal or vertical curves, pavement conditions, environmental or land-use conditions apart from the traffic, which affect driver behavior in the traffic stream. Traffic data need to be collected from different sites within this scope, to model for relationships between inter-vehicular spacing and speeds.

1.6 Organization of the thesis

This thesis is divided into six chapters, as follows-

1. The first chapter focusses on introduction, defining the problem statement and objectives of this thesis.
2. The second chapter provides a comprehensive literature review of proposed work and highlights the shortcomings.
3. The third chapter presents the methodology of field and data collection and extraction of inter-vehicular interactions.
4. The fourth chapter focusses on the analysis and modeling of lateral and longitudinal interactions and overtaking decision modeling.
5. The fifth chapter describes the development of simulation model and its calibration and validation from field data. Further, it also presents some hypothetical scenarios to test the applicability of the developed model.
6. The sixth chapter provides a summary of the work, presents its contribution to the scientific community and explores the future scope.

CHAPTER 2

Literature review

As discussed in the previous chapter, traffic stream in developing countries consists of heterogeneous traffic with weak lane discipline, due to which there are large number of interactions, and existing methodologies may not be able to address the traffic stream behavior. The broad objective of this thesis work is to develop a simulation model which can mimic this stream, with the help of models for inter-vehicular lateral and longitudinal gaps. based on the framework of broad objectives, it is necessary to review existing literature so that previous research works conducted could be inculcated and a new model may be motivated based on these methods. This chapter describes a detailed literature review on the earlier research conducted in this aspect.

- In the first section, various lane-based traffic simulation models (suitable for developed world) and existing modeling approaches to simulating mixed and weak lane-based traffic (suitable for developing world) are described. The drawbacks in these models in replicating mixed traffic conditions are highlighted, and this motivates a study of modeling approaches for inter-vehicular gaps.
- The second section focusses on the previous research on calculation of inter-vehicular gaps, and overtaking decision in a mixed traffic stream. Those researches which have emphasized the lateral gap and longitudinal gap-maintaining behavior, with focus on vehicle type and weak lane discipline are studied. Further, researches to model overtaking decision of a driver in this stream are also reviewed. To develop relationship between inter-vehicular gaps and different variables defining traffic at microscopic level, data collection from field is necessary.
- A peer review of various traffic data-collection methods is presented in the third section, and various methods for collecting data in the present context are shortlisted.
- The fourth section deals with the outcome of this literature review, and gaps in the previous researches pertaining to objective.

2.1 Microscopic modeling of traffic stream

The effort of microscopic simulation modeling of traffic stream is underway since several decades. In the developed world, most of studies of modeling traffic streams are classified as car-following and lane-changing models. They describe driver behavior when one vehicle follows the other (both are essentially cars) or when it changes lanes to overtake. Essentially, for representing the mixed and weak lane disciplined traffic behavior, an ideal simulation model shall replicate (i) Lateral interactions with various vehicle types, (ii) Longitudinal interactions and their relation with amount of staggering, and (iii) Modeling overtaking decisions. Previous studies can be grouped into conventional car-following models, cellular automaton models, and comprehensive models, described in first three subsections, respectively (and presented as summary in Table 2.1). The fourth subsection describes development of simulators, whereas fifth subsection provides concluding remarks about validity of studied models in mixed traffic streams having heterogeneous variety of vehicles.

Table 2.1 A brief summary of traffic simulation models developed

Group	Year	Author(s)	Work upon
Classic car- following model	1953	Pipes	Stated that safe distance headway increases linearly with speed
	1953	Forbes	Considered human factors (aggressiveness) in traffic flow theory
	1959	Helly	Includes acceleration/breaking of LV in GHR model
	1961	Gazi *et al.*	Stated that acceleration depends on speed, spacing and reaction time
	1961	Newell	Developed speed-headway related car following model
	1981	Gipps	Developed model useful for computational tools, providing speed of FV at next time-step. Further modified by Gunay (2007) for weak lane discipline, and Ravishankar and Mathew (2009) for mixed traffic. Metkari *et al.* (2014) developed this model for mixed traffic with weak lane discipline.
	1995	Xing	Combination of GHR and Helly models
	2000	Treiter *et al.*	Developed the intelligent driver model, where acceleration of FV depends on relative speed, gap, etc.
	1992	Kikuchi and Chakraborty	Fuzzy logic based model, divides inputs/ stimuli into fuzzy sets.
Psycho physic al	1963	Michaels	Developed model based on relationship of reaction of driver of FV with change in apparent size of LV
	1974	Wiedemann	Evaluated the headway thresholds in psychophysical model
Heterogeneo us traffic	2000	Khan and Maini	Heterogeneity is addressed by converting into equivalent vehicle factor
	2000	Marwah and Singh	Developed a framework of simulation model for mixed traffic conditions
	2008	Xie *et al.*	2-d optimum speed model using logic similar to pedestrian flow.
Cellular automata (CA)	1992	Nagel *et al.*	Pioneer in development of CA models. Chmura *et al.* (2014) introduced acceleration/deceleration limits, and Li *et al.* (2011) introduced mixed traffic in this model.
	2009	Mallikarjuna and Rao	CA model based on governing of sub-lanes as observed in weak lane discipline traffic
	2010	Gundaliya *et al.*	Grid based approach in CA models for mixed traffic
	2013	Chen *et al.*	Accounted mixed traffic flow behavior in CA models
	2013	Mathew *et al.*	Strip-based approach including tactical overtaking, to extend lane-based traffic modeling to non lane-based
Comprehensive models	1998	Gupta *et al.*	Potential field approach to simulating traffic
	2004	Chakraborty	Driver behavior in 19 different scenarios in potential field modeling approach
	2005	Arasan and Koshy	Model for highly heterogeneous traffic based on maintaining safe lateral/longitudinal gaps
	2007	Maurya	CutSIM cellular model based on calculation of benefit of various possible paths of LV
	2011	Niar *et al.*	Pore space model depending on available spacing between LV's
	2014	Ambarwati, *et al.*	Conducted pore space-density distribution as means of macroscopic modeling of traffic with weak lane discipline

2.1.1 Conventional car-following models

Car-following models describe the processes due to which drivers follow other vehicles in the traffic stream. In developed world, car-following term was used since the traffic stream consisted of mostly cars. However, in the developing world, the term can be replaced by, and hereafter referred as, 'vehicle-following' or simply 'following behavior'. These models have been studied for seven decades (for e.g., Pipes, 1953, stating that safe headway increases with speed). Since car-following attempts to understand the interplay between phenomena at the individual level and global behavior on a more macroscopic scale, it forms as one of the chief processes of modern-day traffic theory. It is clear that a detailed understanding of this key process is now becoming increasingly important as modeling traffic behavior has significant impact on tackling traffic problems. Many old car-following models are developed by now.

2.1.1.1 GHR model and linear (Helly) model

The research team of the General Motors (GM) Company produced five generations of their car following models, all having the basis that the response of the following driver (acceleration or deceleration) is a function of the sensitivity of this driver and the stimulus. Sensitivity-stimulus models were introduced by GM research laboratories and represent the basis of older models. The GHR model represents this group. In this model, acceleration of the follower is a function of follower's speed, relative speed, spacing, and driver reaction time delay. This model was also developed by Chandler *et al.* (1958). The authors (Gazis *et al.*, 1961) also performed several tests in a tunnel in New York for validating the model. Since the GHR model presumes that the acceleration is only proportional to the relative speed, it cannot ensure the achievement of the driving objective to keep a safe distance from vehicles. (Bevrani *et al.*, 2012). When the relative speed approaches zero, there is no response for the following vehicles no matter how far or close it is from the leading vehicle. This is the most well-known model which relates dependency of deceleration of following vehicle (FV) onto the relative speed of leading vehicle (LV) and FV and the current speed of FV. It proposes a stimulus-response type function. The safety distance or collision avoidance model (1959) seeks to specify a safe following distance within which a collision would be unavoidable if FV suddenly decelerates.

Linear (Helly) model (1959) includes the acceleration/braking of the LV into the GHR model. A linear model was proposed, which stated that the acceleration of FV is related to the relative speeds between LV and FV, speed of the FV, the deviation of the relative spacing and the desired following distance, and driver's reaction time. A combination of both the Helly and GHR models was developed by Xing (1995). This model was also calibrated. It contains terms describing relationship of acceleration with relative speed and spacing (GHR model), acceleration/braking from rest (linear model), and behavior under free-flow conditions.

Forbes (1953) was the pioneer in considering human factors in traffic flow theory. The author concluded that, when cars are following each other on a densely packed road, drivers become more alert and aggressive, and a sudden change in driver response time is reflected with the change of headways before and after a leading car aggressively slows down. The study stated that the time headways of the experimental platoon were in the 1 to 1.5 second range while following at constant speed before the slow-down, but about twice as large after the experimental and unexpected deceleration by the lead car.

Newell (1961) investigated car-following model which gave a governing equation for vehicle speed other than acceleration. The inclusion of the functional speed–headway relation entails the Newell model to achieve the objective of driving behavior in a car following. It is regarded as the beginning of study into car-following models with speed–headway relations. Wang *et al.* (2011) also developed three car-following models based on Newell model; by making certain assumptions for perceiving ability of drivers. Treiber *et al.* (2000) proposed the intelligent driver model (IDM). Here, acceleration of FV is related to the speed of FV, maximum acceleration, relative speeds, desired gap and actual gap available. based on this, the model decides the position of FV which is an outcome of intelligent acceleration strategy. The model combines both the free road acceleration and an intelligent braking strategy.

2.1.1.2 Gipps' car following model

Gipps (1981) proposed a car-following model for the response of the following vehicle based on the assumption that each driver sets limits to his/her desired braking and acceleration rates. The model calculates the speed of FV at the next time-step if the speed and conditions at the previous time-steps are input. However, it does not take into account the acceleration or deceleration of vehicles at different stages, and thus may not present realistic reaction of the driver of FV. Based on the presence or absence of an LV, the driver of FV may either (i) accelerate to its desired speed with an increasing acceleration rate; or (ii) select his/her speed to ensure that safe stopping on sudden stopping of LV. The first condition, known as accelerating to desired speed at the free-flow condition, can be adopted for weak lane disciplined traffic too if there is the absence of any interaction of vehicles.

Gunay (2007) have modified the equation for considering the presence of veering in weak lane discipline traffic. In such traffic, the driver also has the opportunity to veer to a safe speed to move parallel to the LV, if it suddenly brakes. This safe speed depends on the allowed width of the corridor between several other LV's, explained further in Section 2.2.1.

2.1.1.3 Fuzzy logic model

The major advancement for the rule-based models is the fuzzy logic model (Kikuchi and Chakroborty, 1992) where such models typically divide their inputs into some overlapping `fuzzy sets' each one describing how adequately a variable fits the description of a `term'. This approach considers that human perceives the environment, uses his/her knowledge and experience to infer possible actions, and responds approximately. Precise (input) variables consist of distance headway, relative speed and acceleration. The consequence of the rules is reaction and position updation of leading vehicle. For example, the rules are of the form 'If at time *t*, the distance headway is very large, AND relative speed is moderately negative, AND acceleration of leading vehicle is negative, THEN at time (*t*+*dt*) follower should accelerate mildly. This model represents the approximate behavior and not by quantitative evaluation. All these models are described in detail by Brackstone and McDonald (1999).

2.1.1.4 Psychophysical car-following model

The psychophysical car-following model (Michaels, 1963) was based on the assumption that drivers can sense the changes in the relative speeds of the leading and following vehicles by analyzing the change in apparent size of the leading vehicles and react according to the visual angle changes subtended by the vehicle ahead. These changes are modelled based on certain thresholds, and quantifying these thresholds and calibrating them was a difficult task, and till today the calibration of threshold parameters vary as per traffic conditions. Calibration was conducted by the visual angle models (Ferrari, 1989) or threshold requirements (Evans and Rothery, 1973). Several studies (Wiedemann, 1974; Bekey *et al.* 1977; Lee, 1976; Wiedemann and Schwerdtfeger, 1987; Wiedemann and Reiter, 1992; Reiter, 1994; Krauss *et al.*, 1999) were conducted to investigate the thresholds and the following vehicle acceleration. Wiedemann (1974) considered four car-following regimes in the psychophysical model- 1. free flow behavior, 2. Closing in behavior, 3. Car-following behavior, and 4. emergency braking situations. The psychophysical model approach is helpful to accurately describe the car-following behavior, but its calibration remains a major issue. Further, none of these models represents car-following in weak lane discipline conditions, wherein vehicles can close in more than the expected safe distance headway at higher amounts of staggering because they have the option to veer if the LV suddenly brakes.

2.1.1.5 Vehicle-following models pertaining to heterogeneous traffic

Earlier studies described heterogeneity in simulation models by converting the vehicle into a standard vehicle using various equivalency factors (Khan and Maini, 2000), and then the usual modeling approach of homogeneous streams is applied. However, this approach may not incorporate vehicle type-wise interactions and their characteristics. Thus, these modeling approaches cannot be used. A framework of traffic simulation model, which can replicate the movement of heterogeneous traffic, has been developed by Marwah and Singh (2000) to analyze the various environment of the road system. Traffic studies have been conducted on different roads of Kanpur metropolis. It includes parameter estimation of different sub-models such as sub-model each for roadway features, traffic input and field data. Different vehicle types, including a majority (up to 65%) of non-motorized vehicles were included in the analysis with different free speeds. Levels of service (LOS) experienced by different vehicles was calculated. This basic structure of simulation model is adopted in several types of research.

A two-dimensional car following model was also proposed by Xie *et al.* (2008). It is based on an optimum speed model for pedestrian flow in lateral and longitudinal directions (Nakayama *et al.*, 2005). Acceleration/deceleration models are considered using the speed differences, and the interactions with various boundaries (including vehicle edges) are considered. If adequate data collection techniques are available, the validity of this model in mixed traffic stream can be explored.

2.1.2 Cellular automaton models

Another series of rule-based models are referred as cellular automata (CA) based models in which the cell is the fundamental unit. These were initially developed by Nagel *et al.* (1992) for freeway traffic. They are described as follows: the time, vehicle position, speed and acceleration are all considered to be discrete variables. Sections are divided into several cells with a fixed length. A cell corresponds to one or several vehicles, or a few cells correspond to a car. Each cell is empty or accommodates the speed of the vehicle. The vehicle speed is defined as the number of cells moving forward in a particular time step (Jia and Gao, 2007). Fukui and Ishibashi (1996) described another such model by enhancing features of that of Nagel's. They imposed restrictions which can reduce the random slowing-down of vehicles of Nagel's model. Chmura *et al.* (2014) have improved Nagel's model by limiting maximum acceleration and deceleration rates.

Li *et al.* (2010) have modified this model for multi-lane traffic conditions, wherein they have included lane-changing behavior also. A similar modeling was done by Lan and Chang (2005) where the authors had represented car and two-wheeler by non-identical particle sizes. Deterministic CA rules were established later and the model was enhanced by the addition of stochastic rules. Mallikarjuna and Rao (2009) have modeled an improved discrete CA model which includes governing of sub-lanes based on the dimensions of the smallest vehicle in traffic that is the two-wheeler. The longitudinal updating of each vehicle is influenced from Kerner *et al.* (2002). The lateral change in position is made governed by a set of rules, which have an incentive criterion (unavailable gap in front based on speed or acceleration) or a safety criterion (occupied cells). The flow-occupancy relationships are calculated for different types of vehicles.

A grid-based analysis approach was adopted by Gundaliya *et al.* (2010) for analyzing heterogeneous traffic. Vehicles follow some stochastic rules depending upon traffic circumstances. Cell size was decided such that it provides a better representation of the unit of a vehicle in heterogeneous traffic. In this model, the lateral movement rules were tested by giving due consideration to the physiology of the drivers' behavior. Chen *et al.* (2013) have defined vehicles in different lengths and maximum speed and have accounted for mixed traffic flow behavior for multi-lane traffic. The traffic flow models have been generated and the authors have concluded that there is a significant improvement in traffic flow and road space usage. The only hindrance is the effect of slow-moving vehicles.

Mathew *et al.* (2013) have devised a strip-based approach for modeling heterogeneous traffic. Here, the lane is divided into strips of narrow widths and the vehicles are assumed to move along the strips as they move about in lanes in the developed world. A model for the longitudinal movement was proposed to take care of the multiple leader and vehicle type dependent following behavior. The lateral movement model allowed tactical overtaking maneuver by a vehicle (in anticipation of better traffic conditions) which may require multiple strip changes. By defining very small widths (but also increasing the complexity of model), continuous lateral movement of vehicles can be modeled. The model is calibrated with field data in Mumbai and show a better representation of mixed traffic movement.

These cellular automaton models may not represent exact microscopic parameters of observed traffic streams. However, they are computationally quite efficient. In most of these CA models, the basis of selection of dimension of a cell remains undefined. Data accuracy increases if cell dimensions are significantly reduced, but there is an increase in the computational time. More troubling, most of these models do not represent lateral friction between adjacent vehicles depending on their speeds or vehicle types. Thus, comprehensive models simulating the traffic stream as a whole need to be studied.

2.1.3 Comprehensive traffic simulation models for heterogeneous weak lane disciplined traffic stream

The comprehensive models are realistic representations of lateral and longitudinal movement of vehicles in the traffic stream. They do not classify the road space in the longitudinal direction (car-following or lane-changing) or do not discretize the road-space. Lateral as well as longitudinal interactions are described together in the same model. Gupta *et al.* (1998) had devised a microscopic traffic interaction model by constraining positions of vehicles depending upon its path. All roadway and traffic features are viewed as obstacles, either dynamic or static. In this model, each obstacle emanates a positive potential (repulsive force field) around it which repel the driver. However, every goal emanates a negative (or attractive force field) potentials which attract the driver. Shape and strength of the potential field depend on the properties of the obstacle; such as; potential emanated by a truck coming in the opposing direction is higher in magnitude than a parked truck. The authors assumed the potential at a point on the road to be the algebraic sum of all the potentials from the various obstacles and goals. The threat to driver's safety increases with the increase of a potential, thus the threat increases with speed. Hence, it was postulated that a sustainable speed (speed at which a driver feels comfortable) at a point is inversely related to the potential at that point. In a similar approach by Chakroborty *et al.* (2004) a comprehensive microscopic model of driver behavior in uninterrupted traffic flow is developed. The authors used a single model to describe driver behavior in 19 different driving scenarios. Here, the responses of drivers are modelled using steering (lateral) and speed (longitudinal) control. For both these microscopic traffic flow models, there is computational inefficiency. One cannot simulate larger traffic streams where one vehicle is interacting with several other vehicles, with different vehicle types and characteristics. Defining and calibrating the potential field functions are not easy from the field data.

Arasan and Koshy (2005) developed a simulation model HETEROSIM suitable for replicating highly heterogeneous traffic flow, depending on the interval scanning technique with known incremental time advance. Vehicles were generated assuming safe lateral and longitudinal gaps, represented in the field. Here, the authors found that lateral clearance between LV and FV depends upon their respective speeds and types. Transverse clearance for two different vehicle type pair can be expressed as a sum of each vehicle type. This inculcates the heterogeneity into practice. A linear variation for both safe distance headway and lateral clearance with speed was assumed. In the developed model, the variation of the longitudinal gap with an increase of staggering was not studied.

Nair *et al.* (2011) have developed a heterogeneous traffic model based on the available spacing between the LVs or between LV and roadside. These spacing are called pores. The multi-class kinematic wave model has been developed by assessing the micro-behavior of each vehicle through pore between vehicles. This approach has been developed to study the behavior of disordered traffic flow with different types of vehicles. Using this approach, the situation compares the behavior of each vehicle such as cars, motorcycles, paratransits, and buses from empirical observation. Fig. 2.1 describes the model proposed by Niar *et al.*

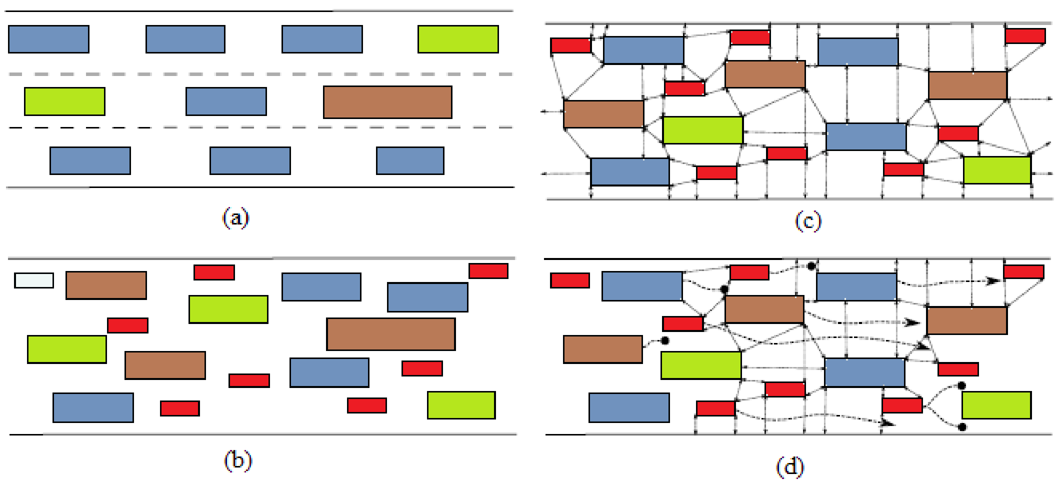

Fig. 2.1 Pore-space model proposed by Niar, *et al.*, 2011. (a) lane-based traffic, (b) non-lane based traffic; (c) vehicles define spacing or pores with interacting vehicles; (d) decisions of vehicular movement.

Ambarwati *et al.* (2014) have conducted an exhaustive empirical analysis of heterogeneous traffic flow in the city of Surabaya, Indonesia. The authors have used pore space as the shortest distance between neighbouring vehicles (measured along the line joining nearest vehicle edges of two neighbouring vehicles). Density is measured in the form of area-occupancy, by studying the occupancy of each image conducted during the recording process. Pore space-density distribution is conducted for car-car, car-2W and 2W-2W pairs. The authors found that pore space decreases with a decrease in the size of vehicle pairs. However, the model complexity increases on a further increase of vehicle pairs.

Maurya (2007) developed the cellular CUTSiM model for heterogeneous traffic. Here, the author assumed that Safe Distance Headway (the headway at which driver feels safe) as well as Lateral Clearance (*LC*) linearly increase with speed. Further, the driver of the following vehicle will choose a path to overtake which will provide a maximum benefit. This benefit is calculated regarding ease to veer towards the gap, its proximity, and speeds of vehicles constituting the gap. This simulation model may represent field traffic conditions accurately, but the main drawback is its calibration parameters which are not easily obtainable from the field. Further, there is no specific relationship between lateral staggering and longitudinal headway, which is generally observed in weak lane discipline.

2.1.4 Development of traffic simulators

Traffic simulators update vehicle positions at different time-steps using various developed algorithms. Benekohal and Treiterer (1988) developed the psychophysical model CARSIM model for simulation of stop-and-go traffic and incorporated a collision avoiding algorithm and a minimum separation constraint for the car following. They have used five situations for describing the degree of response (acceleration). A set of similar conditions were also used in WEAVSIM model developed by Zarean (1987) and Iqbal (1994). FRESIM is another such software developed for microscopic simulation of freeway traffic. (Rakha and Crowther, 2003). CORSIM (CORridor microscopic SIMulation) is a combination of two other micro-simulators; the urban micro-simulator NETSIM and the freeway micro-simulator FRESIM. This has resulted in a simulation model that is capable of representing traffic flow in large urban areas containing both surface streets and freeways and was validated (NSour and Santiago, 1994). Aycin and Benekohal (2000) developed the INTELSIM (Intelligent vehicle simulator) model in which the reaction times of drivers were not restricted by simulation-time steps. Moreover, drivers' perception threshold was considered in car-following. INTELSIM moves follower and leader simultaneously for a continuous time frame using a linear acceleration model. In this model, desired speed is the product of speed and preferred time headway.

VISSIM (Verkehr in den Städten simulator – German word for traffic in towns) model is developed for transit and traffic flow in urban areas as well as interurban motorways on a microscopic level. The psycho-physical traffic flow model of Wiedemann (1974) and the lane-changing algorithm are the building blocks of VISSIM. The models are well-calibrated and validated on motorways in Germany by manual traffic analysis. It is a commercial software, and it claims to validate traffic with weak lane discipline, by means of strip-based approach as devised by Mathew *et al.* (2013). Further, heterogeneous classes of vehicles can be defined and added to the existing traffic stream. Similarly, another simulator AIMSUN is also popular, but both these simulators cannot model variation of headways while following, with the amount of lateral staggering.

Since the inception of most of these simulators was under relatively homogeneous traffic conditions, these models cannot find their application in heterogeneous traffic streams. Metkari *et al.* (2013) have used the CASIM model developed by Maurya (2007) and have added the parameters of Ravishankar and Mathews (2011) (which inculcate the vehicle heterogeneity) and equations of Gunay (2007) for weak-lane based relationships. They have devised a set of rules of basic vehicle-following or free-flow modes, by which every vehicle is updated at every time step consisting of both the criterions. However, the validation is not thorough. There needs to be data which will incorporate more features of vehicular interactions, which are commonly observed in roads of developing countries.

2.1.5 Remarks on simulation modeling approaches in mixed traffic stream

Although there have been some modifications to incorporate mixed traffic conditions in the existing car-following models (Ravishankar and Mathew 2011), there has not been an explicit consideration of weak lane discipline in simulation modeling. The consideration can be made only if a lateral parameter which defines staggering of vehicles is studied, and its effect on other traffic parameters such as speed and headway between leading and following vehicles are investigated. To represent traffic with weak lane discipline, there needs an incorporation of this relationship in a simulation model.

Overtaking of vehicles in a mixed traffic stream does not depend on occupancy at neighboring lanes, but the extent of space availability or lateral gaps between different leading vehicles. Lane-changing models cannot effectively represent overtaking phenomena in mixed traffic conditions. This problem was addressed in few models such as HETEROSIM (2005), CASIM (2007), Gundaliya *et al.* (2007), strip based approach (Mathew *et al.*, 2013) or in pore-space models (Ambarwati, 2014; Niar *et al.* 2009) but a detailed study of variation and modeling of speed with available lateral gaps is not conducted in these models, for a variety of vehicle pairs. Thus, literature which studies these effects needs assessed for incorporation of development of a simulation model.

Hence, a thorough review of literature of modeling of inter-vehicular parameters such as lateral and longitudinal gaps, and overtaking decision modeling is provided in the next section.

2.2 Modeling parameters of traffic in developing countries

The peculiarities of traffic streams in developing countries have been described in Section 1.2. Pertaining to these traffic conditions, limited work was done for modeling weak lane discipline and addressing the heterogeneity. In these streams, vehicles interact longitudinally as well as laterally due to weak lane discipline conditions. When the driver of FV approaches an LV, he/she firstly decides to overtake or follow a leading vehicle. If the decision is to follow, the vehicle interacts longitudinally with leading vehicle, vehicle-following rules dominate the decision of a driver; whereas when it interacts laterally with other vehicles with an intention to overtake them, then lateral clearance maintaining rules dominate the response (decision) of the driver. Driver decision is in the form of acceleration/deceleration or steering. In this section, literature pertaining to different driver behaviors such as following, overtaking and making a decision to overtake are investigated to find an appropriate methodology to be used in simulation models.

2.2.1 Lateral clearance studies

Lateral interactions between adjacent vehicles have been studied since last six decades. May (1953) introduced the concept of lateral friction between vehicles travelling in adjacent lanes, along with various factors affecting flow or providing discomfort to the driver. The author has also calculated the amount of this lateral friction between vehicles in the neighboring lanes. based on traffic arrival pattern of a multi-lane unidirectional highway, Mahalel and Hakkert (1982) concluded that arrival pattern of vehicles in one lane is dependent on the arrival patterns of vehicles in the other lanes.

Nagaraj *et al.* (1990), through the procedure of video-recording the data, observed the clearance gap required for a particular type of vehicle in a mixed traffic flow environment. The road section was a two-lane bidirectional traffic section on a highway. This was the pioneering work to investigate gap maintained by vehicles at different speeds in mixed traffic. However, the context is different (bidirectional roads), and the datasets are outdated with less accuracy.

Gunay (2007) has highlighted the movement of adjacent vehicles in weak lane disciplined conditions and remarked that vehicles tend to shy away from travelling parallel to each other for a longer time. Gunay (2009) have calculated the variation of escape speed of overtaking vehicles in between the gap of two leading vehicles. The variation shows second-degree relationship of escape-speed and width of the escape corridor. The study did not include heterogeneous vehicle types. Pal and Mallikarjuna (2010) have collected data on gap-maintaining behavior between vehicles in a heterogeneous traffic stream. Cell width for the cellular automaton (CA) models (refer Section 2.1.2) need to be decided by gap maintained by vehicles. The authors have evaluated average lateral gap with area occupancy relationship. They have evaluated a variable cell width depending upon the characteristics of the dominant vehicle. In later studies, Mallikarjuna *et al.* (2013) have examined the relationship between lateral gap and vehicle's speed. They found that lateral gaps maintained by vehicles vary with respect to their own speed, type of the adjacent vehicle, and the speed of the adjacent vehicle. The authors also concluded that lateral gaps between vehicles having very little relative speed can be approximated to be normally distributed. Whereas, the lateral gap between vehicles with different speed can be approximated to be lognormal distribution. Here, vehicle pairwise interactions were not investigated. Further, variability in driver behavior was not addressed as a simulation model capable of defining all parameters.

A linear relationship between lateral clearance and speed is assumed in heterogeneous simulation models such as the HETEROSIM model by Arasan and Koshy (2015), CASIM model by Maurya and Chakroborty (2008) and unidirectional model by Metkari *et al.* (2013). In these models, validation was only in the form of macroscopic parameters. VISSIM (2015) has the option of input of lateral interactions between vehicles in the form of a straight line. However, stochastic nature of traffic is not assimilated in this behavior. Moreover, clearance levels are fixed for a particular vehicle type and do not vary as per vehicle pairs.

Previous models have not considered any lateral terms in the equations. Recent research work by Delpiano, *et al.* (2015) involves the introduction of a term called a collateral anomaly. A study has been made to see the effect of vehicle position of neighboring leading vehicle on the following vehicle in a staggered car following. Approaches have also been made by information from a visual angle (Jin *et al.*, 2009); Jin, Wang and Yang, 2010) but they do not adequately represent lateral discomfort. A study has not been made when the vehicle is in overtaking mode. A Recent study by Pal and Mallikarjuna (2016) used the effective width of vehicles to calculate the macroscopic parameter of area occupancy by traffic, at low occupancy levels. Dimayacyac and Palmiano (2016) have studied the lateral clearance change with average speed. The site conditions are mostly homogeneous in nature. The conditions observed are during lane-changing, whereas in developing countries, the phenomenon of lane discipline is not followed. The authors have observed the relationships for various types of cars and heavy vehicles. Studies by Gurumurthy *et al.* (2016) found that lateral and longitudinal gaps maintaining behavior vary as per different vehicle types. Thus, there have been few important studies on the effect of the lateral gap-maintaining behavior of drivers in weak lane discipline traffic (Gunay, 2007; Gurumurthy *et al.*, 2016, Pal and Mallikarjuna, 2013). However, the vehicle heterogeneity in the form of pairwise interactions, or the driver stochasticity is not addressed in most of the models. Very few studies have been undertaken to find out lateral gaps when one vehicle overtakes the another. There is thus, need to study the relationship of the lateral gap with speeds of overtaking and overtaken vehicles accurately for various pairs of vehicles, using sophisticated data collection techniques.

2.2.2 Longitudinal headway studies considering lateral staggering

When a vehicle approaches leading vehicle (LV), it responses either in the form of acceleration/deceleration or a lateral shift. If a vehicle continues to follow a leading vehicle for a long time, it is observed that it stabilizes behind the LV and maintains relative speed almost equal to zero (Sayer *et al.,* 2003; Zhang and Bham, 2007). In traffic stream of developed countries, the basic car-following exists, wherein vehicles follow another vehicle perfectly (i.e. lateral staggering is almost zero) since there is maintaining of lane discipline.

Most traffic simulation models are lane-based, and treat traffic flow in individual lanes separately. However, unlike the basic car-following behavior, the staggered car-following behavior widely exists in traffic with weak lane discipline (Gunay, 2007). For considering non lane-based driving phenomenon in mixed traffic, it is important to consider (i) simultaneous interactions in two dimensions- lateral and longitudinal and (ii) vehicle type-wise or pair-wise interactions.

Gunay (2003) defined the term lane-based driving discipline as the tendency to drive within a lane by keeping as close to the center of the lane as possible. While following in weak lane discipline, the following driver does not assign leadership fully to the vehicle most in front because of the off-centered positions of vehicles. Gunay (2007) investigated the amount of headway with staggering. This investigation is presented in Fig. 2.2. In the basic car following case, FV needs to stop when LV stops, while in the non-lane-based (staggered) car following case, the following driver may have the opportunity to shift and pass the (stopped) leader. Allowed speed determined by Gunay (2007) by the most restrictive of two factors: (a) a speed at which the vehicle can decelerate (at time of passing) to the maximum speed possible after veering to the side of LV; and (b) a speed which should allow the following vehicle adequate time to veer laterally to safely avoid a rear-end collision. The former is called maximum escape speed (MES) by the author and is assumed to be dependent on the width of escape corridor provided adjacent to the LV. Veering time forms the governing factor in the latter part, and depends on the amount of off-centeredness and veering speed of particular vehicle type. Therefore, the following distance between the two consecutive vehicles is a function of the speed allowed by the gap between LV's (depends on the width of escape corridor) and the amount of off-centeredness between them.

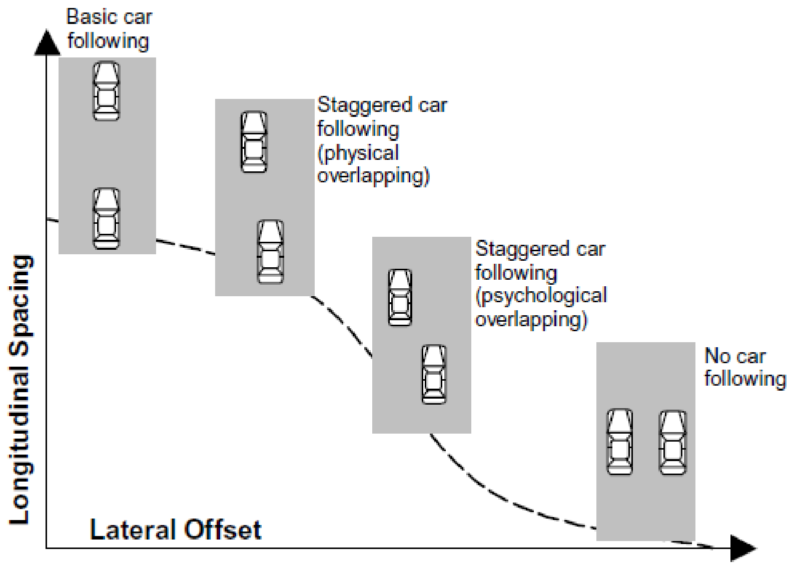

Fig. 2.2 Trend of the relationship between horizontal separations of the LV and FV, and the following distance. *(Gunay, 2007).*

Gunay and Erdemir (2011) also analyzed staggered time headways between the neighboring vehicles on a two lane unidirectional roadway Section without taking the same lane leading vehicle's position into account. When the gap between the two same lane vehicles is small (i.e., 0 < gap < 1.5 seconds), the number of vehicles (travelling in the faster lane) with short neighbouring headways of (0- 1.5 sec) are smaller than the next time interval (1.5- 2.5 sec). Jin *et al.* (2011) developed a theory for staggered car-following based on geometric analysis and proposed a general equation for Time to collision (TTC) based on non-lane based traffic. The TTC was obtained by using visual angle information that can be perceived by drivers directly. TTC was calculated as per Equation 2.1.

$$\frac{1}{TTC} = \frac{\varphi\prime(t)}{\varphi(t)} - \frac{\theta\prime(t)}{\theta(t)} \qquad \ldots 2.1$$

Here, $\varphi(t)$ is the angle described by width of LV onto the driver and $\varphi'(t)$is its derivative. $\theta(t)$ is the is the visual gap angle separating the leading vehicle from the collision position and $\theta'(t)$ is its derivative. Although this approach is novel and can also be applicable in traffic conditions under present study, it is observed that drivers are more concerned with sidewise and front distances rather than angles subtended. Moreover, this paper has calculated lateral gaps in higher discrete intervals of 0.25 m width.

Studies have also found the effect of type of LV or FV on driver behavior, either for homogeneous traffic conditions (Ye and Zhang, 2009*;* Qingyi *et al.*, 2010) or mixed traffic conditions (Kanagaraj *et al.*, 2011). Few studies have investigated the impact of the type of LV on reaction and gap-maintenance of FV. In 2011, Ravishankar and Mathews developed a model that incorporates vehicle-type dependent behavior. The authors modified the widely used Gipp's model for different vehicle-type combinations. Three vehicle classes- namely, car, auto-rickshaw and bus were considered, and the various acceleration and deceleration parameters of Gipp's model were evaluated for each vehicle-type pair from the field using Global positioning system data of LV and

FV. The model cannot yield the reaction of the driver at next time step but calculates the speed at next time-step. Further, the consideration for weak lane discipline is not addressed. In this regard, Metkari *et al.* (2013) have added the parameters obtained from Ravishankar and Mathew (2011) to modified Gipps' car following model by Gunay (2007) to make a simulation model. Although this model suffers from calibration and validation issues, it provides a realistic representation of vehicle- following in such traffic streams.

Thus, it is observed that studies to represent following behavior have been conducted either to represent weak lane discipline or heterogeneous traffic conditions, but not both of them simultaneously. Limited models have been developed for simultaneous representation of both these phenomena, but they are not validated with field data. Thus, there is a need to develop vehicle pair-wise models of a longitudinal gap for weak lane discipline, with speeds of vehicles and staggering.

2.2.3 Overtaking decision modeling

Whenever a vehicle approaches LV, the driver will decide to overtake or follow the LV based on certain traffic parameters. Also, a vehicle stops car-following and begins overtaking the leading vehicle when some traffic parameters in the stream change. There are various factors that would affect driver's decision to depart from the steady car-following state, take a risk and prefer to overtake. There is a need to study these factors and inculcate them in the stream behavior during modeling traffic conditions. The overtaking decision conditions would estimate the situation when car-following (longitudinal interactions) or overtaking (lateral interactions) would be governed. In heterogeneous traffic with weak lane discipline, overtaking decision-making is not in the form of lane-changing as observed in the developed world.

For modeling lane changing decisions, critical issues are the logic that governs the lane changing decision-making process, driver characteristics, and inevitable human uncertainties (Zheng, 2014). Lane-changing models basically consist of three parts (Ahmed, 1999) decision to consider a lane change, choice of a target lane and longitudinal gap-acceptance in the target lane. All three decisions are latent. Decisions to consider a lane change are researched by Yang and Koutsopoulos (1996), where a probabilistic framework was developed depending upon the speed of leading vehicle and opportunity for overtaking. Similarly, Ahmed *et al.* (1996) have used the longitudinal gap between the leading and lagging vehicles as criteria for lane-change. On the other hand, Bar-Gera and Shinar (2005) have assessed overtaking decision by changing the relative speed of FV and LV in a driving simulator and also measured the variation of stable longitudinal headway. The lane-changing decision is also studied by Toledo (2002), Toledo and Farah (2011) or Toledo *et al.* (2003) and these researches conclude that choice of destination lane and decision to accept gap are important aspects. A similar approach is also used by using fuzzy-logic based models in AASIM software developed by Das and Bowles (1999), and the MOBIL lane changing model (2002). But, all these models need to be relooked applied for traffic in weak lane-discipline, where lateral shifts are prominent.

A binary choice model that attempts to capture both drivers' desire to pass and their gap acceptance decisions to complete the desired passing maneuver was developed by Farah *et al.* (2010) and validated by traffic simulator experiments. Drivers were first assumed to decide whether they wanted to pass the lead vehicle or not. Drivers that were interested in passing then evaluated the available passing gap and either accepted it and completed the passing maneuver, or rejected it and did not complete the maneuver. The desire to overtake is the product of desire to pass and desire to accept the gap. This approach is novel and can also be adopted for weak lane discipline conditions.

Kala and Warwick (2013) have heuristically evaluated the overtaking and car-following decisions for an unorganized traffic. As the vehicles move, some uncertainties may arise which are constantly adapted to, and may even lead to either the cancellation of an overtaking procedure or the initiation of one. This approach of evaluation of an overtaking decision can be involved in a simulation model. However, the authors have not considered vehicle heterogeneity or gap-based overtaking decision-making.

The heterogeneous traffic conditions have been studied by limited researchers. Choudhury and Ben-Akiva (2013) have asserted that driving decisions are based on a latent plan approach, consisting of several behavioral algorithms over the travel. They have stated that unobserved factor (the latent plan) can vary dynamically with the change in situation, based on neighborhood variables. The lane-choice, which is discrete, depends upon a maximum utility function for each lane, as studied by Choudhury and Ben-Akiva (2008).

In case of situations for weak lane discipline traffic, there is no concept of a lane, thus studying decision of lateral movement in the form of a lane choice needs introspection. Random utility based models may seem appropriate for capturing lateral movement behavior of mixed traffic. However, the traditional definition of lane-change is not applicable for such traffic, since vehicles perform non-lane based movements, as suggested by Munigety and Mathew (2016). Apart from this, for a driver in weak lane discipline, it is important to consider the effect of surrounding vehicles before making a lateral shift with an intention to overtake. Observing a lateral shift in any vehicle movement can be considered a good indicator of an overtaking decision.

Thus, it is observed that existing literature has primarily focused on lane-based overtaking decisions. Non-lane based acceleration decision model was made by Choudhury and Islam (2016) but the issue of weak lane discipline was considered only to choose the governing latent leader and not for the acceleration component of the model. The overtaking decision model should be based on following principles- (i) should address vehicular heterogeneity; (ii) should consider staggering between vehicles; (iii) should regularly update even during overtaking maneuver; (iv) Observing a lateral shift can be a good indicator of making an overtaking decision.

2.2.4 Remarks on literature review of parameters of traffic in developing countries

For developing a simulation model, several sub-models which determine relationships of various traffic parameters with inter-vehicular gaps need to be developed. These sub-models include-

- *Studies on the lateral clearance between vehicles:* In mixed traffic stream, vehicle movement is affected by friction between adjacent vehicles, which governs their speed. Limited studies were made to calculate the relationship between speeds of vehicles and lateral gaps between them (Pal and Mallikarjuna, 2013; Dimayacyac and Palmiano, 2016).

The developed relationships are not modeled to represent variation across different vehicle types and do not represent realistic stochasticity of driver behavior. A model needs to be developed based on pairwise inter-vehicular distances and speeds.

- *Studies on the longitudinal headways between vehicles:* A stabilized headway between a leading and following vehicle in mixed traffic stream needs a representation of lateral staggering, as proposed by Gunay (2011). Although a large research has been conducted on variation of stable headway with speed, the research is limited for effect of staggering between LV and FV on stable headway. Models have not been made for different vehicle types. To realistically represent vehicle-following behavior in mixed traffic stream, the contribution of both- staggering and speed, needs assessed for different combinations of LV and FV.
- *Overtaking decision modeling:* Few types of research have been conducted to assess overtaking decision of an approaching vehicle based on inter-vehicular gaps, in mixed traffic conditions. A categorical model maybe developed based on observed reaction of the following driver.

2.3 Research related to data collection of gap-maintaining parameters

In this section, methodologies about data collection of parameters of traffic stream with mixed and weak lane disciplined conditions are described. Lateral and longitudinal gap-maintaining characteristics need to be captured from the field and their relationships with speed and other traffic parameters need to be studied. Further, there is a need for an accurate identification technique for various vehicle types. For this purpose, data maybe collected at a point or a short stretch (static collection technique) or moving with the traffic stream (dynamic data collection technique) as shown in Fig. 2.3. There can be further divisions according to the technology used (explained in Fig. 2.3 and described in subsections). The first and second subsections respectively describe static and dynamic data collection methods. The classification of data collection techniques is provided in Fig. 2.3. Various data collection techniques are evaluated based on (i) identification of vehicle types; and (ii) measurement of inter-vehicular distances and speeds.

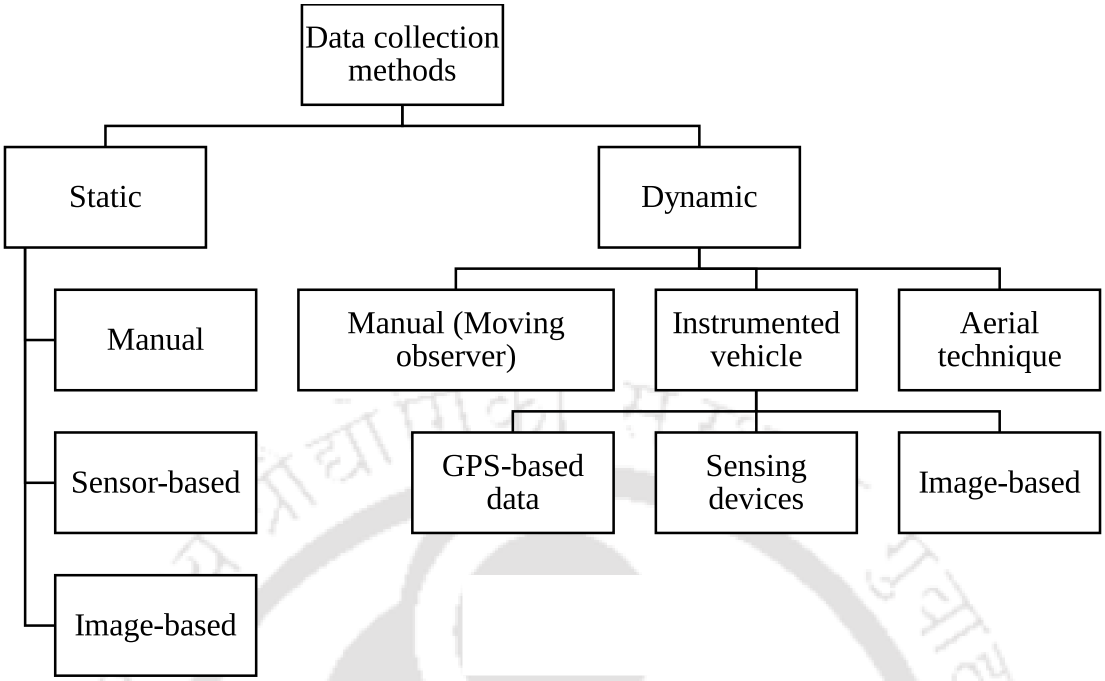

Fig. 2.3 Classification of traffic data collection methods

2.3.1 Data collection by static devices

The static data collection methods involve data collection from a fixed location. They include manual count, sensor-based techniques using waves of different types, and image-based techniques. They can also be classified as intrusive or non-intrusive techniques, depending on the impression left on road section after data collection. Different static traffic data-collection devices are summarized for their applicability in heterogeneous traffic with weak lane discipline in Table 2.2.

Table 2.2 Traffic data collection static devices

S. No.	Method	Description	Advantages	Disadvantages	Applicability to mixed traffic
Intrusive techniques					
1	Pneumatic road tubes (FHWA, 2007)	Difference in pressure change are recorded as traffic passes over pneumatic tubes	Quick data collection methods	Cannot detect vehicle types	Not applicable, cannot classify vehicle types
2	Piezoelectric sensors (Li and Yang, 2006)	Mechanical deformation of piezoelectric material gets recorded to record presence and weight of vehicles	Can record the presence and weight of vehicles	Costly, cannot detect vehicle types of similar weights	
3	Magnetic loops (Kwong *et al.*, 2009)	Magnetic loops arranged in specific formats, generate magnetic field on presence of vehicle	Popularly used in developed world	Costly technique	
Non-intrusive techniques					
1	Manual count	Manual counting and identification of vehicle types	Accurate method of classifying vehicle types	Cannot measure any other traffic parameters such as speed, headway, etc.	Applicable only for vehicle classification.
2	Passive and active infrared (Grabner *et al.*, 2008)	Presence, speed and size of vehicle can be sensed by electronic pulses based on these techniques	Accurate vehicle detection	These methods have limited coverage and are affected by bad weather.	Can be applicable if combined with some other technique for vehicle identification
3	Passive magnetic sensors				
4	Microwave radar (Zwahlen *et al.*, 2005)				
5	Ultrasonic sensors (Kim, 1998)				
6	Video image detection	Vehicle detection and trajectory extraction from video-images of recorded traffic	Data obtained as perceived by drivers, suitable for medium range data	Accuracy changes with change in camera orientations	Can be applicable

2.3.1.1 Identification of vehicle types:

From Table 2.2, it can be observed that intrusive techniques cannot determine different vehicle types in a mixed lane discipline. Although limited identification (in the form of the size of the vehicle, its weight, etc) is possible in the case of few non-intrusive techniques, the precise representation of a vehicle type is possible only by its recorded image or identifying the vehicle type manually. Thus, a video-image detection technique is a requisite to accurately identify various vehicle types. Large researches have been made to identify vehicle types automatically based on their image properties and various image-processing techniques. They calculate detection and position of a vehicle based on the difference in present image and a background image (road section with no vehicles) using various filtering techniques. The main drawbacks of image-processing techniques are the incorrect identification of vehicles, missing of vehicles (especially when vehicle image colour is similar to the colour of roadway), incorrect marking of vehicle size (due to vehicle shadows) etc. A necessary traffic view should be used for this identification. Vehicle-following cannot be effectively studied if a top frontal view is used because FV, in this case, can be shadowed if the size of LV is large enough, and cannot be identified and classified. The incorrect classification can be rectified by manually re-classifying vehicles. Instead, another solution is by manually marking co-ordinate of vehicle position on the image and classifying the vehicle type. This method is tedious, but it has higher accuracy of vehicle classification.

2.3.1.2 Measurement of inter-vehicular gaps:

The measurement of inter-vehicular gaps can be classified based on sensor techniques or image-based techniques.

Sensor-based techniques: For accurate measurement of inter-vehicular gaps, accurate vehicle positions need to be recorded by the measuring device. The exact selection of measuring device depends upon various factors such as availability, cost, accuracy, range, etc. Ultrasonic and infrared sensors have higher accuracy and are of lesser cost. Moving vehicle detection and classification system plays an important role since it gathers all parts of the data used (i.e., vehicle type, speed and distance). Acoustic, seismic, and infrared sensors are also used in vehicle detection and classification systems. Magnetic sensors are less sensitive to noise and Doppler effects. Lan *et al.* (2011) presented novel vehicle detection and classification method by measuring and processing magnetic signals. However, all these devices can be mounted only to the road edges (median or shoulders), thus can provide the position and trajectory of only the nearest vehicle, and its distance from the road edge accurately. Thus, they cannot be used in this form to detect inter-vehicular gaps, and maybe used dynamically if sensors are attached to a vehicle. These setups are described in the further sub-section.

Image-based techniques: Data collection by video-recording is the most popular method used these days. A detailed literature review based on image-sensing of vehicles has been presented by Sun *et al.* (2004). A road section of about 20-100 m lengths can be recorded from a static camera placed away from the roadway. The next step – calculation of lateral and longitudinal positions of vehicles from traffic images – is a challenging task. The Section needs to be laterally divided into sub-sections or strips. There are some efforts in this regard by Metkari *et al.* (2013), Jin *et al.* (2011) and others. In some cases, the road section can be physically marked with strips of known width. However, the more modern methods of camera calibration can be used. Several types of research have been made to calibrate the road section points from their corresponding points visible in the image. Efforts in this regard include those by Fukui (1981), Courtney *et al.* (1984), Bas and Chrisman (1997), Wang and Tsai (1991), Fung *et al.* (2008).

Vehicle trajectory data can be obtained automatically using image-processing softwares which are based on camera calibration techniques. They can basically provide the lateral and longitudinal position of the vehicle. One of such softwares (suitable for developing countries' traffic conditions) is TRAZER or Traffic Analyzer and Enumerator (*website link*). If vehicles are accurately classified, their positions can be calculated to a fair level of accuracy by this method. The accuracy varies as per variation of the focal length of the camera used for recording traffic.

Thus, it is observed that vision based technique (i.e., data collection using recorded video of traffic stream) is the only suitable candidate for collecting traffic data by static means. There are limited applications of vehicle sensing devices, and in spite of their accuracy, they cannot provide inter-vehicular distances. On the other hand, if trajectory data of vehicles could be obtained from their recorded images, inter-vehicular distances can be calculated.

2.3.2 Dynamic data collection

Various traffic data could be collected using the dynamic movement of different vehicles either part of a stream or travelling close to the traffic stream. Some of the common techniques include moving observer method (manual identification and vehicle count), instrumented vehicles and aerial vehicles. The manual count cannot provide inter-vehicular distances, and aerial vehicles are still in development stages, thus are not cost-effective and require large research. They are not used in the present study.

The instrumented vehicle is a vehicle equipped with various instruments to measure desired data as the vehicle traverses through a pre-defined route. The uses of instrumented cars are manifold, of which predominant efforts are used for travel time analysis (Comert *et al.*, 2013). Apart from traffic data collection, they are also used to measure grades, soil strength effect, bridge damping, pavement characteristics and other roadway features. Smart car is an instrumented vehicle of 1995 capable of video-monitoring and recording several driver behaviors. It consists of 4 concealed cameras, and different computer-collected signals such as speed, acceleration, flashers or turn signals being used. These vehicles are in developmental stage since four decades (Helander and Hagvall, 1976). Instrumented vehicles can also be used to calculate travel time distribution of a road network as used by Feng *et al.* (2014).

Alonso *et al.* (2011) have devised the use of ultrasonic sensors in active traffic safety systems to measure the distance between vehicles. Fig. 2.4 shows the adopted diagrammatic setup by the authors. The relative speed between two vehicles was estimated using consecutive samples of this distance. These two quantities are used by the control system to calculate braking and accelerating reactions and adjust the comfortable speed based on these values in addition to maintaining of lateral gaps. As ultrasonic sensors can detect any kind of obstacle, this system can also prevent or reduce collisions. However, there is no co-relation with the absolute speed of the vehicle in the setup used, and a vehicle identification mechanism is not developed.

Fig. 2.4 Experimental prototype developed by Alonso *et al.* (2011)

Chong *et al.* (2013) have used a unique and improved image-processing software for vehicle detection and tracking, from a video taken placed in front of the vehicle. A new algorithm was proposed to detect vehicles using video images which were obtained from video cameras installed in a moving vehicle. The proposed method employed various vehicle features (such as vehicle shadows, rear lights, luminance entropy and edges) to detect vehicles. The proposed vehicle detection algorithm can be used for the development of driver assistance system and autonomous vehicle systems.

A novel approach to detect distances between vehicles was made by Wong and Qidwai (2004) using instrumented vehicles. In this research, the authors have devised collision avoidance of a car using attaching a system consisting of ultrasonic sensors and actuators. The authors have also developed an automatic model car and have evaluated some results. All the processes were processed using a vehicle-electronic control unit. A similar approach was also used by Venter and Knoetze (2013) for measuring lateral distances between two-wheelers and other vehicles to predict safe width of two-wheeler lanes. This approach can be developed for studying lateral distances. Various sensors have also been used for vehicle detection systems. Literature for a video image or vision based sensors has been reviewed by Sun *et al.* (2004). Moving vehicle detection and classification system is popular, with a video image or vision-based sensors being used on a large scale.

The trajectory of a vehicle can also be accurately determined using a high accuracy data logger GPS unit attached to each vehicle. Based on this setup, its position and speed, acceleration and other dynamic parameters can be calculated. Bokare (2008) has evaluated various acceleration-deceleration characteristics of different test vehicles without the influence of other vehicles. The same method can be devised to obtain speeds, accelerations of different vehicles in the traffic stream. However, this method is impossible for studying an entire traffic stream, since every vehicle in traffic stream needs to be fitted with a GPS unit, which is not feasible.

Instrumented vehicles can be developed to measure distances between vehicles, as in Wong and Qidwai (2004), Knoetze *et al.* (2013) or Alonso *et al.* (2011). Further, vehicles can be identified based on image-based identification process provided by Chong *et al.* (2013). However, as described in Section 2.1.3, automated identification processes have their drawbacks, hence an assistance of manual classification is also necessary.

2.3.3 Remarks on data collection techniques

From the research related to methods available for data collection, it can be observed that camera-calibration techniques using video recording are good for measurement of inter-vehicular gaps in the range of 0.5-20 metres, and sensor-based methods are capable of measurement of gaps for lesser ranges, where high precision is required. Vehicle speed data can be obtained by vehicle trajectories either by dynamic methods (GPS techniques) or static methods (vehicle trajectory from images). Softwares developed for traffic data extraction are having the advantage of avoiding manual data extraction, but have a limitation in determining certain traffic parameters, such as identification of vehicle types for which manual method is necessary. It can be concluded that a semi-manual approach needs to be developed for data-collection of mixed traffic streams, to achieve a balance between accuracy in measuring distances, and accuracy of vehicle classification.

2.4 Outcome of the literature review

From this literature review, it is clear that there has not been a unified research which focuses on all aspects about traffic in developing countries like India. Studies have been made of parts, but not over a broader perspective. So that all factors are considered, one needs a broad mechanism which encompasses every aspect such as loose lane discipline, driver behavior, non-standard vehicles etc. After a review of existing literatures on simulation models in developing and developed the world, it is found that piecewise models addressing the issues of either heterogeneity or weak lane discipline have been attempted. However, a holistic model encompassing all the driver behavior features is missing.

The conclusions from reviewing existing simulation models is that to simulate a traffic stream with weak lane discipline and heterogeneous traffic, a comprehensive traffic simulation model needs to be developed on the basis of microscopic models such as- (i) relationship of lateral gaps between vehicles with speeds; (ii) relationship of longitudinal gaps between leading and following vehicles with staggering and speeds; (iii) overtaking decision modeling based on inter-vehicular gaps and other traffic parameters; (iv) other traffic parameters such as acceleration and deceleration of vehicles, lateral and desired speed distribution, etc. Development of these models needs addressed first to simulate mixed traffic stream.

Substantial work has been done for modeling longitudinal gaps with respect to speed. But, majority of this work does not take into account the amount of staggering in this stream, which is a key feature of weak lane discipline traffic. Very few studies have been done in India which includevehicle interaction in both the directions simultaneously. Studies by Ravishankar and Mathews (2011) did not consider weak lane discipline even though heterogeneity was considered. On the other hand, studies such as those by Arasan and Koshy (2005), the CASIM model of Maurya (2007) or that of Metkari *et al.* (2013) considered these parameters but assumed certain relationships. Moreover, these models are not thoroughly validated for greater application. As far as modeling lateral gaps between overtaking vehicles is concerned, few types of research are conducted (Dimayacyac and Palmiano, 2016; Pal and Mallikarjuna, 2016, Arasan and Koshy, 2005), but these works have not focused on all vehicle type aspects and not been able to formulate a model establishing relationship of gap-maintenance with speeds, for different vehicle types and addressing the driver heterogeneity. Further, overtaking decision making of a driver in mixed traffic conditions has not been considered based on inter-vehicular gaps. In some researches, (Toledo *et al.,* 2008,) this decision is considered in the form of lane-changing models, but this may not be applicable in the present context. To develop appropriate models of inter-vehicular gaps with other traffic parameters, large data are required, which could be collected by developing modern data collection methodologies with high precision.

The third section focused on the development of an appropriate methodology for extraction of data. The vehicle detection studies in the western world are sophisticated and advanced, but, similar studies are limited to mixed traffic conditions. For these conditions, either video imagery or moving sensor-based methods are found appropriate. Vehicle trajectory can be accurately calculated using a vehicle equipped with GPS unit. There is a need of a combination of these data collection and extraction methods, for extracting inter-vehicular gap-maintaining data in mixed traffic conditions. For a collection of data for development of a model for inter-vehicular gaps, these methods would be essential. Thus, the first step to proceed for research work is a collection of appropriate traffic data using appropriate methods. These will be discussed in detail in the next chapter.

CHAPTER 3

Methodology for data collection and extraction

For the development of a simulation model, different data-sets are required for replicating behaviors of drivers in different conditions, such as following a vehicle, making an overtaking decision or maintaining lateral gaps. For this purpose, field data collection is essential. The data obtained would be used in modeling inter-vehicular gaps, and these models would be further used to develop a traffic simulation model replicating weak lane disciplined traffic. The overall study framework for this research is depicted in the flowchart in Fig. 3.1.

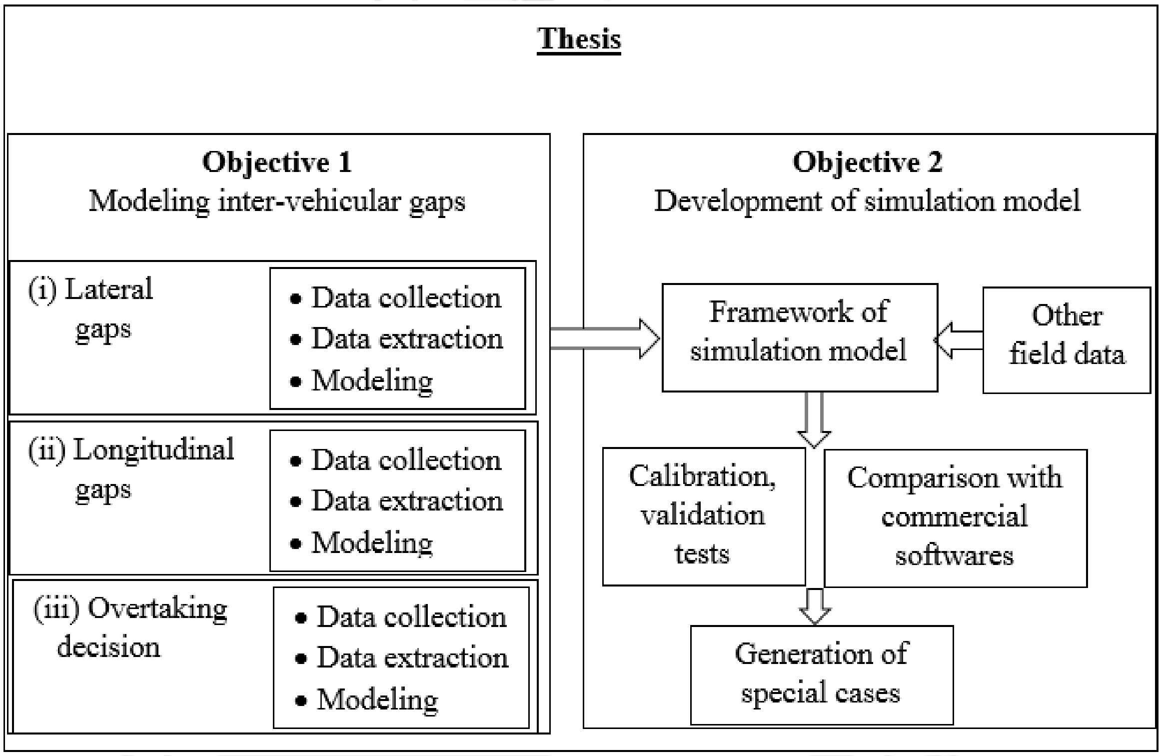

Fig. 3.1 Flowchart depicting the overall study framework adopted in research work

This chapter describes the available methods for traffic data collection and their selection for this study. Further, it describes data-extraction from the field, for lateral and longitudinal gap-maintaining and overtaking decision making. This chapter is divided into the following sections-

- *Representation of interactions between vehicles under heterogeneous traffic with weak lane discipline:* This section describes the interactions between vehicles and the parameters essential for the analysis of behavior in a mixed traffic stream.
- *Adopted methods for data collection of parameters of vehicle interaction:* This section focusses on the selection of the appropriate methods for data-collection of lateral and longitudinal gap-maintaining behavior, from various available traffic data collection methods.

- *Methodology adopted to study lateral interactions:* This section highlights data-collection and extraction for lateral (across the road) gap-maintaining behavior. The data are collected using sensors attached to a moving vehicle.
- *Methodology adopted to study longitudinal interactions*: This section focusses on data-collection and extraction for longitudinal (along the road) gap-maintaining behaviors in mixed traffic conditions. The data are collected by video-recording and camera calibration technique.
- *Vehicle decision making criteria for overtaking*: This section describes data-collection and extraction for overtaking decision modeling, based on inter-vehicular gaps and speeds.

3.1 Representation of interactions between vehicles under heterogeneous traffic with weak lane discipline

Consider a test vehicle moving in a heterogeneous traffic with weak lane discipline. The driver of this vehicle needs to check movement of several vehicles- those ahead of test vehicle as well as those moving alongside test vehicle for safe traversing. These vehicles affect the movement and position of test vehicle as it is maneuvered by the driver in this traffic stream. Such vehicles are called interacting vehicles, since they influence the position of test vehicle in the next instance. Apart from longitudinal interactions, vehicles also interact laterally with test vehicle, since they can veer (move sidewise) in this traffic stream whenever they get gaps between vehicles ahead. Thus, a driver needs to have attention to both- in the front as well as sidewise to safely traverse in such traffic stream. Thus, interactions governing a vehicle position in this stream can be classified as 'longitudinal interactions' and 'lateral interactions'. Their variation with speeds and positions of interacting vehicles, vehicle types, width of road etc., need to be studied in detail.

Parameters influencing the behavior of following-vehicle under the impact of heterogeneous traffic stream may include speeds of interacting vehicles, their lateral and longitudinal positions and gaps between them, the vehicle types, driver behavior, traffic stream density and road geometry. It is assumed that external characteristics (such as land-use, climate, pavement conditions, etc) have negligible influence on behavior of the vehicles. Vehicles are assumed to travel within the road width independent of roadway features such as lane marking, median type and width, etc. Various inter-vehicular parameters arise when a test vehicle interacts with other vehicles, which influence behavior of the driver. They are depicted in Fig. 3.2, and described below.

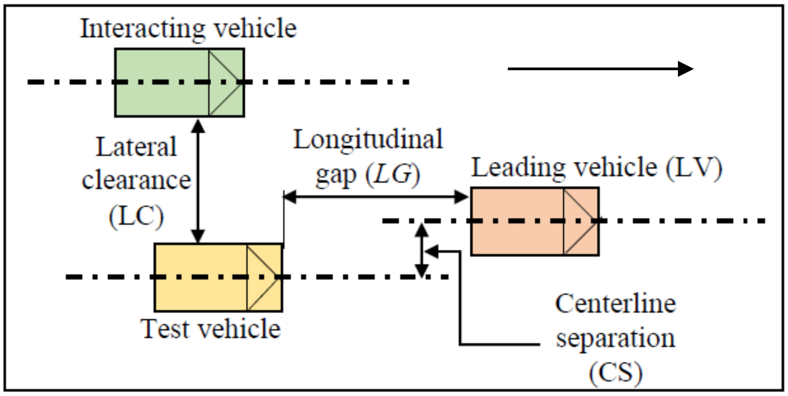

Fig. 3.2. Traffic parameters used in analysis of driver behavior

- Lateral interactions could be represented by means of 'Lateral clearance' (*LC*), or clearance maintained between two adjacent interacting vehicles. They can also be represented by centerline separation (*CS*) or staggering, which is the distance between centerlines of vehicles along the direction of travel. However, drivers are more concerned about *LC* when they drive adjacently without any lane discipline, and they are more concerned about *CS* when they follow a leading vehicle (LV). When one vehicle (following vehicle or FV) follows the other, vehicle widths may influence any other lateral parameter (such as edge to edge separation or extent of overlap). Hence, the direct distance of centerline separation is used for representing staggering of LV and FV.
- During vehicle-following, the difference in the longitudinal positions can be determined using headway between two vehicles. However, the driver of FV perceives the longitudinal gap (*LG*) and not distance headway between two vehicles for his/her reaction. Therefore, in this study, the longitudinal gap (*LG*) is taken into consideration. It is the distance from the back of LV to the front of FV. The longitudinal positions can also be represented in the form of the time gap, which is the time elapsed after passing of back of LV to the front of FV at particular section on the road.
- Speeds of both the vehicles play a crucial role. Vehicles maintain more safety at higher speeds. Thus, inter-vehicular gaps generally increase with the increase of speeds.
- Driver behavior can be quantified in the form of, an amount of risk a driver takes when driving in a traffic stream. This may depend on characteristics such as age, driving experience, familiarity with the road conditions, mental and physical state, strain, etc. Vehicle characteristics such as age of the vehicle, service life, maintenance affect its maneuvering on road stretches.

Several vehicles provide simultaneous stimuli to a test vehicle as it moves in traffic stream. At a particular instance, it is assumed that the following/test vehicle will respond to stimulus of the most dominating vehicles present near it. In denser traffic streams, stimuli from more than one vehicle may affect the position and speed of a particular vehicle and their simultaneous effect need to be studied.

3.2 Adopted methods for data collection of parameters of vehicle interaction

Depending upon the need of study, there are various data collection techniques available. In studying heterogeneous traffic with weak lane discipline, accurate information of the following parameters is essential to be studied-

- Lateral distances between vehicles
- Longitudinal distances between vehicles
- Speeds of vehicles
- Overtaking decision-making of a driver
- Vehicle types

Measurement can be taken at a point (for flow-count), at a small section (for spot speed, flow and position) and a longer stretch, to get relative positions of vehicles and the flow count. In the scope of this thesis, a vehicle to vehicle position is to be found, so information about the absolute position of the vehicle on the road is secondary. Following data collection techniques reviewed in the previous chapter are suitable for this purpose.

i. Data collection by video recording: An observer can calculate speed (from two different positions at different time-steps) and also record position of a vehicle (using camera calibration technique, using video-recording of a traffic stream). Accuracy depends on the video resolution, hence, smaller distances may be inaccurately measured.
ii. Data collection by GPS devices: A GPS device (Global positioning system) records the global coordinates of a vehicle using satellite position data.
iii. Data collection by vehicle detection devices: To measure inter-vehicular distances accurately, one can use ultrasonic or laser detection devices attached to a test vehicle to get inter-vehicular gaps. However, to note vehicle speeds, the devices shall be combined with a GPS device, and there shall be some means to identify vehicle types, too.

From these available methods, appropriate combination needs to be used to collect simultaneous speed and distance data accurately and effectively. For measuring lateral distances, an instrumented vehicle equipped with GPS device was used; whereas for measuring longitudinal distances as well as overtaking decision-modeling, camera calibration technique was used from recorded traffic video. The two subsections highlight the motivation behind using these data collection techniques.

3.2.1 Motivation behind using instrumented vehicle for measuring lateral distances between vehicles

The lateral distance between a pair of interacting vehicles need to be calculated and its variation with speeds of both the vehicles, their vehicle types need to be studied. For this purpose, firstly, video recording technique was considered. It involves gathering trajectories of two interacting vehicles in a traffic stream and calculating their inter-vehicular distance as well as their speed. In this method, accuracy levels of 0.2 m are achieved. Even if image-processing softwares are used to improve accuracy, the centimeter-level accuracy is not achieved by this method. Moreover, the clearance maintained during entire overtaking duration is not recorded by this method, since the trap length of a video camera is less (range upto 50 metres) whereas the overtaking maneuver may continue for greater distances. A setup is required which can provide centimeter level accuracy and at the same time can also obtain speeds of both the vehicles. For this purpose, sensing device needs attached to a probe vehicle. The data collection needs to involve running of a probe vehicle fitted with ultrasonic sensors at its sides, with a GPS device, to get both the readings of vehicle speed and inter-vehicular distances simultaneously. Speed of interacting vehicle can be calculated at a particular instance, if relative speed of these vehicles is known.

3.2.2 Motivation for video-recording for measuring longitudinal distances between vehicles

To find a variation of veering with different vehicle types, speed and longitudinal distance, several methods of traffic analysis were considered. They are listed as follows-

- Longitudinal interactions between vehicles are observed over an extent of 20 meters or higher. Since ultrasonic sensors cannot record distance more than 4 meters, they cannot be used in longitudinal headway analysis. There is the unavailability of sensing devices for obstacles at longer distances in the current study, or the available devices are costly. Data collection using laser sensors was also attempted using attaching a high precision laser sensor ahead of the test vehicle, but the directed beam obtains only longitudinal distance and not the lateral staggering. Thus, the available device (laser sensors) cannot obtain centerline separation between vehicles and larger number of such devices need attached to test vehicle which is not feasible. Hence, this method is not used in current study.
- An instrumented vehicle equipped with GPS: It is necessary to note the trajectory of LV and FV vehicles. Instrumented vehicles can provide trajectories, but it is not feasible to use a large number of instrumented vehicles to obtain the large trajectory database of interacting vehicle pairs for different vehicle types. Further, to study the impact of multiple leading vehicles on FV, one may require more than two GPS-equipped vehicles, which is not feasible due to limit on a number of GPS equipment.
- Video image-processing: Data could be extracted from the field using modern methods of video recording and processing. There are commercial softwares which detect vehicles from a video in the field and detect their coordinates. One such commercial software which can be used for vehicle detection and noting of trajectories is TRAZER. It requires a top-frontal view of moving traffic, and then based on the face structure and shape of the vehicle, it classifies vehicles into four broad categories. However, it is observed that in such a video, there is shadowing of FV by the LV, due to which it is not possible to note the image co-ordinates of FV every instance. Further, the processing time required increases in the denser traffic stream. Many times a vehicle is wrongly classified or missed during classification, and a manual correction is needed. Image processing involving detection of vehicles is difficult to be developed for a traffic stream with a large variety of vehicles varying significantly in their operating characteristics but not their sizes (e.g. LCV, cars and motorized three-wheelers).

- Thus a semi-manual method of identification is employed. The manual method of noting vehicle coordinates for each interacting vehicle at each video frame will be too laborious. Thus, software is developed which can note coordinates of vehicles at a mouse click.

While playing the recorded traffic video, image-coordinates of interacting vehicles at desired frames in video file are noted by a mouse click, using a program developed in MATLAB. These image coordinates are converted into coordinates in the real field (i.e., the plane of the road) to find out lateral or longitudinal distance with respect to edges of the road. For this purpose, literature is reviewed, and the best possible method involves that by Fung *et al.* (2003).

3.3 Methodology adopted to study lateral interactions

Lateral or sidewise interactions of vehicles are common in a traffic stream with no lane discipline. Two vehicles are moving sidewise in a traffic stream keep a certain distance (clearance) between them which may vary as per their speeds, vehicle type, driver behavior, and external factors as well (width of the road, day or night conditions etc). In the present study, the lateral interactions are captured using an instrumented vehicle consisting of the ultrasonic sensor device, GPS and video camera.

3.3.1 Instruments used for data collection

During lateral interaction of vehicle pair, four chief parameters viz. test vehicle speed, interacting vehicle speed, lateral clearance between test vehicle and interacting vehicles and vehicle type of interacting vehicles need to be determined. Other parameters such as road width in the form of number of lanes, time of recording (day or night); are also considered.

The instrumented vehicle used in this thesis consists of equipments used to measure the speed of the interacting vehicles and lateral clearance between them simultaneously. The main instruments used in this experiment are-

i. Ultrasonic sensor assembly
ii. GPS device equipped with video cameras.

Fig. 3.3 shows the instruments which are part of the sensor assembly in the vehicle, used to measure lateral clearance.

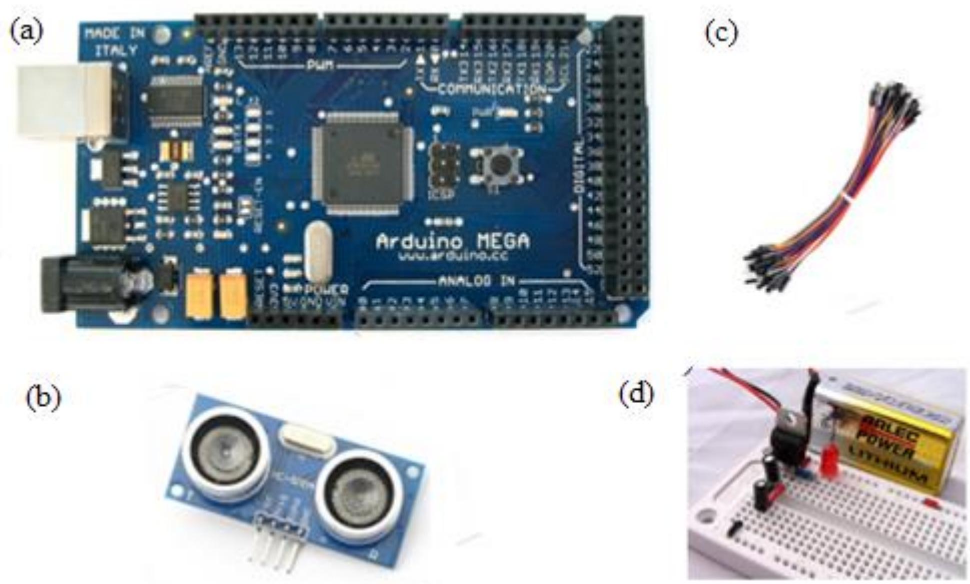

Fig. 3.3 Equipments used for measuring lateral clearance- (a) Microcontroller board, (b) Ultrasonic sensor, (c) Connecting wires and (d) Breadboard with power supply.

3.3.1.1 Ultrasonic Sensor assembly

Features

To measure the lateral spacing between vehicles, ultrasonic sensors are used. These sensors can trigger particular ultrasonic pulse and can calculate the distance between themselves and required an object, based on the time taken between triggering of pulse and receiving of reflected 'echo' pulse from the object.

Working

When a pulse is triggered, the sensor monitors for reflected waves and microcontroller board keeps track of time-lag to the accuracy of one millisecond. Knowing the speed of ultrasonic waves in air (~344 m/s) and time lag, one can calculate the total path length for the reflected wave (i.e., twice the lateral spacing between instrumented vehicle and object). The range of these sensors is upto 4 meters. For this setup, it is restricted to 2.5 meters, since it is assumed that vehicles do not interact laterally beyond a lateral distance of 2.5 meters (Siddiqui, 2013). The assumption is based on the fact that two vehicles travelling in neighboring lanes (3.5 m width) have less interaction with each other even at higher speed.

Sensor positioning in vehicle

Six sensors (four in case of a two-wheeler used as an instrumented vehicle) are attached on either side of vehicles, one each in front, middle and backside, as shown in Fig. 3.4 (a). They are placed at the height of 80-100 cm from ground level, to ensure that every interacting vehicle is detected. The distance between two sensors is noted as inter-sensor distance.

Conical angle correction factor of ultrasonic sensor

The sensors emanate ultrasonic pulse in a conical direction as shown in Fig. 3.4. The cone angle for each sensor is calibrated in the lab; and based on this and the distance maintained from the sensor, a correction is made dynamically, and inter-sensor distance is accordingly corrected. (For example, corrected distance between sensor 1 and 2 in Fig. 3.4 (a) is AL if the vehicle is overtaking test vehicle, and CN if test vehicle is overtaking another vehicle.) If echo pulse is not detected, or if the object is beyond the stipulated range of the sensors (i.e., 250 cm), then the sensors are programmed to record a ‘null’ reading marked as 0.

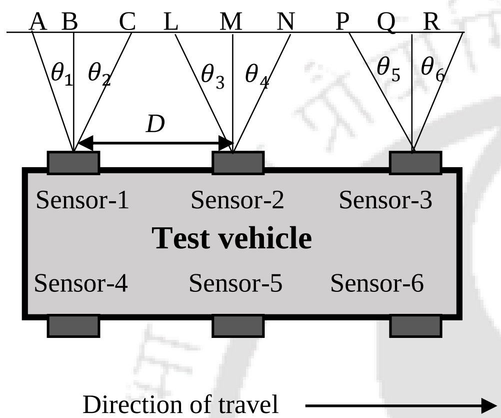

(a)

Timestamp (ms)	Sensor-1 (cm)	Sensor-2 (cm)	Sensor-3 (cm)	Speed (km/h)
725100	0	0	0	56.025
725300	0	0	0	55.889
725500	0	0	0	56.067
725700	A $\boxed{188}$	0	0	56.277
725900	190	0	0	56.661
726100	182	L $\boxed{195}$	0	56.424
726300	190	187	P $\boxed{201}$	56.392
726500	187	176	190	56.421
726700	172	173	178	56.568
726900	C $\boxed{169}$	172	174	56.406
727100	0	163	170	56.481
727300	0	173	164	56.395
727500	0	N $\boxed{152}$	150	56.653
727700	0	0	150	56.251
727900	0	0	140	56.273
728100	0	0	142	56.269
728300	0	0	136	56.157
728500	0	0	R $\boxed{151}$	56.171
728700	0	0	0	55.844
728900	0	0	0	56.054
729100	0	0	0	55.763

(b)

Fig. 3.4: Illustration showing sensor readings corresponding to time of detection.

Microcontroller board and related accessories

The ultrasonic sensors are operated and controlled by a microcontroller board which is further connected and controlled from a program, as shown in Fig. 3.4 (a). ‘Arduino mega’ microcontroller board is selected for this purpose. The program code is written in a C++ based open project Arduino 1.0.5. The program triggers pulses at the highest frequency available, and this is adjusted to 10 Hz, matching the frequency of Video V-box (GPS setup). A 5 Volt DC supply is required to trigger pulses in the sensors. Connecting wires are required to connect sensors to the power supply as well as microcontroller board. A 12 Volt DC battery is required for the power supply.

3.3.1.2 GPS with video cameras

Test vehicle speed is calculated using video V-box (manufactured by Racelogic company). This consists of an accelerometer attached with a high accuracy Global Positioning System (GPS) data-logger. It updates vehicle position from satellite signals and thus calculates the speed at every time step, which is set at 0.1 seconds in this case. At the same time, it also has provisions for recording traffic data using two cameras. Thus there is a simultaneous collection of vehicle speed and traffic video. Since the present methods for determining vehicle types using any software are not accurate, capturing of a video is essential during the run. At a later stage, there needs a manual detection of vehicle types using the video recorded from V-box. Fig. 3.5 shows instruments for analyzing lateral clearance with speed.

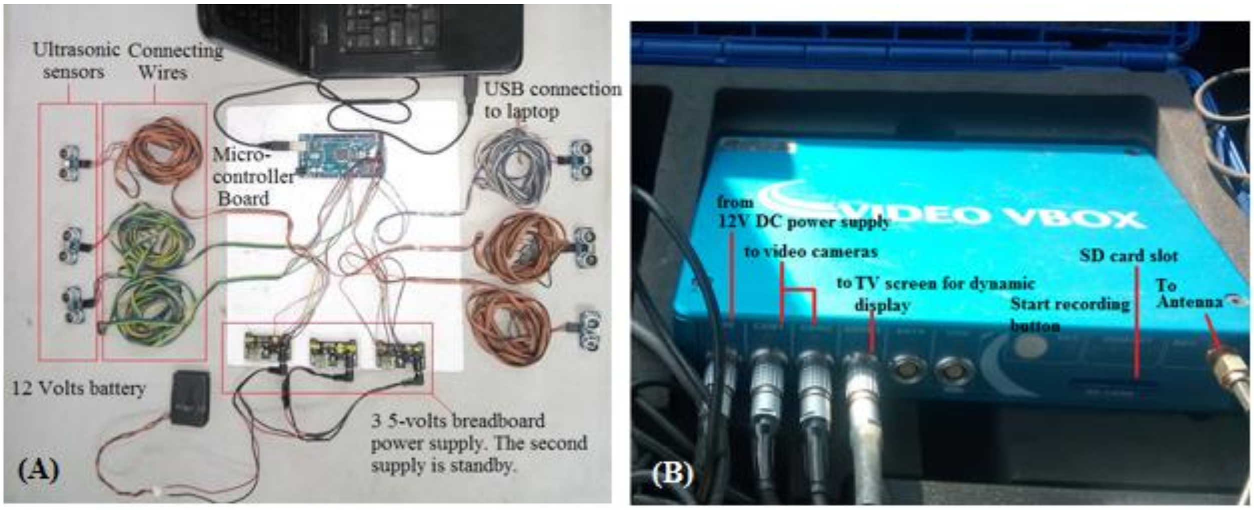

Fig. 3.5 Instruments used for analyzing lateral clearance and speed data (a) Sensor assembly setup; (b) Video V-box for measuring the speed of test vehicle.

3.3.2 Data extraction from instruments

Data extraction from both the instruments (sensor assembly and video V-box) involves file generation, synchronizing and refining the data.

3.3.2.1 File-generation

The vehicle data extraction from the instruments involves the creation of three files:

1. A file generated by a microcontroller (file A) saves readings of six sensors in the form of the distance of any obstruction in centimeters for each sensor along with a particular time stamp.
2. A second file generated by V-box (file B) saves speed of test vehicle with a time stamp.
3. A third file (file C) is generated manually by using video obtained from the V-box. The observer notes manually the time of interaction of interacting vehicle, an indicator whether the vehicle has been overtaken or overtaking the test vehicle, and its vehicle type (whether it is categorized as a hatchback car, sedan car, SUV, van, three-wheeler, bus, truck, two-wheeler or LCV). The timestamp readings of this file matches with the VBox speed-file, since both (video as well as speed file) are generated by the same instrument.

3.3.2.2 Synchronizing data of video V-box and sensor assembly

Video V-box and sensor-setup run independently and collect data at different starting times. Starting time-step of both the equipment needs to be matched with each other for synchronization. For this purpose, a physical obstruction is placed in front of any sensor, when the vehicle is stationary. Video V-box and sensor setup are started. As soon as vehicle attains a non-zero speed, the obstruction is removed from that sensor. Thus, the instance where a reading corresponding to physical obstruction for particular sensor ceases to exist in file A, and a non-zero speed reading begins for the video V-box (in files B and C); is the starting datum. With this synchronization, one gets the data of sensor-distances and speed (along with the time stamp) from GPS together. Table 3.1 describes this exercise. The reader can notice the detection of obstruction reading before point P in sensor-2. The other sensors are giving 'null' or 0 reading since their waves hit obstacles beyond 2.5 m. In this case, points P in file A and Q in file B are the matching points.

Table 3.1 Synchronization of data for V-box and sensor files

No.	**Sensor data readings (File A) (cm)**				**V-box readings (File B)**	
	Time-stamp (milliseconds)	Sensor-1	Sensor-2	Sensor-3	V-box time (sec)	Speed (km/h)
115	5139300	0	5	0	65.1	0
116	5139400	0	3	0	65.2	0
117	5139500	0	3	0	65.3	0
118	5139600	0	3	0	65.4	0
119	5139700	0	5	0	65.5	0
120	5139800	0	6	0	65.6	0
121	5139900	0	5	0	65.7	0
122	5140000	0	4	0	65.8	0
123	5140100	0	4	0	65.9	0
124	5140200	0	5	0	66.0	0
125	5140300	0	2	0	66.1	0
126	5140400 **P**	0	0	0	66.2 **Q**	0.841
127	5140500	0	0	0	66.3	1.012
128	5140600	0	0	0	66.4	1.232
129	5140700	0	0	0	66.5	1.413
130	5140800	0	0	0	66.6	1.58
131	5140900	0	0	0	66.7	1.703
132	5141000	0	0	0	66.8	1.901
133	5141100	0	0	0	66.9	2.17
134	5141200	0	0	0	67	2.364

3.3.2.3 Refining obtained data

The data obtained from sensors consist of several unwanted readings such as those reflected from the median, electric poles, trees and other street furniture. Most of readings are 'null' readings if vehicle is not interacting to any obstruction/vehicle within 2.5 m. The determination of vehicle interaction time in File 'C' helps to eliminate any unwanted data.

The three files A, B and C; are combined together by matching the time-stamp. The process of all data collection and creation of a master file is presented in Fig. 3.6.

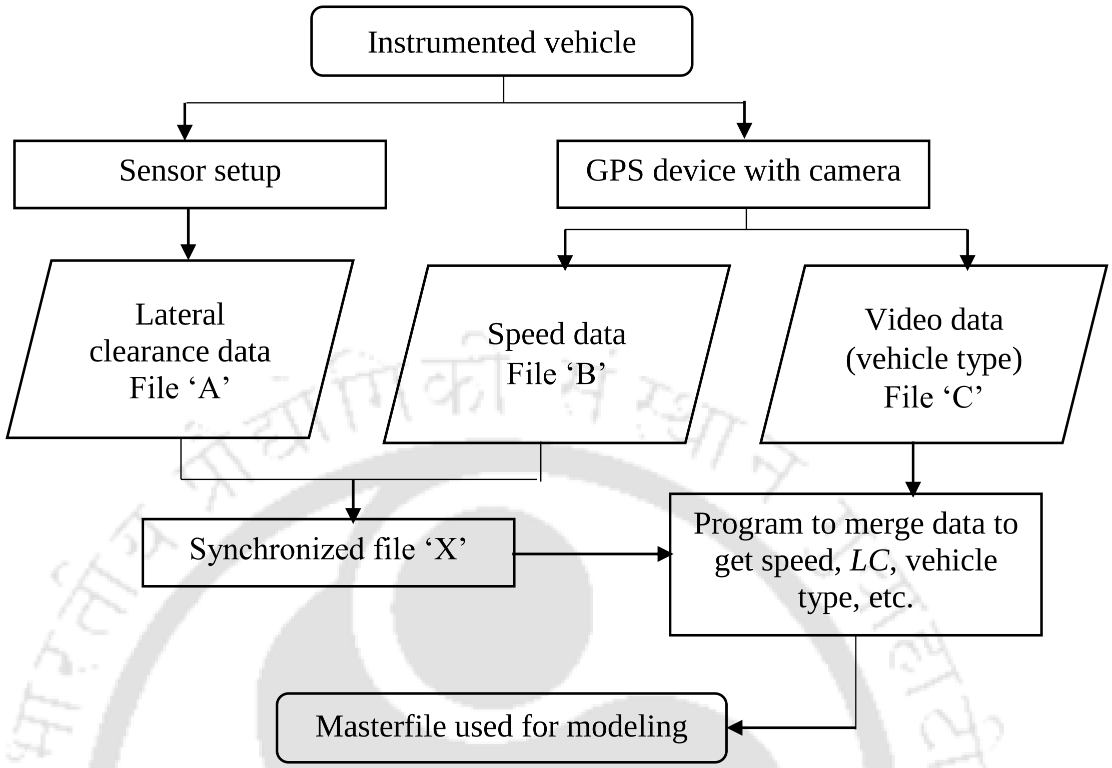

Fig. 3.6. Flowchart mentioning file handling in developing lateral clearance-speed relationship

In this way, at a particular speeds, one can calculate accurately the lateral distance maintained between vehicles at a particular speed of test vehicle. Speed of interacting vehicle (v_{IV}) can be found from speed of test vehicle (v_{TV}), inter-sensor distance (*D*) shown in Fig. 3.4 (a), and difference in detection time between these two sensors (Δt) by formula given in Equation 3.1. If interacting vehicle overtakes test vehicle, positive sign is used in Equation 3.1, else, negative sign is used.

$$v_{IV} = v_{TV} \pm \frac{\mathrm{D}}{\Delta t} \qquad \dots 3.1$$

3.3.3 Estimation of accuracy

The methodology developed is tested for its accuracy for determining (i) speed of test vehicle, (ii) Speed of interacting vehicle, and (iii) Measurement of lateral distance. The least count of ultrasonic sensors to measure inter-vehicular distances is 1 cm. Least count of speed as measured by GPS device is 0.001 km/h.

There is 0.05% error in measuring distance by the GPS device Video V-box, as obtained from the technical specifications of Racelogic, the manufacturer of video V-box used in this experiment (Source: User manual of Video V-Box). The error is also reflected in the speed measurement of the test vehicle. Error in measurement of the speed of interacting vehicle depends on the calculation of relative speed, which depends on the distance between two sensors (Equation 3.1). If the distance between two sensors increases, accuracy increases. To determine the accuracy, a test vehicle was made to pass beside several parked vehicles to predict their speeds. An ideal instrument setup should predict the speed of other vehicles as zero. However, a deviation was observed. Error increases as relative speed between vehicles increases. The data in Fig. 3.7 shows the trend of error to relative speeds of 40 km/hr. This error is due to the relative lower frequency of sensors (10 Hz) as compared to higher relative speeds. Error varies with the relative speed of vehicles, and not with individual speeds of vehicles.

Accuracy of measurement of lateral distances is conducted in controlled conditions in laboratory, and a comparison between actual distance (measured by laser distance meter) and distance measured by sensors is compared. The error is primarily due to least count (1 cm) of the sensors, amounting to a maximum of 0.5 cm error. The minimum inter-vehicular distances measured by the sensors is 50 cm, thus maximum error to measure the distance is 1%.

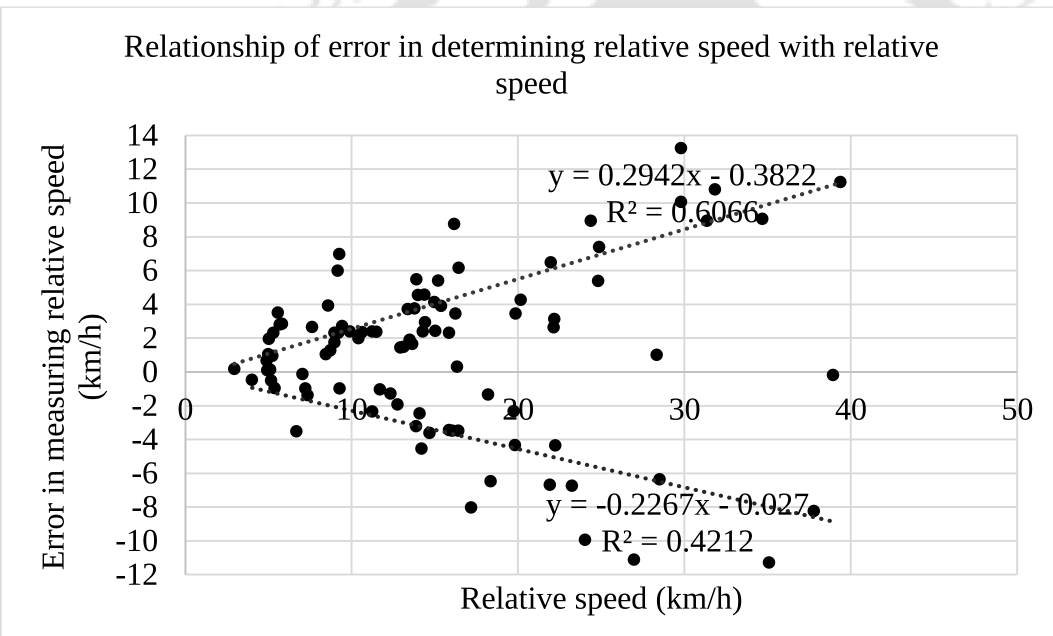

Fig. 3.7 Relationship of error in relative speed between two interacting vehicles, with actual obtained relative speed.

From Fig. 3.7, it is observed that at 10 km/h relative speeds, the average error in estimating speed of interacting vehicle is about 2 km/h. In the field, it is observed that maximum relative speeds achieved are not beyond 40 km/h, and 85th percentile relative speed is 32 km/h, which correspond to errors of 6 km/h and 8 km/h, respectively. This error does not exceed more than 20%. This error is positive as well as negative. Since the error in determining speed of test vehicle is negligible, the error in determining average speed is halved.

3.3.4 Data collection locations for lateral interaction study

To study gap-maintaining behavior of drivers in urban traffic stream, the methodology developed is applied to develop various instrumented vehicles used in different cities, and data collection is conducted to obtain speeds of interacting vehicles as well as their lateral clearance maintained. The driver behavior may vary significantly from location to location across different regions. Therefore, to capture this variation for effectively representing driver behavior, six different cities in India are selected. They include Delhi, Mumbai, Bangalore, Pune, Kolkata and Guwahati, which are million-plus population cities distributed across different regions in India. Instrumented vehicles need to be driven as part of the traffic stream. In the current study, the focus is on lateral interactions of vehicles on mid-block section, hence data at intersections, or locations with significant interruptions due to pedestrians or encroachment are eliminated during analysis.

Fig. 3.8 provides photographs of some instrumented vehicles used in field data collection for lateral clearance analysis.

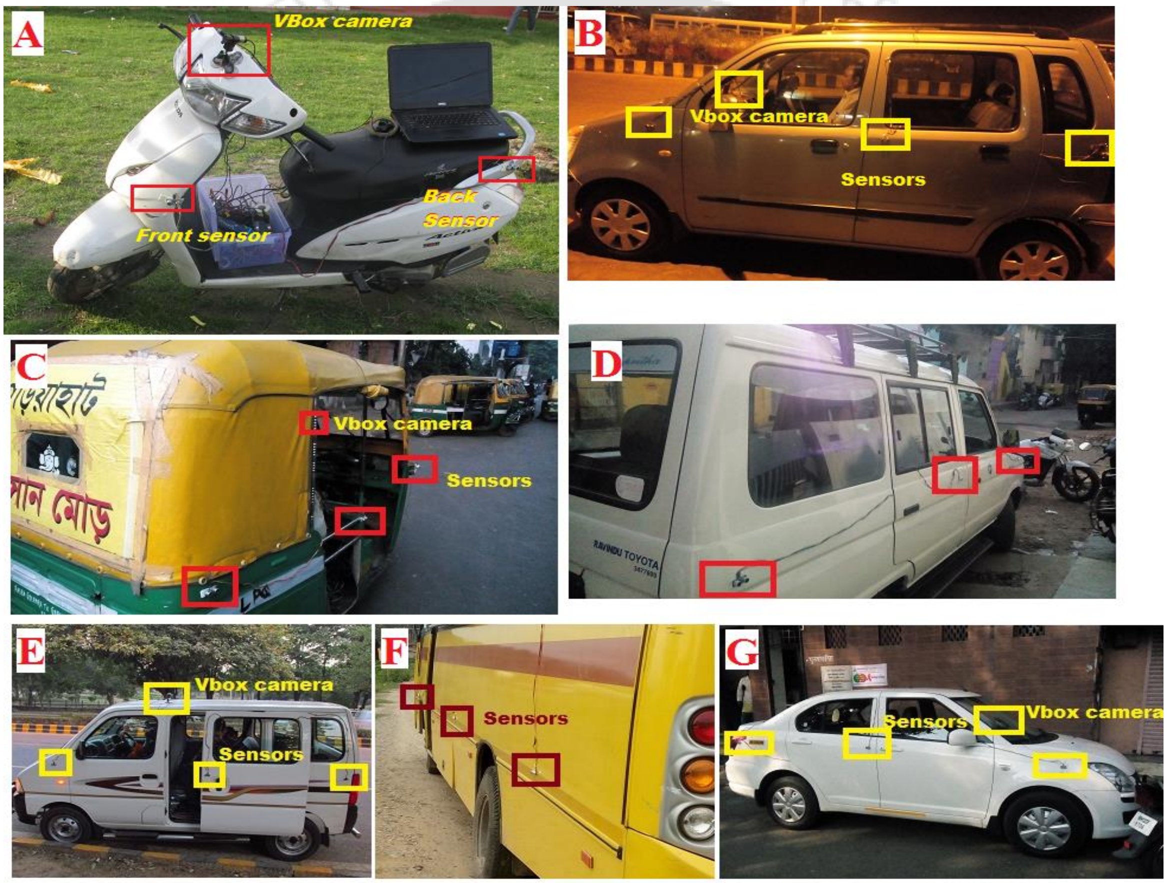

Fig. 3.8 Photographs of some instrumented vehicles used in analysis of lateral clearance data- A: Two-wheeler, B: Hatchback car, C: Three-wheeler, D: SUV, E: Van, F: Bus, and G: Sedan car.

Table 3.2 provides a list of road stretches covered for lateral distance analysis along with vehicles used. Travel route of instrumented vehicles in different cities is finalized such that roads of different widths should be covered. All the selected road surfaces were in good condition. Tick mark indicates that particular instrumented vehicle was used in the city.

Table 3.2 Details of vehicles and locations used for collecting lateral distance analysis data.

S. no	City	Road stretches	Test Vehicles						
			Hatch back	Sedan	SUV	Van	3W	2W	Bus
1	Delhi	Outer ring road, Inner ring road, Nelson Mandela road, Africa Ave, GT road, Mehrauli-Badarpur road, Mehrauli-Gurgaon road.	✓	✓	✓	✓	✓		
2	Guwahati	Guwahati bypass, GS road.	✓	✓	✓	✓	✓	✓	✓
3	Kolkata	EM bypass, VIP road, CIT road, Gariahat road, DPS road (Tollygunge), Manicktala Vivekananda Road, Chittaranjan Ave, Rash Behari Ave.	✓	✓	✓		✓	✓	
4	Bengaluru	Mysore Road, Bellary Road, CV Raman road, West chord road, Outer Ring Road, Hosur Road, NICE road, TCM Royan road (Majestic), Racecourse road.	✓	✓	✓		✓	✓	
5	Pune	Bibwewadi Road, Sinhagad Road, Ambedkar-Wellesley road, Old Bombay-Poona Highway, Pune bypass, Ganeshkhind road, Tilak road, Karwe road.	✓	✓	✓		✓	✓	
6	Mumbai	Link road, Western Express Highway, Eastern express highway, Pedder Road, Marine Drive, Bandra Worli Sea Link, Jogeshwari-Vikhroli link road.	✓	✓	✓		✓	✓	

The common route traversed by instrumented vehicles in different cities is shown in Fig. 3.9..

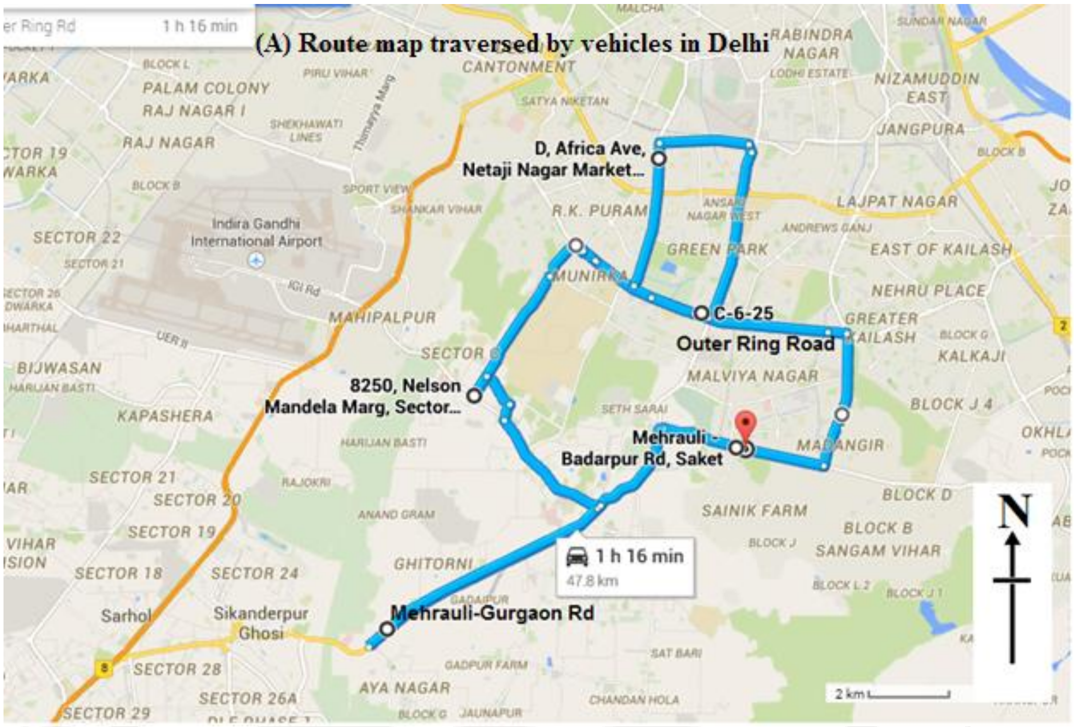

Fig. 3.9 (a) Route travelled by instrumented vehicles in Delhi

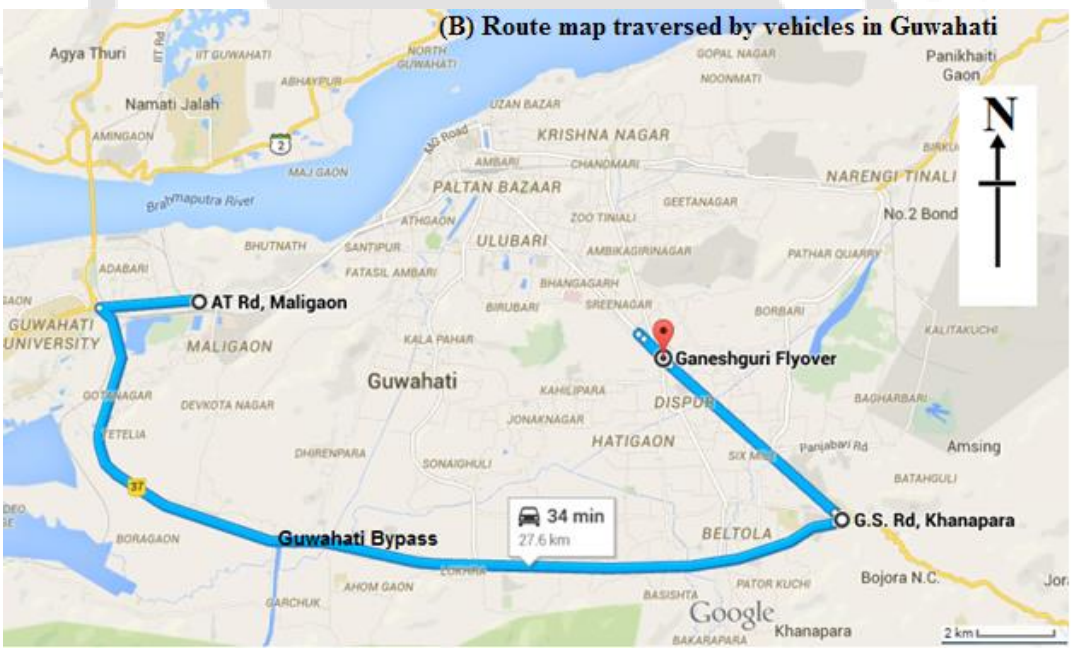

Fig. 3.9 (b) Route travelled by instrumented vehicles in Guwahati

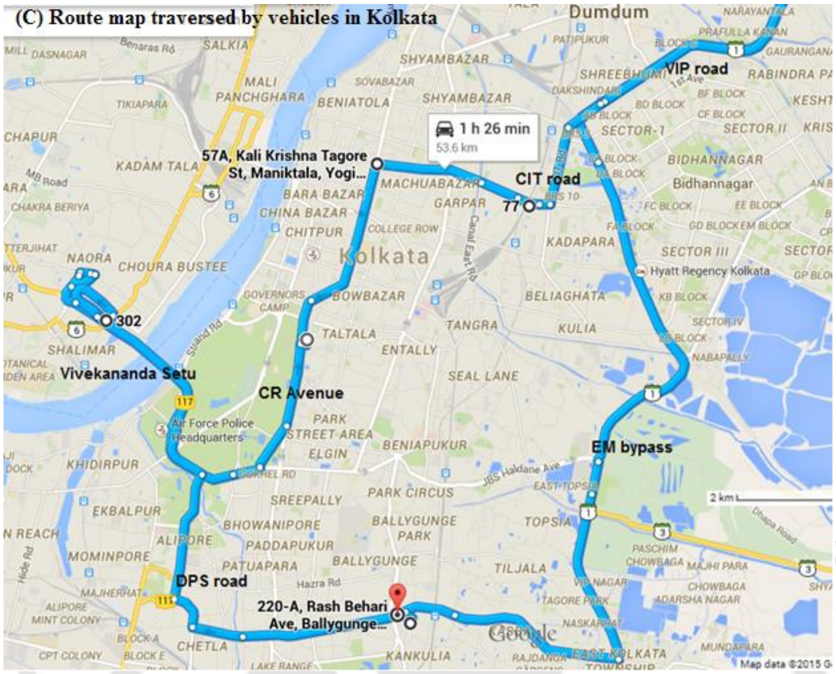

Fig. 3.9 (c) Route travelled by instrumented vehicles in Kolkata

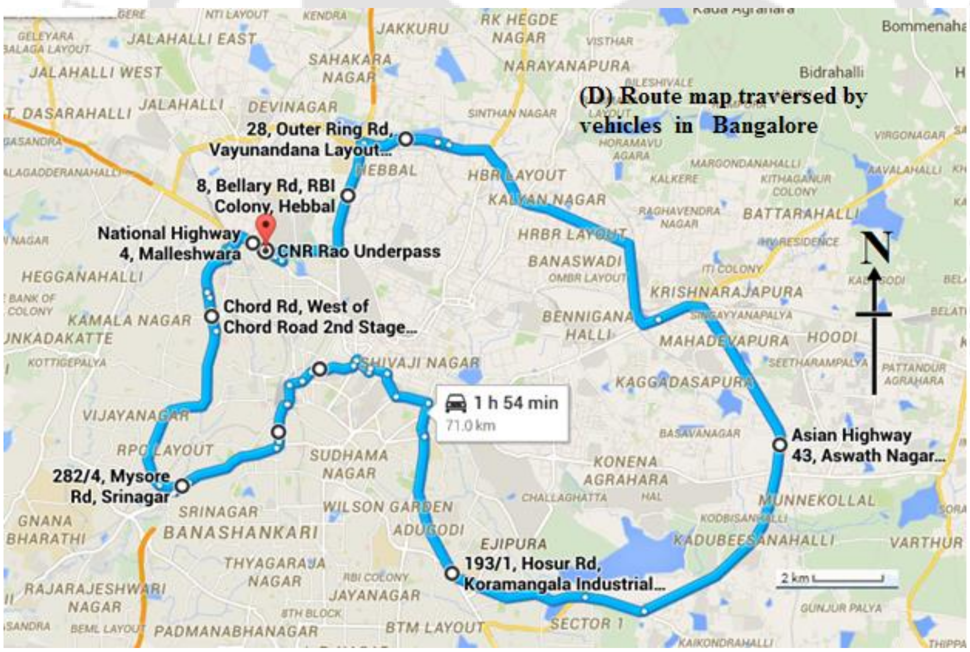

Fig. 3.9 (d) Route travelled by instrumented vehicles in Bengaluru

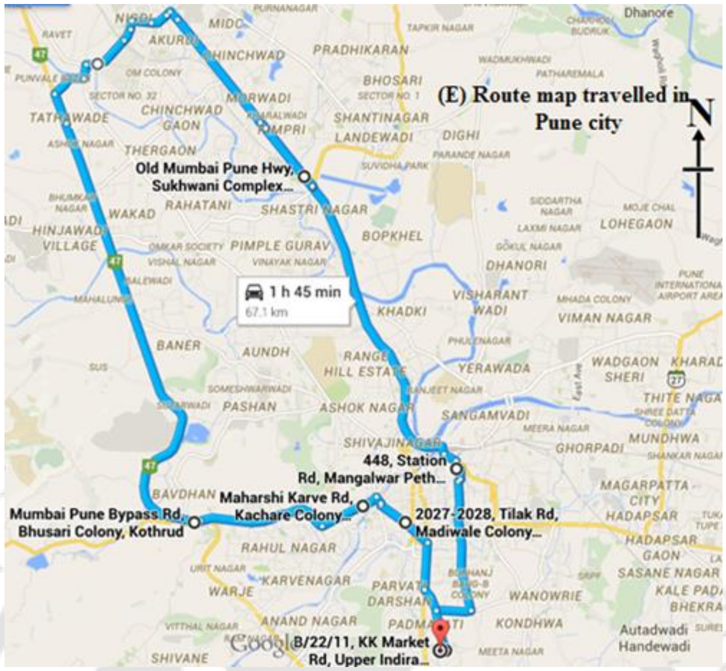

Fig. 3.9 (e) Route travelled by instrumented vehicles in Pune

Fig. 3.9 (f) Route travelled by instrumented vehicles in Mumbai

3.4 Methodology adopted to study longitudinal vehicle interactions

Most vehicle interactions in heterogeneous streams are dominated by vehicle- following behaviors in a staggered pattern. Due to lack of lane discipline, a general staggering behavior between leading and following vehicle (LV and FV) is observed in the traffic stream. If a vehicle closes-in a slow-moving leading vehicle and does not get an opportunity to pass for a long time due to traffic conditions, it gets stabilized behind the leading vehicle, maintaining a certain longitudinal distance headway with it, at certain speeds and centerline separation (*CS* – lateral distance between centers of LV and FV). The relative speed between LV and FV in this case will be minimum.

Longitudinal distance headway of a stable vehicle-following case may depend upon *CS*, type of leader and follower vehicles, driver behavior, and their respective speeds. To study this variation, camera-calibration technique is used (refer Section 3.2.3).

This section describes this technique to capture field coordinates from recorded traffic video, evaluates its accuracy, and presents the details of selected traffic streams for data collection.

3.4.1 Camera-calibration technique for data extraction

Camera-calibration technique used for collecting traffic data from video recording focusses upon a low-distortion stationary image camera and a monocular traffic image sequence. Vanishing point technique is used for calibration, and width of a fixed rectangle needs to be measured in field to accurately determine coordinates in the real world. Road needs to be straight without any horizontal or vertical curves. A set of equations that computes camera parameters from image coordinates of calibration pattern and width of the road is used from literature (Fung *et al.*, 2003).

The relationship between the image coordinates (x and y) of video recorded by camera, and the real-world coordinates (X and Y) of a plane surface in field is defined in terms of pan angle p, tilt angle t, swing angle s, focal length f, and camera distance l. Various quantities are described in Fig. 3.10. The error rate of data extraction does not depend on any of the above parameters in this methodology and is thus used for analysis.

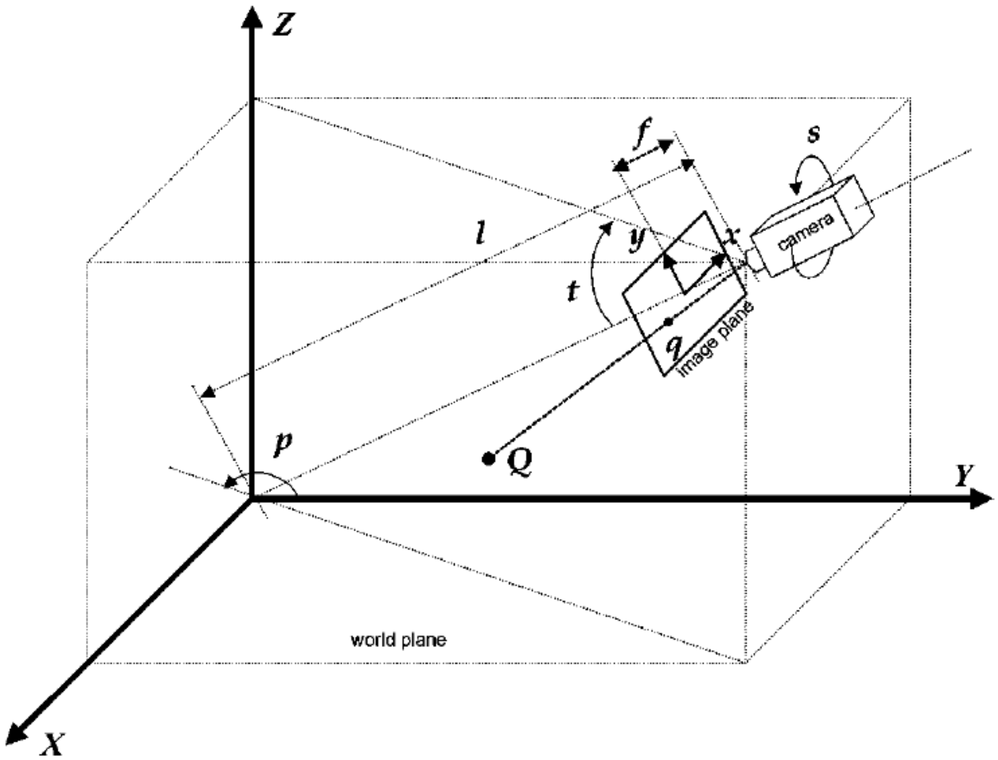

Fig. 3.10 Employed camera calibration model adopted from Fung *et al.* (2003).

Four end points (preferably lying on edges of a road) are selected to form a calibration pattern of rectangle *ABCD*, as described in Fig. 3.11.

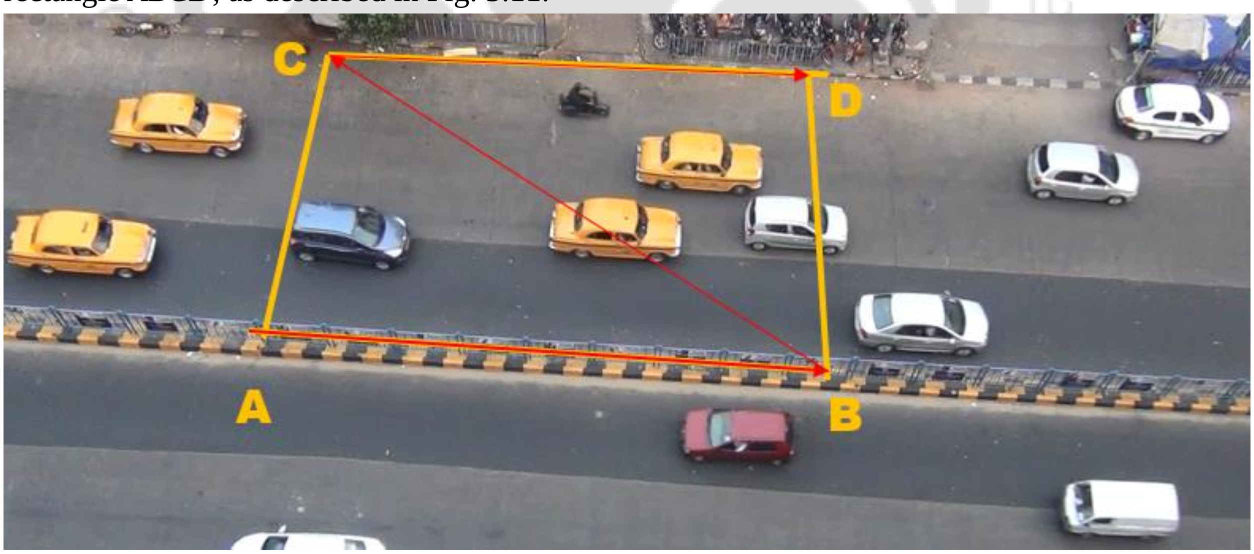

Fig. 3.11 Marking pattern used in converting image coordinates to real world coordinates.

The world coordinates of *A*, *B*, *C*, and *D* are (X_A,Y_A,0), (X_B,Y_B,0), (X_C ,Y_C,0), (X_D ,Y_D,0). Four end points marked on the ground representing a rectangle in the field is presented in Fig. 3.11. The width of this rectangle is *w* in the world coordinate system (Real world width BD as shown in Fig. 3.11). As per Fung *et al.* for any point *Q* on the road surface,
X_Q and Y_Q is calculated as

$$X_Q = \frac{\left[l \sin p\,(x_q \sin s + y_q \cos s) \;+ l \sin t \cos p\;\,(x_q \cos s - y_q \sin s)\right]}{x_q \cos t \sin s + \;y_q \cos t \cos s + f \sin t}$$

And

$$Y_Q = \frac{\left[-l \cos p\,(x_q \sin s + y_q \cos s) \;+ l \sin p \cos t\;\,(x_q \cos s - y_q \sin s)\right]}{x_q \cos t \sin s + \;y_q \cos t \cos s + f \sin t}$$

$$l = \frac{w(f \sin t + \;x_A \cos t \sin s + \;y_A \cos t \cos s)\,(f \sin t \;+ x_C \cos t \sin s + \;y_C \cos t \cos s\,)}{\begin{bmatrix} -(f \sin t + \;x_A \cos t \sin s + y_A \cos t \cos s) \\ (x_C \cos p \sin s - x_C \sin p \sin t \cos s + \;y_C \cos p \cos s + \;y_C \sin p \sin t \sin s) \\ + (f \sin t + \;x_C \cos t \sin s + y_C \cos t \cos s) \\ (x_A \cos p \sin s - x_A \sin p \sin t \cos s + \;y_A \cos p \cos s + \;y_A \sin p \sin t \sin s) \end{bmatrix}}$$

$$f = \frac{\chi_{BD} \cos p \cos t}{\begin{pmatrix} \beta_{BD} \sin p \cos s - \beta_{BD} \cos p \sin t \sin s \\ + \alpha_{BD} \sin p \sin s + \alpha_{BD} \cos p \sin t \cos s \end{pmatrix}},$$

$$\tan p = \frac{\sin t\,[(\beta_{BD}\chi_{AC} - \;\beta_{AC}\chi_{BD}) \sin s \;+ (\alpha_{AC}\chi_{BD} - \alpha_{BD}\chi_{AC}) \cos s]}{[(\alpha_{BD}\chi_{AC} - \;\alpha_{AC}\chi_{BD}) \sin s \;+ (\beta_{BD}\chi_{AC} - \beta_{AC}\chi_{BD}) \cos s]}$$

$$\sin t = -\left\{\frac{\begin{pmatrix} [(\alpha_{BD}\chi_{AC} - \;\alpha_{AC}\chi_{BD}) \sin s \;+ (\beta_{BD}\chi_{AC} - \beta_{AC}\chi_{BD}) \cos s] \\ [(\alpha_{CD}\chi_{AB} - \;\alpha_{AB}\chi_{CD}) \sin s \;+ (\beta_{CD}\chi_{AB} - \beta_{AB}\chi_{CD}) \cos s] \end{pmatrix}}{\begin{pmatrix} [(\alpha_{CD}\chi_{AB} - \;\alpha_{AB}\chi_{CD}) \cos s \;+ (\beta_{AB}\chi_{CD} - \beta_{CD}\chi_{AB}) \sin s] \\ [(\beta_{BD}\chi_{AC} - \;\beta_{AC}\chi_{BD}) \sin s \;+ (\alpha_{AC}\chi_{BD} - \alpha_{BD}\chi_{AC}) \cos s] \end{pmatrix}}\right\}^{1/2}$$

$$\tan s = \frac{\begin{pmatrix} -\beta_{AB}\beta_{Ac}\chi_{BD}\alpha_{CD} + \beta_{AC}\beta_{AB}\chi_{CD}\alpha_{BD} \\ +\beta_{BD}\beta_{CD}\chi_{AB}\alpha_{AC} - \beta_{AB}\beta_{BD}\chi_{CD}\alpha_{AC} \\ -\beta_{BD}\beta_{CD}\chi_{AC}\alpha_{AB} - \beta_{CD}\beta_{Ac}\chi_{AB}\alpha_{BD} \\ +\beta_{AB}\beta_{BD}\chi_{AC}\alpha_{CD} + \beta_{CD}\beta_{Ac}\chi_{BD}\alpha_{AC} \end{pmatrix}}{\begin{pmatrix} -\beta_{AB}\alpha_{CD}\chi_{AC}\alpha_{BD} + \beta_{AC}\alpha_{CD}\chi_{AB}\alpha_{BD} \\ -\beta_{AC}\alpha_{BD}\chi_{CD}\alpha_{AB} - \beta_{CD}\alpha_{AB}\chi_{BD}\alpha_{AC} \\ -\beta_{BD}\alpha_{CD}\chi_{AB}\alpha_{AC} + \beta_{AB}\alpha_{AC}\chi_{BD}\alpha_{CD} \\ +\alpha_{AB}\beta_{BD}\chi_{CD}\alpha_{AC} + \alpha_{BD}\beta_{CD}\chi_{AC}\alpha_{AB} \end{pmatrix}},$$

Where,

$$\alpha_{AB} = x_B - x_A,\ \ \beta_{AB} = y_B - y_A,\ \ \chi_{AB} = x_A y_B - x_B y_A, \qquad \ldots 3.2$$

Similarly, α_{AC}, α_{BD}, etc., can be calculated.

By using these formulae, one can transfer image coordinates (x_q and y_q) into real world coordinates (X_Q and Y_Q) and obtain vehicle positions.

3.4.2 Development of data extraction software for extracting longitudinal interactions

Data extraction software is developed in MATLAB programming language. It is used for noting the vehicle coordinates as they travel in the traffic stream, at a particular time-frame. The image coordinates from a video are extracted and converted into real coordinates by using a MATLAB code. Two output files are generated- (i) vehicle details such as type, size (length, width), and (ii) vehicle coordinates at different time frames. The user inputs the video frame rate in the MATLAB code in addition to the video path of traffic video file recorded in .avi format. After running the code, user can see the first image of recorded traffic video in a window, with four buttons. A snapshot is shown in Fig. 3.12 (a). The four buttons are-

1. ‘Load image’ loads the video from requisite address path on MATLAB software so it can read video details;
2. ‘Run’ button executes the playing function for video.
3. ‘Pause’ button pauses the video and converts current frame in an image and opens it in a new window for marking image coordinates.
4. ‘Play’ button resumes the playing of video after data extraction.

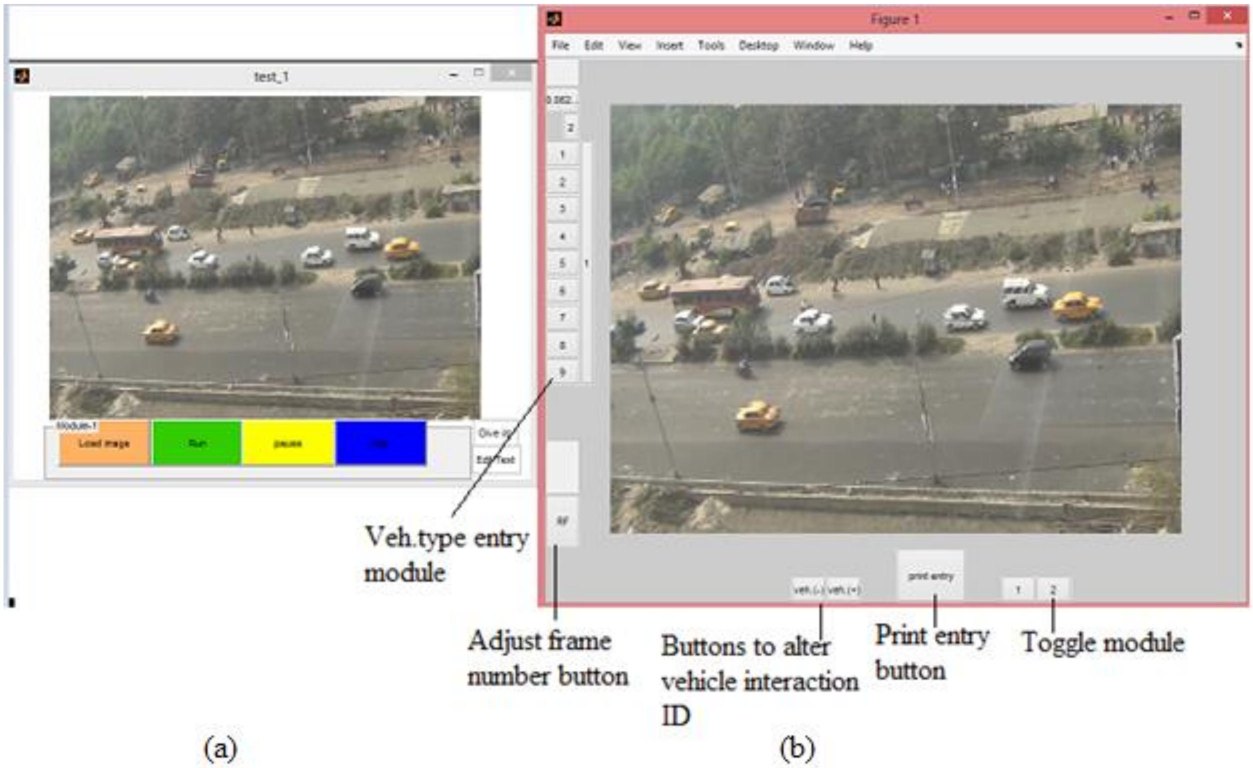

Fig. 3.12 Snapshot of developed software in MATLAB for extracting vehicle trajectory data.

A user needs to click on ‘Play’ button. After noticing any vehicle interaction in the video, he/she needs to pause the video so that he/she can mark the vehicle coordinates. A new window containing a larger image of the current frame (Fig. 3.12 (b)) pops up after pressing the pause button. Clicking on any part within this image records the pixel coordinates of mouse position in a text file. Apart from the image, following modules are also visible-

- Toggle button module- Two files are to be generated- (i) File ‘P’ keeps track of vehicle properties (size, type) and (ii) File ‘Q’ notes their trajectory coordinates at different time intervals. Thus, to keep track of which data to be entered where, a module is created with buttons 1 and 2 in the same window. User can toggle between the files where he/she desire the output.
- Vehicle type details module- vehicle type details (numeric only) can be entered using software in file P, by means of a vehicle code number.
- Print entry button- This button is used to record frame number and vehicle pair interaction number (VPIN) (for file P); or record and increment the VPIN (for file Q). A user needs to press this button after recording every interaction, close the pop-up window and play the video again.
- Change vehicle ID module- It consists of ‘+’ and ‘-’ buttons to increment or decrement VPIN. This module is useful in dense traffic, when, at a given time, there are more than one interacting pairs of vehicles in section.

- Adjust frame number buttons- A user can manually enter the required number of frames by which he/she wants to rewind video from the current frame during play. The default value is set as 10 frames. It is useful in dense traffic, or it is also useful when the user wants interaction at fixed time intervals.

To note the vehicle size, user clicks on three extreme visible corners of a vehicle in popup window. Software stores three coordinates, and vehicle length, width and coordinates of fourth corner are calculated. To note trajectory, user needs to click on one particular corner of each of the vehicles at different frames, by repeatedly playing the video.

The data need to be entered in a particular sequence. Fig. 3.13 provides the algorithm for operating the developed software.

3.4.3 Prerequisites for video-recording of traffic stream

The prerequisites for video-recording of traffic stream are-

1. There should not be an overlapping of the image of LV onto the image of FV. Since the study is to be made for longitudinal vehicles' interactions, a data extractor should be able to clearly see the coordinates of corners of FV and LV. Therefore, a top-side view taken from a higher vantage point, from either edge of the road is preferred. A sample screen-shot of such a video is shown in Fig. 3.11.
2. The road should not have any horizontal or vertical curve (A constant vertical gradient is permitted since road surface will still lie on a plane).
3. Coordinates of corners of a perfect rectangle (which lies on a perfect plane) need to be determined on the field. For this purpose, trap length and sides of the road are determined and marked in the field. (as in Fig. 3.11)

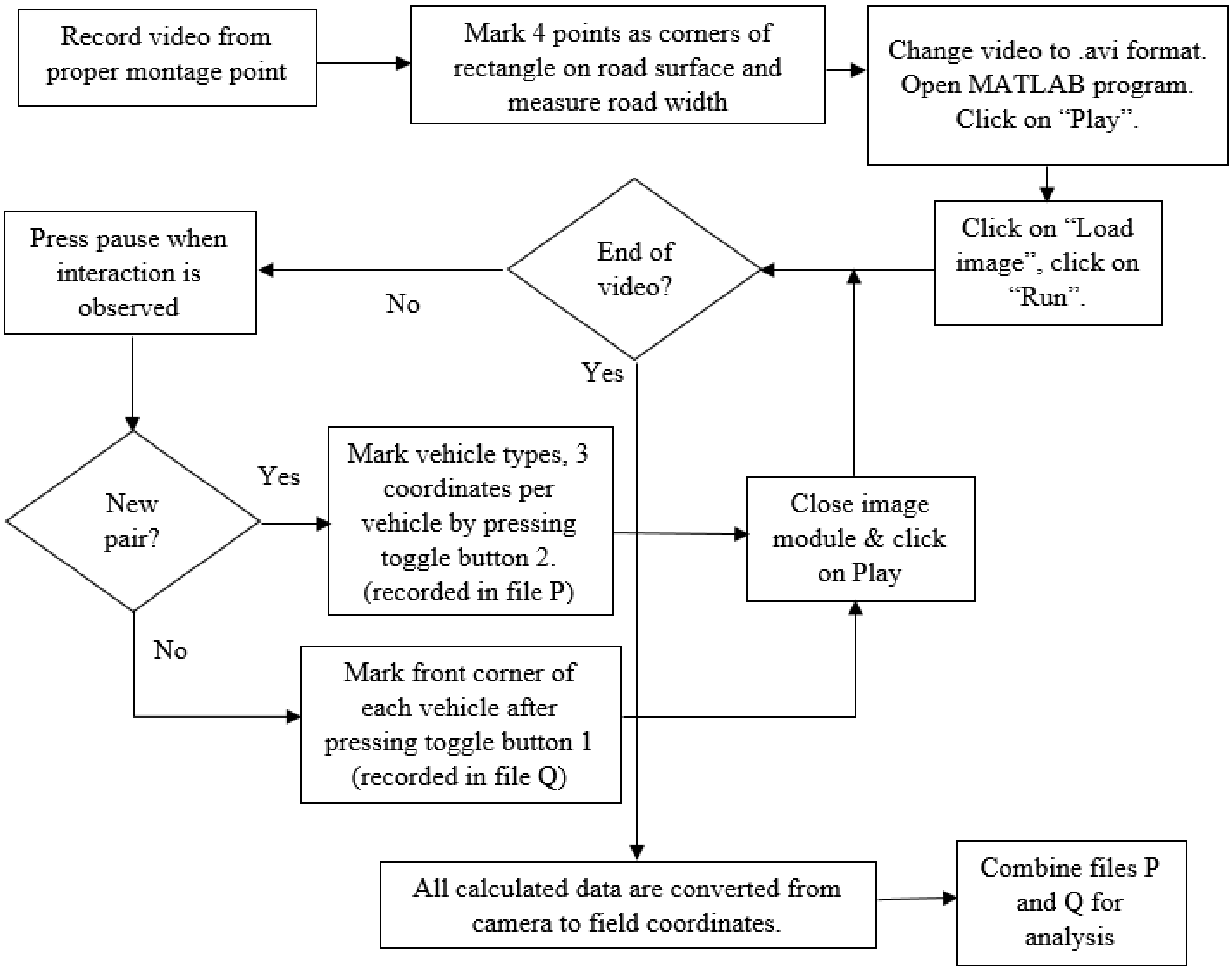

Fig. 3.13 Algorithm for operating developed software for data extraction from recorded videos.

3.4.4 Checking accuracy of data extraction

The developed methodology is checked for accuracy of extracted data, which may be affected by a possible human error in making a mouse click at an accurate location on the image. This human error aggravates to a larger error in marking real-world position if the zooming of the camera is less (i.e., higher section trap length).

3.4.4.1 Error evaluation of a particular mouse click

Data accuracy depends upon how accurately an extractor clicks on the exact corner of the vehicle. This error is due to human perception capability, and may vary from person to person. An extractor may make an erroneous mouse click with a fixed standard deviation radius on the screen, represented in the form of pixels. This error is independent of traffic section or video. To evaluate this error, a fixed width can be repeatedly measured by the extractor, and error with actual width may be compared. An exercise is carried out in this aspect, and 100 cars belonging to only a particular model of a taxi (known width) are marked for their widths by clicking on two extreme points. This exercise is carried by nine different enumerators covering different ages, different genders and different educational qualifications. Since width is calculated by two mouse clicks, variance of error of one mouse click will be halved, and standard deviation will be divided by $\sqrt{2}$. It is observed that there is an average standard deviation of error equal to 6 pixels for one mouse click. These 6 pixels on screen may correspond to different lengths in the field, due to different zooming and capturing of trap lengths. Table 3.3 mentions the average error calculation for each site.

Table 3.3 Average standard deviation of error in recording position in field

City	Location	Recorded road width in video (m)	Standard deviation of error in field; from one mouse click in m
Bengaluru	Mekhiri circle	23.5	0.176
Bengaluru	Rajajinagar	13.0	0.121
Guwahati	Guwahati bypass	7.0	0.057
Kolkata	EM bypass near Ruby	17.5	0.169
Kolkata	Ballygunge	23.5	0.136
Kolkata	Ultadanga (CIT road)	13.0	0.134
Mumbai	Western Express Highway, Jogeshwari	38.5	0.246
Mumbai	Link road, Malad	31.5	0.273
Mumbai	Jogeshwari Vikhroli Link Road	23.5	0.094
Pune	Sinhagad road	17.5	0.160
Pune	Shivajinagar	10.5	0.078
Pune	Old Bombay Pune road	13.0	0.075
Pune	Pune bypass	13.0	0.089

Details of these locations are discussed in the next subsection (3.4.5). From Table 3.3, it is observed that the high range in deviation of error in the field from one mouse click is due to higher trap-widths of road locations. The average longitudinal gaps maintained by vehicles are in the range of 5-30 meters. The error calculated from this table obtains 5-20% random error in calculating the longitudinal gap. The error is positive as well as negative.

3.4.4.2 Accuracy of software for calculating speed

Error in the evaluation of the precise position of a point (Table 3.3) on the field results in an error in measuring speed. To obtain this error, a vehicle attached with high accuracy GPS data logger (Video V-box, make Racelogic, with an accuracy of 0.05 km/h) was driven in the same Section where a video of traffic stream is taken. The speed of vehicle at the points where a vehicle crosses the recorded sections is extracted from V-box. Same vehicle positions are also marked using developed softwares, at every three video frames (frequency of video V-box speed data is 10 Hz, and the frame rate is 30 fps, thus recorded frequency is three frames). The speed of vehicle is calculated using both methods. It is observed that speed of V-box is similar with calculated speed. There is some mismatch at higher speed levels. A simple t-test gives result as similar at 5% significance level (P (T<=t) one sided =

0.472, t critical = 1.65. Root mean square error is 8.79, mean percent error is 0.49% for sample size 106.

3.4.5 Data collection details

Video recording for longitudinal gap analysis is carried out at a total of 13 locations across 5 cities, namely Guwahati, Kolkata, Pune, Mumbai and Bengaluru as per details in Table 3.4. Mid-block urban arterial sections of various road widths are chosen on the basis that there should not be any major intersection obstructing traffic movement within 500 m from video recording area. The sites were selected as per the prerequisites of camera-calibration technique described in Fung *et al.* (2003). The video-recording is conducted on the same routes taken by the test vehicle for data-collection of lateral interactions, so that the traffic stream behavior recorded in both cases would be similar. The effect of external factors such as pavement conditions, the weather was not affecting traffic flow.

The traffic videos recorded in Table 3.4 are played, and interacting vehicles are searched. A pair of LV-FV is considered as interacting, if there is some lateral overlapping between them, and the time headway maintained between them is less than 4 seconds. As per the details provided in the flowchart in Fig. 3.13, data are extracted from all sites and files are generated. Obtained master-file after combining data from all the locations consists of (i) Vehicle positions i.e., x and y coordinate of front center of LV and FV, (ii) speeds of LV and FV, (iii) their vehicle types, (iv) Longitudinal gap and centreline separation between LV and FV. These parameters are calculated and compared for modelling purpose. The results are shown in the next chapter.

Table 3.4 Details of video recording locations for collection of data for longitudinal analysis.

S no .	**City**	**Road**	**Location**	**Co-ordinates**	**Date**	**Time**	**Width of road (m)**	**Trap length**	**Vantage point**
1	Guwahati	Guwahati bypass	Games Village	26.110969, 91.775307	16-Jan-15	10:30-13:30	7.6	20 m	Big tripod
2	Kolkata	Gariahat main road	Gariahat	22.523450, 88.365460	17-Nov-14	15:30-18:30	12.1	25 m	High-rise building
		EM bypass	Ruby hospital	22.516173, 88.401297	18-Nov-14	10:00-13:00	7.8	35 m	High-rise building
		CIT road	Ultadanga Manicktala ESI hospital	22.588642, 88.392702	20-Nov-14	16:00-18:30	10	20 m	roadside building
3	Bengaluru	West Chord Road	Magadi underpass	12.975530, 77.548691	29-Nov-14	10:00-12:30	7.6	20 m	Above underpass
		Bellary road	Mekhiri circle	13.013816, 77.583933	30-Nov-14	16:30-19:30	11.2	30 m	Above Underpass
4	Pune	Sinhagad road	Nilayam bridge	18.500427, 73.849189	04-Dec-14	11:00-13:00	10.4	35 m	High-rise building
		Ganeshkhind road	Sancheti hospital underpass	18.529474, 73.852457	04-Dec-14	14:00-16:00	9	45 m	Above Underpass
		Pune bypass	Sus-pashan exit	18.544651, 73.774851	05-Dec-14	11:00-13:30	11.2	60 m	At top of deep cutting
		Old Bombay-Poona Highway	PCMC corporation	18.627916, 73.804295	05-Dec-14	16:30-19:30	7.8	50 m	Above Underpass
5	Mumbai	Western Express Highway	Ismail Yusuf College (Jogeshwari East)	19.132249, 72.855302	07-Jul-14	10:00-11:30	17.5	45 m	High-rise building
		Jogeshwari Vikhroli Link road	Powai garden	19.122868, 72.898468	14-Jul-14	15:30-16:30	10.8	20 m	Foot over-bridge
		Link road	Saidham complex (Malad West)	19.204389, 72.834261	08-Jul-14	18:30-20:00	14	40 m	High-rise building

3.4.6 Data extraction for multiple-vehicle interactions

In dense traffic streams, it is observed that more than two vehicles may interact together. In other words, a FV has stabilized behind following two LV's simultaneously, and it is maintaining minimum relative speed with them. This illustration is shown in Fig. 3.14 for different cities.

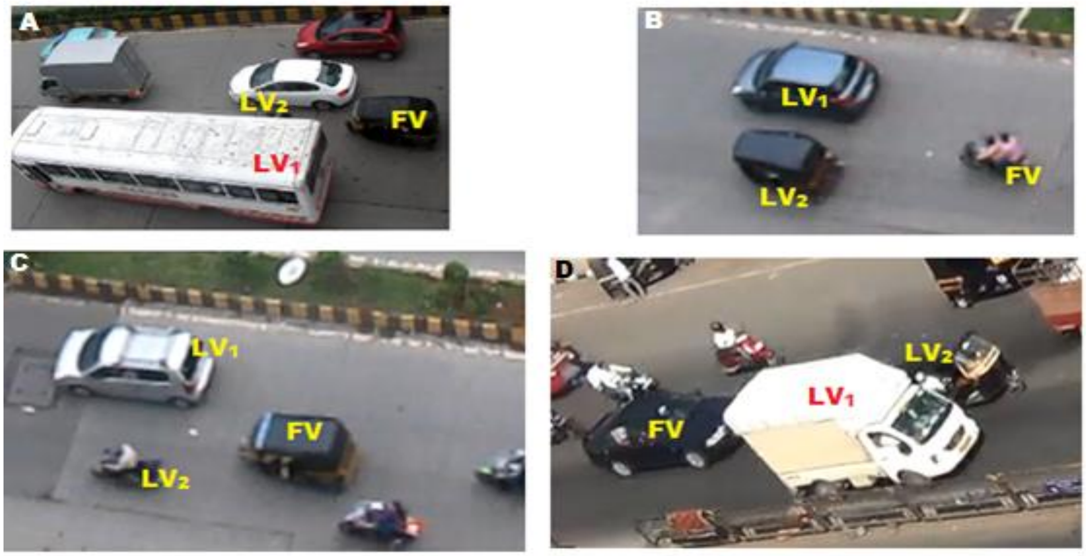

Fig. 3.14 Snapshot of two or more vehicles influencing a single vehicle observed in field

To model this phenomenon, there needs an assessment as to whether the behavior is governed by combined effect of individual LV's, or there is any compromise on safety. For this purpose, field data are extracted in a similar manner, using the same program developed in MATLAB, but two leading vehicles are considered instead of one. Data are collected for sample 100 'triplets' of vehicles (LV_1-LV_2-FV) each in the sections of Jogeshwari-Vikhroli Link road, Linking road (Mumbai), Bellary road (Bengaluru), Sinhgad road (Pune) and EM Bypass (Kolkata), mentioned in Table 3.4. The program records vehicle types, speeds, lateral and longitudinal gaps between each interacting pair. The data are analyzed and results are mentioned in the next chapter.

3.5 Data collection of overtaking decision-making criteria

In heterogeneous traffic, when the driver of a vehicle approaches a slow-moving LV ahead of it, he/she may make a decision to overtake, based on various parameters and overall traffic situation ahead of him/her. The parameters influencing his/her decision to overtake may depend upon the lateral and longitudinal distance to LV, relative and average speeds of LV and FV, and the traffic situation ahead of LV. If the driver decides to follow, the FV will stabilize behind LV and will travel at similar speed. However, if the driver decides to overtake, the FV may accelerate or decelerate and at the same time veer to overtake the LV. The exact decision of driver is latent, and it is assumed that when FV makes a lateral shift with respect to the position of LV, the driver of FV has decided to overtake LV. Fig. 3.15 shows this veering maneuver. To study factors affecting the decision to overtake, traffic data from six sections, namely, Jogeshwari-Vikhroli Link road and

Linking road (Mumbai), Bellary road (Bengaluru), Sinhgad road (Pune); and EM Bypass and Ballygunge (Kolkata) (described in Table 3.4) is used for this purpose.

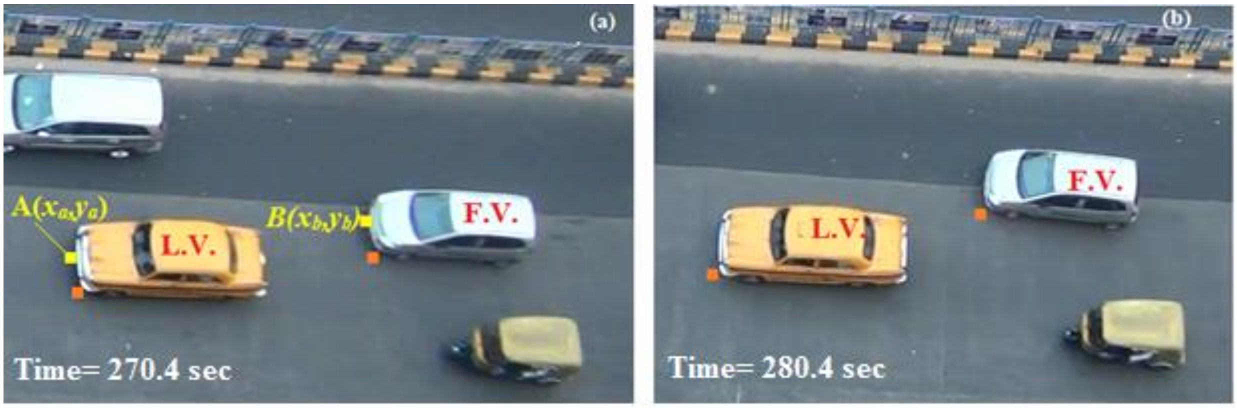

Fig. 3.15 Video snapshots indicating overtaking decision of the following vehicle (a) Before making the decision and (b) After making the decision

From the traffic video, vehicle pairs are chosen and marked along with their decision to overtake. The output file saves average and relative speeds of LV and FV, longitudinal gap and centerline separation. The output variable 'overtaking decision' is noted in the form of categorical input- 1 (Decided to follow) and 2 (Decided to overtake). The presence of hindrance to overtaking (in the form of another vehicle or road edge) is also noted as a categorical input- 0 (No hindrance) and 1 (presence of hindrance). This variable is an indirect representation of traffic situation ahead of LV. A total of 3,013 data points corresponding to several LV-FV vehicle-pairs are determined. Significant data (>50 data points) are obtained for nine vehicle pairs, having total 2708 data-points- namely, cars following other cars, three-wheelers, heavy vehicles, two-wheelers and LCVs; three-wheelers following other three-wheelers; two-wheelers following cars, three-wheelers or other two-wheelers. Data from one of the carriageways each, from the sites Bellary road (Bengaluru), Sinhagad road (Pune) and Linking road (Mumbai) are separated and used for validation for these pairs, whereas the model for these pairs is developed using data from remaining sections or carriageways.

3.6 Summary

This chapter highlighted data collection exercise for (i) lateral interactions, (ii) longitudinal interactions between vehicles, and (iii) overtaking decision-modeling for a following vehicle, in mixed traffic stream with weak lane discipline. Approximately 25% of total data is separated for validation and not used for modeling purpose. Data are collected from mid-block sections located within six cities of India, namely Delhi, Mumbai, Kolkata, Bengaluru, Pune and Guwahati. Data for lateral interactions are collected using test vehicles equipped with sensors and GPS devices to measure the spacing and speeds, whereas data for longitudinal interactions and overtaking decision modeling are collected by video camera mounted on the side of a mid-block stretch and extracted using trajectory data by means of a mouse-click. Table 3.5 highlights magnitude of data collected from each city for lateral, longitudinal interactions and overtaking decision making.

Table 3.5 Magnitude of data collected from each city

Interaction	**Name of city**						**Total data**
	Delhi	Mumbai	Kolkata	Bengaluru	Pune	Guwahati	
Lateral interactions	1163	886	1174	1310	918	565	6016
Longitudinal interactions	0	3100	3509	3481	2847	1119	14056
Overtaking decision-modeling	0	889	917	674	533	0	3013

CHAPTER 4

Modeling of inter-vehicular gaps

Inter-vehicular gaps are essential to be studied and modeled for replicating the heterogeneous traffic conditions in developing world. The modeling of these inter-vehicular gaps will be useful and building blocks for the development of simulation model, which can replicate the real-world traffic conditions. After the data-collection work discussed in the previous chapter, this chapter highlights the modeling of inter-vehicular gaps in heterogeneous traffic stream with weak lane discipline. This chapter is divided into the following sections-

- Analysis and modeling of lateral clearance between vehicles: This section focusses on analysis of lateral clearance between vehicles using sensors as well as camera calibration techniques. The lateral clearance (LC) maintaining behavior is modeled and validated. Effect of constrained overtaking by driving in the gap between two vehicles is also checked, and the differences of constrained and unconstrained overtaking are evaluated.
- Analysis and modeling of longitudinal gaps: Analysis of longitudinal interactions between leading and following vehicles is conducted in this section. The analysis includes variation of longitudinal gap with centerline separation and average speeds, its validation, and multiple vehicle interactions.
- Overtaking decision-making criteria: This section presents a position and speed based criterion for overtaking decisions.
- Other parameters evaluated from field data: This section focusses on calculation of other parameters such as the distribution of lateral and desired vehicle speeds, overtaking time, etc., necessary for calibrating a traffic simulation model.

4.1 Analysis and modeling of lateral clearance between vehicles

This section describes analysis of lateral clearance (LC) between two interacting vehicles, with their average speed ($\bar{v}$). First sub-section describes the effect of various parameters such as average speed, relative speed, day-night conditions and roadway width on LC. Second sub-section describes model development of LC with $\bar{v}$ using sensor data. Third sub-section describes the city-wise variation of developed model. Fourth sub-section describes results obtained using data from camera calibration techniques and compares it with results obtained by sensor data. Fifth sub-section describes shying away behavior due to heterogeneity of interacting vehicle pairs. Sixth sub-section compares lateral interactions in dense traffic (constrained) with unconstrained interactions. Seventh sub-section focusses upon effect of road width and day/night conditions on lateral clearance between vehicles.

4.1.1 Effect of various traffic parameters on lateral clearance

From analysis of lateral clearance data from sensors (Refer Section 3.3), information about three traffic parameters are obtained- (i) speeds of interacting vehicles, (ii) lateral clearance maintained between them during overtaking, and (iii) their vehicle types; at various road widths and traffic conditions. In this subsection, these traffic parameters are checked for their significant effect on the lateral clearance data. The elaborate description is provided in Table 4.1.

Table 4.1 Effect of various traffic parameters on lateral clearance (Overall data, sample size: 6,016)

Variable	**Statistical test**	**Obtained value**	**Inference**
Average speed*	Pearson's Coefficient of correlation	0.386	Average speed has medium correlation with lateral clearance.
Relative speed*		0.043	Relative speed has quite weak correlation with lateral clearance.
Speed of overtaking vehicle		0.271	Speed of overtaking vehicle has weak to medium correlation with lateral clearance.
Speed of overtaken vehicle		0.263	Speed of overtaken vehicle has weak to medium correlation with lateral clearance.
Width of road		-0.045	Width of the road has quite weak correlation with lateral clearance.
Day/Night conditions	ANOVA test between day and night condition at 5% significance	$p = 0.032$	There is significant difference between datasets of day and night conditions

*Average and relative speeds are calculated between two interacting vehicles

From Table 4.1, it is observed that lateral clearance has correlation with average speed and speeds of individual vehicles. Thus, for modeling variation of lateral clearance between vehicles, average speed can be considered as an appropriate independent variable. Speeds of overtaken and overtaking vehicle have equal impact on lateral clearance.

There is quite weak effect of width of the road or relative speed on maintaining of lateral clearance, whereas there is a significant difference in day or night conditions. The road width might be having weak effect on lateral clearance-maintaining, because vehicle-vehicle interactions are more concerned with distance and speeds between vehicles rather than the road width.

4.1.2 Model development using sensor data

As discussed in the previous subsection, lateral clearance (LC) and average speeds ($\bar{v}$) of different vehicle types are considered as dependent and independent variables, respectively. A total of 6,016 vehicle pair interactions (of various vehicle types and pairs) are obtained by data-collection described in Section 3.3. During data-collection, it is observed that vehicles rarely interact beyond 250 cm (Siddiqui, 2013). The maintained lateral clearance between two vehicles is due to the combined contribution of both these vehicles. This statement will give rise to two fundamental assumptions-

- If x and y are two different vehicle types, $LC_{(x\text{-}y)}$ is the same as $LC_{(y\text{-}x)}$; and

- Average speed of interacting vehicles affects the lateral clearance, rather than individual speeds. Moreover, the coefficient of correlation of *LC* with average speed is higher than individual speeds.

The interacting vehicle-pairs which have been considered in this study are cars with other cars, three-wheelers, two-wheelers, LCVs and heavy vehicles (combined data of buses and trucks), three-wheelers with other three-wheelers, cars, two-wheelers and heavy vehicles and two-wheelers with other two-wheelers, three-wheelers and cars.

4.1.1.1 Trend of obtained data of LC with speed

A scatter plot of average speed of test vehicle and interacting vehicle, versus lateral clearance for all the cities is presented in Fig. 4.1.

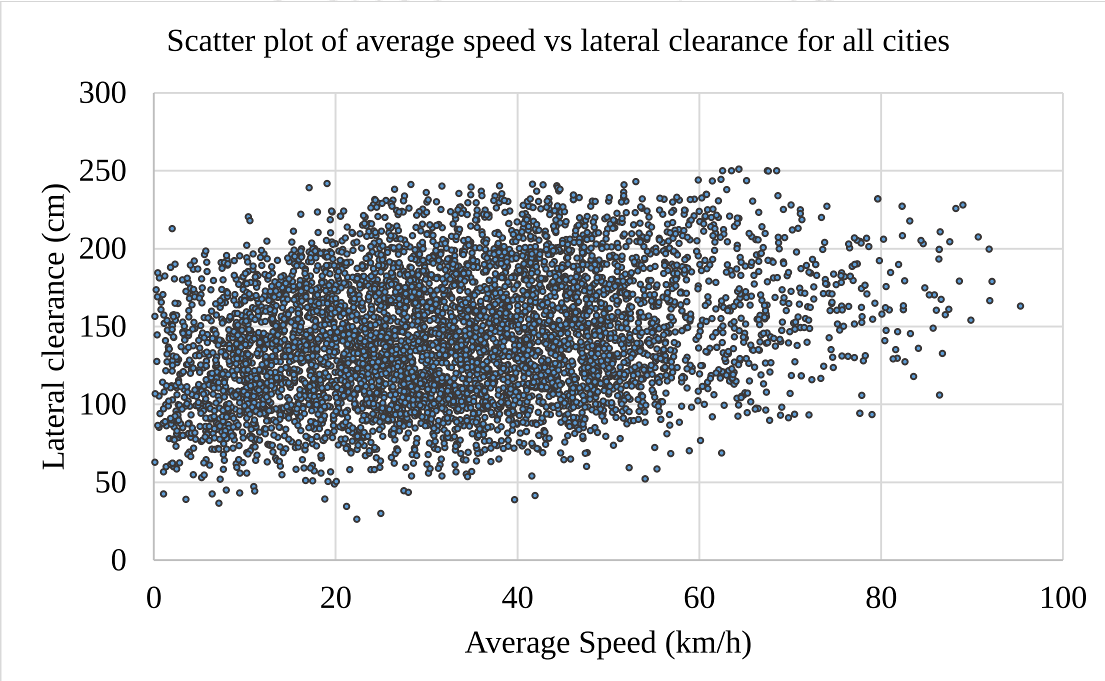

Fig. 4.1 Scatter plot of average speed with lateral clearance for all data

It is observed that a general increasing trend of *LC* is observed with an increase of speed. As drivers drive at higher speeds, they maintain higher degrees of safety, thus maintaining higher *LG*. To understand the trend of this graph in a better manner, it is preferable to divide the data into 10 km/h speed interval groups and 25 cm lateral clearance groups, and calculate their frequency. Frequency of vehicles belonging to each lateral clearance and speed group is expressed as percent of total vehicles for that a particular speed group. Fig. 4.2 depicts the contour plot of frequency observed (in percentage) between lateral clearance and average speed of interacting and test vehicle. Numbers on the chart show percentage of vehicles maintaining the particular lateral clearance range for a given average speed interval.

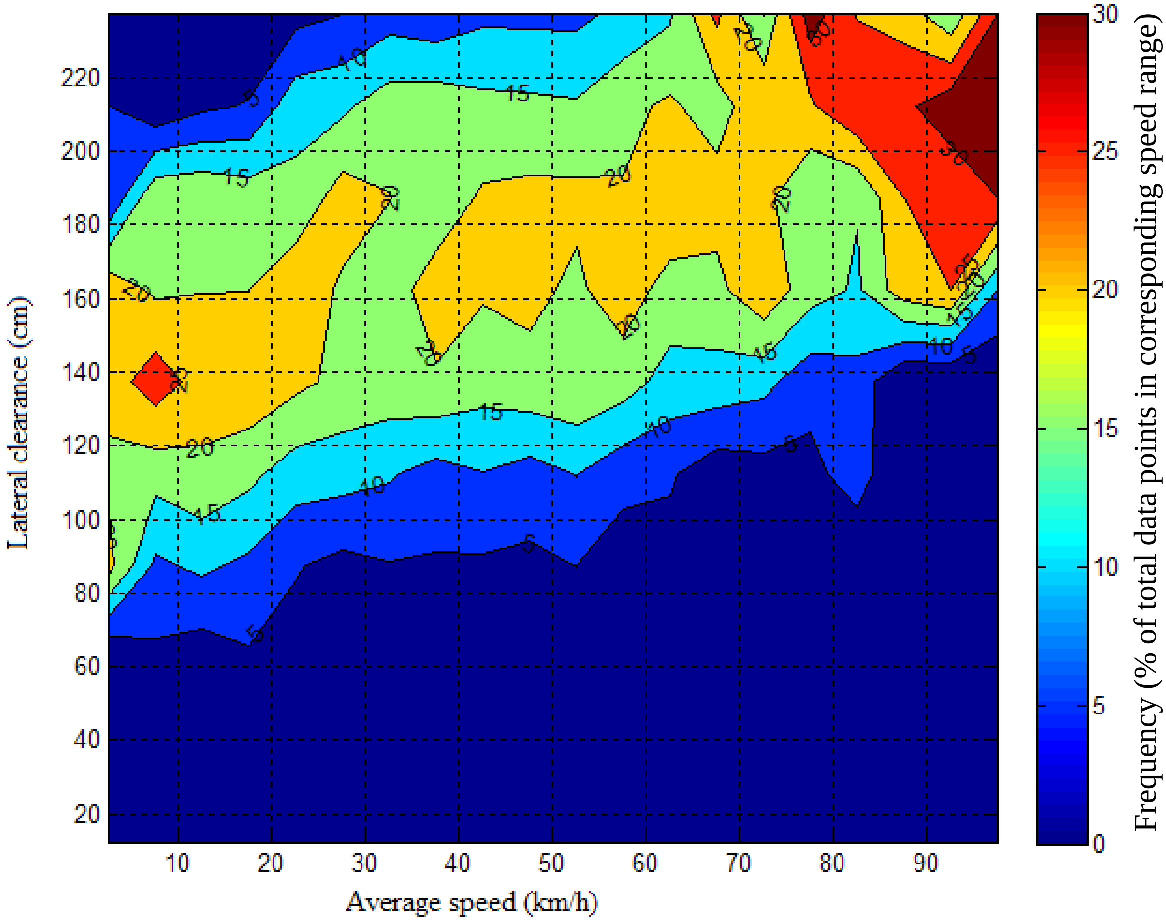

Fig. 4.2 Contour plot for representation of observed frequency between lateral clearance and average speed of interacting and test vehicle

From the obtained contour plot and from positive value of correlation coefficient between lateral clearance and average speed in Table 4.1, it is clear that *LC* increases linearly with average speed ($\bar{v}$). The graph can be best represented as a statistical linear model. A linear model is chosen since increasing the degree of equation does not improve the fitting of regression curve.

4.1.1.2 Structure of developed model

The model proposed for *LC* with average speed ($\bar{v}$) relationship comprises of a deterministic part (regression line) and a stochastic part (residual distribution). The general equation of this model can be represented as Equation 4.1, where *LC* is lateral clearance between vehicles, $\bar{v}$ is average speed, φ is residual terms about the mean, *m* is slope and *c* is intercept.

$$LC = m\bar{v} + c + \varphi \qquad \ldots 4.1$$

Residuals also need to be checked for heteroscedasticity and auto-correlation. Goldfeld-Quandt test is used to check heteroscedasticity and Durbin-Watson statistic is used for auto-correlation test.

- Goldfeld- Quandt (GQ) test for heteroscedasticity basically does F-test between divided sample. GQ test gives F_{GQ} for lower 3/8th data (1503 data points) and middle 1/4th data

(2256 data points) as 1.113, whereas F_{GQ} for middle 1/4th and higher 3/8th data as 1.003 These values are less than $F_{critical}$ = 1.115 at 0.01 significance levels. Thus, the residual data have similar means.

- Further, K-S test is also applied to this divided data, to confirm that the residual distributions remain consistent with speed. The *p*-value of K-S test between lower 3/8th data and middle 1/4th data is 0.123, whereas this value between middle 1/4th and higher 3/8th data is 0.104 (greater than 0.05). Thus, residuals have similar distribution across the means at various speed levels.
- Value of Durbin Watson statistic (autocorrelation test) is 1.86, which is close to 2. Since the value is close to 2, it means weak auto-correlation between consecutive residual terms.

Thus, residuals are found to be homoscedastic with very less auto-correlation. It indicates that the spread of data about the regression line remains consistent with speed. The reason for this maybe because the available road width for overtaking does not change, so drivers travelling at lower speeds also have a wide range of lateral clearances to choose from. Since driver behavior is a natural phenomenon, distribution of residuals is close to normal distribution (*p*=0.03 for all combined data of all vehicle types), and is not grossly non-normal. Thus, the assumption of regression analysis can hold true.

To model the distribution of residual terms about the regression line, it is compared against best-fitted common distributions such as normal, log-normal, beta, etc., using K-S test. This comparison is shown in Fig. 4.3.

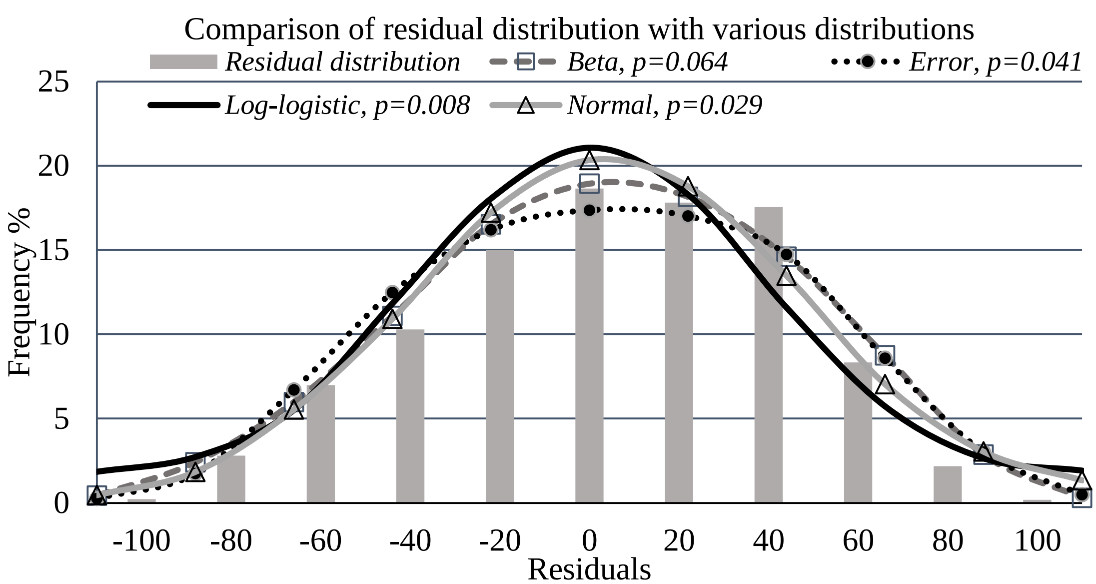

Fig. 4.3 Residual probability density function (lateral clearance data) plotted with common distributions

It can be concluded that residual distribution is statistically similar to Beta distribution. The distribution is determined by four parameters namely $a,\ b,\ \alpha_1$ and α_2. Here, a and b are upper and lower boundary parameters, respectively, whereas $\alpha_1$and α_2 are shape parameters. Variation of Beta distribution frequency function *f(x)* with the residual (*x*) is shown in Equation 4.2.

$$f(x) = \frac{1}{B(\alpha_1,\alpha_2)} \cdot \frac{(x-a)^{\alpha_1-1}(b-x)^{\alpha_2-1}}{(b-a)^{\alpha_1+\alpha_2-1}} \qquad \ldots 4.2\ (a)$$

$$B(\alpha_1, \alpha_2) = \int_0^1 t^{\alpha_1-1}(1-t)^{\alpha_2-1}dt \quad (\alpha_1, \alpha_2 > 0) \qquad \ldots 4.2(b)$$

Beta-distribution is a close-ended distribution with maximum and minimum thresholds on maintenance of lateral clearance. The phenomenon is also observed in real traffic, since interacting vehicles may not venture below or above a given threshold for safe maneuvering.

4.1.1.3 Model development for various interacting vehicle pairs

LC and $\bar{v}$ is also calculated for certain interacting vehicle pairs whose data are significantly observed in field, and a model is developed for these vehicle pairs. Buses and trucks are considered in a single category as heavy vehicles (HV) since noticeable difference in speeds, vehicle sizes and maneuverability were not observed between these two vehicle types in various urban sections studied. Different interacting vehicles pairs included in this study are – cars with other cars, two-wheelers, three-wheelers, HV and LCVs; three-wheelers with other three-wheelers, cars, two-wheelers and HVs; and two-wheelers with other two-wheelers. Other vehicle pairs are not considered due to less sample size observed in collected data. Before proceeding for modeling, it is checked if there is any significant difference among the relationships between different vehicle pairs. These test results are presented in Table 4.2, for slopes (lower wedge in Table 4.2) and intercepts (upper wedge in Table 4.2) of LC with $\bar{v}$ relationship.

Table 4.2 Comparison of slopes and intercepts of various vehicle pairs at 5% significance levels

Vehicle pairs		Car-Car	Car-3W	Car-2W	3W-3W	3W-2W	2W-2W	Car-HV	Car-LCV	3W-HV		
		Intercepts↓										
Car-Car	*Slopes↓*		Y	N	N	N	N	Y	Y	N	*Intercepts↑*	Car-Car
Car-3W		N		N	N	Y	Y	Y	N	N		Car-3W
Car-2W		N	N		N	N	N	Y	Y	N		Car-2W
3W-3W		Y	Y	N		N	N	N	N	N		3W-3W
3W-2W		Y	Y	Y	N		N	N	Y	N		3W-2W
2W-2W		N	N	N	Y	Y		N	Y	N		2W-2W
Car-HV		N	N	N	N	Y	N		N	N		Car-HV
Car-LCV		Y	N	Y	Y	Y	N	Y		N		Car-LCV
3W-HV		N	N	N	N	N	Y	Y	N			3W-HV
		Slopes↑										

Y=Significant difference. N= No significant difference.

From Table 4.2, it is observed that there is a significant difference between intercepts and slopes for a large number of vehicle pairs at 5% significance levels. (For intercepts: 10/36 pairs, for slopes: 15/36 pairs). Thus, vehicle pair-wise relationships need to be obtained. Further, it is also checked if there is significant difference amongst the relationships between different pairs, keeping one interacting vehicle type constant. These test results are presented in Table 4.3. It can be observed that two-wheelers maintain lesser gap (with other vehicles) than cars and three-wheelers (with other vehicles). Further, it can be observed that although cars and three-wheelers maintains similar gaps at lower speeds, three-wheelers (with other vehicles) maintain larger gaps at higher speed.

Subsequent rows under each vehicle type represent deviation in intercept and slope estimate for a particular interacting vehicles pair with respect to overall behaviors of that vehicle type (with other vehicles). It is observed that three-wheelers behave significantly different with cars as compared with other vehicles (Probability of T value mentioned in bold). Due to the high maneuverability of three-wheelers, cars maintain higher gaps with them even at lower speeds. A similar observation can be made in case of car-2W interactions. Such comparison results of regression lines of *LC* and $\bar{v}$ are also mentioned in Fig. 4.4 (a) to Fig. 4.4 (c). Cars are observed to behave significantly different with themselves as compared to other vehicles. Linear statistical equations are modeled. Model parameters (slope, intercept, coefficients of Beta distribution) are calculated for each pair, and mentioned in Table 4.4.

Table 4.3 Comparison of vehicle pairs with overall behavior

Pair	Intercept (c)				Slope (m)			
	Deviation	Std. Err.(σ)	T	Prob>|T|	Deviation	Std. Err. (σ)	T	Prob>|T|
Three wheelers with other vehicles: c=129.6 (σ 5.2), m=0.962 (σ 0.2).								
3W-Car	7.555	6.67	1.133	0.258	-0.516	0.242	-2.128	**0.034**
3W-2W	-7.504	7.327	-1.024	0.306	0.205	0.272	0.754	0.451
3W-3W	-0.872	9.337	-0.093	0.926	0.171	0.372	0.461	0.645
3W-HV	0.821	11.791	0.07	0.945	0.139	0.457	0.305	0.76
Two-wheelers with other vehicles: c=119.76 (σ 6.2), m=0.541 (σ 0.2).								
Car-2W	5.461	6.328	0.863	0.388	0.069	0.207	0.334	0.738
3W-2W	-3.728	6.668	-0.559	0.576	0.248	0.218	1.14	0.255
2W-2W	-1.733	12.019	-0.144	0.885	-0.317	0.396	-0.8	0.424
Cars with other vehicles: c=126.51 (σ 1.9), m=0.550 (σ 0.05).								
Car-Car	-9.125	2.392	-3.415	**0.001**	0.128	0.064	1.994	**0.046**
Car-2W	-1.297	2.655	-0.488	0.625	0.061	0.076	0.801	0.423
Car-3W	-2.482	3.024	-0.821	0.412	0.096	0.085	1.124	0.261
Car-HV	-0.657	3.511	-0.187	0.851	0.144	0.094	1.521	0.128
Car-LCV	13.561	6.209	2.184	**0.029**	-0.429	0.173	-2.478	**0.013**

Bold values in table indicate rejection of null hypothesis at 5% significance levels

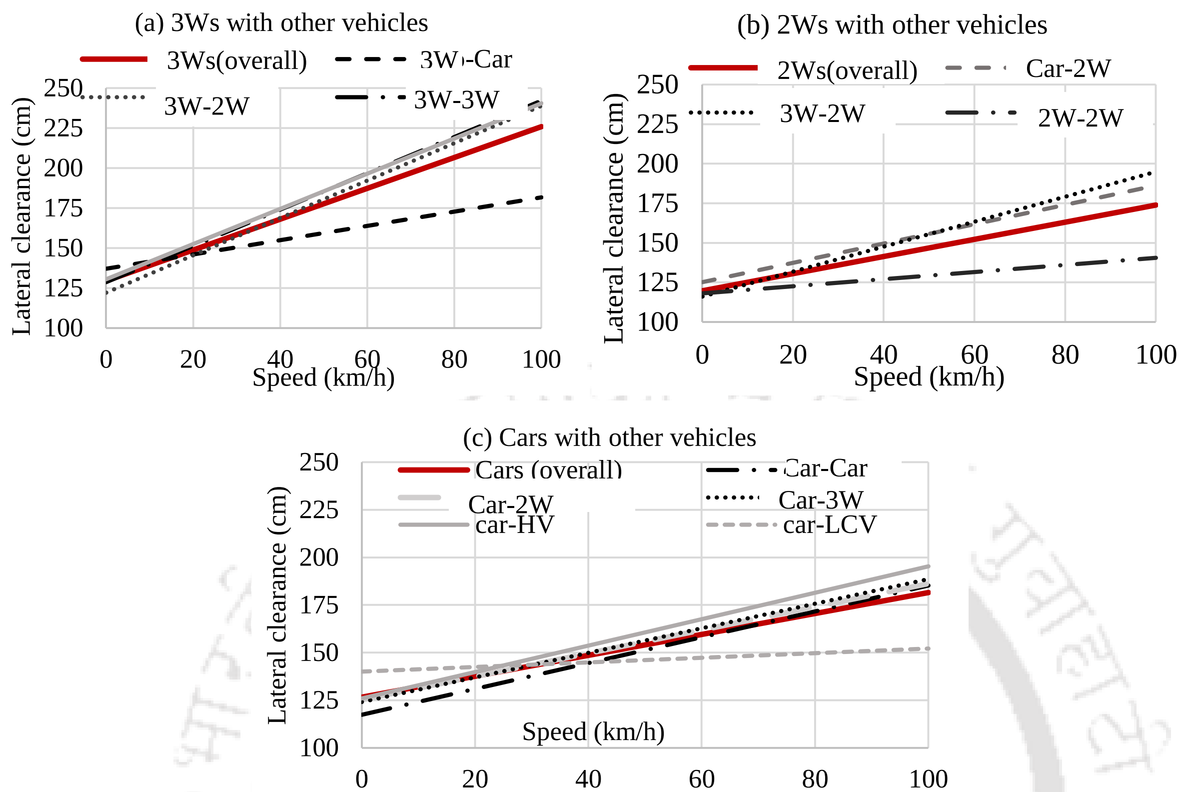

Fig. 4.4 Comparison of vehicle pair behavior with overall behavior of (a) Three wheelers; (b) Two-wheelers; and (c) Cars.

Table 4.4 Parameter estimation for different vehicle pairs

Vehicle pair	Sample size	Regression line		Coefficients of Beta distribution				
		slope	intercept	α_1	α_2	*a*	*b*	*p*-value of fit
All combined	**6,016**	**0.641**	**122.3**	**4.496**	**4.671**	**-117**	**147.94**	**0.063**
3W-3W	140	1.037	114.55	1.861	2.338	-89.79	112.73	0.787
3W-2W	417	0.739	117.27	3.803	4.222	-120.18	133.77	0.305
3W-HV	131	0.985	123.86	2.235	2.633	-100.97	118.31	0.892
2W-2W	87	0.224	118.02	1.511	1.856	-68.93	84.553	0.782
Car-3W	897	0.642	124.12	4.263	4.995	-120.59	141.41	0.601
Car-2W	1372	0.612	125.16	6.522	8.496	-131.13	170.92	0.057
Car-Car	2246	0.681	117.31	3.971	4.891	-106.9	131.94	0.116
Car-HV	538	0.675	126.35	2.264	2.789	-88.39	108.85	0.997
Car-LCV	139	0.132	139.78	1.711	2.213	-74.98	96.641	0.861

Obtained parameters from Table 4.4 can be used for modeling gap-maintenance between vehicles in a heterogeneous traffic stream. One may also compare estimates of average behavior of different types of vehicle pairs, based on regression slopes and intercepts presented in Table 4.4. By this comparison, for particular $\bar{\boldsymbol{v}}$, vehicles maintain lesser *LC* with vehicles of their own vehicle types. This is evident from slope and intercept equations for car-car, 2W-2W and 3W-3W. Two-wheelers maintain the least LC amongst the overall behavior of vehicle types of cars, three-wheelers and two-wheelers. Cars and three-wheelers maintain larger LC with LCVs. However, three-wheelers and cars maintain relatively lesser slope (of LC with speed) with heavy vehicles than their own types, since it was observed that heavy vehicles, due to their weak maneuverability and acceleration capability, are frequently overtaken by many of vehicles even by taking significant risk.

The coefficients a and b of beta-distribution provide information about the spread of data about the best-fit regression line. Since vehicles may predict the behavior of their own vehicle types more accurately than other types, spread of data (indicated by $(a - b)$) about the best-fit line for car-car, 3W-3W and 2W-2W pairs is lesser than other combinations. Moreover, for all the pair combinations, $|a| < |b|$, or the extent of residual-spread towards higher threshold is greater than spread towards lesser threshold (due to safety concerns at lower thresholds). The coefficients α_1 and α_2 represent nature of distribution about this spread. If $\alpha_1 > \alpha_2$ then the data are more skewed towards higher thresholds. Lower absolute values of α_1 and α_2 indicate a flatter distribution. It is observed that for all the vehicle pairs, $\alpha_2 > \alpha_1$ or in other words, more number of vehicles tend to maintain a lateral clearance closer to the lower threshold. A flatter distribution is obtained when two-wheelers interact with two-wheelers, cars interact with heavier vehicles (LCVs, buses, trucks), and three-wheelers interact with three-wheelers or heavy vehicles (as inferred from values of α_1 and α_2). K-S test was applied between the best-fit beta distribution and residual distribution; and p-value of comparison of these two distributions is shown in the last coloumn of Table 4.4. It is observed that residuals follow beta distribution at good significance. Table 4.5 provides average lateral clearance values as estimated from best-fit regression lines for these vehicle pairs.

Table 4.5 Average values of lateral clearance for various vehicle pairs at different speeds

Vehicle pair	**Average *LC* (cm)**		
	0 km/h	**30 km/h**	**60 km/h**
All combined	122.3	141.53	160.76
3W-3W	114.55	145.66	176.77
3W-2W	117.27	139.44	161.61
3W-HV	123.86	153.41	182.96
2W-2W	118.02	124.74	131.46
Car-3W	124.12	143.38	162.64
Car-2W	125.16	143.52	161.88
Car-Car	117.31	137.74	158.17
Car-HV	126.35	146.6	166.85
Car-LCV	139.78	143.74	147.7

4.1.1.4 Comparison with previous literature

Previous researchers have calculated inter-vehicular gaps using static data-collection techniques (such as video-recording), whereas this research uses a dynamic method to record these gaps. In previous literatures, the researchers were not able to record average value over the entire overtaking duration due to limitations on trap length in video-recording techniques. Table 4.6

presents the comparison of average *LC* values for car-car pair as obtained from this research with previous researches.

Table 4.6 Comparison of *LC* values with previous researches for car-car pair

Research	Average *LC* (m) for car-car interaction	
	0 km/h	50 km/h
Current study	1.173	1.581
Arasan and Koshy (2005)	0.600	1.000
Mallikarjuna, *et al.* (2013)	0.850*	1.500*#
Dimayacyac and Palmiano (2016)	0.500	1.470
Gunay (2011)	0.800*	1.600*

* estimated value. # extrapolated value.

It can be inferred that the obtained *LC* is comparable with the data from Mallikarjuna *et al.* (2013) as well as Gunay (2011) at higher speeds, due to a similarity in traffic behavior of studied traffic in these researches with that studied in this paper. However, at lower speeds, reported *LC* is found higher than these studies. This may be due to accuracy in *LC* measurement in previous researches, as in the adopted methodology, accuracy decreases with increase in vehicle density. The values estimated by Dimayacyac and Palmiano (2016) is showing higher sensitivity to speed, since the traffic studied was more organized and followed lane discipline.

4.1.2 Variation of developed model across cities

It was observed from Fig. 4.1 that the combined trend of *LC* maintained by interacting vehicles from different cities increases with average speed. However, this observed relationship may change from one city to other due to change in drivers and vehicles' characteristics. A multiple comparison test i.e., analysis of covariance (ANCOVA) is conducted to evaluate the behavioral change in *LC* with $\bar{v}$, among the interacting vehicle pairs of each city and results are presented in Fig. 4.5. Fig. 4.5 provides the spread of obtained slopes and intercepts of best-fit regression lines for each city. Here, data are combined for all vehicle types and all road widths for each city.

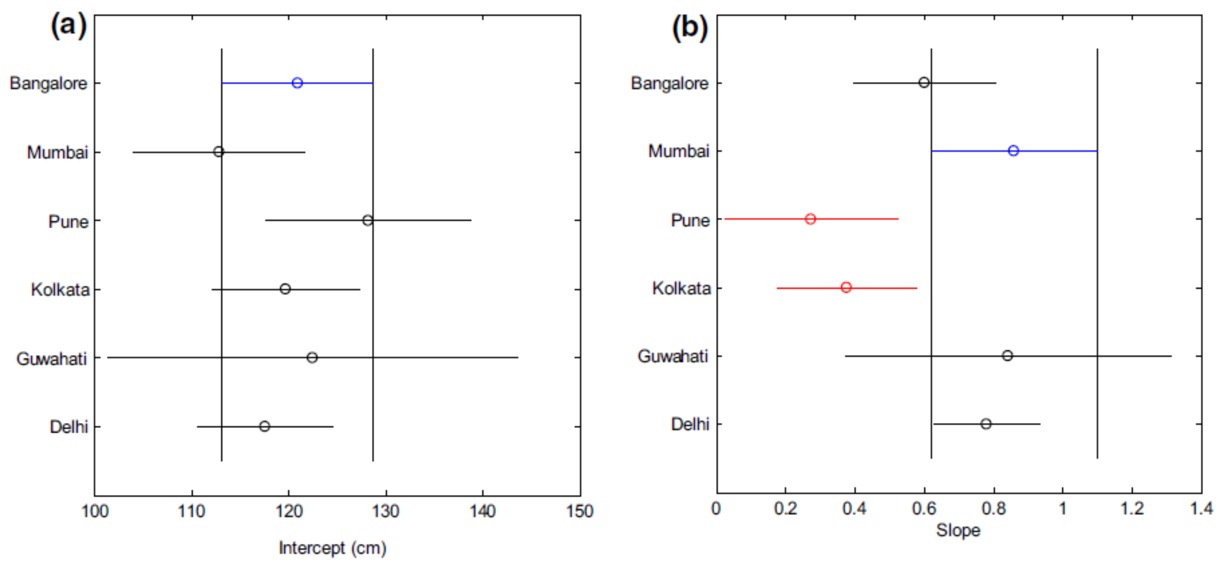

Fig. 4.5 Comparison of range of slopes and intercepts for different cities

It is observed that slopes of *LC*-speed relationship of vehicles in Pune and Kolkata significantly differ with those of Mumbai and Delhi. Guwahati city has a higher range of slope and intercept variation, since predictability of accuracy of slope or intercept is less due to lesser data-points of Guwahati city.

Fig. 4.6 provides the linear plots of fitted regression lines for various cities.

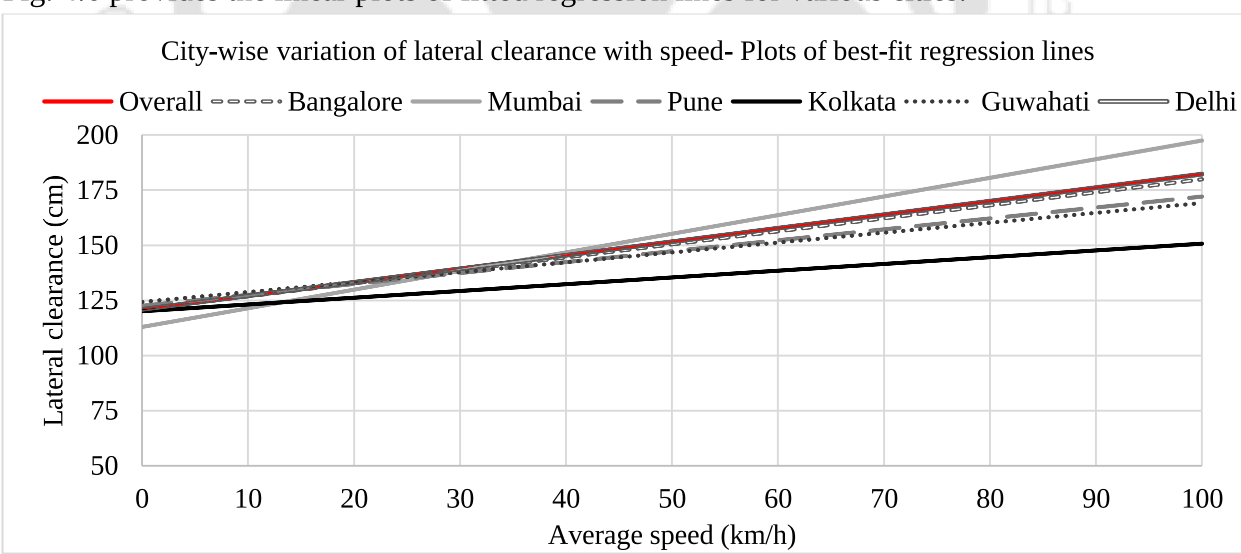

Fig. 4.6 Comparison of obtained regression lines of *LC* with speed relationship for different cities

Table 4.7 compares *LC* with $\bar{v}$ relationships for interacting vehicle pairs in different cities, with the relationship developed for combined data of all cities. It is observed from T-values of Table 4.7, that vehicles maintain statistically similar intercepts of regression lines in all the cities. It means that at lower speeds there is no observable difference in vehicle behavior in different cities.

However, drivers in Pune and Kolkata maintain significantly lesser slope of *LC* with $\bar{v}$ as those of other cities, whereas Mumbai and Delhi maintain significantly higher slope; as evident from statistics values marked in bold, in the last coloumn of Table 4.4. In other words, when maintaining lateral clearance, drivers of Mumbai and Delhi are more sensitive to speed whereas those of Pune and Kolkata are less sensitive. Since the study requires aggregate behavior of vehicles across all cities, entire dataset of all cities is taken for analysis.

Table 4.7 *LC* data comparison of different cities

City	Sample size	Intercept (All cities' estimate: 120.883, Std. Err. 2.232).				Slope (All cities' estimate: 0.615, Std. Err. 0.053).			
		Deviation	Std. Err.	*T*	Prob>|*T*|	Deviation	Std. Err.	*T*	Prob>|*T*|
Bengaluru	1310	0.123	3.854	0.032	0.975	-0.025	0.099	-0.25	0.803
Mumbai	886	-8.101	4.288	-1.889	0.059	0.256	0.113	2.263	**0.024**
Pune	918	9.671	4.971	1.945	0.052	-0.351	0.119	-2.959	**0.003**
Kolkata	1174	-2.565	3.757	-0.683	0.495	-0.188	0.097	-1.933	0.053
Guwahati	565	4.223	8.069	0.523	0.601	0.143	0.183	0.781	0.435
Delhi	1163	-3.351	3.51	-0.955	0.34	0.164	0.077	2.134	**0.033**

4.1.3 Modeling for lateral clearance with camera calibration data

Lateral clearance analysis is also conducted using camera calibration techniques for a limited number of vehicles, since the dynamic vehicle movement has the disadvantage of not accounting difference in driver behavior. Fig. 4.7 shows scatter plot of average speed of test vehicle and interacting vehicle in km/h, versus lateral clearance in cm, obtained by camera calibration technique discussed in Section 3.4. An ANOVA test is performed between lateral clearance obtained by both the techniques, and it is found that there is a statistical similarity between data obtained by both the techniques (p=0.381).

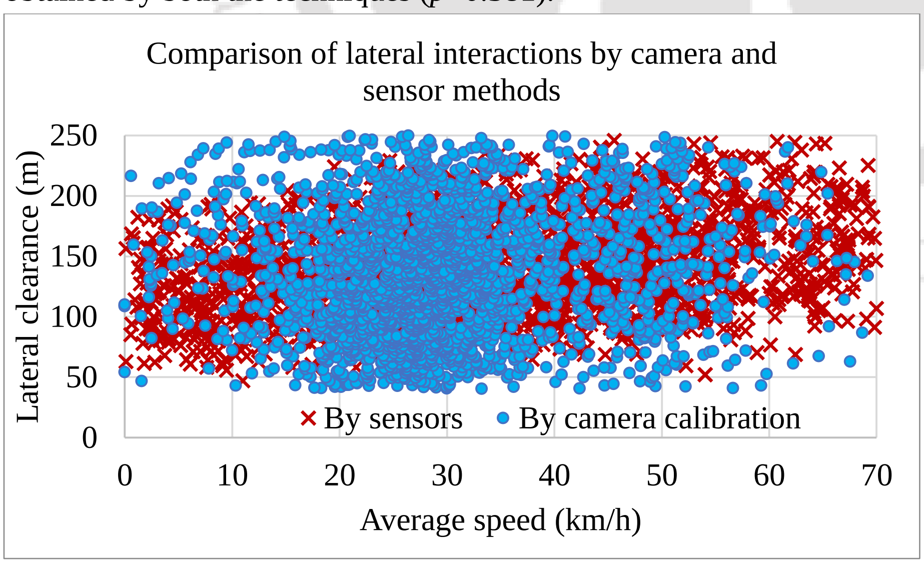

Fig. 4.7 Lateral clearance with average speed relationship using camera calibration technique for car-car pair

The data obtained by sensor-based techniques have greater precision levels, hence they are used for modeling purpose.

4.1.4 Shying away behavior of heterogeneous interacting vehicles

An attempt is made to verify a hypothesis that the *LC* maintained between two interacting vehicles is the result of individual contribution of each vehicle. For a given average speed between two interacting vehicle types *x* and *y*, $LC_{(x\text{-}y)}$ should be the average of $LC_{(x\text{-}x)}$ and $LC_{(y\text{-}y)}$ for this hypothesis to hold true. To test this hypothesis, *LC* and $\bar{v}$ relationships (regression lines) observed from field data for homogeneous vehicle pairs (like car-car, 2W-2W and 3W-3W) are compared with those of heterogeneous vehicles pairs combinations (like car-2W, car-3W, 3W-2W, etc). Sample size and model coefficients are provided in Table 4.5. Fig. 4.8 presents the results of such comparison graphically for each vehicle pair. For example, Fig. 4.8 (a) presents the observed *LC* and $\bar{v}$ relationships for 3W-3W (AA), 2W-2W (BB), and 3W-2W (AB) along with the computed 3W-2W (AB) relationship based on the average value of $LC_{(A\text{-}A)}$ and $LC_{(B\text{-}B)}$. It is observed that values of regression lines $LC_{(A\text{-}B)}$ is more than the average value of $LC_{(A\text{-}A)}$ and $LC_{(B\text{-}B)}$. One possible reason for this can be that driver of one vehicle type is less confident about the behavior of other vehicle types, hence maintains more *LC* with them than with the same vehicle type. Similar results were obtained when tested for two-wheeler and car pairs (refer Fig. 4.8 (c)). In case of 2W-3W (AA) and car-car (CC) test, similar result has been observed at lower speed but at higher speed averaged value of $LC_{(A\text{-}A)}$ and $LC_{(C\text{-}C)}$ is found to be higher than the field $LC_{(A\text{-}C)}$.

From Table 4.2, for car-3W, 2W-3W and car-2W pairs, it can be calculated that there is 8.7%, 0.85% and 6.76% increase in intercept; and -25.37%, 14.1% and 35.15% increase in slope of $LC_{(x\text{-}y)}$ regression line with speed, respectively, as compared to average of $LC_{(x\text{-}x)}$ and $LC_{(y\text{-}y)}$. Comparisons for heterogeneous pairs ($LC_{(x\text{-}y)}$) are made with average of $LC_{(x\text{-}x)}$ and $LC_{(y\text{-}y)}$ in Fig. 4.8. From this exercise, it can be concluded that lateral clearance between two different vehicle types cannot be taken as the combined contribution of two similar type of vehicles' individual behaviors. There is a general shying away when interaction of dissimilar vehicle types is considered.

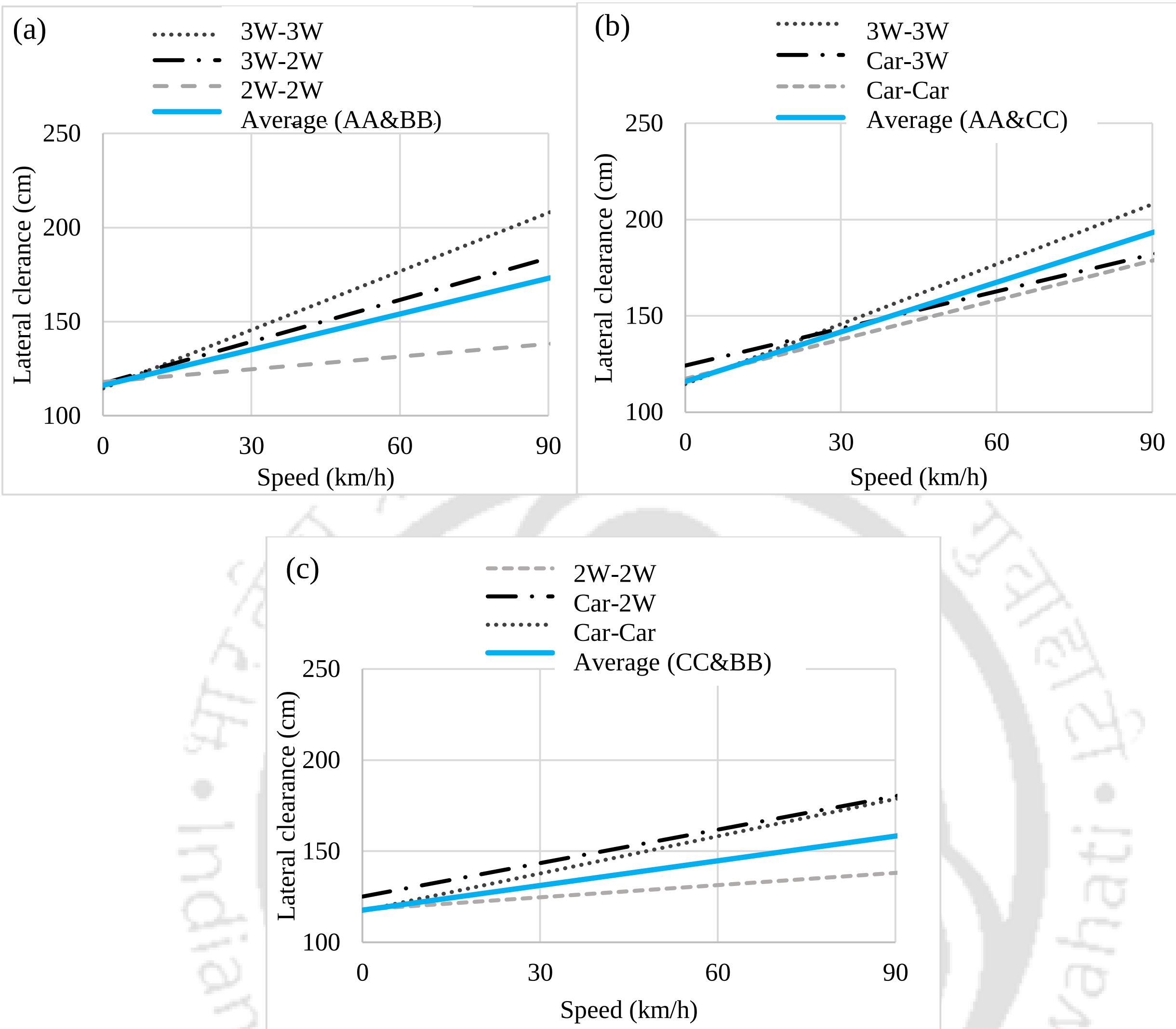

Fig. 4.8 Comparison of heterogeneous pair of vehicle with average of respective homogeneous interactions for **(a)** 3W-2W, **(b)** 3W-car, and **(c)** car-2W interactions

4.1.5 Analysis of simultaneous multiple lateral interactions

If vehicles interact simultaneously on both sides of the test vehicle, there is simultaneous influence of both these vehicles on test vehicle equipped with sensors. Interaction of vehicles are decided based on vehicle's detection by the sensors fitted on both sides of the vehicles (refer to Fig. 4.2). The necessary condition for multiple vehicle interactions is that a vehicle should be detected in at least one sensor of one side of the test vehicles, while at least one sensor on opposite side also detects another vehicle, at the same time-step, as shown in Fig. 4.9. This illustration is shown in Fig. 4.9.

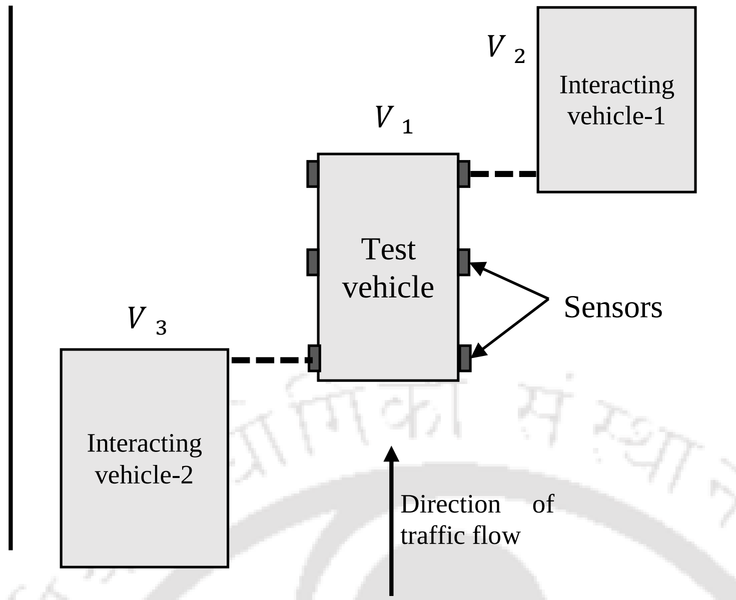

Fig. 4.9 Necessary condition of detecting interacting vehicles for multiple vehicle interactions

4.1.5.1 Conditions for constrained interaction

Four conditions may arise when vehicle interacts laterally with one or more vehicles-

1. Interaction is only on one side.
2. Interaction is on both sides, and test vehicle is overtaking both the vehicles (Fig. 4.9, $v_1 > v_2, v_3$).
3. Interaction is on both sides, and test vehicle is being overtaken by other two vehicles. ($v_1 < v_2, v_3$)
4. Interaction is on both sides, and test vehicle is overtaking one vehicle and being overtaken by other vehicle. ($v_2 > v_1 > v_3$).

Case 1 is considered as unconstrained lateral interaction for analysis. Case 2 is considered as constrained lateral interaction. Cases 3 and 4 are ambiguous and not considered for comparison, since it is difficult to conclude whether test vehicle is in constrained or unconstrained condition. The situation of test vehicle overtaking both vehicles by moving in the gap between them, is a definite indicator of constrained lateral interaction. If Case 2 is observed, then interaction with both the vehicles are assigned as constrained interactions. Data of different vehicle pairs from Cases 1 and 2 are compared with each other. To avoid constraining due to median or road edges, the data obtained from carriageways with less than three lanes width is removed. Data for both the cases are modeled as per Equation 4.1 and 4.2.

4.1.5.2 Modeling and comparison of constrained behavior

Regression equations (slopes and intercepts) and Beta-distributed residuals are calculated for some vehicle-pairs (car-car, car-3W, car-2W, and 3W-2W) with significant data for both the conditions. Both the regression equations are plotted in Fig. 4.10 for each vehicle pair. The comparisons of slopes and intercepts of constrained conditions with unconstrained conditions for various pairs are shown in Table 4.8. Last coloumn in this table presents *p*-statistic of fit of beta distribution with actual residuals from field data.

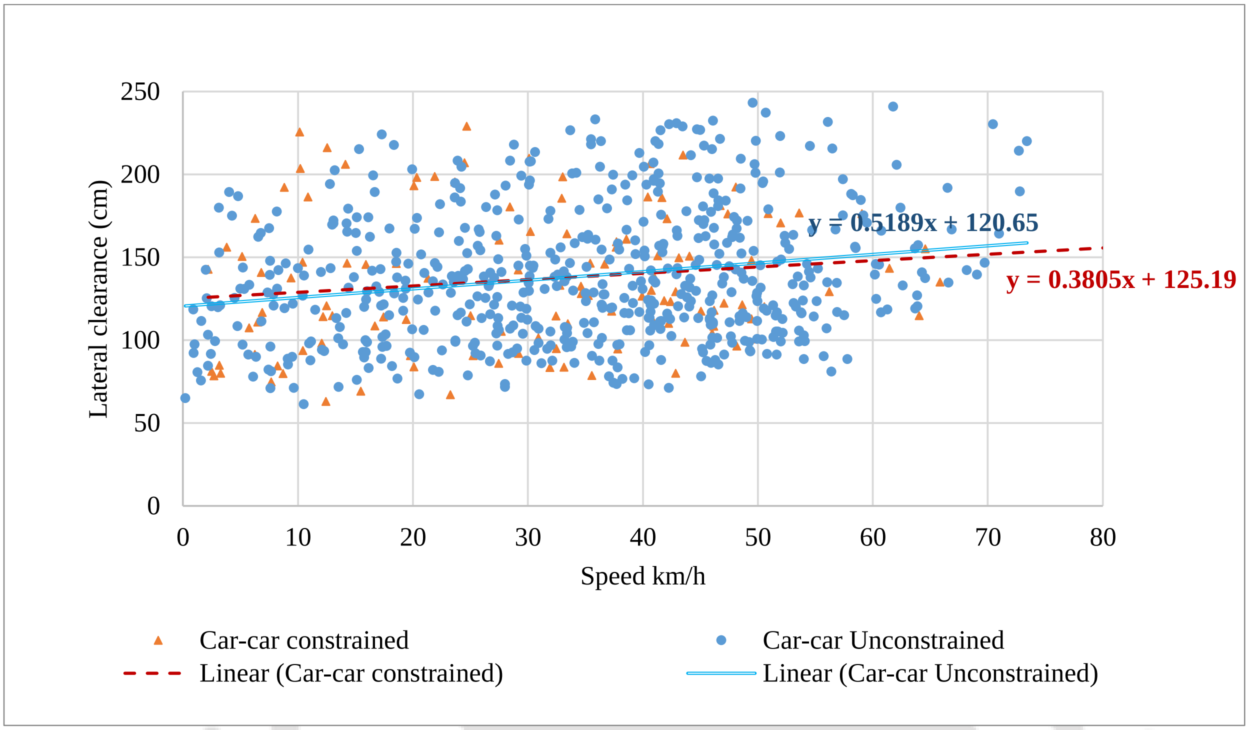

Fig. 4.10 (a) Plots of speed-lateral clearance relationships for constrained, unconstrained cases for Car-car pairs

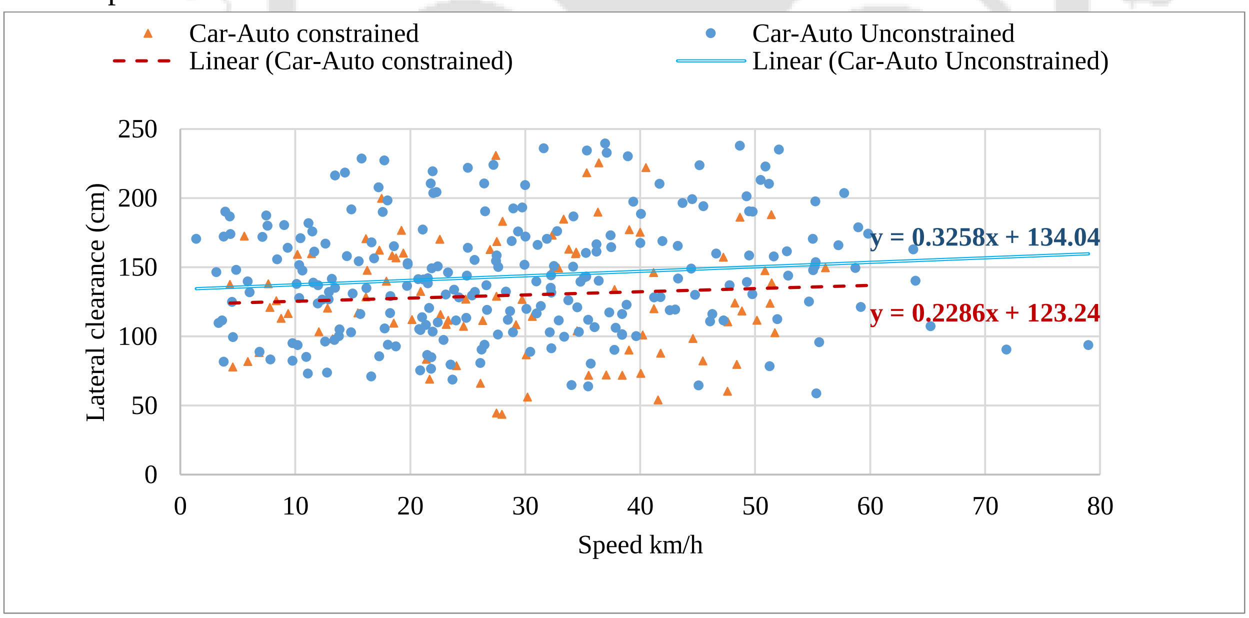

Fig. 4.10 (b) Plots of speed-lateral clearance relationships for constrained, unconstrained cases for Car-3W pairs

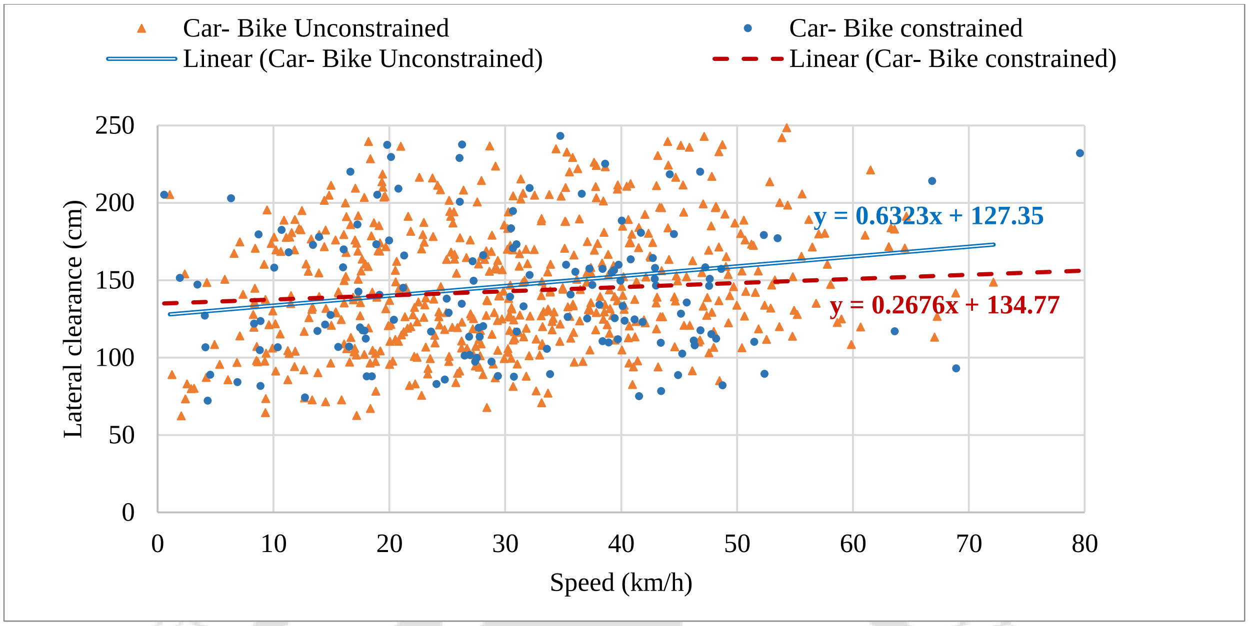

Fig. 4.10 (c) Plots of speed-lateral clearance relationships for constrained, unconstrained cases for Car-2W pairs.

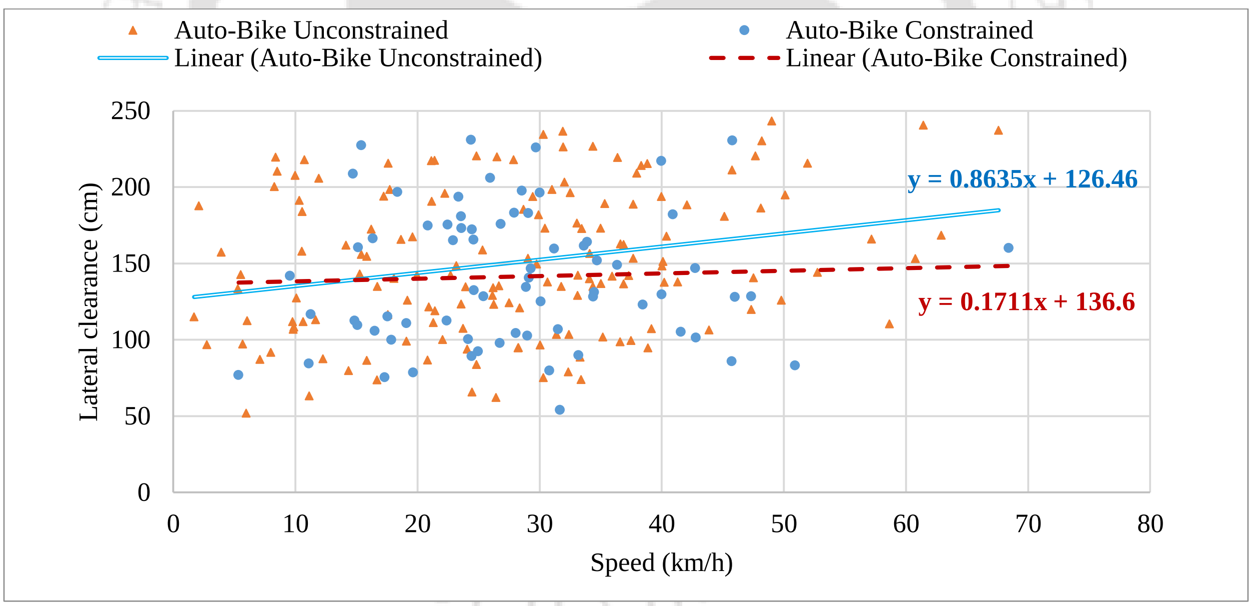

Fig. 4.10 (d) Plots of speed-lateral clearance relationships for constrained, unconstrained cases for 3W-2W pairs.

Table 4.8 Comparison of lateral clearance with average speed models for constrained and unconstrained conditions

Vehicle pair	Condition	Sample size	Regression line		Parameters of beta distribution of residuals				
			Slope	Intercept (cm)	α_1	α_2	*a*	*b*	*p*-value
Car-Car	Unconstrained	585	0.519	120.65	3.016	1.854	-72.05	118.31	0.034
	Constrained	122	0.381	125.19	2.154	1.379	-67.96	106.96	0.054
3W-Car	Unconstrained	243	0.326	134.04	7.668	4.634	-118.72	196.68	0.045
	Constrained	95	0.229	123.24	2.712	2.085	-96.63	125.81	0.059
Car-2W	Unconstrained	553	0.632	127.35	2.875	2.058	-79.31	112.31	0.051
	Constrained	141	0.267	134.78	2.193	1.339	-82.83	58.63	0.055
3W-2W	Unconstrained	151	0.864	126.46	1.276	1.322	-87.57	86.59	0.075
	Constrained	67	0.171	136.6	2.063	1.868	-91.84	103.12	0.071
Validation data Car-car	Unconstrained	414	0.51	121.03	4.164	2.412	-81.69	141.44	0.028
	Constrained	75	0.312	125.12	1.864	1.325	-74.86	107.4	0.083

From Table 4.8, following inferences can be observed-

- There is an increase of lateral clearance with increase in average speed for both the cases- constrained as well as unconstrained and for all vehicle pairs.
- There is a reduction in slopes by 26.67%, 29.75%, 57.77% and 80.19% for car-car, 3W-car, car-2W and 3W-2W pairs. It may mean that at moderate and higher speeds, vehicles maintain lesser gap during constrained overtaking than unconstrained overtaking. Slopes of data from constrained and unconstrained cases are compared with each other using ANCOVA comparison and they are not significantly similar except for car-car case at 5% significance levels. (*p*=0.088, 0.046, 0.035 and 0.041 between slopes of constrained and unconstrained behavior for car-car, 3W-car, car-2W and 3W-2W pairs). This indicates that drivers behave significantly different at higher speeds, under constrained and unconstrained overtaking conditions.
- At lower speeds (<20 km/h), the value of *LC* maintained by vehicles at constrained condition is higher than unconstrained conditions. This information is derived only from best-fit lines. However, in Fig. 4.10, one can observe that at lower speeds, there is no significant change in lateral clearance-maintenance. An ANCOVA test on intercepts also confirms the result. (p=0.067, 0.348, 0.219 and 0.078 between intercepts of constrained and unconstrained interactions, for car-car, 3W-car, car-2W and 3W-2W pairs).
- Two-wheelers have a higher capability to veer, thus may maintain lesser gaps during constrained cases. Moreover, when vehicles of larger size like three-wheeler or car overtake the two-wheelers, there is not much risk due to collision with a two-wheeler. So, lesser gaps maybe maintained with two-wheelers during constrained overtaking. This property is reflected from the coefficients of slope for constrained conditions of car-2W and 3W-2W pairs. There is a high compromise (58% for car-2W pair and 80% for 3W-2W pair) when constrained relationship is compared with unconstrained relationship (Fig. 4.10

(c), (d)). On the other hand, for cars maintaining gap with other cars, there is not a significant change in relationships as observed from Fig. 4.10 (a).

- From the residual coefficients a and b of constrained and unconstrained cases, one can conclude that there is less spread of data about the regression line (indicated by the difference between a and b) for constrained case as compared with the unconstrained case (except for 3W-2W pair). In the analysis, value of parameter $\alpha_1 > \alpha_2$ or the distributions are skewed towards the lower sides for almost all vehicle pairs.

4.1.5.3 Validation for constrained case

Validation is performed using MANOVA test, only on car-car dataset, because data for *constrained* situations observed for other vehicle types were insignificant (sample size < 50). About 40% data are kept aside for validation. The speed-lateral clearance plot and regression lines are plotted similar to models described earlier. Validation exercise is performed to check whether lateral clearance-speed relationships of constrained and unconstrained conditions differ significantly with change in datasets. Fig. 4.11 compares the constrained and unconstrained conditions for validation data of car-car pairs. Table 4.9 provides various statistical tests on field and validation constrained and unconstrained data.

These results for compromise in lateral clearance in constrained overtaking conditions will be helpful in modeling traffic with weak or no lane discipline. Here, vehicles tend to squeeze in between two vehicles due to lack of proper lanes. These results, if used along with basic pairwise lateral clearance maintenance between two vehicles can reflect lateral interactions between vehicles in weak lane discipline traffic, as observed in developing countries.

Table 4.9 Validation exercise for checking constrained-unconstrained behavior on car-car pairs

Hypothesis	*p*-value	Reject (0) or accept (1) hypothesis at 95% confidence
Significant similarity between constrained data of model, validation	0.245	1
Significant similarity between unconstrained data of model, validation	0.314	1
Significant similarity between constrained and unconstrained slopes of validation	0.052	1

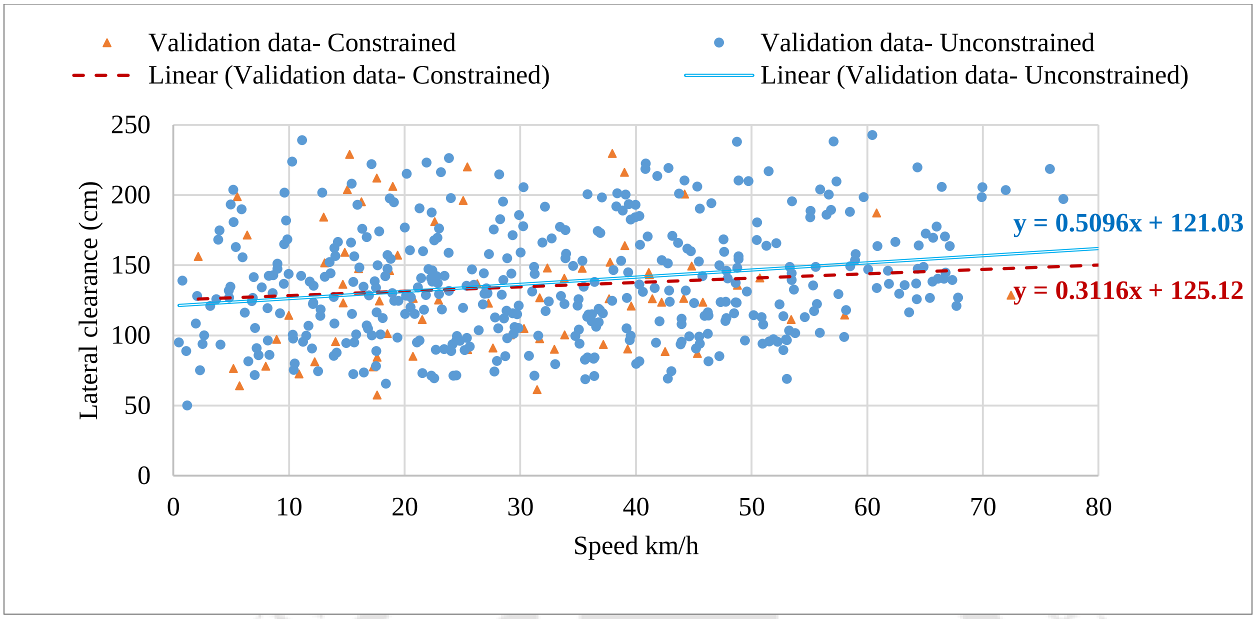

Fig. 4.11 Constrained and unconstrained condition data for validation dataset of car-car pair

4.1.6 Effect of width of road and day/night conditions on speed-*LC* relationship

During manual vehicle identification of interacting vehicles through video-camera, an approximate width of road was also noted in terms of number of lanes. Paved shoulders are classified as having half-lane width. Data are segregated widthwise, and regression lines are fitted for each width group for *LC* with average speed.

Data are segregated widthwise, and 3d regression plane is fitted. The aim is to find width where *LC* is minimum for given speed. Partially differentiating obtained regression surface (Equation 4.3, second degree with N, first degree with $\bar{v}$) gives N=4.59, or about 4.5 lane width. It means at this width, vehicles achieve maximum squeezing in. The graphical representation is shown in Fig. 4.12. However, it is observed that the increase or decrease in lateral clearance with number of lanes is not significant (Pearson's coefficient of correlation is -0.043), thus width of the road do not hold significant effect in effect on lateral clearance maintenance.

$$LC = 149 - 13.79N + 0.553\bar{v} + 1.5N^2 + 0.02\bar{v}N \qquad \dots 4.3$$

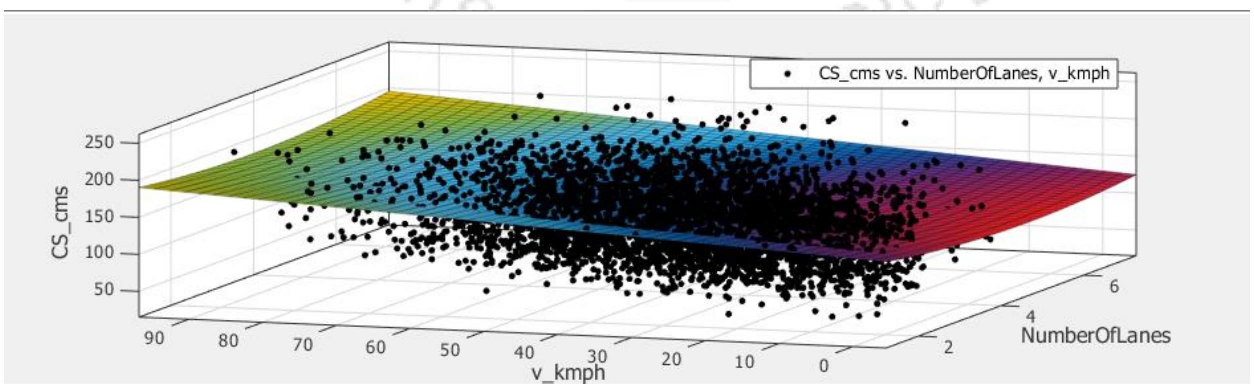

Fig. 4.12 Parameters of *LC* with average speed relationship varying with number of lanes.

The obtained results are presented in Table 4.10. From the results, one can conclude that there is no significant trend of slopes and intercepts for *LC*-speed relationship based on road width. However, vehicles tend to maintain least *LC* at four-lane road width (two lanes with paved shoulders), equivalent to 14 m road-space. *LC* increases roughly with increase in road width after this width.

Table 4.10 Parameters of *LC* with average speed relationship varying with number of lanes.

Approximate number of lanes	Parameters of straight line relationship of speed with *LC*	
	Slope	Intercept
1.5	1.00	105.34
2	0.57	130.37
2.5	0.37	129.58
3	0.56	120.81
3.5	0.72	142.95
4	0.75	122.88
5	0.87	111.03
6	0.92	105.34
7	0.88	109.83

Time of the day (day or night time) was also taken into consideration during vehicle identification. Those vehicles which run during day as well as night were segregated. Plot of *LC* with average speed was calculated separately for day and night conditions. It is observed that, vehicles tend to keep significantly more *LC* during the daytime than night time (refer Table 4.1), as against what was expected. Linear regression trends give night time *LC* with average speed slopes and y-intercept as 0.371 and 119.9 (0.33 and 117 for car-car), as against 0.697 and 123.4 (0.791 and 119.69 for car-car) for the same vehicles during day time. One of the reasons for this can be the urgency of vehicles to return to the destination during night-time, due to which they take higher risks.

4.2 Analysis and modeling of longitudinal gaps

This section describes variation of longitudinal parameters such as longitudinal gap and time gap, with the centerline separation (lateral parameter), and speeds of vehicles. The data for longitudinal gap are collected and extracted as mentioned in Section 3.4. Here, four parameters are of main interest- speed of leading vehicle (LV), speed of following vehicle (FV), centerline separation between them (*CS*); and longitudinal gap between LV and FV. In the first subsection, preliminary observation of *LG* data and its comparison with earlier studies is provided. Variation of longitudinal gap with two variables- centerline separation (*CS*) and average speeds ($\bar{v}$) is shown in second subsection, and its validation is provided in the third subsection. A theory regards to threshold conditions of steady state flow is described in fourth subsection. Comparison of multiple vehicle interactions in a denser traffic stream with single vehicle interactions is mentioned in fifth subsection.

When a FV approaches and begins to follow a LV, it needs to adjust its speed to equal the speed of LV. The driver needs to accelerate or decelerate; and after some duration, the FV stabilizes itself behind the LV, so that the speed difference tends to zero. This is called as steady state. A study of inter-vehicular gaps maintained at this state is required, since drivers target to reach this position from LV where they feel safe. The longitudinal gap maintained between them corresponds to a minimum stable distance headway for safe vehicle-following. This value changes as per driver behavior, speeds, staggering and vehicle types. It is observed from literature that vehicles can be considered in a steady following state if absolute relative speed between LV and FV is observed to be less than 5 km/h (Sayer *et al.*, 2003; Zhang and Bham, 2007). Thus, in collected data, the data-points having relative speed greater than ±5 km/h are removed, since they do not meet the above assumption.

4.2.1 Preliminary observation of longitudinal gap data and its comparison with earlier studies

As FV approaches LV and begins closing-in to LV, it starts adjusting its speed to maintain a constant longitudinal gap between them as per their centerline separation (*CS*) (distance between center of width of two vehicles) between them and the lateral clearance. The *CS* is a measure of off-centeredness of vehicles from maintaining disciplined vehicle-following. In heterogeneous traffic conditions, driver of FV is actually unable to perceive the position of front of LV and perceives the position of back of LV with better precision. Therefore, longitudinal gap (*LG*) between the back of LV and front of FV is considered instead of distance headway in the analysis. The following preliminary observations are made-

1. Obtained *LG* between LV and FV is plotted against *CS* and $\bar{v}$, keeping the other variable constant. *LG* is observed to decrease with *CS* at various speed levels, and increase with speed at various *CS* levels. This variation is presented in Fig. 4.13 (a) and (b) respectively.

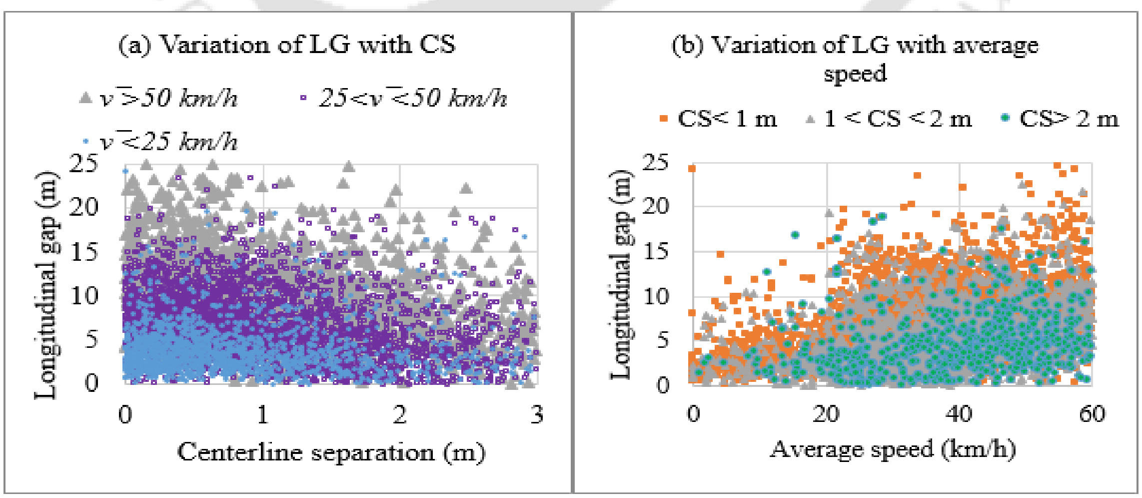

Fig. 4.13 A plot of *LG* with (a) centerline separation (*CS*), and (b) with speed ($\bar{v}$)

2. There is weak correlation between *CS* and $\bar{v}$ (coefficient of correlation = 10^{-5}), thus these variables can be used as independent variables.

Gunay (2007) had examined the variation of time headway between LV and FV with centerline separation, at relatively homogeneous traffic conditions. Obtained dataset is compared with Gunay (2007) and time headway is calculated for every pair of LV and FV. It is the ratio of longitudinal headway and speed of FV. From the data collected, data of a particular site (Western Express Highway in Mumbai) is selected so that site conditions (road width, vehicle composition, city characteristics, etc) matches with those in Turkey, as mentioned in Gunay (2007). The plot of time headway with centerline separation obtained from this (Mumbai) site for car-car pair is mentioned in Fig. 4.14 (a).

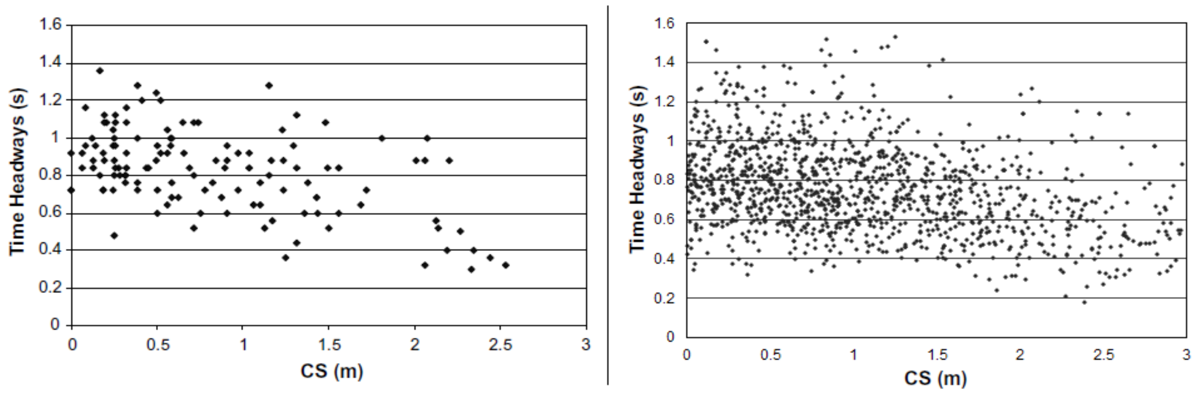

(A) CS vs time headway plot from Gunay (2007); (B) CS vs time headway data from similar field conditions.

Fig. 4.14 Comparison of obtained time headway with centerline separation data with that of Gunay (2007).

From Fig. 4.14, it is observed that as *CS* increases, the time headway decreases for both the researches. The average values of time headways are also observed to be similar from Fig. 4.14. Thus, there is consistency in observed data with the previous literature.

4.2.2 Variation of longitudinal gap with centerline separation and average speeds

In this analysis, centerline separation and speed are used as independent variables whereas longitudinal gap is used as dependent variable. Scatter plot of 3 variables- average speed ($\bar{v}$), longitudinal gap (*LG*) and centerline separation (*CS*) are extracted for every vehicle-type pair (sample size >100). As stated in Section 3.4.1, data of three sites are segregated for validation purpose.

4.2.2.1 Modeling of LG with $\bar{v}$ and CS

The modeling of *LG* with *CS* and $\bar{v}$, can be represented as a composition of deterministic part and a stochastic part.

Deterministic part can be represented by choosing a suitable polynomial function. Single degree polynomial functions are found to be reasonably fit the scatter plot, since increasing degree of equation for both the variables does not significantly improve R^2 value of the fit. General equation of curves is given in Equation 4.4, where *a* and *b* are coefficients of $\bar{v}$ and *CS*, respectively, *c* is the constant term; and φ is residual term about the best fit curve.

$$LG = a\,(\bar{v}) + b(CS) + c + \varphi \qquad \ldots 4.4$$

A sample curve fit (snapshot from MATLAB software) for the car-car plot is shown in Fig. 4.15. A similar trend is also observed for other vehicle pairs.

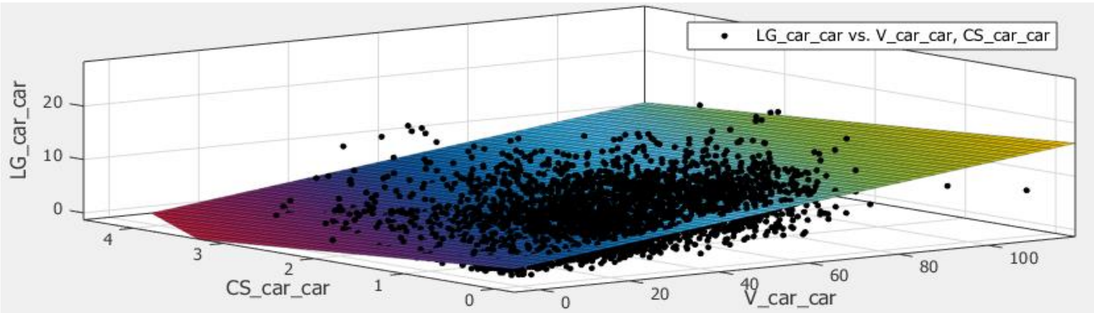

Fig. 4.15 Scatter plot and deterministic curve of model for longitudinal gap with centerline separation and speed

4.2.2.2 Residual analysis

The residuals obtained from subtracting obtained *LG* from actual field value of *LG* are calculated and need to be modeled. Since the samples are large in number (>100) the normality test on residuals is not relevant.

The plot of residuals against the longitudinal gap (from the regression equation) is given in Fig. 4.16 (a). Applying the Goldfeld Quandt (GQ) test on the residuals, (F-test between divided sample) gives F_{GQ} for lower 3/8th data and middle 1/4th data as 3.449, whereas F_{GQ} for middle 1/4th and higher 3/8th data as 1.842. These values are greater than $F_{critical}$, which is 1.114 at 5% significance. Thus, it can be concluded that the residuals are heteroskedastic. The heteroscedasticity is also visible in Fig. 4.16(a). If *LG* increases, the spread of residuals decreases, because at higher *CS* and lower average speed levels, vehicles tend to follow closer to the LV because the confidence of veering quickly to the side of FV on sudden braking by FV is higher. Thus higher values of longitudinal gap are not observed. If a higher value of *LG* at higher *CS* is observed, there is a possibility that there is no interaction between the vehicles. Thus, the spread of residuals decreases at lower *LG* levels. Residuals (φ) are calculated, and divided by (1+ $a\,(\bar{v}) + b(CS) + c'$) for addressing the concern of heterogeneity. New residual terms are calculated and plotted in Fig. 4.16 (b). They are compared with commonly observed distributions in Fig. 4.16 (c). It is observed that they follow a distribution statistically similar to Burr distribution (4-parameter) at good significance levels by K-S test. Similar fits are observed by changing the LV and FV pair. General form of equation of Burr distribution (frequency distribution about the regression plane) is mentioned in Equation 4.5.

$$f(x) = \frac{\alpha k \left(\frac{x-\gamma}{\beta}\right)^{\alpha-1}}{\beta\left(1+\left(\frac{x-\gamma}{\beta}\right)^{\alpha}\right)^{k+1}} \qquad \ldots 4.5$$

The possible reason for obtaining a Burr distribution is, there is restriction on *LG* on one side that *LG* cannot be negative, whereas on the other side, there is no upper limit for maintaining *LG*. This is the property of Burr distribution.

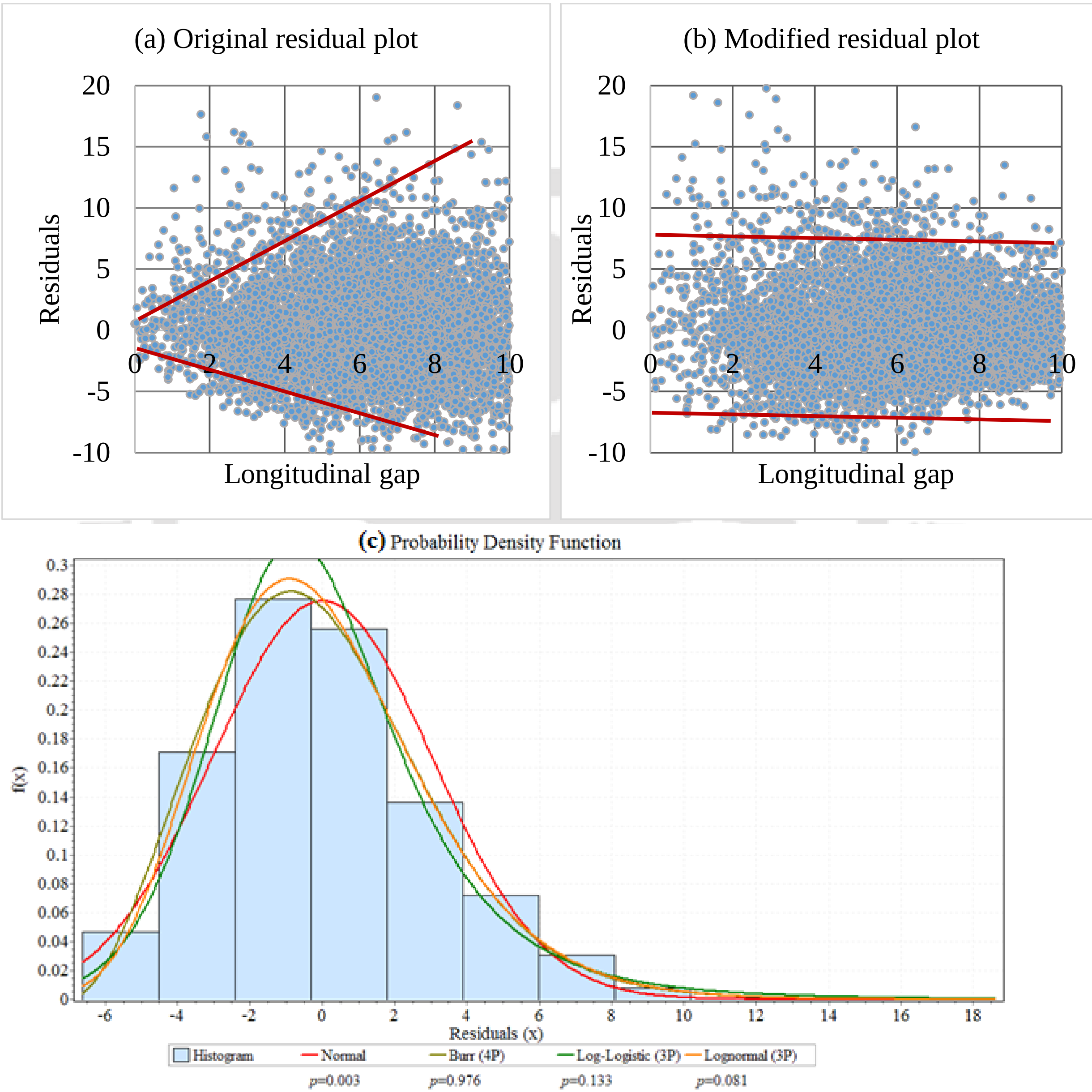

Fig. 4.16 Residual plot of longitudinal gaps, and transformations (a) Original plot, (b) plot after modification, (c) residual distribution compared with standard distributions

Coefficients *a*, *b*, *c* of Equation 4.4 and parameters of Burr distribution (from Equation 4.5) for different LV and FV pairs are shown in Table 4.11. The last row presents the *p*-value of fit of observed data with fitted Burr distribution with the coefficients.

Table 4.11 Coefficients and residual parameters for plot of *LG* with *CS* and speed.

LV	FV	Sample size	Coefficients of Equation 4.4 (Modelled data)			Burr (4P) distribution parameters of modified residuals				
			a	*b*	*c*	*k*	α	β	γ	*p-value*
Car	Car	4356	0.11	-1.25	3.38	1.25	3.37	1.13	-1.15	0.091
3W	Car	2187	0.03	-1.05	6.09	5.96	1.95	2.68	-1.02	0.145
2W	Car	1885	0.04	-0.5	3.97	6.88	1.67	3.32	-1	0.409
LCV	Car	512	0.08	-1.42	4.26	3.44	1.95	1.91	-1.02	0.211
Heavy	Car	617	0.17	-0.8	1.78	1.55	3.19	1.14	-1.02	0.714
Car	3W	345	0.08	-1.62	4.38	12.21	1.56	5.14	-0.96	0.048
Car	2W	489	0.07	-0.3	2.5	15.47	1.63	5.87	-1.01	0.085
Car	LCV	220	0.11	-1.05	2.81	3.13	2.22	1.78	-1.07	0.331
3W	3W	608	0.01	-1.23	7.23	168.74	1.54	30.92	-1.01	0.896
3W	2W	291	0.09	-1.01	1.73	0.91	3.29	0.75	-0.94	0.423
2W	3W	117	0.04	-1.28	4.32	133.19	1.51	28.85	-1.02	0.035
Heavy	Heavy	108	0.26	-1.52	2.66	2.81	3.59	1.84	-1.34	0.064
2W	2W	89	0.03	-0.21	3.32	3.73	1.54	2.2	-0.99	0.101

4.2.2.3 Interpretation of obtained results

From Table 4.11 one can infer the following results about longitudinal gap-maintaining behavior of different vehicle types during staggered vehicle-following-

- It is observed from the obtained coefficients *a* and *b* for all vehicle pairs in Table 4.11, and also in Fig. 4.15 that *LG* increases with the increase in $\bar{v}$ or decrease in *CS*. As *CS* increases, driver of FV feels more confident of a veering maneuver on sudden stopping of LV, thus, he/she can maintain lesser *LG*. At higher speeds, drivers are more cautious so *LG* increases with increase in $\bar{v}$.
- There is higher sensitivity to speed when heavy vehicles are being followed, as is evident from values of the coefficient *a* in Table 4.11. On the other hand, it is observed that sensitivity to speed when three-wheelers and two-wheelers are being followed is less, maybe due to smaller size of three-wheelers and two-wheelers. For example, there is a *LG* gain of just 0.3 m for a speed increase of 10 km/h when a car follows three-wheeler (at *CS*=0), but the *LG* gain is 1.1 m when a car follows another car for the same speed increment.
- There is higher sensitivity to centerline separation (as evident from high absolute values of coefficient *b*), when three-wheelers follow cars, other three-wheelers, or two-wheelers; or when cars follow LCVs. This higher sensitivity is also observed in case of heavy vehicles.

On the other hand, two-wheelers are less sensitive to centerline separation change when they follow or are being followed. The reason for this may be due to lesser width of a two-wheeler, it needs to veer less for overtaking maneuver, thus maintaining *LG* with a two-wheeler does not change significantly with change in centerline separation.

- It is observed that vehicles maintain comparatively less longitudinal gap with smaller vehicles (such as two-wheelers) than with larger vehicles like cars or LCVs or trucks. At 30 km/h and zero *CS*, *LG* for 2W-car, car-car, LCV-car and heavy vehicle-car pairs are 5.18 m, 6.67 m, 6.68 m and 6.88 m, respectively.

4.2.2.4 Road-width wise variation of LG with CS and speed

The variation of *LG* with *CS* and speed is conducted for car-car pairs segregated site-wise with different road widths. The data are presented in Table 4.12. It is observed that there is no significant and observable trend followed by either the slopes and intercepts or the actual *LG*, with an increase in road width. A conclusion can be made that longitudinal gap-maintaining behavior may not depend on the width of roadway, and is purely a vehicle-dependent characteristic. (coefficient of correlation of *LG* with width of road is 0.01).

Table 4.12 Road width wise classified variation of *LG* with *CS* and speed

Road Section	Width of road (m)	Coefficients of Eq. 5.6 for car-car pair		
		a	*b*	*c*
PCMC, Pune	7.3	0.129	-1.271	2.995
Guwahati bypass	7.4	0.213	-1.538	0.040
Rajajinagar, Bangalore	7.6	0.214	-1.069	0.003
Mhatre pul, Pune	7.8	0.293	-0.409	0.230
EM bypass, Kolkata	8.1	0.155	-1.544	0.985
Pune bypass	8.2	0.154	-0.510	0.057
Shivajinagar, Pune	9.0	0.176	-0.681	0.099
JVLR, Mumbai	10.8	0.125	-0.946	0.019
Mekhiri circle, Bangalore	11.2	0.165	-0.723	0.265
Ballygunge, Kolkata	12.1	0.169	-0.179	0.120
Link road, Mumbai	14.1	0.172	-0.019	0.229
Western Express Highway, Mumbai	17.5	0.067	-1.464	5.271

4.2.3 Validation of variation of *LG* with *CS* and speed

1000 data-points corresponding to each vehicle-pair for different *CS* (0-4 m) and $\bar{v}$ (0-80 km/h) ranges are generated randomly using coefficients from Table 4.11 and the equations 4.4 and 4.5, and longitudinal gap is calculated. This is termed as 'modeled data' and used to compare with validation data from field.

As described in Section 3.4, data of three locations- Bellary road in Bangalore, Old Bombay-Poona Highway in Pune, and Linking road Mumbai from Table 3.4 are separated for validation, whereas data from remaining sites are used for model development. The validation is conducted in two parts- (i) Statistical similarity of overall data at different *CS* and $\bar{v}$ ranges; and (ii) Similarity of distributions of residual terms.

4.2.3.1 Validation of overall dataset

For determining similarity between the dataset of validation and model, modeled data and raw data of validation are discretized into groups of different *CS* and $\bar{v}$ levels. T-test is applied between the two datasets at various levels, for the null hypothesis that means of two samples are significantly equal. Highlighted cells in Table 4.13 indicate the rejection of null hypothesis.

Table 4.13 T-test between modeled data and validation data for different *CS* and speed levels

Vehicle pair (LV-FV)		Car-Car				Car-2W			Car-3W		
CS, m		0-1	1-2	2-3	3-4	0-1	1-2	2-3	0-1	1-2	2-3
Speed range, km/h	0-20	0.00	0.12	0.26	0.37	0.06	0.71	N.D.	0.49	0.32	0.15
	20-40	0.00	0.79	0.26	0.00	0.02	0.16	0.46	0.08	1.00	0.11
	40-60	0.29	0.22	0.00	0.07	0.87	0.01	0.01	0.00	0.07	N.D.
	60-80	0.00	0.00	0.00	0.03	N.D.	0.46	N.D.	N.D.	N.D.	N.D.
	80-100	0.37	N.D.	0.48	N.D.	N.D.	N.D.	N.D.	N.D.	N.D.	N.D.
Vehicle pair (LV-FV)		2W-3W			2W-Car			3W-Car			
CS, m		0-1	1-2	2-3	0-1	1-2	2-3	0-1	1-2	2-3	3-4
Speed range, km/h	0-20	0.27	0.22	N.D.	0.00	0.00	N.D.	0.55	0.82	N.D.	N.D.
	20-40	0.24	0.84	0.46	0.01	0.10	0.29	0.00	0.15	0.02	0.02
	40-60	0.47	0.00	0.17	0.01	0.15	0.77	0.86	0.00	0.00	0.38
	60-80	N.D.	N.D.	N.D.	0.07	0.87	0.25	N.D.	0.05	0.17	N.D.

N.D. Indicates no data available from validation dataset for comparison.

In Table 4.13, for every vehicle pair, highlighted cells (significantly different data) are less in number than non-highlighted cells (significantly similar dataset) (total 44 of 66 cells show similarity in data). A conclusion can be derived that, the datasets used for validation and modeled data are significantly similar for majority of vehicle pairs.

4.2.3.2 Validation of residuals

Since residuals are not normal, K-S test is used for comparing the distributions of field data with distribution of modelled data (Antoniou *et al.*, 2014). Table 4.14 presents K-S test results conducted at 5% significance.

Table 4.14 Validation of relationships for longitudinal gap with centerline separation and speed

LV	**FV**	**Sample size (validation data)**	**Coefficients of Equation 4.4**			***p*-value after validating residuals for K-S test**
			a	***b***	***c***	
Car	Car	2331	0.085	-1.051	4.449	0.073
Car	3W	106	0.063	-0.003	2.814	0.314
2W	Car	118	0.077	-0.944	4.627	0.063
2W	2W	266	0.023	-0.781	4.445	0.081
2W	3W	108	0.042	0.463	2.922	0.21
3W	Car	302	0.101	-0.748	2.953	0.548
Car	2W	103	0.031	-1.423	3.919	0.881

From Table 4.14, it is observed that for all vehicle pairs, the residuals of validation data can replicate modelled dataset. Thus, the models are well validated for overall mean and residuals.

4.2.4 Optimal position of FV in steady state flow using developed model

From the above discussions, one may obtain the position of FV corresponding to the estimated longitudinal gap to be maintained by FV, if information about centerline separation and average speed is available. This longitudinal gap is estimated as per the best-fit plane given in Equation 4.4. In other words, using Equation 4.4, one can calculate the position of front center of FV under these *CS* and $\bar{v}$ values, for a steady state vehicle-following. If locus of all such points is found for different values of centerline separation (at a particular speed), it will be a pair of straight lines with opposite slopes, intersecting at the backside of centerline of LV, as shown in Fig. 4.16. This intersection point will correspond to zero *CS* and maximum *LG*. The domain of these straight lines will be restricted to the back edge of leading vehicle (or zero *LG* and maximum *CS*). On increasing the average speed, threshold locus moves away from the LV, as per positive value of coefficient *a* in Equation 4.4. Fig. 4.17 shows the loci for longitudinal position of FV's front center, at different speed levels. This discussion is for a FV driver who is having behavior corresponding to the best fit line. The residual plot helps to quantify driver behavior. To quantify the aggressiveness of driver, risk factor can be considered in the form of percentile of data. Average-behaved driver will have behavior 50th percentile data, or 50% of longitudinal gaps below his/her behavior. The highest risk-taking driver will have 100% *LG* maintenance data below his/her *LG* maintained. The discussion about risk taking is further mentioned in the next chapter.

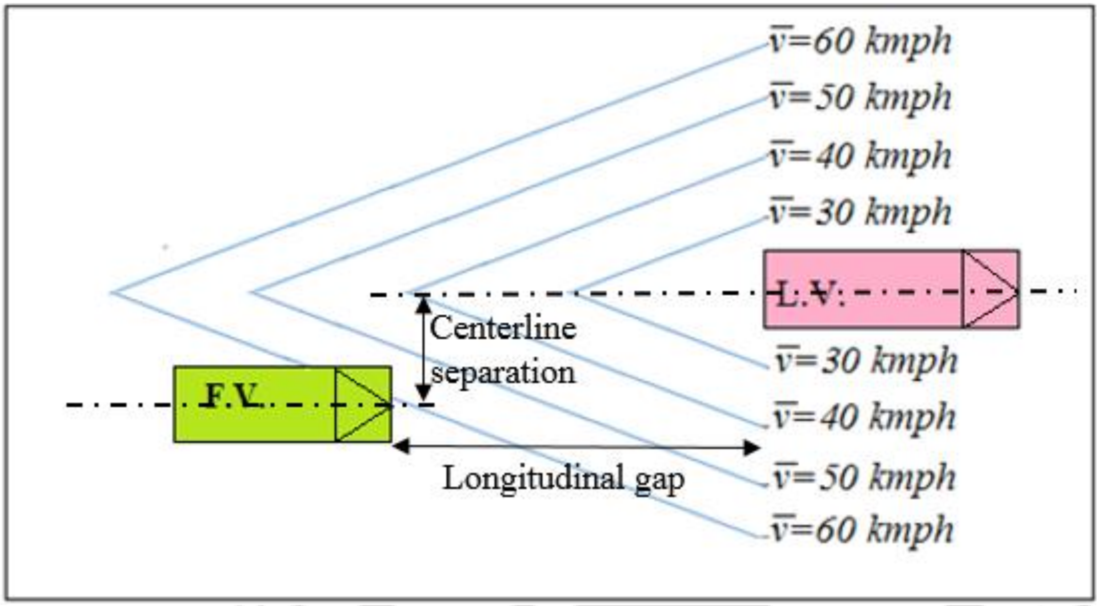

Fig. 4.17 Loci of FV's front center, with varying average speeds

4.2.5 Multiple vehicle interactions in mixed traffic stream

The recorded videos from five different locations were also used to extract multiple vehicle interactions, that is, an FV following two LV's, namely LV_1 and LV_2. This phenomenon can be frequently observed in mixed traffic stream with higher density. During multiple vehicle interactions, when FV approaches LV_1 and LV_2, it has a fixed *CS* with each of the vehicles, CS_1 and CS_2. If only pairwise interactions are considered, then corresponding to individual vehicle pairs (FV-LV_1 pair, and FV-LV_2 pair) two *LG*'s would be obtained, assuming that there is no second LV. This illustration is showed in Fig. 4.18.

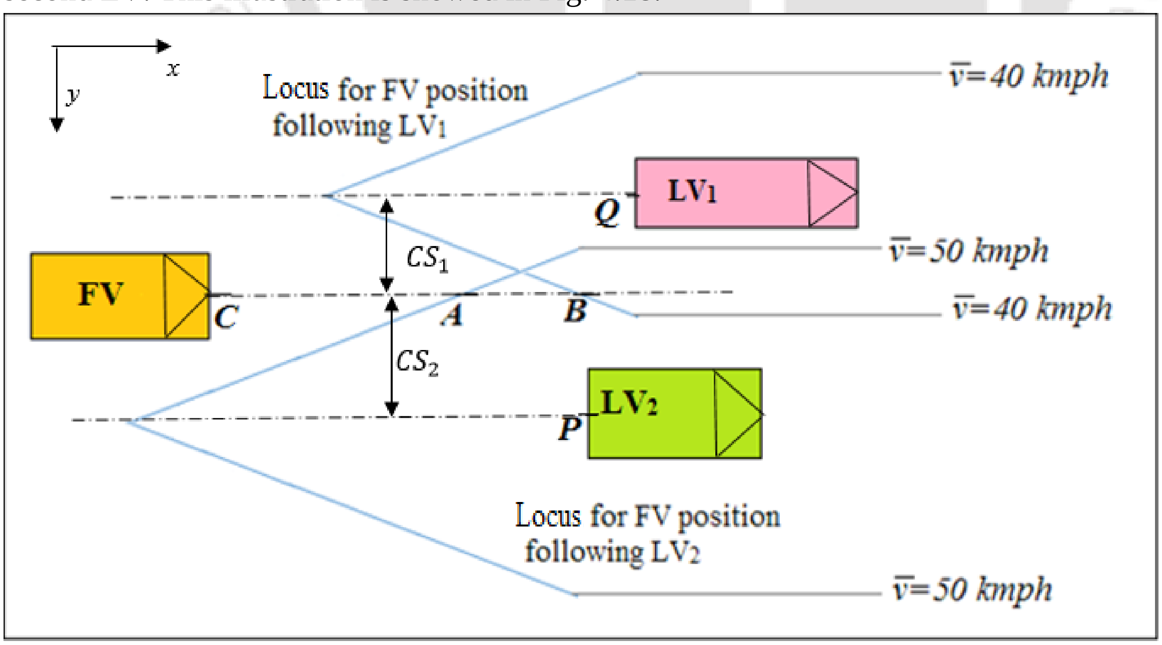

Fig. 4.18 Locus of FV in the presence of multiple LVs in vehicle-following case

In this subsection, two values of LG's are compared-

- Corresponding to FV following only one LV (LV_1 or LV_2) assuming the other LV is absent. This is denoted by LG_{single}. The values of these LG's are obtained using the relationships developed in Section 5.2.3. Since CS_1, CS_2, $\bar{v}_1$, $\bar{v}_2$ obtained from field data, LG_1^{single} and LG_2^{single} can be calculated using Equation 4.4 and coefficients from Table 4.11. They are represented by $(x_Q - x_B)$ and $(x_P - x_A)$, respectively, in Fig. 4.18. Since it is a pairwise representation assuming the third vehicle is absent, the data of LG_1^{single} and LG_2^{single} are merged. This condition is known as unconstrained condition.
- The second group of longitudinal gaps are the actual LG maintained by FV in the field with each of LV_1 and LV_2. They are denoted by LG_1^{double} and LG_2^{double}, respectively. It is represented by $(x_Q - x_c)$ and $(x_P - x_C)$, respectively in Fig. 4.18. LG_1^{double} and LG_2^{double} are measured during data extraction from field. The data of LG_1^{double} and LG_2^{double} are merged. They are segregated depending upon different statistically significant combinations of type of LV and FV. This condition will be referred as constrained condition.

4.2.5.1 Development of model for pairwise following at constrained conditions

In this subsection, the presence of second LV is not considered quantitatively in the form of vehicle type, or *LG* and *CS* maintained by FV with it, while following the system of two LV's. Data of relationship of LG_1^{double} with CS_1 and $\bar{v}_1$ and that of LG_2^{double} with CS_2 and $\bar{v}_2$ are combined to make a model to represent constrained condition of vehicle-following. The model consists of a deterministic part in the form of a best-fit line and a stochastic part in the form of residual distribution similar to Equation 4.4. Single degree polynomial functions are found to be reasonably fit the scatter plot. General equation of curves is given in Equation 4.6, where *a* and *b* are coefficients of $\bar{v}$ and *CS,* respectively, *c* is the constant term; and *φ* is residual term about the best fit curve.

$$LG^{double} = a\,(\bar{v}) + b(CS) + c + \varphi \qquad \ldots 4.6$$

The model is calculated for different LV-FV pairs of significant data (>50 data points). Residuals are calculated and they are found to be heteroscedastic. As *LG* increases, the spread of residuals also increase, since longitudinal safety margin for following vehicles to follow increases. Necessary adjustment for heteroscedasticity was made. Residuals were divided by obtained value of *LG* i.e., divided by $a(\bar{v}) + b\,(CS) + c$'. Modified residuals are found to be Burr-distributed. The model was developed for several vehicle pairs, namely each vehicle type followed by car, car followed by three-wheeler, two-wheeler and LCV, and three-wheelers and two-wheelers following each other. The obtained set of parameters of model for each pair is mentioned in Table 4.15. Parameters of obtained model for FV following LV in constrained case are also validated. 30% field data are kept separate for validation and not used in model development. Vehicle pairs (LV-FV) having significant dataset (>50 data-points) for validation include car-car, car-3W, 3W-car, car-2W and 3W-2W. Model is developed for the validation data also, and mentioned in Table 4.15.

Table 4.15 Coefficients of model equation for vehicle-following in constrained case

LV	FV	Sample size*	Coefficients of Equation 4.6 (Modeled data)			Burr (4P) distribution parameters of modified residuals			
			a	***b***	***c***	***k***	***α***	***β***	***γ***
Car	Car	500	0.12	-1.13	1.18	3.83	4.31	21.23	-31.23
3W	Car	134	0.09	-1.88	3.21	156.23	4.42	27.02	-7.85
2W	Car	93	0.11	-1.24	1.13	63.84	3.5	22.91	-6.30
LCV	Car	88	0.06	-1.78	3.69	147.21	5.02	32.92	-11.20
Heavy	Car	55	0.13	-0.95	0.74	0.52	7.41	45.31	-74.54
Car	3W	137	0.09	-1.64	2.24	21.53	5.65	37.82	-61.29
Car	2W	138	0.04	-0.07	0.56	4.16	55.43	97.84	-94.61
Car	LCV	55	0.07	-1.65	4.08	4.16	12.87	24.99	-21.71
3W	3W	102	0.06	-1.37	2.40	26.43	6.76	19.46	-11.23
3W	2W	124	0.14	-1.52	0.02	4.20	5.47	10.46	-7.63
2W	3W	54	0.22	-0.49	3.32	35.11	26.47	55.70	-47.73
2W	2W	120	0.01	-0.96	1.46	35.95	9.92	21.31	-15.61
Validation data									
Car	Car	200	0.09	-1.75	3.64	3.25	11.94	25.37	-39.90
Car	3W	55	0.14	-1.86	3.04	0.48	8.86	61.83	-14.40
3W	2W	50	0.03	-1.13	1.92	0.69	20.09	15.07	-8.19
3W	Car	54	0.18	-1.45	1.22	41.71	8.09	20.52	-20.31
Car	2W	55	0.05	-1.94	3.12	189.21	4.625	27.22	-7.99

* Sample size for pairs apart from those chosen for validation include the entire dataset.

From Table 4.15, following conclusions can be derived-

- There is a higher intercept value when three-wheelers, LCVs or cars are being followed.
- There is a lower intercept value when two-wheelers follow other vehicles.
- Further, when two-wheelers follow or are being followed, there is less sensitivity with *CS* as compared to other vehicles, since they require less space to make a lateral movement.
- There are lower intercept values as compared with the unconstrained behavior observed in Table 4.11, since drivers could perceive situation behind LV with ease, if they are following two vehicles.

The validation exercise is mentioned in Table 4.16. For comparing whether the two datasets of model and validation are statistically different, raw data of both these datasets are discretized into groups of different *CS* and $\bar{v}$ levels. T-test is applied between the two datasets at various levels, for the null hypothesis that means of two samples are significantly equal. Highlighted cells in Table 4.16 indicate the rejection of null hypothesis. A conclusion can be derived that, the datasets used for validation and modeling are significantly similar for majority of vehicle pairs. Coefficients *a* and *b* of Equation 4.6 for validation and modeling are also similar, (as observed from Table 4.15).

There is difference in coefficient *c*, due to which the null hypothesis is rejected at lower *CS* and lower speeds (Table 4.16). 58 out of 67 cells in Table 4.16 show similarity in compared data.

Table 4.16 P-values of t-test between model and validation dataset for different *CS* and $\bar{v}$ levels for various vehicle pairs. N.D. indicates no data for comparison.

LV-FV Pair		(a) Car-car					(b) car-3W			
CS, m		0-1	1-2	2-3	3-4	4-5	0-1	1-2	2-3	3-4
Speed, km/h	0-12	0.00	0.86	0.89	N.D.	N.D.	N.D.	0.07	0.35	N.D.
	12-24	0.14	0.34	0.04	0.81	N.D.	N.D.	0.00	0.34	0.29
	24-36	0.00	0.13	0.37	0.59	N.D.	0.39	0.56	0.01	0.09
	36-48	0.60	0.79	0.00	0.68	N.D.	N.D.	0.80	N.D.	0.26
	48-60	0.40	0.00	0.09	0.25	0.07	N.D.	N.D.	N.D.	N.D.

LV-FV Pair		(c) Car-2W			(d) 3W-2W			(e) 3W-car		
CS, m		0-1	1-2	2-3	0-1	1-2	2-3	0-1	1-2	2-3
Speed, km/h	0-10	0.18	N.D.	N.D.	N.D.	N.D.	N.D.	0.10	N.D.	0.41
	10-20	N.D.	0.19	0.15	0.96	0.12	0.86	0.83	0.01	N.D.
	20-30	0.00	0.55	0.01	0.39	0.57	0.92	0.95	0.18	0.76
	30-40	N.D.	0.53	0.47	0.53	0.08	0.87	N.D.	0.89	0.39
	40-50	N.D.	N.D.	0.82	0.79	0.80	N.D.	N.D.	0.08	0.60

4.2.5.2 Comparison of relationships of single and multiple vehicle following

Parameters obtained in Table 15 are compared with *LG* for individual vehicle pairs (assuming no effect of LV_2) calculated mentioned in Section 4.2.2 (Table 4.11). For comparing whether the two datasets are statistically different, firstly the raw data of both the cases are discretized into groups of different *CS* and $\bar{v}$ levels. T-test is applied between datasets of constrained and unconstrained following, within each group. This exercise is carried for different vehicle pairs. Table 4.17 mentions parameters of T-test obtained. Highlighted cells indicate rejection of null hypotheses that means are significantly different.

Table 4.17 P-values of t-test between constrained and unconstrained vehicle following for different CS and $\bar{v}$ levels for various vehicle pairs. N.D. indicates no data for comparison.

LV-FVPair		(a) Car-car					(b) 3W-car				(c) 2W-car		(d) Car-2W		
CS, m		0-1	1-2	2-3	3-4	4-5	0-1	1-2	2-3	3-4	0-1	1-2	0-1	1-2	2-3
Speed, km/h	0-12	0.01	0.00	0.00	0.00	N.D.	0.77	0.31	0.00	N.D.	0.34	0.63	0.07	0.13	N.D.
	12-24	0.00	0.03	0.05	0.00	N.D.	0.02	0.00	0.05	0.01	0.10	0.36	0.00	0.01	0.06
	24-36	0.00	0.26	0.01	0.02	0.00	0.39	0.00	0.03	0.01	0.26	0.81	0.00	0.00	0.00
	36-48	0.30	0.00	0.20	0.00	0.00	0.45	0.73	0.15	0.14	0.58	0.01	0.00	0.44	0.00
	48-60	0.01	0.00	0.00	0.03	0.00	N.D.	0.00	0.13	N.D.	0.02	0.13	N.D.	0.02	0.02

LV-FVPair		(e) Car-3W			(f) 3W-3W			(g) 2W-2W		(h) LCV-car			(j) HV-Car		
CS, m		0-1	1-2	2-3	0-1	1-2	2-3	0-1	1-2	0-1	1-2	2-3	0-1	1-2	2-3
Speed, km/h	0-10	0.84	0.41	0.01	0.19	0.01	N.D.	N.D.	0.89	0.68	0.03	N.D.	0.84	0.44	N.D.
	10-20	0.00	0.00	0.05	0.03	0.00	0.01	0.00	0.02	0.46	0.28	0.62	0.27	0.45	N.D.
	20-30	0.29	0.78	0.00	0.03	0.01	0.05	0.00	0.00	0.11	0.03	0.01	0.56	0.06	0.27
	30-40	N.D.	0.60	0.37	0.46	0.01	0.50	0.00	0.00	0.45	0.79	0.06	N.D.	N.D.	N.D.
	40-50	0.75	0.52	N.D.	0.41	0.33	0.03	0.11	N.D.	0.67	0.99	0.56	0.30	0.69	0.65

From Table 4.17, it can be concluded that, for most vehicle pairs, there is observable difference at 5% significance levels (63 of 123 cells in Table 4.17). The difference is not significantly observed when two-wheelers are followed because vehicles actually do not feel the constraining due to two-wheelers, since two-wheelers are smaller in size. However, the difference is also not significantly observed in case of heavy vehicles like truck, bus and LCV being followed. This is because of the large size, constraining remains consistent, influence to follower is dominated by heavy vehicle, thus vehicles take greater precautions when closing in during following heavy vehicles and rather closely follow the other leading vehicle (if it is not a heavy vehicle).

Further, percentage decrease in LG for constrained case when compared with unconstrained case, is calculated and presented for a few vehicle pairs (cars following three-wheelers, two-wheelers, other cars, heavy vehicles, three-wheeler following three-wheeler, two-wheeler following three-wheeler) for various values of CS and $\bar{v}$. This information is obtained from the coefficients of best fit regression lines for constrained and unconstrained cases, from Table 4.11 and Table 4.15. The results are presented in Fig. 4.19. Similar results can be obtained for other vehicle type combinations too, mentioned in Table 4.15.

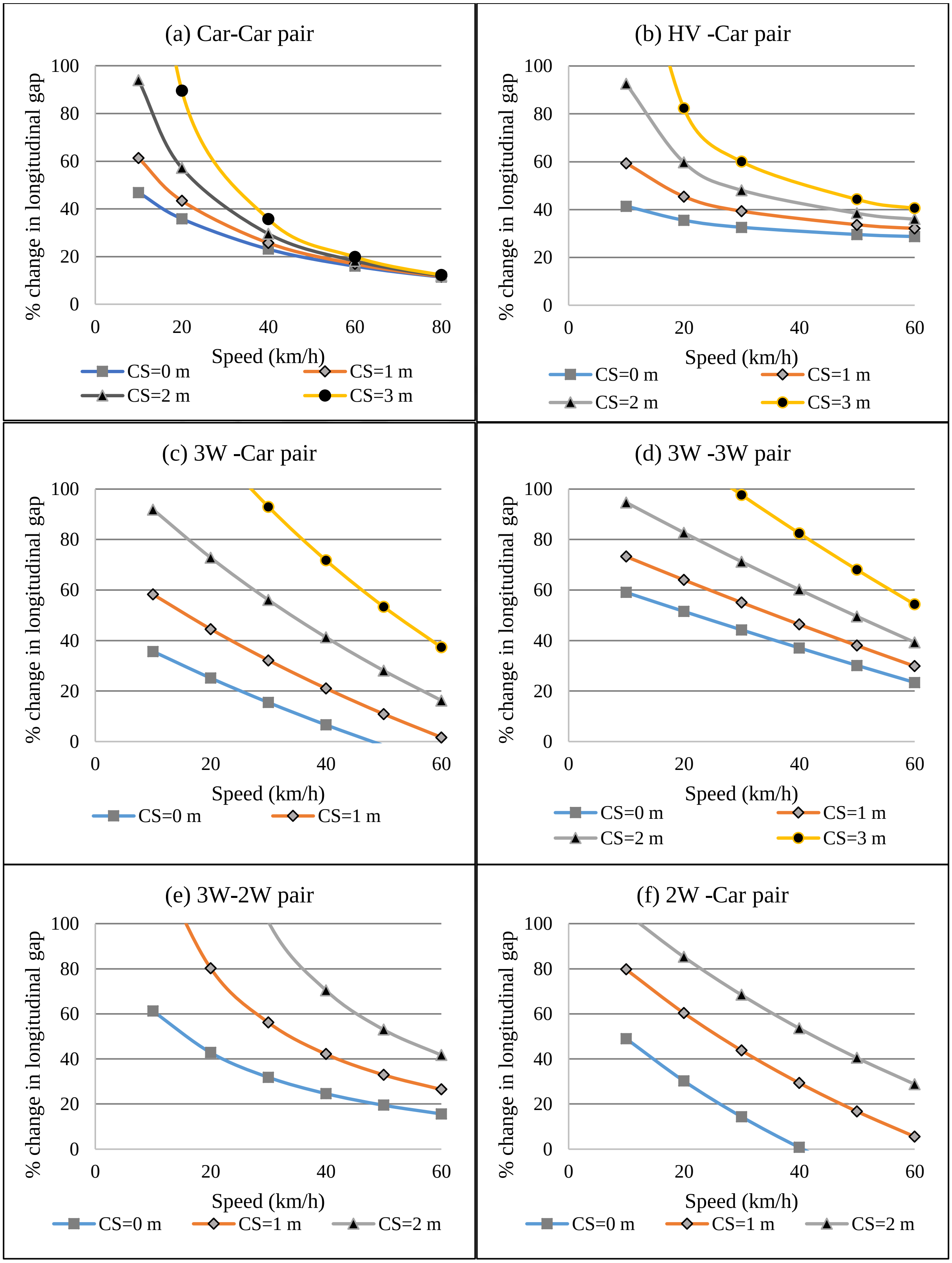

Fig. 4.19 Decrease in longitudinal gap during constrained following, for various vehicle pairs, at different speed and *CS* levels

It is observed that, for all the vehicle pairs, there is a general decrease in intercept in constrained conditions, as compared with unconstrained conditions. There is a higher percentage decrease of LG with increase of CS and decrease of $\bar{v}$. With decrease in speed, there is higher percentage decrease of LG because at lower speeds, aggressiveness to achieve desired speed may increase. Driver of FV tries to maximize speed at lower speed levels, so comes closer to LVs as compared with unconstrained situations. At higher CS levels, vehicle feels more comfortable since they can perceive situations ahead of LVs, thus decreasing the LG levels. If decrease is more than 100%, it indicates that front bumper of FV has crossed rear bumper of one of LV's, but FV is still following other LV. Such cases are ambiguous and not considered. Percentage decrease is more, when smaller size vehicles such as two-wheelers and three-wheelers are followed.

The reason for decrease in LG can be drawn to queuing patterns. When moving in a traffic stream with no lane discipline, there is a general observance of a diamond-shape queuing pattern. A driver of FV follows two LV's with a lower value of LG since he/she can clearly observe road space ahead of the LV's and anticipate the decisions of LV's with better precision or predictability.

4.2.5.3 Effect of level of constraining

In the previous section, no information about the third vehicle (i.e., second LV) was taken into consideration. The level of constraining is measured here as the amount of lateral clearance (CS_{LV}) between LV_1 and LV_2 which is equal to ($CS_1 + CS_2$). Average longitudinal gap ($\overline{LG}^{double}$) of LG_1^{double} and LG_2^{double} is used as the dependent variable. Average speed is taken as average of all three vehicles, $\bar{v}$. A single degree relationship was fitted with $\bar{v}$ and CS_{LV} as the independent variables. The regression equation obtained is represented by equation. 4.7, with Burr-distributed modified residuals, φ.

$$\overline{LG}^{double} = 0.061\,\bar{v} - 0.577\,CS_{LV} + 3.207\,\varphi \qquad \ldots 4.7$$

A negative coefficient with CS_{LV} implies a decrease of $\overline{LG}^{double}$ with an increase of CS. If lateral clearance between two LV's increases, then driver of FV would try to squeeze in his/her vehicle in between the two LVs. Risk associated with sudden braking of LV's reduce if CS increase. Further, due to higher CS_{LV}, FV can peep the scenario ahead and anticipate the LV's action. If the gap becomes larger than the width of FV (plus a safety psychological margin), the FV would pass through the gap in the overtaking mode, if it decides to overtake.

4.2.5.4 Representation of two leading vehicles as a single vehicle

An attempt is made to represent two LVs in the form of a single, combined vehicle system and it is checked whether its behavior matches with single vehicle vehicle-following. The result is conducted for both LVs as cars. Fig. 4.20 shows this representation. For this purpose, effective CS is taken as $CS_{EFF} = 0.5 \times |CS_1 - CS_2|$. CS_{EFF} gives the eccentricity between FV and combined vehicle system, or the lateral placement of centerline of FV with respect to centerline of system. Average longitudinal gap ($\overline{LG}^{double}$) of LG_1^{double} and LG_2^{double} is used as the dependent variable. Average speed is taken as average of all three vehicles, $\bar{v}$. This exercise is conducted for all three vehicle types as cars. Data are considered upto a certain range of constraining, or lateral clearance between the sides of both LVs is less than 3 m, so that the two vehicles are considered as a group by the FV, and not individual vehicles. A single degree relationship was fitted with $\bar{v}$ and CS_{EFF} as the independent variables. The regression equation obtained is represented by equation 4.8, with Burr-distributed modified residuals, φ.

$$\overline{LG}^{double} = 0.061\,\bar{v} - 0.187\,CS_{EFF}1.745 + \varphi \qquad \ldots 4.8$$

A negative coefficient with CS_{EFF} implies a decrease of $\overline{LG}^{double}$ with an increase of effective CS. It is observed that $\overline{LG}^{double}$ obtained for combined system at lower CS_{EFF} values (<2 m) is significantly less than LG_{single} (obtained from Table 4.11). However at higher CS_{EFF} levels (>3.5-4 m), the result matches with that obtained from LG_{single} at similar levels of CS_{EFF}. There is a rise in slope coefficient of CS_{EFF}.

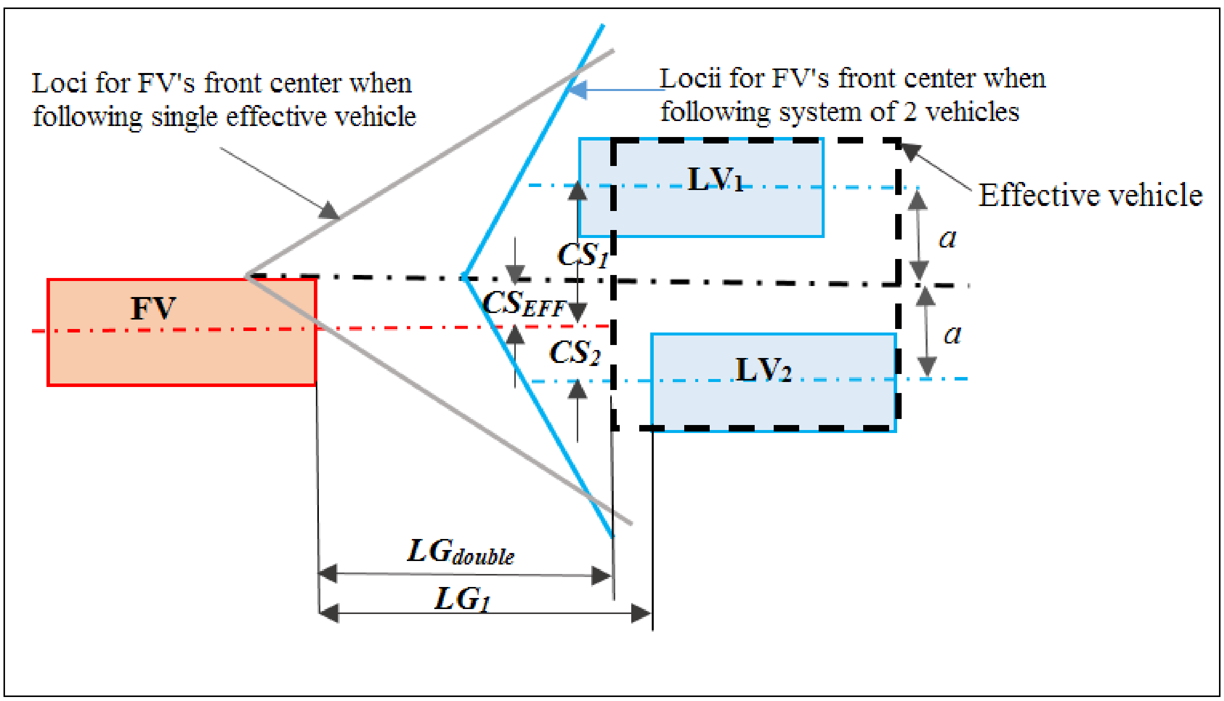

Fig. 4.20 Representation of system of two closely spaced leading vehicles as effective vehicle

The result can be interpreted as the situation in Fig. 4.20. Consider two cases, case 1, in which a car is following a system of two closely-spaced cars; and case 2, in which it is following a single hypothetical vehicle equal to the width of two cars plus the gap maintained in between them, with other characteristics similar to a car. Since the driver of FV will try to overtake, he/she will feel safer at higher CS_{EFF} and thus close-in to the system at higher values of CS_{EFF}. Hence with the increase in CS_{EFF}, the LG will decrease. At higher CS_{EFF} levels (>3m), driver of vehicle maintains similar LG as with case 2. However, at lower values of CS, in case 1, driver can peep in the gap and perceive situation of traffic with better precision, thus maintains lesser LG with the system than it will maintain with a single vehicle of equivalent width. In simulation models, if vehicle-following behavior with a group of similarly behaving vehicles is to be considered as a combined (aggregate) behavior with a large vehicle with average properties of all vehicles, then necessary adjustments to *LG* need to be provided at lesser *CS* values.

4.3 Overtaking decision-making criteria

Overtaking decision-making criteria study is conducted to assess the parameters influencing the decision to overtake for a following vehicle, when it is approaching the leading vehicle. Using the data extracted in Section 3.5, average speed, relative speed of LV and FV is calculated. A high correlation between speeds of LV and FV is observed, so average speed and relative speed are used as predictor variables instead of speeds of LV and FV. Longitudinal gap and centerline separation is also calculated and decision to overtake is noted as categorical input (1 or 2) at the instance the driver of FV is perceived to make a decision.

The analysis includes modeling, interpretation and validation of results. Logistic regression methods are used to estimate coefficients for predictor variables influencing decision to overtake, and are mentioned in the first subsection. Inferences drawn from these coefficients for different vehicle types, are mentioned in second subsection. The model is validated for car-car, 3W-3W and car-2W pairs in the third subsection.

4.3.1 Modeling of overtaking decisions

For various vehicle-types, log-odds (z) expresses the natural logarithm of the ratio between the probability that overtaking will not occur to the probability that it will occur. Predicted probability (p) of overtake occurring can be calculated by

$$p = 1 - [\frac{1}{1+e^{-z}}] \quad \text{…4.9 (a)}$$

where, z is log-odds to overtake and given by,

$$z = \ln\left(\frac{probability\ to\ follow}{probability\ to\ overtake}\right) = \beta_0 + \beta_1\bar{v} + \beta_2 v_{LV|FV} + \beta_3 LG + \beta_4 CS + \beta_5 H \quad \text{…4.9 (b)}$$

Using equation 4.9 one can obtain probability to overtake depending on various predictor variables. Probability to follow is obtained by subtracting probability to overtake from unity. The coefficients β_0, β_1,…, β_5 express the effects of the predictor variables- average speed ($\bar{v}$), relative speed ($v_{LV|FV}$), longitudinal gap (*LG*), centerline separation (*CS*), and hindrance to overtake (*H*); on the log odds of following versus overtaking (z). Logistic regression analysis is performed on each vehicle-pair, and the results obtained are mentioned in Table 4.18. Table 4.18 mentions the following-

- The first row mentions the vehicle type-wise leader-follower pairs used for analysis. The sample sizes used for analysis for each vehicle pairs are mentioned in the next row. The data of car-car, 2W-car and 3W-3W do not contain data kept separately for validation. Sample sizes of validation data for these pairs are 401, 62 and 51, respectively. Third row gives the deviance of fit of regression equation, which is a likelihood test giving the deviation of the fitted model with a saturated (intercept-only) model.

- The next set of rows states the values of estimated coefficients (β_0 to β_5) as per logistic regression technique, for each vehicle pair. Higher absolute value of coefficient indicates higher increase per unit change of the corresponding predictor variable. Negative value indicates decrease of the odds to follow, upon increase of corresponding predictor variable.
- The third set of rows gives the standard error of these coefficients for each vehicle pair.
- Data for each vehicle pair are separated as per decision to overtake or follow into two datasets. These two datasets for particular predictor variables are compared with each other using T-test, with the null hypothesis that they are significantly similar. The fourth set of rows mentions the *p*-value of this comparison, for each predictor variable and each vehicle pair. A *p*-value less than 0.05 indicates that the data for corresponding predictor variable for that vehicle pair, separated as per decision to overtake and decision to follow; are significantly different. It implies that drivers maintain statistically different values of these predictor variables during overtaking and during following.
- The fifth set of rows indicates percentage increase in odds to overtake, with 5% increase of predictor variable. 95% confidence intervals are calculated for the range of each predictor variable, and the increases are maintained at 5% of this confidence interval. This set of rows basically gives sensitivity of predictor variable on the decision to overtake. The values of last row in this set (for β_5) show increase of chances to overtake on introducing a hindrance to overtake.

Table 4.18. Overtaking decision model estimates for various vehicle-pairs

Vehicle types		Car-Car*	2W-Car*	3W-Car	LCV-Car	Heavy-Car	3W-3W*	Car-2W	3W-2W	2W-2W
Sample size		717	144	186	170	210	107	111	84	79
Deviance of fit		766.130	150.059	158.278	156.631	215.598	94.313	115.221	53.264	87.612
Estimated coefficients	β_0	-0.232	-0.669	-0.980	-2.078	-0.131	-1.522	-3.363	-5.747	1.021
	β_1	0.031	-0.003	-0.048	0.015	-0.001	0.085	0.007	0.000	-0.023
	β_2	-0.032	-0.142	-0.009	-0.099	-0.109	0.026	-0.060	0.029	0.012
	β_3	0.022	0.025	0.283	0.091	0.015	0.377	0.131	0.517	0.210
	β_4	-1.546	-0.392	-1.950	-2.066	-0.754	-3.982	0.408	-0.399	-1.779
	β_5	0.885	2.223	2.251	2.857	1.955	-0.266	1.606	3.834	-0.262
Standard error of coefficients	β_0	0.314	0.724	0.711	0.768	0.602	1.215	0.817	1.863	0.827
	β_1	0.008	0.019	0.022	0.016	0.014	0.046	0.023	0.050	0.023
	β_2	0.020	0.046	0.044	0.050	0.036	0.056	0.054	0.077	0.066
	β_3	0.029	0.075	0.080	0.074	0.053	0.124	0.077	0.171	0.097
	β_4	0.164	0.283	0.413	0.476	0.244	0.856	0.262	0.640	0.789
	β_5	0.205	0.478	0.478	0.600	0.386	0.567	0.533	1.080	0.600
p-value for coefficients	β_0	0.459	0.355	0.168	0.007	0.828	0.211	0.000	0.002	0.217
	β_1	0.000	0.866	0.031	0.355	0.948	0.062	0.774	0.994	0.337
	β_2	0.098	0.002	0.830	0.048	0.002	0.646	0.270	0.706	0.854
	β_3	0.458	0.735	0.000	0.223	0.773	0.002	0.089	0.002	0.030
	β_4	0.000	0.165	0.000	0.000	0.002	0.000	0.119	0.532	0.024
	β_5	0.000	0.000	0.000	0.000	0.000	0.639	0.003	0.000	0.662
% increase in odds to overtake, on 5% increase in predictor	β_0	N.A.	N.A.	N.A.	N.A.	N.A.	N.A.	N.A.	N.A.	N.A.
	β_1	-8.879	0.935	13.726	-4.354	0.273	-11.405	-1.879	0.077	7.753
	β_2	3.198	14.606	0.923	9.435	11.931	-2.819	6.278	-3.130	-1.289
	β_3	-1.888	-2.014	-16.790	-5.779	-1.330	-17.563	-11.689	-39.842	-21.226
	β_4	23.052	6.261	31.242	29.892	12.234	57.383	-6.738	5.583	13.697
	β_5	-58.709	-89.172	-89.468	-94.254	-85.844	30.495	-79.921	-97.838	29.963

* Data for these vehicle pairs do not include those kept aside for validation; N.A.=not applicable

To understand graphically the variation of decision to overtake with increase of each predictor variable, datasets are generated at different values of predictor variable, and probability to overtake is calculated and this trend is plotted in Fig. 4.21 for car-car pair, with varying each predictor variable, at presence or absence of hindrance, by keeping other predictor variables constant. The values for predictor variables kept constant are relative speed = 10 km/h, average speed = 40 km/h, centerline separation = 1 m, longitudinal gap = 20 m.

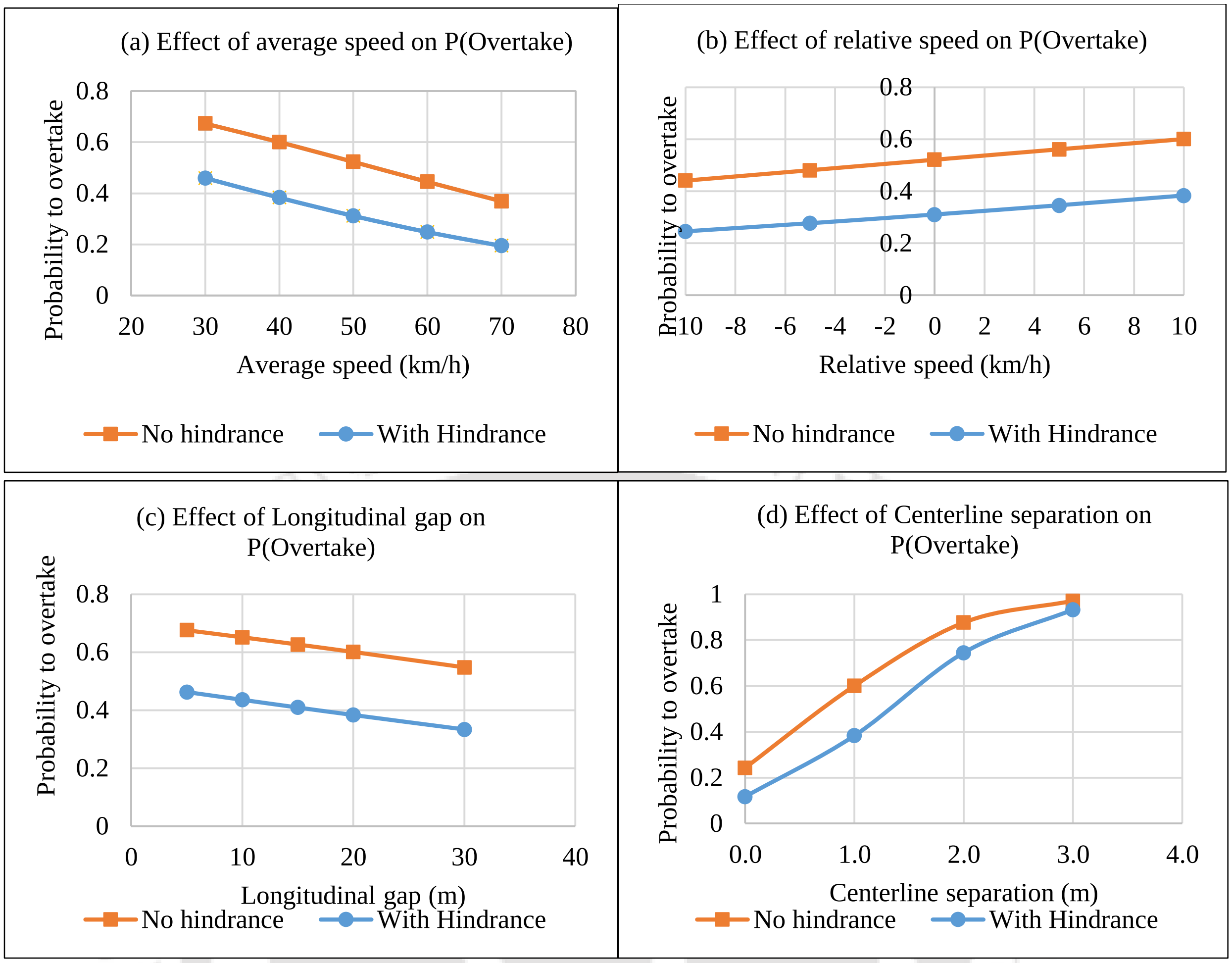

Fig. 4.21 Variation of probability to overtake with change in different predictor variables.

4.3.2 Interpretation of model estimates for various vehicle pairs

This subsection is divided into interpretation of obtained coefficients, their goodness of fit with respect to the decision to overtake, and sensitivity analysis.

4.3.2.1 Interpretation of obtained coefficients

From Table 4.18, various obtained coefficients for different predictor variables and different pairs can be interpreted as follows-

- The coefficient β_0 is the constant term, which indicates overall probability without the influence of any predictor variable. Its value is negative for almost all the pairs, indicating that vehicles have a greater overall tendency to overtake the LV than following it. The tendency is higher for two-wheelers overtaking cars or three-wheelers, or cars overtaking LCVs. The reason is, in mixed traffic conditions, two-wheelers can move in between the gaps of vehicles and seldom follow them. However, when a two-wheeler approaches other leading two-wheelers, it has overall more tendency to follow them. The value of β_0 has a higher standard deviation, indicating a larger variation in overall tendency of driver behavior to overtake.

- The coefficient β_1 indicates influence of average speed on odds to follow. It is observed that, generally, as average speed increases, odds to follow decrease (in case of car-car, LCV-car and car-2W pairs, which have a majority of traffic stream). However, in other vehicle pairs, it is seen to increase with the increase of average speed.
- The coefficient β_2 indicates influence of relative speed on odds to follow. There is increase of probability to overtake as relative speed increases in majority of vehicle pairs, as is evident from values of β_2. The reason behind this maybe that, as relative speed of FV with respect to LV increases, time to collision decreases and driver of FV may not feel comfortable following the LV, compelling him/her to decide to overtake.
- The coefficient β_3 indicates influence of longitudinal gap on odds to follow. For all vehicle types, as longitudinal gap increases, probability to overtake decreases. Predicted values of β_3 are positive. There is greater decrease for vehicles following a slow-moving vehicle such as three-wheeler.
- The coefficient β_4 indicates influence of centerline separation on odds to follow. Its value is negative for all the vehicle pairs, indicating that as centerline separation increases, odds to follow decreases. This is evident from the fact that when FV approaches LV with a higher centerline separation, the drivers can easily perceive overtaking situation ahead, and the they require lesser maneuvering for overtaking the LV. Thus, tendency to make an overtaking decision increases. There is greater increase if a faster-moving vehicle type (car) is following a slower-moving vehicle (three-wheeler, LCV). However, the sensitivity is less for a two-wheeler following other vehicle. This is because as centerline separation increases after certain amount, the LV will no longer affect position of two-wheeler, or in other words, there would not be any vehicle-following. The weak lane disciplined behavior is evident from this observation of coefficient of β_4.
- The coefficient β_5 indicates influence of presence of hindrance on odds to follow. Its value is positive for most of the vehicle pairs. This indicates that presence of hindrance (categorized as 1) strongly dissuades the decision to overtake.

4.3.2.2 Interpretation of goodness of fit of variables

From Table 4.18, if the obtained *p*-value is less than 0.05, it implies that drivers maintain statistically different values of particular predictor variables during overtaking and during following. It is observed that the *p*-value for average speed and longitudinal gap is high in several vehicle pairs, implying that these variables have little impact on the decision to overtake. The driver will not solely decide to overtake on these factors. This inference matches with those obtained by Bar-Gera and Shinar (2005). On the other hand, *p*-value for centerline separation and hindrance to overtake is less than 0.05 in several vehicle pairs, implying that drivers can perceive hindrance and centerline separation with more precision and may take the decision to overtake mostly based on these factors.

4.3.2.3 Sensitivity analysis on various predictor variables

In Table 4.18, sensitivity analysis is conducted by checking percentage increase of odds to overtake, on increasing the predictor variables by 5% of their confidence interval range. This is carried to compare the effect of various variables on the decision to overtake with each other. It is observed that for all vehicle pairs, the introduction of a hindrance to overtake severely impacts the decision to overtake. The decision to overtake also depends on centerline separation; since on increasing centerline separation by 5%, there is 5.6-57.4% increase in the odds to overtake. Most vehicle pairs are more sensitive to a hindrance to overtake and centerline separation than other variables. Relative speed is more significant variable, when the LV is a two-wheeler; whereas, when two-wheelers are the FV, they are more sensitive to longitudinal distance than other variables. A slight change in relative speed will compel the FV to overtake a two-wheeler (since it is easier to overtake than other vehicles). On the other hand, two-wheelers have a very low tendency to follow (as discussed in 4.2.1) and try to find gaps to avoid following; thus, their decisions are sensitive to change in longitudinal gap.

4.3.3 Validation

The validation includes a check for effectiveness of model using residual interpretation and calculating percent correct predictions for model data and a separate dataset for validation.

4.3.3.1 Check for effectiveness of model

To check the effectiveness of the model, Pearson's residual values are calculated, and their details (standard deviation and percentage absolute values above 2.0) are mentioned in Table 4.19. It is observed that for all vehicle pairs, less significant amount of residuals has the undesirable absolute value greater than 2. The standard deviation is also less than one for most vehicle pairs. In order that modeled coefficients (β_0, β_1,…, β_5) fit the existing data well, the decision to overtake was modeled based on the criteria that overtaking decision is made when probability of overtaking exceeds probability of follow (or exceeds 0.5). The decisions are checked for all vehicle pairs and the percentage of correct predictions are given in Table 4.19.

Table 4.19 Effectiveness of modeled coefficients on model and validation data

Vehicle types		Car-car	2W-Car	3W-Car	LCV-Car	Heavy-Car	3W-3W	Car-2W	3W-2W	2W-2W
Pearson's residuals	Standard deviation	1.003	0.963	0.898	0.944	0.976	0.902	0.416	0.327	0.436
	% Absolute values above 2.0	5.858	0.697	1.115	0.976	1.534	0.697	0.000	0.000	0.000
% correct predict-tions for	Model data	75.014	71.224	78.378	77.778	75.714	76.415	75.891	90.271	74.683
	Validation data	80.376	68.306	N.A.	N.A.	N.A.	62.500	N.A.	N.A.	N.A.

N.A.=Not applicable.

4.3.3.2 Cross-validation

The same exercise as mentioned in 4.3.1 is used to predict responses of the validation dataset, which is not used for modeling purpose. Coefficients obtained from regression model are used to model the new dataset used for validation. Percentage correct predictions are given in Table 4.19. For all the vehicle pairs, model can correctly predict behavior higher than the null model which gives a random value prediction (50% accuracy). The average prediction rate is comparable to the model data.

4.4 Other parameters evaluated from field data

From the field traffic video recording, other vehicle parameters such as lateral speed of vehicles, desired speed, etc., are calculated by means of camera calibration technique. They are discussed in detail below.

4.4.1 Lateral speed

Lateral speed is the speed with which vehicle traverses laterally during any overtaking or veering maneuver. During a particular veering phenomenon, lateral speed is assumed to be constant for a particular vehicle. When data for vehicle-following behavior were extracted, veering speeds were also noted as per Equation 4.10.

$$Lateral\ speed = \frac{\text{Absolute difference in lateral position of vehicle}}{\text{difference in time−stamp}} \quad \ldots 4.10$$

These lateral speeds depend upon driver behavior and vehicle types, and are found to observe negative exponential distribution. (General form as per Equation 4.11). In equation 4.11, λ is the decay rate of negative exponential distribution. Parameters of lateral speed for various vehicle types are provided in Table 4.20.

$$f(x) = \lambda e^{-\lambda x} \quad \ldots 4.11$$

Table 4.20 Parameters of distribution of lateral speed during overtaking

Vehicle type	Lateral speed during overtaking		
	Mean, m/s	85th percentile (m/s)	λ, overtaking
Three-wheeler	1.082	2.848	0.624
Car	1.033	2.825	0.677
Bus	1.034	2.729	0.677
Two-wheeler	1.233	3.253	0.568
Truck	0.935	2.467	0.749
LCV	1.030	2.717	0.680

From Table 4.20, it can be inferred that smaller sized vehicles like two-wheelers and three-wheelers have higher lateral speeds than larger sized vehicles. Mean overtaking lateral speed is always higher than the lateral speed while adjusting to follow a leading vehicle.

4.4.4 Overtaking time

During data-extraction for lateral clearance, the time required to overtake a particular vehicle was also calculated as a difference in time between start of detection of first sensor and end of detection of last sensor for a particular vehicle interaction, as shown in Fig. 4.22.

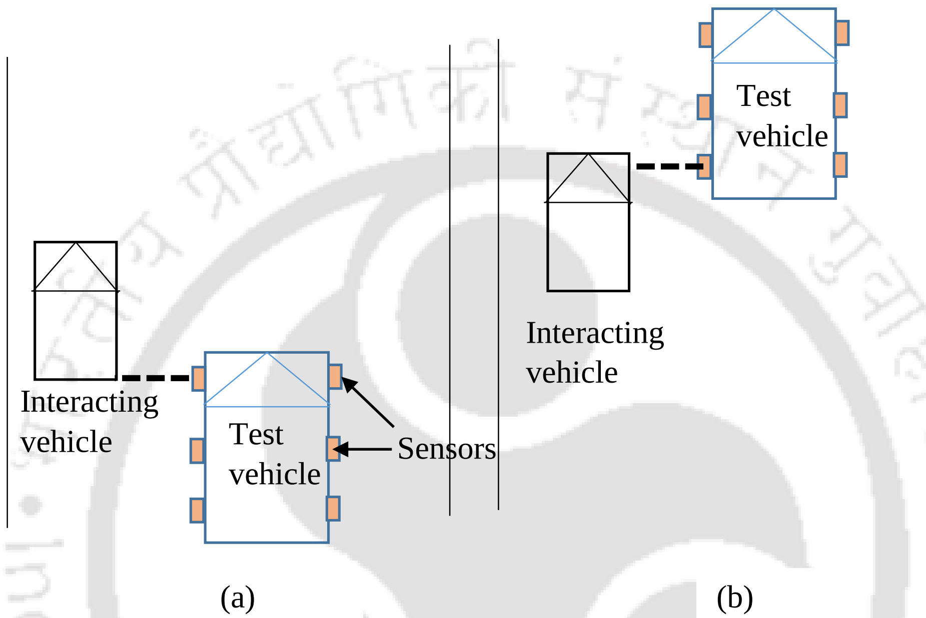

Fig. 4.22 (a) Starting and (b) ending condition for calculation of overtaking time

For all overtaking maneuvers, overtaking time distribution is observed to follow log-logistic distribution (two parameters). The general equation of this distribution is shown in Equation 4.12. The variation is studied and given in Table 4.21. Vehicle pairwise relationships are calculated. First vehicle indicates overtaking vehicle and second vehicle indicates overtaken vehicle.

$$f(x) = \frac{\alpha}{\beta}\left(\frac{x}{\beta}\right)^{\alpha-1}\left(1+\left(\frac{x}{\beta}\right)^{\alpha}\right)^{-2} \qquad \ldots 4.12$$

It is observed from Table 4.21 that mean overtaking time is lower for smaller size vehicles such as three-wheelers and two-wheelers. This parameter is crucial since, during overtaking, vehicles tend to avoid travelling parallel to each other. Using 85th percentile data of overtaking time, one can obtain the desired time for which vehicle can stay side by side with another vehicle. This will obtain the desired speed necessary to overtake a vehicle travelling at a particular speed, to avoid discomfort due to travelling side-by-side.

Table 4.21. Parameters of log-logistic distribution for overtaking time required (in seconds)

Vehicle pair	Parameters of log-logistic distribution		p-value	Sample size	Time to pass (seconds)	
	α	β			Mean	85th percentile
3W-3W	1.59	1.918	0.137	77	1.90	12.30
3W-2W	1.715	1.888	0.563	215	1.88	10.58
Car-2W	1.968	2.177	0.545	677	2.19	9.73
Car-3W	1.963	2.46	0.411	470	2.48	10.90
Car-Car	2.204	2.499	0.129	1191	2.53	9.57
Car-LCV	1.74	2.273	0.753	116	2.27	12.24
Car-Heavy	1.761	2.858	0.259	326	2.88	15.98

4.4.3 Vehicle dimensions

Heterogeneous traffic involves a variety of vehicles with different makes and models for each vehicle type. Thus, a fixed dimension for a vehicle cannot be used. From field data, vehicle dimensions of vehicle types used for analysis are calculated. Mean and variation of these values is mentioned in Table 4.22.

Table 4.22 Vehicle dimensions adopted from field for study

Vehicle type	Length (m)		Width (m)	
	Mean	S.D.	Mean	S.D.
Two-wheeler	1.83	0.17	0.74	0.08
Three-wheeler	2.92	0.08	1.35	0.04
Car	3.75	0.87	1.49	0.23
LCV	5.97	1.67	1.79	0.44
Bus	9.21	1.12	2.44	0.30
Truck	6.74	1.49	2.38	0.21

4.5 Summary

From this chapter, relationships for inter-vehicular gaps (lateral and longitudinal), overtaking decision-making and some other parameters were evaluated. They are summarized below.

Analysis and modeling of lateral interactions:

1. There is a significant correlation between average speed on maintaining of lateral clearance. There is quite weak correlation between relative speed and width of road on lateral clearance.
2. Inter-vehicular lateral clearance increases with increase in average speed between two vehicles. The model for lateral clearance with speed can be represented by a deterministic

straight line with positive slope and Beta-distributed residuals can represent the stochastic nature.

3. Results vary for different vehicle types. The average lateral clearance maintained by different vehicle pairs is mentioned in Table 4.4. Cars and three-wheelers maintain more clearance with heavy vehicles and LCV's, whereas two-wheelers maintain the least lateral clearance. Further, it is observed that vehicles maintain lesser lateral clearance between vehicles of the same type than vehicles of other type. Due to this behavior, lateral clearance cannot be assumed as the sum of individual contribution of vehicles constituting the clearance.
4. During constrained overtaking case, when a vehicle interacts with vehicles on both sides simultaneously, there is compromise in maintaining lateral clearance at higher speeds (except for car-car pair). At 50 km/h average speed, average lateral clearance decreases from 146.6 cm to 144.2 cm, 150.3 cm to 134.7 cm, 159.0 cm to 148.1 cm and 169.6 cm to 145.5 cm for car-car, car-3W, 3W-2W and car-2W pairs, respectively.

Analysis and modeling of longitudinal interactions:

1. Longitudinal gap (*LG*) between leading and following vehicles increases with the increase of average speed and the decrease of centerline separation. The model for longitudinal gaps with speed and centerline separation can be represented by regression plane (deterministic part), having positive slope with speed, and negative slope with centerline separation. Further, the Beta-distributed residuals can represent the stochastic nature of driver behavior.
2. For car-car pair, the average *LG* varies from 3.38 m at 0 km/h to 9.98 m at 60 km/h for *CS*=0 m, and from 2.13 m at 0 km/h to 8.73 m at 60 km/h for *CS*=1 m.
3. Two-wheelers and three-wheelers are observed to have least *LG*. Vehicles are more sensitive to speed changes when they follow vehicles of larger sizes. For instance, at 30 km/h, *LG* for 2W-car, car-car, LCV-car and heavy vehicle-car pairs are 5.18 m, 6.67 m, 6.68 m and 6.88 m, respectively.
4. If vehicle follows two vehicles simultaneously, then it compromises significantly on maintenance of longitudinal gap. The compromise is higher if a smaller vehicle is following a larger vehicle. The percentage change of *LG* with the introduction of second leading vehicle is mentioned in Fig. 4.19, for different vehicle pairs, speeds and centerline separations. As lateral clearance between two leading vehicles decreases, average longitudinal gap increases.

Overtaking decision-making criteria:

1. The decision to overtake is influenced by change in lateral clearance and relative speeds. It is also influenced by any hindrance to overtake in the form of other vehicles or road edges, and longitudinal gap. It is not significantly affected by average speeds for all considered vehicles.
2. The probability to overtake can be represented by logistic regression models for individual vehicle-pairs. It is observed that probability to overtake increases with increase of

centerline separation and relative speeds, and decreases with average speed and longitudinal gap.

3. Based on negative values of constant term of regression model, it can be concluded that vehicles have overall higher tendency to overtake than follow, and two-wheelers have higher tendency to overtake.
4. For car-car pair, there is 8.9% decrease, 3.2% increase, 1.9% decrease, and 23% increase in probability to overtake on 5% increase of average speed, relative speed, longitudinal gap and centerline separation, respectively. Similar relationships are obtained for other pairs mentioned in Table 4.18.

CHAPTER 5

Development of driver behavior model

As discussed in Chapter 1 (Section 1.3), modeling of lateral and longitudinal gaps between vehicles in mixed traffic stream with their speeds, and the overtaking decision-making criteria based on these gaps, are the key inputs or approaches modeling such traffic streams. Chapter 3 presented methodology to collect field data for modeling these parameters, whereas Chapter 4 developed their relationships based on field data. Based on these relationships, this chapter discusses the development of a comprehensive simulation model. It is divided into the following sections-

- *Framework of driver behavior model*: This section focuses on various rules that govern the driver behavior as a vehicle moves in the traffic stream.
- *Structure of simulation model:* This section focuses on vehicle generation, updating the vehicle position and printing of necessary results.
- *Calibration and validation of model*: This section describes the calibration and validation of developed model and compares it with commercially available software VISSIM.
- *Application of the developed model:* This section discusses simulation of specific cases generated by this simulation model, which are not possible to experiment in the field.
- The fifth section summarizes the work in this chapter.

The driver behavior model developed uses the inputs from inter-vehicular gap models and field data for which it is simulated. It is an outcome of lateral clearance model, longitudinal vehicle-following model and overtaking decision model. These models are used to develop the framework of simulation model, as described in Fig. 5.1.

Free flow module	Vehicle-following module	Overtaking module
• Desired speed • Acceleration/deceleration characteristics	• Lateral clearance vs average speed • Acceleration/deceleration characteristics	• Longitudinal gap vs centerline separation, speed • Acceleration/deceleration characteristics

Fig. 5.1 Modules in simulation model and input data requirement for each of them

5.1 Framework of driver behavior model

The developed driver behavior model obtains positions of vehicles at every discretized time duration. For every time-step, every vehicle's driver behavior gets affected by presence or absence of vehicles within certain road stretch ahead of it (referred here as Interaction Range); which he/she can perceive. Interaction range (*IR*) is the threshold distance ahead of the subject driver/ vehicle, within which driver can perceive and react to the presence of other vehicle(s) and road geometry. The IR is assumed to consist of sum of distances covered during drivers' reaction time (T) and braking. Therefore, IR can be calculated from Equation 5.1.

$$IR = v_t T + C_1 {v_t}^2 \qquad \ldots 5.1$$

Where v_t represents the current speed of vehicle and C_1 is a proportionality constant (evaluated in Section 5.4).

Based on presence or absence of other vehicles in its neighborhood, particular vehicle can be in any of these three situations (i) Free-flow behavior; (ii) Vehicle-following behavior; and (iii) Overtaking behavior. If other interacting vehicles are absent within interaction range, the vehicle will be in free-flowing behavior. If interacting vehicles are present, the model calculates number of interacting vehicles at the front and back of test vehicle which affect its movement. In the presence of a leading vehicle, the driver chooses either to follow or veer to overtake it, based on driving comfort or benefit offered by either situation. This offered benefit can be calculated depending upon longitudinal gap between vehicles, their centerline separation, their average and relative speeds and presence of other vehicles making hindrance to overtake. A detailed description of this benefit calculation is provided in Section 4.3. The traditional term 'car-following' will be replaced by 'vehicle-following'. Thus, the proposed simulation model consists of three modules, namely free flow, vehicle-following and overtaking. Fig. 5.1 highlights the input data for the three modules.

5.1.1 Free flowing module

Desired speed is maximum speed at which driver feels safe at existing road conditions. It is the property of individual vehicle type and driver combination. Different drivers and vehicles travelling in a stream, at their desired speeds (without the influence of traffic) constitute a stream traveling at free-flow speed. When the movement of any vehicle is not influenced by other vehicles, it is free to accelerate to its desired speed. The free-flowing case involves calculation of a speed at every time-step as per Gipps' (1981) equation presented in Equation 5.2. This equation uses variable acceleration values – zero at desired speed and maximum acceleration at zero-speed, which ultimately governs the time required to achieve its desired speed under free-flowing behavior.

$$v_{t+T}^{a} = v_t + 2.5 a_{max} T \left[1 - \frac{v_t}{V}\right] \sqrt{0.025 + \frac{v_t}{V}} \qquad \ldots 5.2$$

v_t is the current speed, a_{max} is the desired acceleration for particular vehicle type (given in Table 5.1), T is driver reaction time and V is the desired speed the vehicle.

5.1.2 Vehicle-following module

When a test vehicle or following vehicle (FV) approaches a LV and decides to follow, it reacts in such a way to minimize relative speed while maintaining a stable longitudinal gap with leading vehicle (LV). Vehicles with near zero relative speed at stable longitudinal gap (LG) are referred to be in stable following situation. These vehicles maintain a stable gap depending upon average speed of LV and FV ($\bar{v}$), their vehicle types, centerline separation (*CS*) or staggering between LV and FV (refer Equation 4.4 and Table 4.11). Field data on this stable longitudinal gap are collected and modeled in detail in Section 4.2.

If the test vehicle is not in stable following condition, it will react to achieve a stable headway, depending upon its deviation from *LG* (represented as *S*). Its reaction (acceleration or deceleration) can be obtained from Equation 5.3.

$$a_{FV} = \left(\frac{v_t{}^2 - v'_{LV}{}^2}{2 \times S}\right) \quad \ldots 5.3$$

where, a_{FV} is acceleration or deceleration of FV, v_{FV} is current speed of FV, v'_{LV} is perceived speed of LV by FV and S is the deviation from LG. The approach of a vehicle when it follows a LV is shown in Fig. 5.2.

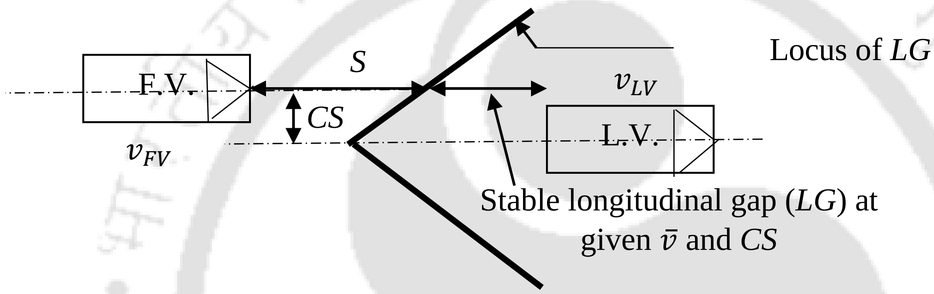

Fig. 5.2 Representation of different parameters under approach to stable vehicle-following

Due to human perception limitation, driver of FV may not be able to perceive speed of LV accurately. The perception error of FV's speed is assumed a function of speed of LV (v_{LV}), deviation of FV from stable longitudinal gap (*S*) and aggressive/risk-taking nature of driver of FV. The distribution of aggressive nature of drivers (risk factor or *R*) for error-perception is assumed as a truncated normal distribution with values 0 for most conservative and 1 for most risk-taking driver. It is assumed that most aggressive drivers may have best perception capabilities with least error (say, zero error, i.e., $v'_{LV} = v_{LV}$), whereas most conservative drivers may make a maximum error on positive or negative side randomly changing with every time-step. The perceived speed of LV can be calculated from Equations 5.4 (a) for positive error and 5.4 (b) for negative errors.

$$v'_{LV+} = v_{LV} + v_{LV}C_2(1-R)\left(1 + \frac{S}{IR - LG}\right) \quad \ldots 5.4\ (a)$$

$$v'_{LV-} = v_{LV} - v_{LV}C_3(1-R)\left(1 + \frac{S}{IR - LG}\right) \quad \ldots 5.4\ (b)$$

Where, C_2 and C_3 are site-specific calibration constants for positive and negative speed perception, respectively, and their values are determined from Section 5.4. IR is the interaction range, *R* is risk factor, LG is stable longitudinal gap (calculated from Equations 4.4, 4.5 and Table 4.11) and

S is deviation from LG. Perception error values are assumed to increase linearly with deviation from LG, and it is are assumed to be doubled at the interaction range (IR), corresponding to deviation $IR - LG$. Fig. 5.3 presents variation of perceived speed of LV with change in (a) risk factor and (b) deviation from stable LG. If more than one LVs are present, the LG is calculated as per Table 4.15.

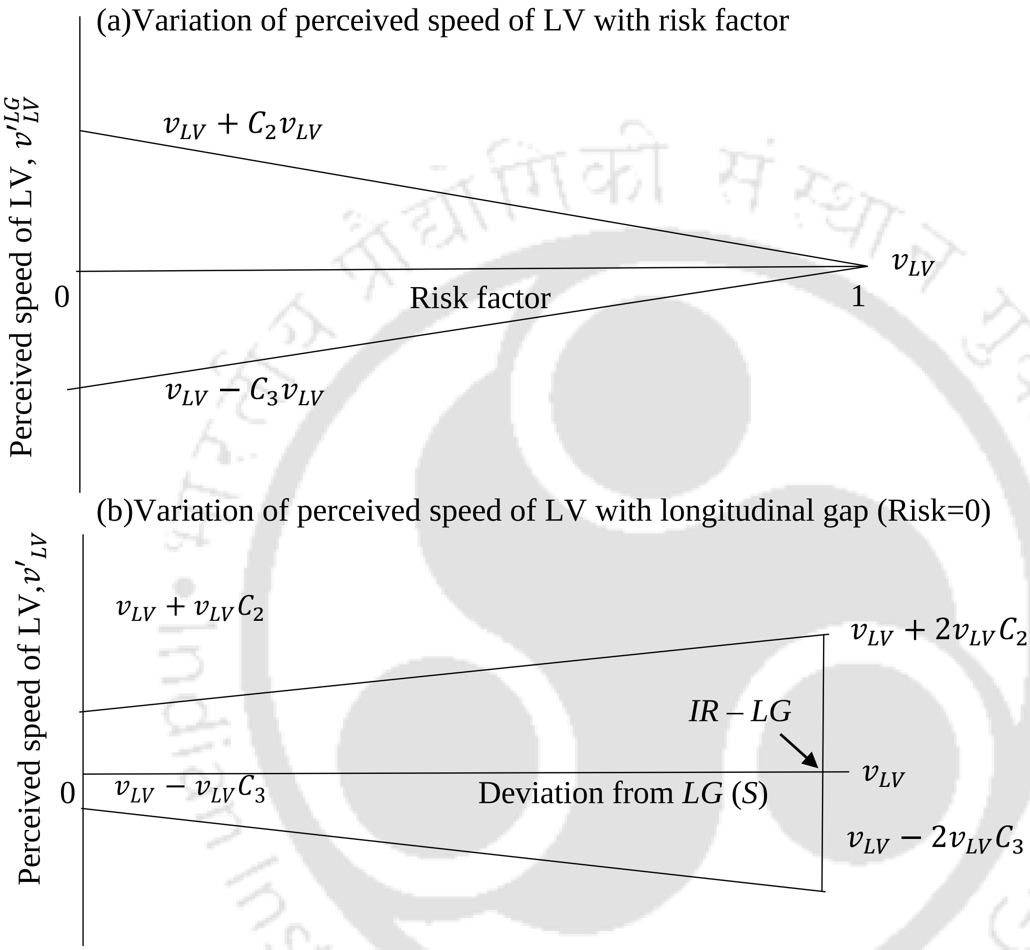

Fig. 5.3 Variation of perceived speed of LV with a change in (a) risk factor and (b) deviation from LG.

In case of zero relative speed between LV and test vehicle, predicted reaction is zero (as per Equation 5.3). However, zero relative speed situation will not last long, as perception error keeps varying on positive or negative side randomly at every time-step, which implies that v'_{LV} will keep changing randomly over time, even for same v_{LV}. Predicted acceleration or deceleration values are bounded by maximum permissible limits (a_{max}) for desired acceleration. However, in emergency situations (extreme cases) emergency deceleration limits may be applied which are C_4 times the normal braking limits. The value of C_4 is calibrated in Section 5.4.

5.1.3 Overtaking module

If the driver decides to overtake the LV, the path to be taken by FV depends upon the gaps between interacting vehicles present within the interaction range of FV and speed offered by them. The gap offering maximum speed with minimum veering required is selected for overtaking, and vehicle accelerates or decelerates towards that gap depending upon speed offered, along with simultaneous veering.

5.1.3.1 Calculation of speed offered by a gap between interacting vehicles

Fig. 5.4 shows different gaps available to a test vehicle with three interacting vehicles (A, B and C) within its interaction range (*IR*).

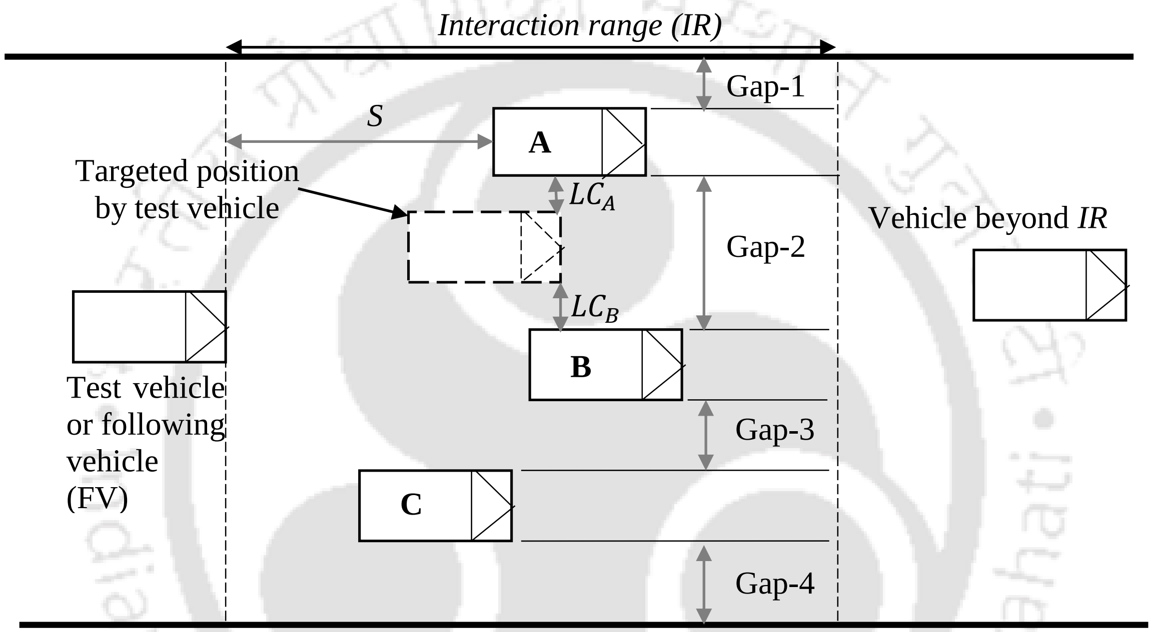

Fig. 5.4. Gap identification by test vehicle between LVs within *IR*, for its overtaking procedure

Initially, the width of each available gap is calculated. If this width is less than the width of test vehicle, speed offered by the gap will be zero. Else, available clearance offered by the two vehicles constituting that gap (say, gap 2 for vehicles A and B in Fig. 5.4) is the difference of width of that gap and width of the vehicle. This is the sum of contribution of clearance offered by each vehicle. If FV chooses to veer towards that gap, then its speed at that gap will be a function of lateral clearance offered (Refer Section 4.1). Using relationships of Section 4.1, Lateral clearance offered by vehicles A and B (LC_A and LC_B) can be calculated as

$$LC_A = m_1\bar{v}_1 + c_1 + \varphi_1 \quad \dots 5.4$$

$$LC_B = m_2\bar{v}_2 + c_2 + \varphi_2 \quad \dots 5.5$$

If the gap leaves a space greater than 2.5 meters, then unconstrained overtaking relationships are used (Table 4.4). Otherwise, constrained overtaking relationships (Table 4.8) are used. $\bar{v}_1$ is average of perceived speed of vehicle A and speed offered by gap *k* to FV, and $\bar{v}_2$ is average of perceived speed of vehicle B and speed offered by gap *k* to FV. φ_1, the residual term obtained between relationship of FV and vehicle A, is taken as percentile of average risk factor (*R*) constituted individually by drivers of vehicle A and FV (Detailed discussion for risk factor is provided in Section 5.2.1). Similarly, φ_2 is also obtained. The values of $m_1, m_2, c_1,\ c_2$ are presented in Section 4.1. (Table 4.4, 4.8 for unconstrained and constrained interactions respectively)

$$\bar{v}_1 = \frac{v'_A + v_k}{2} \quad \text{… 5.6 (a)}$$

$$\bar{v}_2 = \frac{v'_B + v_k}{2} \quad \text{… 5.6 (b)}$$

But, for a particular gap k,

$$y_k = \text{width of gap } k = LC_A + LC_B + w_{FV}, \quad \text{…5.7}$$

where w_{FV} is width of FV. The only unknown variable v_k can be calculated from Equations 5.3 to 5.7, and represented in Equation 5.8.

$$v_k = \frac{2}{m_1 + m_2}\left(y_k - w_{FV} - c_1 - c_2 - \frac{m_1 v'_1}{2} - \frac{m_2 v'_2}{2} - \varphi_1 - \varphi_2\right) \quad \text{... 5.8}$$

5.1.3.2 Calculation of goodness of overtaking opportunity offered by each gap

Goodness of a particular gap depends upon veer required by the vehicle to reach the gap and speed offered by each gap. Veer required by a vehicle to reach a particular gap k, (Δy_k) can be calculated as difference in lateral coordinates of centerline of test vehicle and center of gap. Goodness of a gap k in a road of width w (G_k) can be calculated by Equation 5.9.

$$G_k = \frac{\frac{v_k}{V} \times C_5 - \frac{\Delta y_k}{w}}{(1 + C_5)} \quad \text{… 5.9}$$

Here, V is the desired speed of test vehicle, C_5 is a measure of proportion of preference given to proximity of a gap (k) and its speed offered (v_k). This is a field-specific constant and needs to be calibrated as per procedure described further in Section 5.4.2. Goodness for a particular gap increases with increase in speed offered and decreases with increase in lateral distance required to reach that gap. Goodness of all gaps are calculated and gap offering maximum goodness (G_{k_max}) is is chosen for vehicle movement at next time step.

5.1.3.3 Vehicle movement after selection of priority-gap

Once the gap with maximum goodness is selected, vehicle is assumed to accelerate/decelerate uniformly to the speed offered by gap chosen to overtake and simultaneously veer. The amount of acceleration (a) can be calculated from third kinematic equation, and provided in Equation 5.10.

$$a = \frac{{v_{G_{k\_max}}}^2 - {v_t}^2}{2S} \qquad \dots 5.10$$

where $v_{G_{k\_max}}$ is speed offered by gap having maximum goodness, S is the longitudinal gap between the nearest interacting vehicle constituting the gap and FV (shown in Fig. 5.4).

The vehicle is assumed to perform a simultaneous lateral shift with a uniform veering speed (evaluated from field data and presented in Section 4.4.2) which will change as per driver's aggressiveness or risk taking behavior as well as vehicle type.

5.2 Structure of the simulation model

The developed comprehensive simulation model updates position of every vehicle at the end of discretized time-step, which is chosen equal to the mean perception-reaction time of the drivers considered as 1 second (adopted from Hugemann, 2002). The model consists of vehicle generation, driver-behavior model governing vehicle position, and printing of necessary macro and microscopic parameters of the simulated traffic stream. For simulation of selected field stretch, the length of road (excluding generation zone and warm-up zone) and traffic composition is kept similar to the field. Vehicles are generated at the 'vehicle-generation zone' located at 0.5 km of initial stretch of road. The vehicles are allowed to interact in the 'warming-up zone' spread over 1 km after the generation zone. All the macro and microscopic stream parameters are collected from remaining stretch of the road.

5.2.1 Vehicle generation

Based on observed traffic flow and composition, vehicles are generated in the vehicle-generation stretch and placed in such a way that they maintain a safe gap with neighboring vehicles in both lateral and longitudinal direction. Every generated vehicle is assigned- (i) Vehicle type and corresponding desired speeds as per field traffic composition and vehicle-type wise desired speed distribution; and (ii) Risk factor to incorporate variability in aggressiveness of driver behavior, and (iii) Interaction range.

In the real world, aggressive nature of driver is variable. To incorporate this behavior, a risk factor is defined for each driver. It may be defined as percentage of drivers taking risk lesser than the driver under consideration. Further, it is assumed that a driver maintains the same amount of aggressiveness while displaying each of the driving behaviors such as lateral speed, lateral clearance, longitudinal headway, overtaking decision-making, etc. Therefore, the least aggressive driver will maintain highest lateral clearance, longitudinal headway, and lowest lateral speed and will choose to overtake in the least possible scenarios; whereas the most aggressive driver will present a reverse behavior.

5.2.2 Updating the vehicle position

At every time-step T, all vehicle lateral and longitudinal positions are updated based on previous (lateral and longitudinal) positions and calculated speed for present time-step using Equation 5.11.

$$v_{t+T} = v_t + aT \qquad \text{... 5.11 } (a)$$

$$x_{t+T} = x_t + \left(\frac{v_t + v_{t+T}}{2}\right)T \qquad \text{... 5.11 (b)}$$

$$y_{t+T} = y_t + v_{veer}T \qquad \text{... 5.11 (c)}$$

where *x* and *y* represent longitudinal and lateral positions of vehicle, v_{veer} is lateral speed, and suffixes *t* and *t+T* represent the current time-step and next time-step.

5.2.3 Printing of results

Microscopic as well as macroscopic parameters need to be captured from model, to compare them with the field for validation purposes. Macroscopic parameters include speed, flow and density plot at a fixed time interval, whereas microscopic parameters in mixed traffic stream include speed distribution of every vehicle type, time headway distribution, the relationship of lateral clearance with speed for different vehicle types, *x* and *y* coordinates of all vehicles on the road section to show the weak lane discipline, the relationship of longitudinal headway with centerline separation and average speed for vehicle-following behaviors.

These microscopic and macroscopic characteristics are captured at particular section(s) located downstream of generation and warming-up zone. The flow of section is captured in terms of vehicles per 5-minute and one-minute intervals. Speed for macroscopic calculations is average speed of all vehicles during 1-minute and 5-minute interval. The lateral and longitudinal separations between overtaking and following vehicles respectively are calculated similar to the calculations in field (in Sections 3.2 and 3.3), from vehicle trajectories.

5.2.4 Flowchart of simulation model

Flowchart given in Fig. 5.5 represents the overall framework of the developed simulation model.

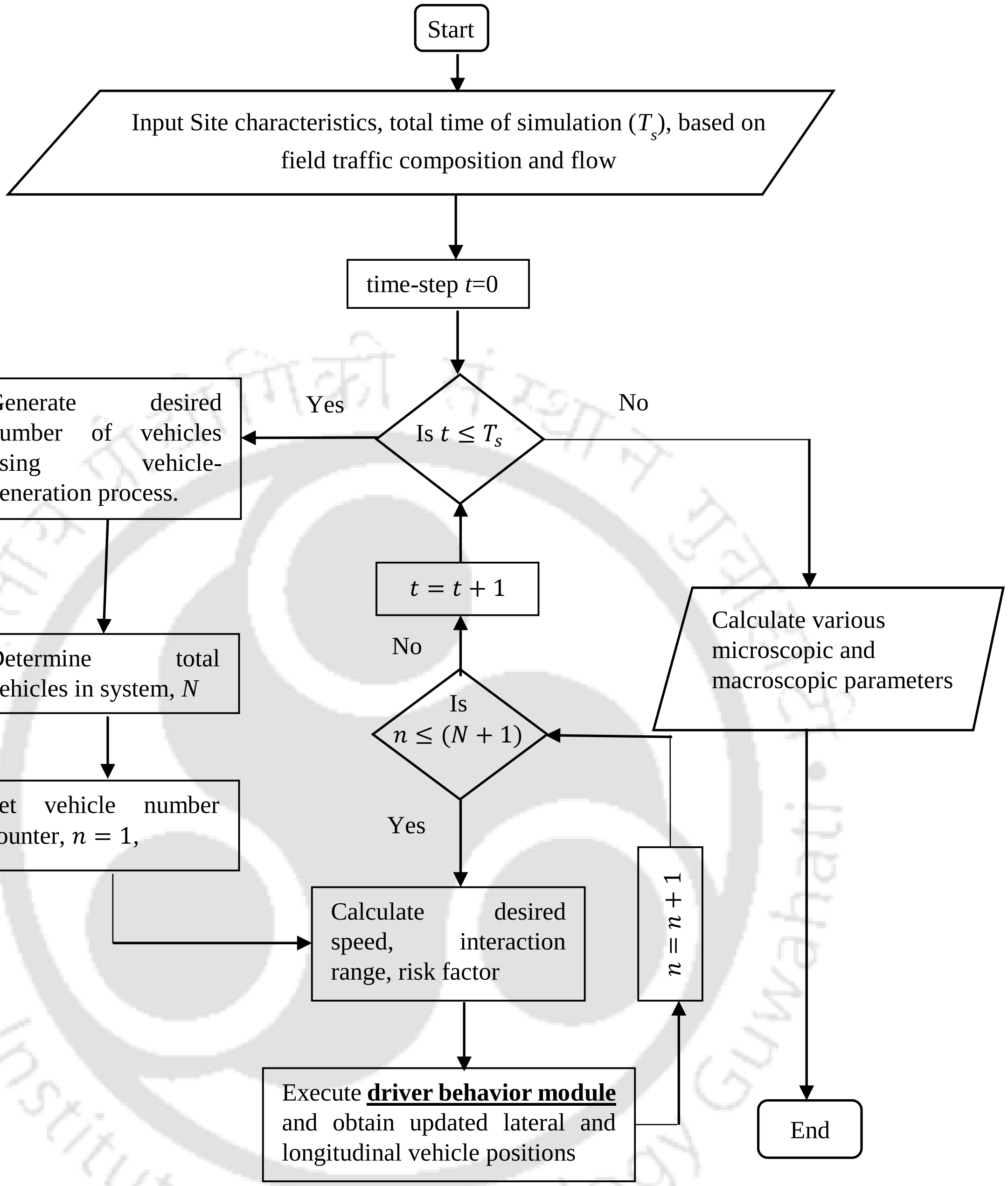

Fig. 5.5. Flowchart showing the framework of developed simulation model

The driver behavior model highlighted in this flowchart is mentioned in detail in the flowchart in Fig. 5.6. The driver behavior model also mentions the different modules which the vehicle needs to go through for determining the position at next time step.

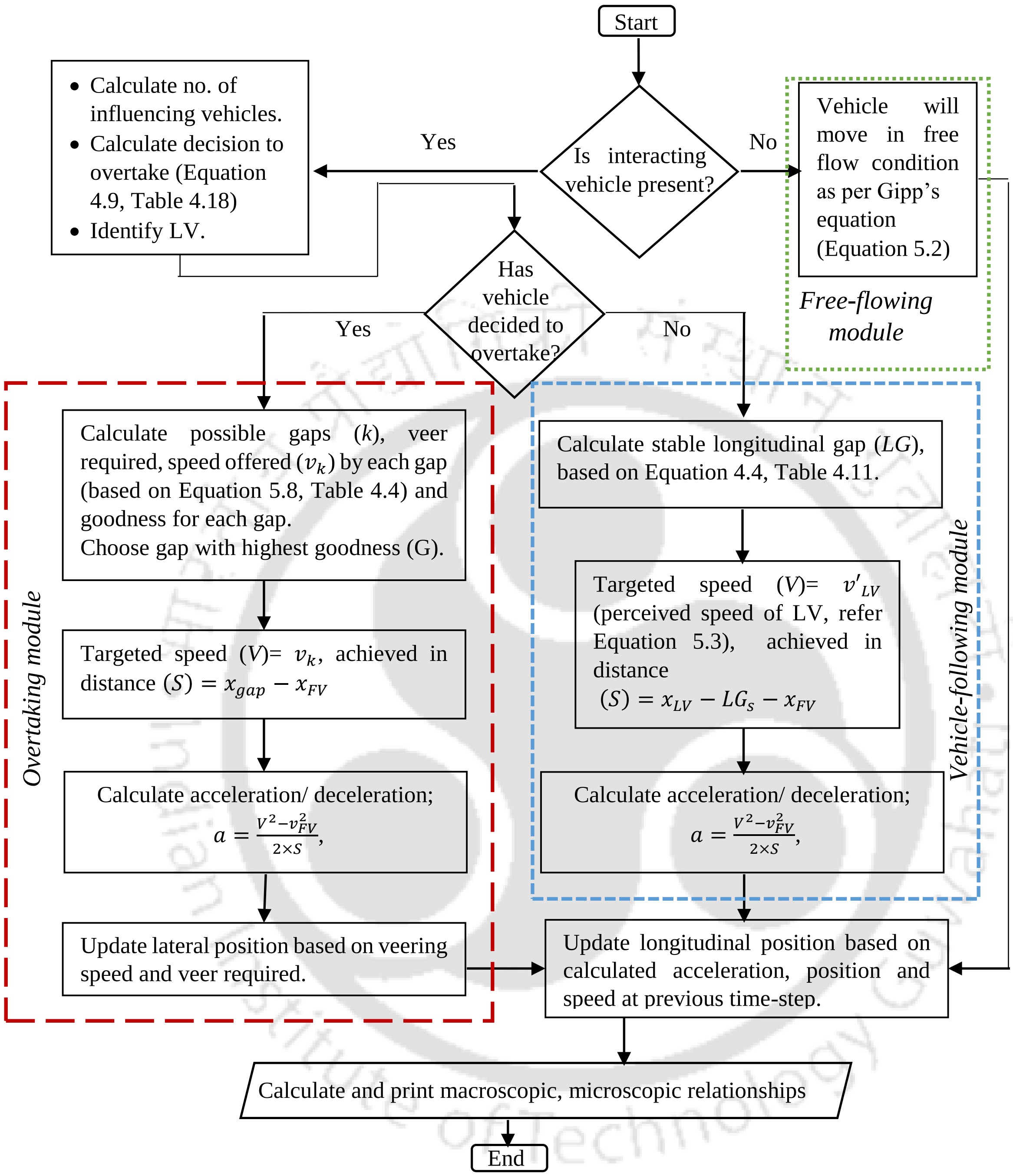

Fig. 5.6 Flowchart of driver behavior model used in simulation program

5.3 Calibration and validation of model

The aim of a simulation model is to mimic the traffic conditions at a given site. For this purpose, a traffic site is chosen (Outer Ring Road underpass, near BEL circle, Bengaluru) and various macroscopic and macroscopic parameters are extracted from the field. Values of some parameters (such as desired speed, composition, sizes, etc) can be directly determined from the field, whereas, values of certain parameters in the model and cannot be obtained directly. Values of these parameters are determined by calibrating the developed model from field data by minimizing the difference between simulated and field parameters using genetic algorithms. The first subsection presents various input parameters from field, whereas the second subsection presents calibration of unknown model parameters presented in earlier subsections. The third subsection presents calibration of a popular and commercial software VISSIM, which can generate (and model) the mixed, no lane disciplined traffic as observed in developing countries.

5.3.1 Input parameters measured from the field

The input parameters from the field include roadway features and traffic parameters of selected field section.

5.3.1.1 Roadway features

A straight Section with good pavement conditions and absence of intersecting traffic is selected from a dual carriageway arterial road of Bengaluru city (Outer Ring road), with a carriageway width of 11.5 m, and Section length 5 km. It consists of three lanes (each lane of 3.5 m width) with paved shoulders. Traffic data are collected from 4 pm to 7 pm on a weekday with clear weather, which constitute the lean peak hour and peak hour intervals. Out of these data, those captured during 4 pm – 6 pm are used for calibration, whereas the remaining data are used for validation purpose.

5.3.1.2 Traffic parameters

Table 5.1 provides values of various traffic input parameters used in the simulation model. The average observed traffic flow in the field was 4000 vehicles/hour. Various traffic parameters such as composition, vehicle dimensions, lateral and desired speeds are obtained from the field. The values of maximum desired acceleration and deceleration rates are adopted from Bokare, (2013). Maximum deceleration rate during emergency situations is assumed C_4 times desired deceleration.

5.3.2 Calibration of unknown model parameters

Various model parameters (C_1, C_2, … C_5) described earlier in Section 5.1 are calibrated in this subsection. The values of these parameters are tuned between certain ranges using genetic algorithms (GA), to obtain behavior of simulated stream similar to the field traffic stream by minimizing the error between two streams.

Table 5.1 Input parameters in simulation model from field data

Vehicle type			3W	Car	Bus	2W	Truck	LCV
Traffic composition (%)			8.11	43.39	3.08	40.90	1.89	2.63
Vehicle dimensions	Length (m)	Mean	2.92	3.75	9.21	1.83	6.74	5.97
		Standard deviation	0.08	0.87	1.12	0.17	1.49	1.67
	Width (m)	Mean	1.35	1.49	2.44	0.74	2.38	1.79
		Standard deviation	0.04	0.23	0.30	0.08	0.21	0.44
Lateral speed	Mean, m/s		1.08	1.04	1.03	1.23	0.94	1.03
	85th percentile (m/s)		2.85	2.83	2.73	3.25	2.47	2.72
	λ (negative exponential)		0.62	0.68	0.68	0.57	0.75	0.68
Desired speed distribution (km/h)	Mean, km/h		49.57	76.32	60.19	59.94	51.77	59.90
	Standard deviation		6.41	17.66	11.63	14.08	12.94	14.98
Desired acceleration, a_{max} m/s^2			1.32	2.56	1.21	2.31	1.00	1.86
Desired deceleration, m/s^2			2.65	3.34	2.11	3.18	1.67	1.98

5.3.2.1 Description of calibrated parameters

The following parameters calibrated within their ranges, using genetic algorithms:

1. Parameter C_1 for calculating interaction range: In Equation 5.1, the term $C_1\, v_t^{\,2}$ represents distance covered during braking ($v_t^{\,2}/2 \times \text{deceleration}$). The minimum deceleration may be assumed as 1 m/s^2 whereas maximum deceleration as per Fambro *et al.* (2000) is 4.5 m/s^2. Therefore upper and lower limits of C_1 (0.5 and 0.1, respectively) can be calculated from these values ($1/(2 \times \text{deceleration})$). Literature doesn't yield any study related to estimation of interaction range of a driver in weak lane disciplined traffic, therefore, the constant C_1 in Equation 5.1 is also considered for calibration from field data. The interaction range may or may not be site-specific.
2. Error in the perception of speed of LV by following driver (C_2 and C_3): It is basically the percentage incorrect speed perception of LV by the least risk-taking driver. Details about calculation of these errors are mentioned in Section 5.1.2. The perceived LV speed error limits maybe calculated based on the assumption that drivers would estimate negative error (positive relative speed or approaching the LV) with better accuracy than positive error. The maximum error threshold is estimated from FHWA's relative speed threshold with inter-vehicular spacing graph, for observation time 1 second (adopted from Evans and Rothery, 1973).
3. Ratio of normal braking to emergency braking (C_4): The ratio of maximum deceleration (emergency breaking) to normal deceleration values are defined by a site-specific calibration constant C_4. The maximum limit for emergency braking is based on the

assumption that drivers would not brake harder than g, the acceleration due to gravity, even in the worst possible scenario (Kudarauskas, 2007).

4. Ratio of speed offered by a gap to its proximity while calculating priority (Gap-priority): It is the calibration constant C_5 used in Equation 5.9.

These five parameters with their ranges are used as inputs to the objective function, described in Table 5.2. With various trial and errors (using GA), the parameters are assigned values by GA tool. Objective function is described further.

Table 5.2 Model parameters used for calibration by GA

S. no.	Parameter used for calculation of	Parameter	Lower limit	Upper limit
1	Interaction range	C_1	0.100	0.500
2	Perceived LV speed positive error	C_2	0.000	0.100
3	Perceived LV speed negative error	C_3	0.000	0.050
4	Emergency braking	C_4	1.000	3.000
5	Gap-goodness (speed or proximity)	C_5	0.200	5.000

5.3.2.2 Objective function

The optimization objective-function f used in this algorithm consists of error terms for deviation of model traffic from speed-flow relationship (macroscopic stream property) and speed distribution (microscopic property) relationships of the field; and is mentioned in Equation 5.12.

$$f = 2.0 - NRMSE_1 - NRMSE_2 \quad \text{... 5.12 (a)}$$

$$NRMSE_2 = \text{average}(NRMSE_{car}, NRMSE_{Bike,}\ NRMSE_{Auto}) \quad \text{... 5.12 (b)}$$

$where, NRMSE_1$ is the normalized root mean square error between obtained speeds for particular per-minute flow level of model and field (for 1 hour duration); and $NRMSE_{car}, NRMSE_{Bike,}\ NRMSE_{Auto}$ are the normalized root mean square errors between discretized frequency of speed distribution of car, two-wheeler and three-wheeler, respectively between field and model. The normalized MSE was used since the speed distribution and speed-flow relationships provide different values of errors and they need to be normalized to be combined to calculate a resultant error term.

5.3.2.3 Genetic Algorithms used to optimize model flow

The genetic algorithm consists of an objective function described by Equation 5.12 and proceeds as per following steps-

1. The algorithm begins by creating a random initial population of size 10, within the initial range mentioned in Table 5.2. One individual of the population consists of a set of values for respective parameters, within the initial limits.
2. The algorithm then creates a sequence of new populations. At each step, the algorithm uses the individuals in the current generation to create the next population. To create the new population, the algorithm performs the following steps:
    - Score each individual of the current population by computing its fitness value by running the simulation program using the current values of the individual;
    - Select the parents based on their fitness using Roulette wheel technique.
    - The next generation is produced in three ways- (i) Directly pass some better fitness valued individuals to next generation (maximum 20% of the population); (ii) Produce children by crossover; (iii) Produce children by mutation. The next generation is produced only if there is an improvement to the objective function.
3. The algorithm is run for several generations and each generation produces an optimized value less than or equal to the earlier generations' value. Table 5.3 provides the optimized value by each generation and Fig. 5.7 highlights the optimization of objective function after each generation. In Table 5.3, best *f(x)* represents minimum value of optimization function amongst function values for all individuals in the population for the current generation, whereas mean *f(x)* represents their mean.

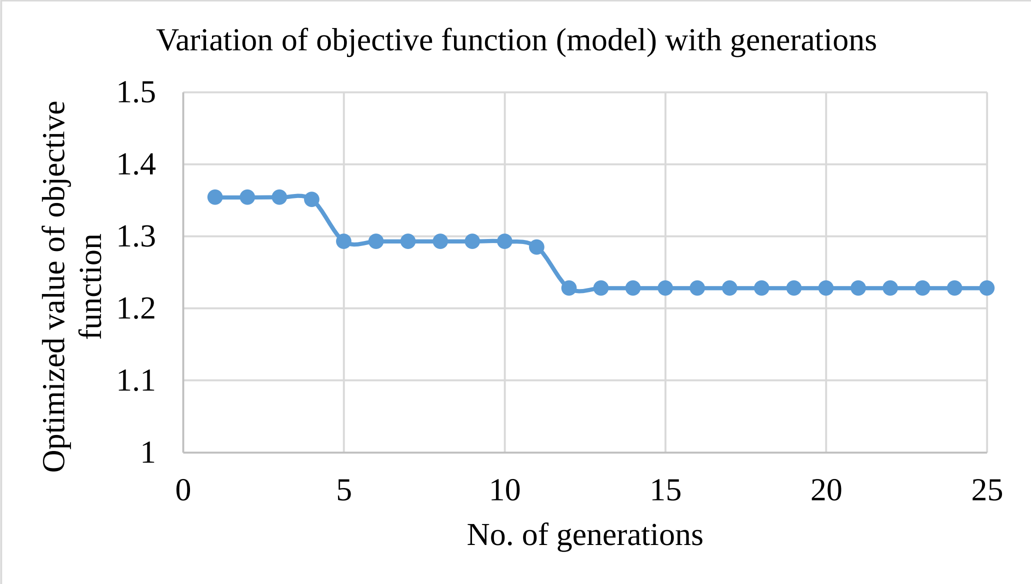

Fig. 5.7 Variation of objective function values after each generation of GA

4. From Fig. 5.7 and Table 5.3, it is observed that beyond 14th generation, the value of objective function remains consistent. Thus, the algorithm is terminated at the 25th generation. The obtained optimized values for C_1, C_2, C_3, C_4 and C_5 are 0.272, 0.085, 0.035, 2.57 and 0.556, respectively at the 25th generation.
5. The developed model is run with these optimized values and various parameters are calculated for further evaluation.

Table 5.3 Optimized value of objective function after each generation

Generation	Best *f(x)*	Mean *f(x)*	No. of stalled generations
1	1.354	8.103	0
2	1.354	4.985	1
3	1.354	2.013	2
4	1.351	2.591	0
5	1.293	1.51	0
6	1.293	1.444	1
7	1.293	1.523	2
8	1.293	1.423	3
9	1.293	1.395	4
10	1.293	1.345	5
11	1.285	1.357	0
12	1.228	1.335	0
13	1.228	1.321	1
14	1.228	1.321	2
15	1.228	1.318	3
16	1.228	1.317	4
17	1.228	1.317	5
18	1.228	1.324	6
19	1.228	1.617	7
20	1.228	1.343	8
21	1.228	1.317	9
22	1.228	1.589	10
23	1.228	1.406	11
24	1.228	1.323	12
25	1.228	1.317	13

5.3.3 Calibration of VISSIM model parameters

VISSIM is a microscopic, discretized time and behavior based simulation model developed to analyze the full range of functionally classified roadways and public transportation operations.

Initially, a traffic stretch is simulated (for its traffic properties and roadway features) in VISSIM's graphic user interface (GUI) tool, similar to the field conditions. Vehicle classes and composition are defined similar to field conditions used in calibration of developed model. Further, several driver behavior parameters used as input include the following- (i) Acceleration-deceleration curves are adopted from Bokare (2013); (ii) Lateral clearance-maintaining behavior, adopted from Table 4.4 and Equation 4.1, are used as inputs in the form of clearance maintained at 0 km/h and 50 km/h in the VISSIM model, mentioned in Table 5.4.

Table 5.4 Lateral clearance values used as input in VISSIM model

Vehicle type		Three-wheeler	Car	Bus	Two-wheeler	Truck	LCV
Average Lateral distance (m)	0 km/h	1.14	1.17	1.35	1.18	1.35	1.49
	50 km/h	1.66	1.51	1.69	1.29	1.69	1.51

VISSIM uses Wiedemann-99 vehicle-following model to estimate the following behavior of simulated vehicles. The different variables for vehicle-following include look-ahead distance, look-back distance and Wiedemann-99 parameters CC0 to CC9 which need to be calibrated. All the parameters are not sensitive enough to affect the output. Sensitivity analysis using Latin hypercube sampling was conducted by previous researches Manjunatha, *et al.* (2013), Mathew and Radhakrishnan (2010), and Siddharth and Ramadurai (2013) and it was found that that the parameters CC0, CC1, CC7, CC8, maximum look-ahead and look-back distances are sensitive. The upper and lower limits for variables to be optimized are given in Table 5.5. The values are adopted from Mathew and Radhakrishnan (2010).

Table 5.5 Upper and lower limits for different vehicle-following parameters used in VISSIM for optimizing traffic stream

S. no.	VISSIM parameter	Lower limit	Upper limit
1	W99CC0	0.0	4.0
2	W99CC1	0.0	4.0
3	W99CC2	0.0	10.0
4	W99CC7	0.1	1.5
5	W99CC8	0.0	4.0
6	Look ahead distance (max)	10.0	200.0
7	Look back distance (max)	10.0	200.0

The vehicle-following sensitive parameters are optimized between the ranges given in Table 5.5, using Genetic Algorithms. The process is similar to that described in Section 5.3.2. VISSIM model is run for various iterations corresponding to different random seeds. The obtained optimized values are 3.748, 1.495, 1.519, 0.625, 1.267, 194.504 and 142.930 for parameters CC0, CC1, CC7, CC8, look ahead distance and look back distance, respectively. Fig. 5.8 provides the graph of optimized values of the objective function with number of generations for calibrated VISSIM parameters. From the graph, it is observed that beyond 17th generation, the value of objective function remains consistent. Thus, the algorithm is terminated at the 25th iteration. The simulation model is run using optimized values, and information of macroscopic parameters can be obtained from flow counters placed at particular sections in VISSIM, whereas information of microscopic parameters can be obtained using trajectory data of individual simulated vehicles by VISSIM. These parameters are compared with the developed model in the next subsection.

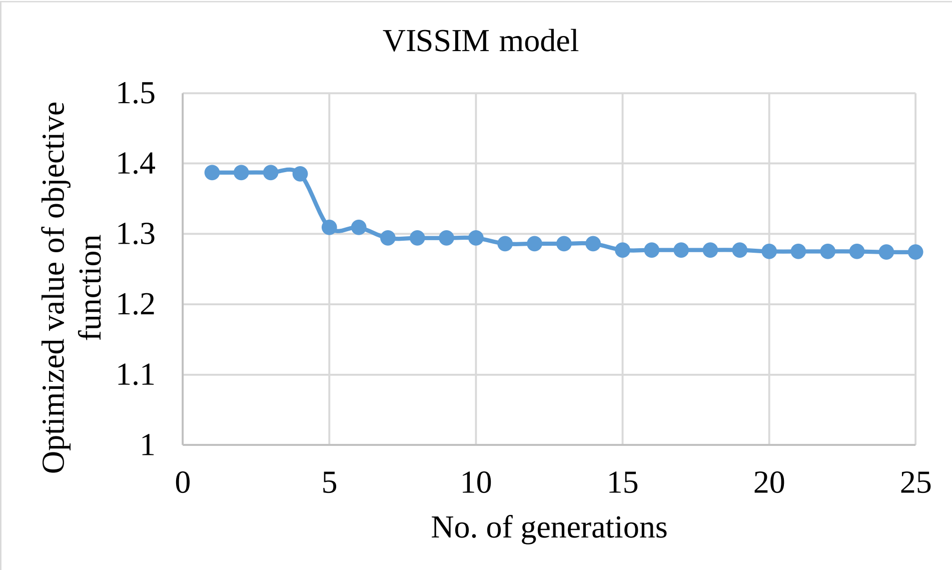

Fig. 5.8 Graph of optimized values of objective function with number of generations for VISSIM model

5.3.4 Validation of developed model and VISSIM with field data

Validation is the process to determine whether the simulation model is an accurate representation of the system under study. The model is validated in two aspects- Microscopic and macroscopic validations. Macroscopic validation involves checking speed-flow-density curves of field and model. Microscopic validations involve comparison of speed distribution, lateral clearance-maintaining behavior, longitudinal vehicle-following behavior and relationships between longitudinal and lateral speeds and accelerations; between field and modelled data. Traffic data from the same site for a different time duration (6 pm – 7 pm) are used for validating developed model and VISSIM simultaneously.

5.3.4.1 Speed-flow relationship

Relationship of per-minute flow and average speeds of vehicles from the field (validation data), VISSIM and model are extracted and validated with each other using RMSE. The RMSE for speed-flow diagram between model and field, and between model and VISSIM are 0.312 and 0.334, respectively. Thus, a conclusion can be drawn that model performs comparable to VISSIM. The comparison of speed-flow relationships is shown in Fig. 5.9 (a).

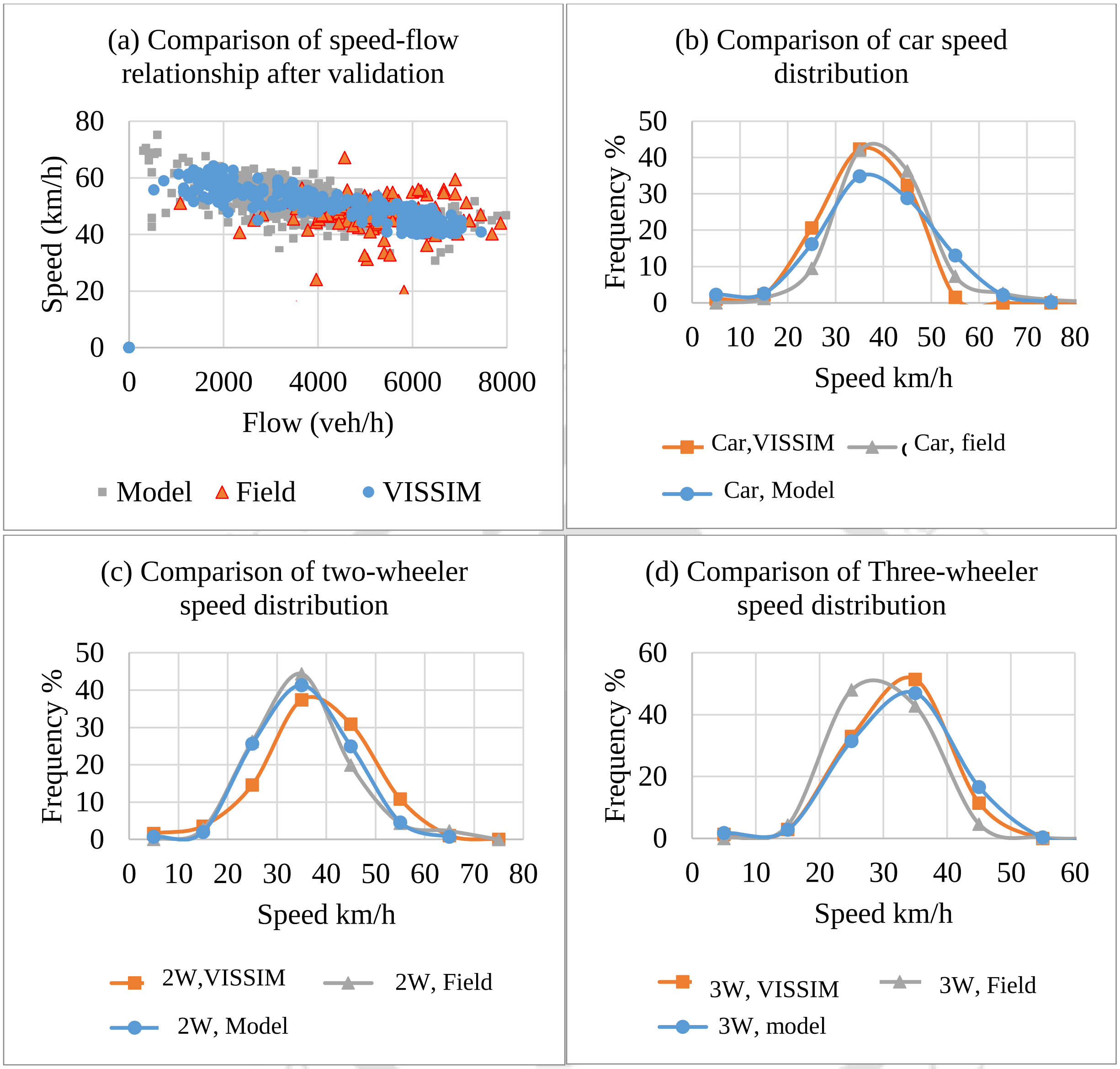

Fig. 5.9. Comparison of streams of VISSIM and developed model with field data for (a) Speed-flow relationship; Speed distribution of (b) cars, (c) two-wheelers and (d) three-wheelers.

5.3.4.2 Vehicles' speed distribution

Obtained speeds of individual vehicle types are extracted from field, as well as model and VISSIM. Vehicle speed distribution diagrams for these three datasets are plotted for each of cars, two-wheelers and auto-rickshaws and compared with each other. It is observed that RMSE for speed distribution of cars, two-wheelers and three-wheelers between model and field are 0.248. 0.174, 0.360, respectively, whereas the same values between VISSIM and field are 0.204, 0.226 and 0.339, respectively. It indicates that model can replicate the field conditions similar to VISSIM model. The comparison of speed distributions of cars, two-wheelers and three-wheelers are presented in Fig. 5.9 (b), (c) and (d) respectively.

5.3.4.3 Time headway distribution

Difference between arrival timings at a section over the entire width of the road, between two consecutive vehicles (referred as time-headway in the developed world) is calculated for field, VISSIM and model. As vehicles do not follow lane discipline, traditional lane-based time headway calculation is not possible. Arrival time difference distributions of field, VISSIM and model are plotted against each other and shown in Fig. 5.10. The calculated arrival-time headways are discretized in intervals of 0.5 seconds each and it is observed that RMSE between field and model is 0.314, whereas RMSE between VISSIM and model is 0.307. K-S test applied between discretized datasets of field and modeled data gives p-value 0.139, whereas between field and VISSIM data as 0.154. It indicates that developed model can behave comparable to VISSIM and field conditions.

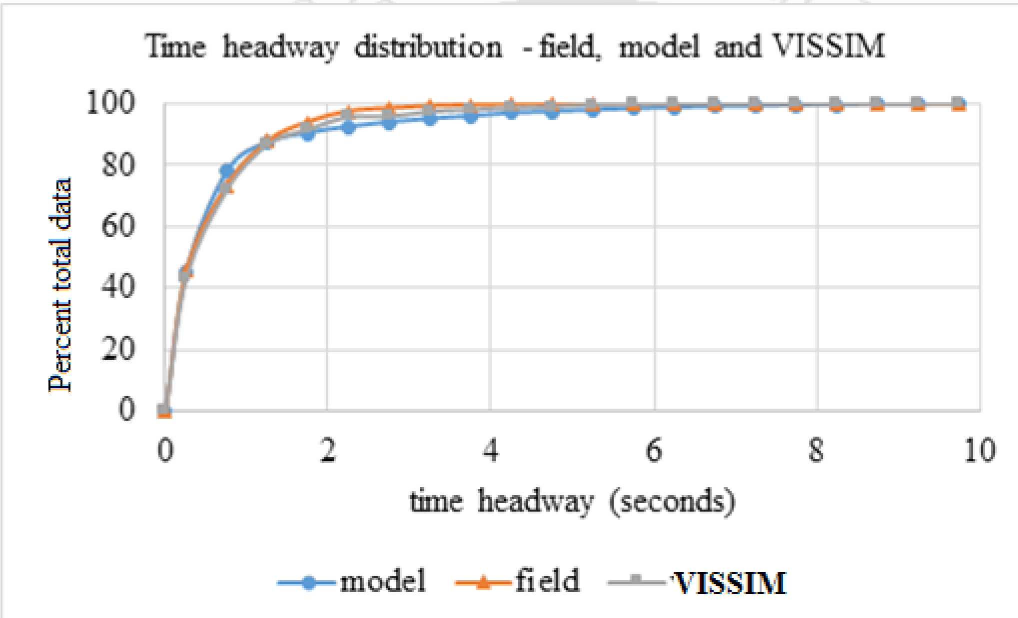

Fig. 5.10 Comparison of time headway distribution of field, model and VISSIM data

5.3.4.4 Lateral maneuvers by vehicles

The frequency and intensity of change in lateral position of a vehicle over a particular distance is an important indicator of driver behavior for heterogeneous and weak lane discipline traffic. In lane disciplined traffic, this behavior is depicted by 'lane changes per unit longitudinal distance'. However, in traffic with weak lane discipline, lateral maneuvers are not discrete in the form of lanes, but can vary over continuous width of the road. In a fixed longitudinal stretch of road (50 m), the total lateral maneuvering performed by each vehicle is evaluated in the field as well as VISSIM and developed model. Frequency of these calculated lateral maneuvers in the developed model and VISSIM is expressed per 10 m road width (discretized in groups of 0.5 m) and compared with the field maneuvers. These comparison results are presented in Fig. 5.11 for (a) all vehicles, (b) two-wheelers and (c) cars. The difference between field and simulation models can be expressed in terms of RMSE. It is observed that RMSE between model and field are 0.109 (all vehicles), 0.084 (cars) and 0.112 (two-wheelers); whereas the same values between VISSIM and field are 0.536, 0.487 and 0.522, respectively. Similarly, applying K-S test between model and field, *p*-value of test between model and field is 0.364 (all vehicles), 0.362 (cars) and 0.521 (two-wheelers), whereas the same values between VISSIM and field are 0.241, 0.171 and 0.211, respectively. Thus, model can perform better than VISSIM to represent lateral maneuvers by vehicles.

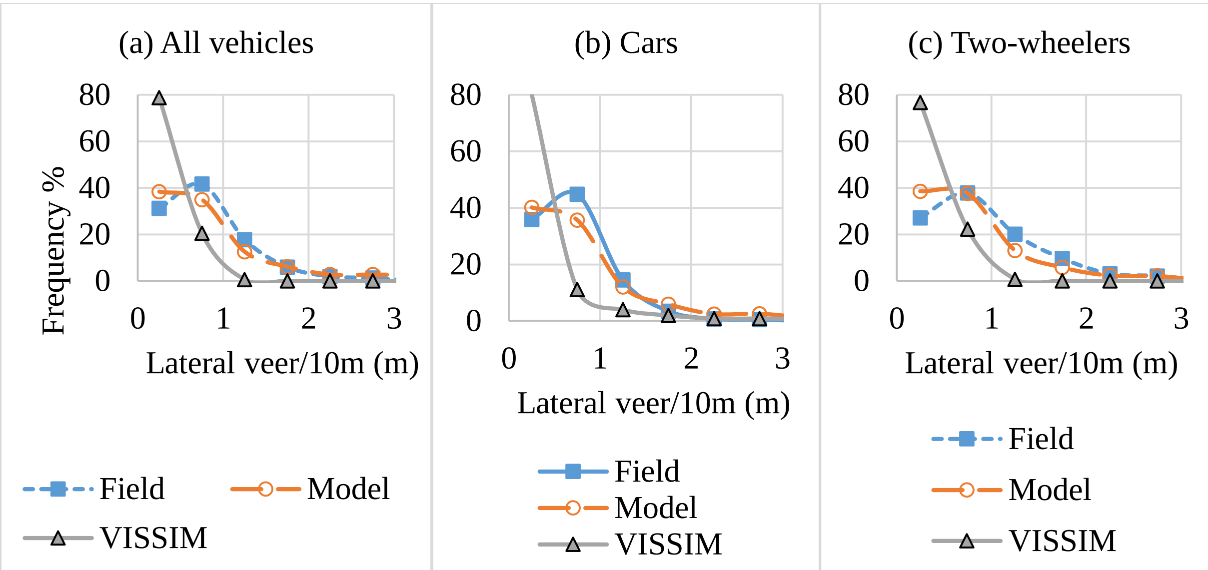

Fig. 5.11 Validation of lateral maneuvers for every 10 m longitudinal distance for VISSIM and developed model, for (a) All vehicles, (b) Cars and (c) Two-wheelers

5.3.4.5 Lateral speed distribution for all vehicles

Lateral speed distribution is extracted from field from vehicle trajectories, and compared with the model and VISSIM data for various vehicle types. It is observed that the distributions of field and model are statistically similar by K-S test (p=0.389). However, it is observed that there is less statistical similarity between VISSIM and field data (p=0.056). The plot of lateral speed distribution for field, VISSIM and model, for cars is shown in Fig. 5.12. A similar result is also observed for other vehicle types.

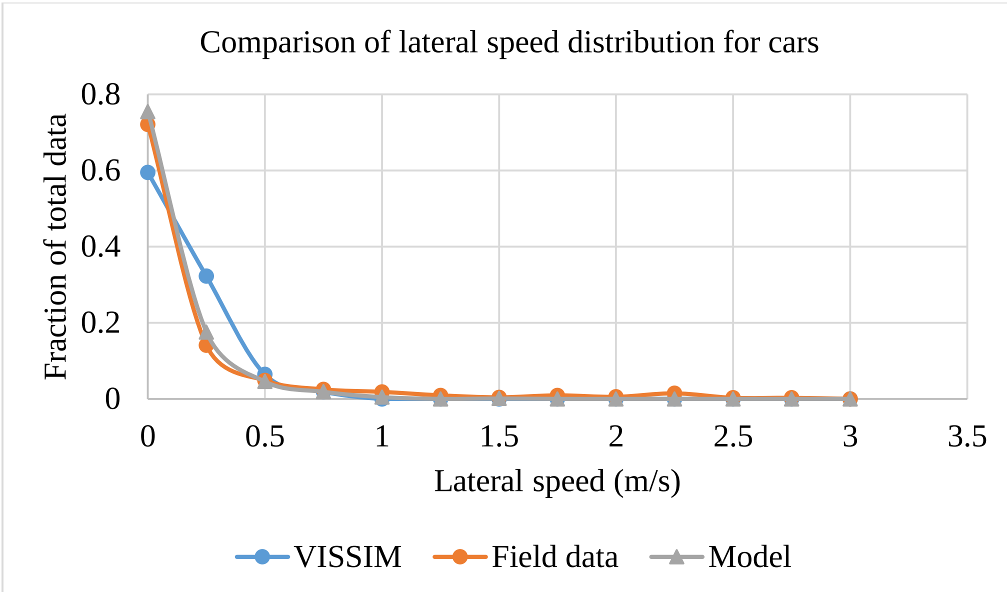

Fig. 5.12 Comparison of lateral speed distribution of field, VISSIM and model, for cars

5.3.4.6 Vehicles' lateral and longitudinal position on the road

After the model is run, lateral and longitudinal positions of each vehicle are noted at every time step and recorded in a file. A snapshot is taken at any random time step and the vehicle positions are plotted for 1 km stretch. The snapshot is given in Fig. 5.13. It indicates that the weak lane discipline characteristic is reflected in the model. It also indicates that vehicles' lateral positions are evenly distributed across the width of the road. Due to asymmetry in X and Y scales, there is an impression regarding very close longitudinal proximity of vehicles with each other, but in the simulation model, they are maintaining sufficient gaps.

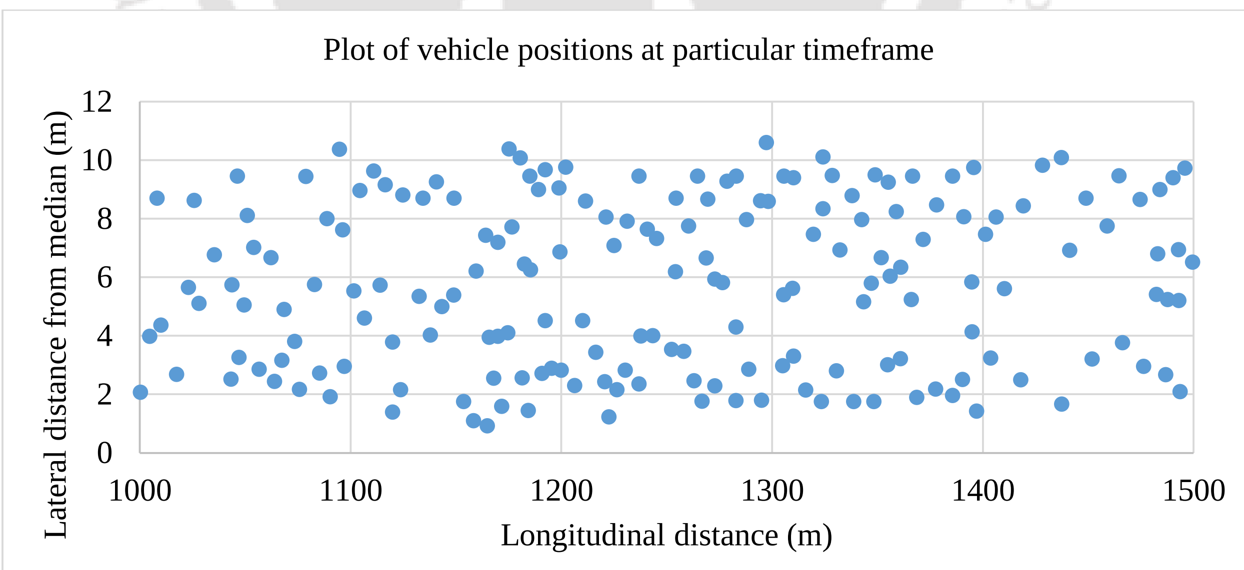

Fig. 5.13. Graphical representation of simulated vehicles along roadway length. Each point represents the center of the front edge of a vehicle.

5.3.4.7 Longitudinal gap-maintenance with speed and centerline separation

The face-validation of, whether vehicles observe the same rules governing vehicle-following in the model, as devised in Section 4.2 is conducted by extracting longitudinal gap, average speed and centerline separation of leading-following vehicle pairs in VISSIM and developed model. The criteria for selection of such pairs are (i) time headway shall be less than 2 seconds; (ii) there should be lateral overlapping, and (ii) relative speed of LV and FV is less than 5 km/h. Relationship of longitudinal gap (dependent variable) with centerline separation and average speeds (as independent variables) is developed using scatter data for LV-FV types obtained from the model. The relationship obtained from simulation model is similar to Section 5.3, i.e., linear variation with Burr-distributed residuals. The coefficients of relationship for few vehicle pairs (as obtained from the simulation model) is described in Table 5.6.

For validating the field and developed relationship, raw data from field as well as model are discretized into several centerline separation and average speed groups and T-test is performed on each group (presented in Table 5.7). N.D. indicates no field data available for that group. In Table 5.7, the null hypothesis is that data from each groups of speed and centerline separation ranges for field and simulation model are statistically similar at 5% significance levels. The shaded cells indicate the ranges of speed and centerline separation for the particular vehicle types, where data of field and model are not statistically similar.

Table 5.6 Coefficients of modeled equation and residual parameters from simulation model

Vehicle types		Coefficients of modelled equation 4.4			Parameters of modified Burr distributed residuals			
LV	FV	*a*	*b*	*c*	*k*	*α*	*β*	*γ*
Car	Car	0.07	-0.39	4.6	1.08	0.91	18.85	-12.73
Car	3W	0.13	-0.24	1.54	0.78	2.13	16.56	-1.39
Car	2W	0.05	-0.02	3.23	1.46	3.38	3.4	-0.82
3W	2W	0.06	-0.27	3.63	13.6	1.7	5.68	-1.22
2W	2W	0.07	-0.1	2.38	5.24	1.49	3.89	-2.49
2W	3W	0.1	-0.08	1.05	1.33	31.93	14.61	-9.42
3W	Car	0.14	-0.69	1.11	4.02	95.31	2.09	-2.05
2W	Car	0.08	-0.18	1.46	51.39	82.48	1.45	-0.1
LCV	Car	0.11	-0.25	1.08	3.37	6.31	4.13	-0.97
Heavy	Car	0.2	-0.88	0.25	0.76	5.6	9.09	-1.11

Table 5.7 T-test results for groups of speed and centerline separation ranges, for different vehicle pairs, for validation of simulation model with field data for vehicle-following behavior

LV-FV pair		2W-3W			Car-3W			Car-2W			Car-Car			
Centerline Separation (m)		0-1	1-2	2-3	0-1	1-2	2-3	0-1	1-2	2-3	0-1	1-2	2-3	3-4
Speed range (km/h)	0-10	N.D.	N.D.	N.D.	N.D.	N.D.	N.D.	0.12	0.08	N.D.	0.10	0.14	0.42	N.D.
	10-20	0.71	N.D.	N.D.	0.25	0.81	N.D.	0.49	0.26	N.D.	0.75	0.23	0.12	0.49
	20-30	0.02	0.41	N.D.	0.69	0.25	0.36	0.26	0.38	0.08	0.09	0.00	0.09	0.47
	30-40	0.85	0.30	0.46	0.01	0.36	0.09	0.07	0.00	0.00	0.00	0.00	0.38	0.23
	40-50	0.03	0.83	N.D.	0.01	0.01	0.09	0.04	0.07	0.88	0.00	0.16	0.29	0.15
	50-60	0.67	0.16	0.59	0.09	0.11	0.00	0.11	0.36	0.44	0.05	0.22	0.82	0.34
	60-70	N.D.	N.D.	N.D.	N.D.	N.D.	N.D.	0.12	0.10	N.D.	N.D.	0.08	0.68	N.D.
LV-FV pair		3W-Car			LCV-Car			2W-Car			HV-Car			
Centerline Separation (m)		0-1	1-2	2-3	0-1	1-2	2-3	0-1	1-2	2-3	0-1	1-2	2-3	3-4
Speed range (km/h)	0-10	N.D.	N.D.	N.D.	0.33	0.74	N.D.	0.54	0.04	N.D.	N.D.	N.D.	N.D.	N.D.
	10-20	0.83	N.D.	N.D.	0.72	0.00	0.41	0.25	0.28	N.D.	N.D.	N.D.	N.D.	N.D.
	20-30	0.27	0.01	0.28	0.01	0.01	0.53	0.05	0.01	N.D.	0.78	0.17	0.48	N.D.
	30-40	0.69	0.22	0.15	0.95	0.22	0.55	0.00	0.03	0.10	0.21	0.86	0.11	0.47
	40-50	0.80	0.30	0.18	0.05	0.21	0.02	0.03	0.03	0.94	0.13	0.57	0.16	0.81
	50-60	0.80	0.30	N.D.	0.22	0.72	0.07	0.65	0.07	0.10	0.48	N.D.	0.22	N.D.
	60-70	N.D.	N.D.	N.D.	N.D.	N.D.	N.D.	0.56	0.52	0.87	N.D.	N.D.	N.D.	N.D.

The exercise in Table 5.7 fails to reject the null hypothesis for majority of speed and centerline separation ranges (total 82 of 105 cells or 79% of cells in Table 5.7).

This exercise is also conducted on VISSIM datasets and mentioned in Table 5.8.

Table 5.8 T-test results for groups of speed and centerline separation ranges, for different vehicle pairs, for validation of VISSIM model with field data for vehicle-following behavior

LV-FV pair		2W-3W			Car-3W			Car-2W			Car-Car		
Centerline Separation (m)		0-1	1-2	2-3	0-1	1-2	2-3	0-1	1-2	2-3	0-1	1-2	2-3
Speed range (km/h)	0-10	N.D.	N.D.	N.D.	N.D.	N.D.	N.D.	0.00	0.00	N.D.	0.02	0.01	0.00
	10-20	0.02	N.D.	N.D.	0.00	0.01	N.D.	0.08	0.04	N.D.	0.00	0.00	0.00
	20-30	0.02	0.41	N.D.	0.00	0.00	0.00	0.00	0.05	0.00	0.00	0.00	0.00
	30-40	0.00	0.01	0.00	0.00	0.00	0.00	0.00	0.00	0.00	0.00	0.00	0.00
	40-50	0.00	0.00	N.D.	0.00	0.00	0.00	0.00	0.00	0.00	0.00	0.00	0.00
	50-60	0.00	0.00	0.00	0.00	0.00	0.00	0.00	0.00	0.00	0.00	0.00	0.00
LV-FV pair		3W-Car			LCV-Car			2W-Car			HV-Car		
Centerline Separation (m)		0-1	1-2	2-3	0-1	1-2	2-3	0-1	1-2	2-3	0-1	1-2	2-3
Speed range (km/h)	0-10	N.D.	N.D.	N.D.	0.00	0.00	N.D.	0.00	0.00	N.D.	N.D.	N.D.	N.D.
	10-20	0.00	N.D.	N.D.	0.01	0.03	0.00	0.02	0.06	N.D.	N.D.	N.D.	N.D.
	20-30	0.01	0.00	0.00	0.02	0.00	0.00	0.03	0.00	N.D.	0.00	0.00	0.00
	30-40	0.00	0.00	0.00	0.00	0.00	0.00	0.00	0.00	0.00	0.00	0.00	0.00
	40-50	0.00	0.00	0.00	0.00	0.00	0.00	0.00	0.00	0.00	0.00	0.00	0.00
	50-60	0.00	0.00	N.D.	0.00	0.00	0.00	0.00	0.00	0.00	0.00	N.D.	0.00

Surprisingly, it is observed that there is a large difference between datasets of VISSIM and field. The plot of *LG* with speed for field data, VISSIM and developed model is presented in Fig. 5.14 for two *CS* levels, for car-car data.

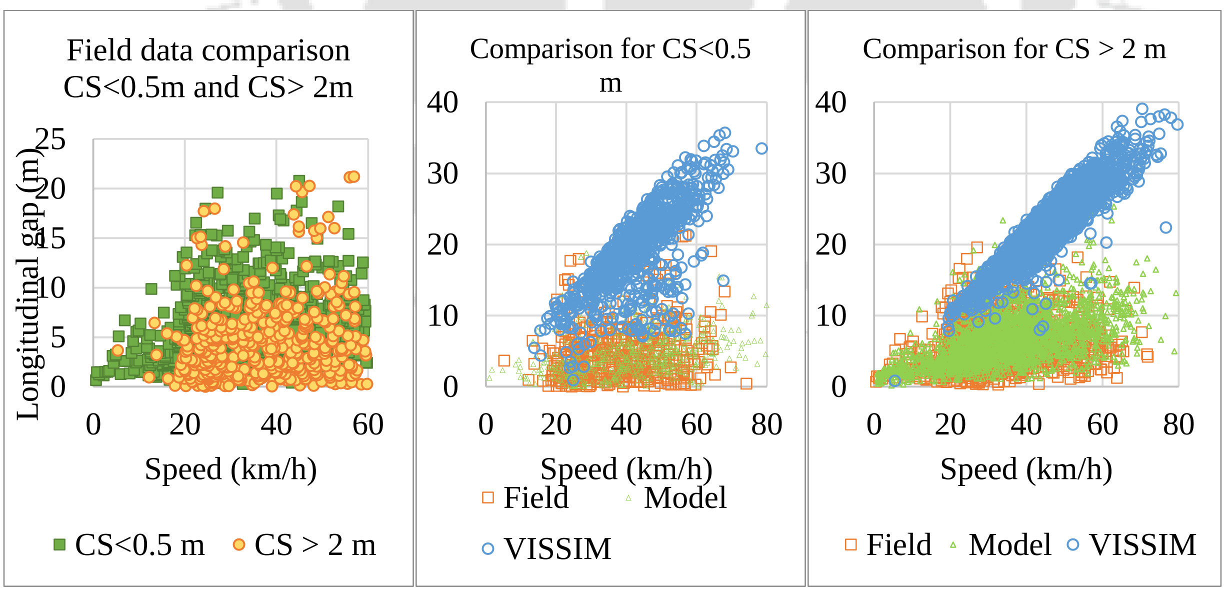

Fig. 5.14. Comparison of *LG* data with *CS*<0.5 m and *CS*>2 m for field, model and VISSIM

It is observed from Fig. 5.14 that although the data extracted from simulation model (*LG* with speed at different *CS* levels) are similar to field trend, the *LG* obtained from VISSIM data is statistically higher.

5.3.4.8 Lateral clearance maintaining behavior with speed

Similar to validation of longitudinal gap-maintenance behavior, the validation for lateral clearance data with average speeds of overtaking and overtaken vehicles are also conducted for certain vehicle pairs. It is considered that vehicles do not interact laterally above 2.5 m lateral clearance, so *LC* data above this limit are not considered. The simulation model also follows an increasing linear relationship of lateral clearance with average speeds (coefficient of correlation 0.367) with beta-distributed residuals across the best fit line, as obeyed by the field data. The slopes and intercepts of regression lines and various coefficients of Beta distribution (Refer Equation 4.2) are provided in Table 5.9.

Validation for certain vehicle pairs (car-car, 3W-car, 2W-car, three-wheeler two-wheeler, car-heavy vehicles and car-LCV) pairs are conducted by discretizing speed in 10km/h intervals, and T-test is conducted at each speed intervals for various pairs. The validation exercise is mentioned in Table 5.10. The exercise fails to reject the null hypothesis that data from speed ranges for field and simulation model are statistically similar at 5% significance levels, for a majority of cells (34 of 48 cells or 70% cells with data).

Table 5.9 Developed regression model with residual distribution as obtained from modelled data

Vehicle pair	Regression line		Coefficients of Beta distribution			
	slope	intercept	α_1	α_2	a	b
All combined	**0.38**	**122.43**	**5.10**	**5.78**	**-130.19**	**199.38**
3W-3W	0.14	122.83	2.59	3.74	-86.59	120.02
3W-2W	0.34	124.43	4.19	3.98	-139.11	151.51
3W-HV	0.98	110.81	2.45	2.92	-87.20	123.98
2W-2W	0.60	114.88	1.31	2.30	-102.39	113.38
Car-3W	0.09	129.96	5.92	7.11	-134.19	128.91
Car-2W	0.30	125.59	5.19	4.10	-148.19	161.25
Car-Car	0.46	119.55	6.18	2.19	-121.30	147.39
Car-Heavy	0.88	107.08	2.10	3.48	-93.20	124.31
Car-LCV	0.36	123.82	1.91	2.45	-83.49	100.08

A similar exercise is also conducted for data obtained from VISSIM simulation. However, it is observed that in the obtained VISSIM data, there is very less correlation of lateral clearance with average speeds (coefficient of correlation is 0.023) for all the vehicle pairs. Further, clearance maintained by vehicles in VISSIM is observed to be higher than input field data. A comparison of the plot of data for VISSIM, field and model for car-car pairs is shown in Fig. 5.15.

Thus, although model can reflect the increasing trend behavior of lateral clearance with speed significantly, the VISSIM model is unable to reflect this behavior.

Table 5.10 T-test results for groups of speed ranges, for different vehicle pairs, for validation of simulation model with field data for lateral clearance-maintaining behavior

Speed ranges (km/h)	0-10	10-20	20-30	30-40	40-50	50-60	60-70	70-80
Car-Car	0.044	0.346	0.295	0.029	0.012	0.009	0.075	0.740
Car-3W	0.062	0.073	0.051	0.190	0.039	0.021	0.399	N.D.
3W-3W	0.917	0.476	0.017	0.069	0.048	0.733	N.D.	N.D.
3W-2W	0.060	0.621	0.081	0.495	0.141	0.382	0.003	N.D.
Car-LCV	0.929	0.141	0.037	0.379	0.229	0.283	0.435	N.D.
Car-Heavy	0.956	0.828	0.022	0.005	0.087	0.033	0.047	0.887
3W-HV	N.D.	0.799	0.645	0.181	0.461	0.73	N.D.	N.D.

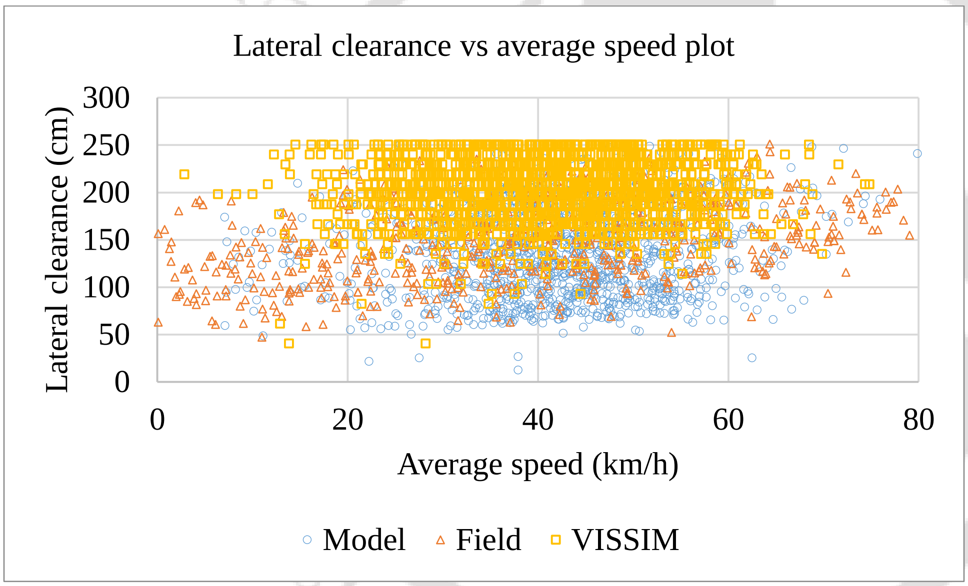

Fig. 5.15 Plot of lateral clearance with speed for field, developed model and VISSIM data

5.3.4.9 Verification of obtained vehicle composition

The composition of vehicles generated in the model should be similar to the field composition. For this purpose, vehicles are generated for four different random seeds which allow different aggregate compositions. The overall composition is observed to be similar to the field. Table 5.11 gives variation of field and model compositions (percent of total) for different vehicle types.

Table 5.11 Vehicle composition obtained from field and model

Vehicle	Truck	Car	3W	Bus	2W	LCV	Total
Field composition %	1.8	43.4	8.1	3.1	40.8	2.6	100
Model composition %	0.5	43.8	11.1	2.8	40.7	1.1	100

5.4 Application of the developed model

The model has been calibrated and validated at microscopic and macroscopic levels. Now, it can be used to generate specific cases of traffic flow to study and experiment with different traffic conditions. This section focusses on simulation of specific traffic cases using the developed model, which is not possible in real-world traffic stream without disturbing flow of traffic. Some specific cases used in the study include calculation of road capacity, a variation of capacity with free flow speed, road width wise effect on capacity and effect of segregation of traffic.

5.4.1 Capacity of the road section

The selected calibrated and validated traffic stream is simulated for various speed and density ranges averaged over 5-minute durations. A generalized single regime model is found to fit better in obtained speed-density plot in Fig. 5.16 (a) (RMSE 5.4, $R^2 = 0.92$). Dual regime models are not attempted since they reflect inconsistency of driver behavior at the boundary condition of free and congested regime. Equation of this model is given in Equation 5.13, where u is stream speed, k is stream density, k_j is jam density and u_f is free flow speed. Estimated values of u_f, k_j, l and m are 58.94, 591.8, 2.427 and 0.621, respectively.

$$u^{1-m} = {u_f}^{1-m}\left[1 - \left(\frac{k}{k_j}\right)^{l-1}\right] \qquad \dots 5.13$$

Assuming flow as a product of speed and density, a model with same coefficients (u_f, k_j, l and m) is fitted with speed-flow diagram, presented in Fig. 5.16 (b), and the capacity of Section is estimated as 6,300 vehicles per hour. Jam density observed from Speed-density plot is 590 vehicles/km, whereas free flow speed is 59 km/h. Although cars with free flow speed > 75 km/h have substantial composition (43%), slower moving vehicles constitute remaining composition and have free flow speeds less than 60 km/h, They are observed to hinder movement of faster moving vehicles at moderate density levels (50-150 veh/km). Due to this, overall stream free flow speeds as per best fit equation are lower than expected.

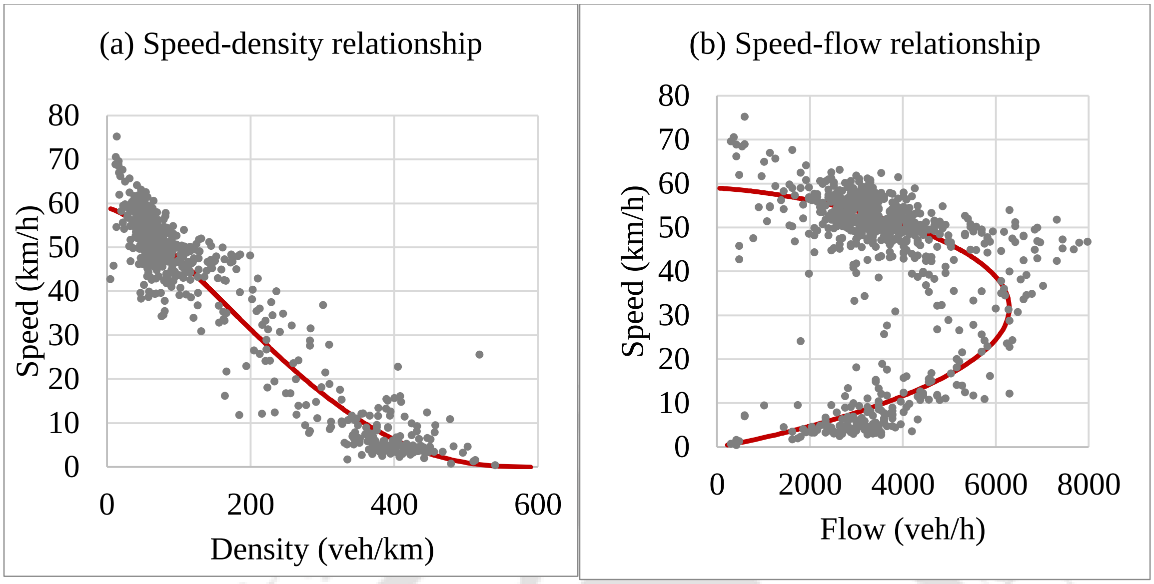

Fig. 5.16. (a) Speed-density; and (b) Speed-flow relationships of simulated section

5.4.2 Effect of free-flow speed on capacity

Homogeneous (car-only) traffic streams with different free-flow speeds are generated at different flow levels, and their capacities are calculated based on speed-flow diagrams. Variation in desired speeds of cars is fixed to the extent of 10% of mean value to represent the free-flow speed. As expected, it is observed that the section capacity increases with increase in free-flow speed, from 4,940 cars/h for desired speed 50 km/hr to 8,140 cars/h for desired speed 120 km/hr for 3-lane road, constituting 100% cars. The variation of capacity with different desired speed levels is shown in Fig. 5.17. It is observed that capacity varies linearly with increase in free-flow speed. The results are synonymous with Dhamaniya and Chandra (2017) till free-flow speeds of 90 km/h.

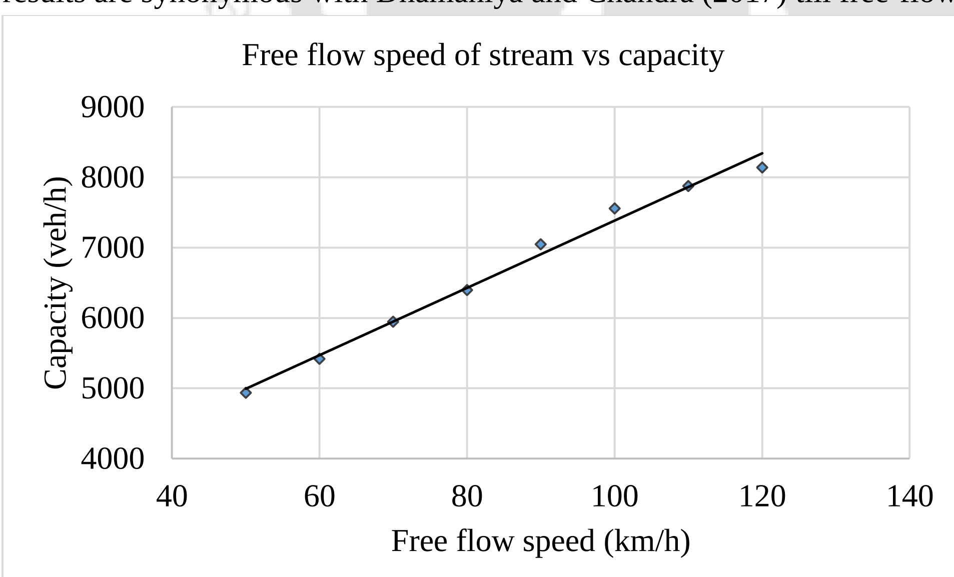

Fig. 5.17 Variation of capacity with free flow speeds for homogeneous simulated stream

5.4.3 Effect of road width on capacity

Homogeneous (cars-only) as well as heterogeneous traffic streams (composition provided in Table 5.1) are generated at different road widths from 3.75 m wide (single lane) to 14 m wide (4 lanes). As expected, it is observed that capacity increases with increase in road width for both the streams. For homogeneous traffic, the capacity per lane does not show a significant increase with width, and varies from 2,300-2,500 veh/h/lane. However, in case of heterogeneous traffic streams, the capacity of section per meter width does not remain consistent with the width of the road, but decreases from 771 vehicles/m/hr (for single lane carriageway) to 578 vehicles/m/hr (for four lane carriageway). This trend is also observed in previous researches (Chandra and Kumar, 2003). The result is not synonymous with HCM-2000 which mentions a proportional increase in capacity with number of lanes. As the road width increases, drivers feel more comfortable and try to maintain more safety. There are less constrained overtaking conditions. Further, it is observed that this decrease is steady with width of road, because fixed-width vehicles in homogeneous traffic are not able to squeeze in between smaller gaps, as against vehicles of smaller width present in heterogeneous traffic. The capacity for heterogeneous streams is lower than homogeneous streams (at same width), due to presence of slow-moving vehicles like three-wheelers. The trend of capacity per meter width with width of the road for heterogeneous traffic is presented in Fig. 5.18.

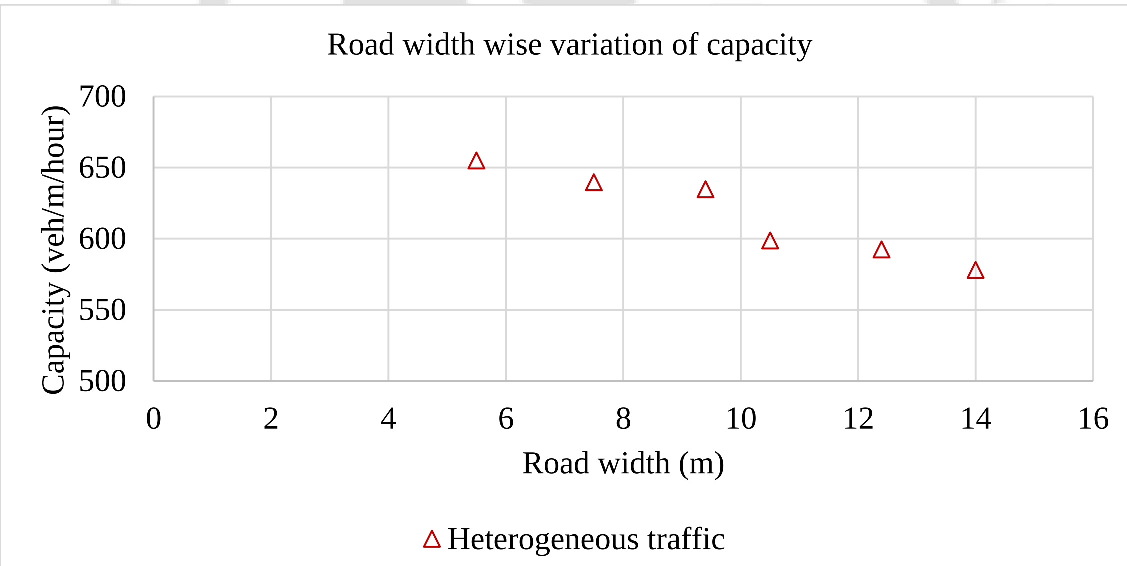

Fig. 5.18 Effect of road width on capacity of roadway for heterogeneous traffic

5.4.4 Effect of segregation of buses on the traffic stream

In order that public transport gets preference over other modes of transport, buses are segregated from other vehicle types by providing a separate bus-lane for their speedy transport, called as Bus Rapid Transit or BRT. This traffic management can also be simulated for an 11.5 m wide road by generating two traffic streams- (i) Simulated road width 7.75 m, without buses; and (ii) Simulated road width 3.75 m, exclusively for buses. The capacities for individual simulated streams are added and compared with original traffic stream without segregation. The flow and speed levels achieved by combined traffic streams are compared with the usual stream on 11.5 m wide roadway width, and presented in Fig. 5.19.

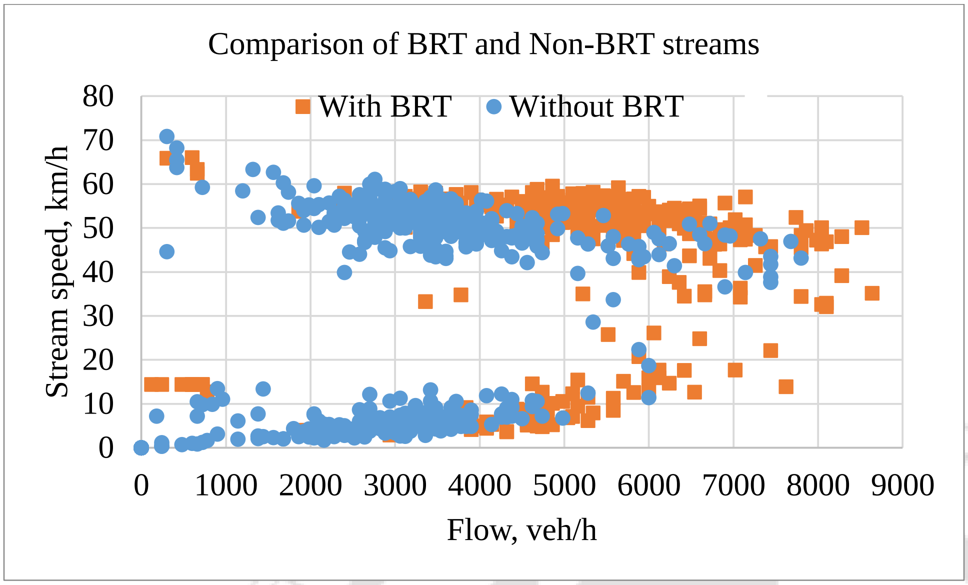

Fig. 5.19 Comparison of BRT and non-BRT traffic streams

The average speeds obtained at various speed levels for BRT and non-BRT traffic are presented in Table 5.12.

Table 5.12 Stream speeds at various flow ranges with and without BRT system

Flow range, vph	Average stream speed (Km/h) No BRT	Average stream speed (km/h) With BRT	% improvement
0-1000	67.42	68.68	1.42
1000-2000	55.64	57.63	3.58
2000-3000	51.87	53.91	3.93
3000-4000	50.35	53.28	5.82
4000-5000	47.46	52.34	10.28
5000-6000	39.06	45.36	16.13
6000-7000	30.23	36.65	21.24

It is also observed that the capacity of section increases from 6300 vph to 7450 vph. At the capacity condition, higher number of buses are generated (8.2% as against 3.1% without BRT). There is maximum improvement to speed of buses (21% improvement) at capacity. The segregation of this stream will be useful at flow levels 4000 vph or higher, since there would be greater than 10% improvement in flow. This observed result is also synonymous to previous literature (Arasan and Vedagiri, 2009).

5.5 Summary

This chapter has described the development of a simulation model based on models for inter-vehicular lateral and longitudinal gaps, for heterogeneous traffic with weak lane discipline in mid-block sections. Further, it has described its calibration and validation with field data and evaluated its performance with a commercial simulation model VISSIM. Few applications of the model are also highlighted.

Development of simulation model

- The developed comprehensive simulation model updates position of every vehicle (using parallel update scheme) at discretized time-step of 1 seconds, which is assumed equal to the average perception-reaction time of the drivers. It consists of generation zone, where vehicles are generated and assigned parameters as per field traffic conditions.
- Movement of a vehicle (driver behavior) depends on presence of leading or adjacent vehicles to it, which govern speeds to be maintained during vehicle-following or overtaking, respectively. The choice of overtaking or following is formulated depending on inter-vehicular gaps.
- Speed maintained during overtaking depends on available gap between vehicles, calculated based on inter-vehicular lateral clearance relationship with speed devised in Chapter 5.
- The reaction while approaching a slow moving vehicle to follow it depends on distance from stable longitudinal gap (which depends on speed and staggering, calculated in Chapter 5).
- Based on obtained reactions, speeds and positions of vehicles at next time step are updated depending on speeds and positions at the previous time-steps.
- Various microscopic and macroscopic parameters are calculated from simulation model.

Calibration and validation of developed simulation model

- The developed simulation model is site-specific. Field parameters such as roadway features, traffic composition, desired lateral and longitudinal speeds are extracted from a field section for calibration and used as input in simulation model.
- Values of additional unknown parameters in simulation model are calculated indirectly so that the error between field traffic characteristics and simulated stream characteristics is minimum. The model is calibrated using genetic algorithms.
- A commercial traffic model VISSIM is also calibrated using the same logic, and results obtained from both–VISSIM and developed model are compared with field data.
- The developed model is observed to perform comparable to VISSIM, while representing macroscopic characteristics and microscopic characteristics like time headway distribution, speed distribution, etc. It is observed to perform better while calculating lateral maneuvers of vehicles or relationship of lateral and longitudinal gaps with speed.

Application of developed model

The developed model is used to calculated capacity of given roadway feature. It is also devised to calculated effect of road width, desired speed and segregation of traffic stream on roadway capacity. The results are observed in tune with previous literatures.

CHAPTER 6

Conclusions and future scope

6.1 General

The research work in this thesis focuses on development of driver behavior model based on maintaining of inter-vehicular lateral and longitudinal gaps in heterogeneous traffic stream with weak lane discipline. To develop this model, inter-vehicular lateral clearances during overtaking are obtained from the real world traffic streams by high-accuracy ultrasonic sensors attached to an instrumented vehicle running as a part of traffic stream, and a high accuracy GPS device fixed in-vehicle to obtain its speed. Longitudinal gaps between leading and following vehicles in traffic stream are calculated with the help of a camera calibration technique for converting image coordinates from video to real-world coordinates. Single degree regression models with Beta and Burr-distributed residuals are respectively developed for variation of inter-vehicular lateral clearances with speeds, and longitudinal gaps with speed and amount of staggering. Further, overtaking decision model is developed based on inter-vehicular gaps and vehicle speeds. These three models are used as input to the developed simulation model, consisting of separate modules for free flow, vehicle-following and overtaking behavior. This model is well-calibrated using Genetic Algorithms and validated with field data at microscopic and macroscopic levels. The model's performance was compared to a commercial software VISSIM. Further, it was used to generate specific cases of interest to a traffic engineer, such as estimating the capacity of different sections, calculating the effect of desired speed, road width or vehicle segregation on the capacity of stream.

This chapter presents the summary of research conducted in this thesis. The second section highlights the key findings in this research. The contribution of developed research for the scientific community is showcased in the third section. The fourth section explores the future scope of this research work.

6.2 Conclusions

The key findings from this research can be summed up as follows-

6.2.1 Analysis and modeling of lateral interactions

Lateral clearances (*LC* – the clear distances between sides of adjacent vehicles) are evaluated between various pairs of vehicles as they move in the traffic stream, and their variation with the speeds of vehicles are studied. High accuracy sensors attached to the sides of a vehicle measure the lateral clearances as it overtakes or gets overtaken by other vehicles. The observations from this study are-

- A significant correlation is observed between average speed ($\bar{v}$) and lateral clearance, but there is quite weak correlation between relative speed and width of road on lateral clearance.

- LC increases for increase in average speed between two vehicles. The model for lateral clearance with $\bar{v}$ can be represented by a deterministic part and stochastic part. The deterministic part consists of a linear relationship with positive slopes (m) and intercepts (c), whereas the stochastic part consists of Beta-distributed residuals (φ) which are homoscedastic with $\bar{v}$. The residuals address the driver variability in LC behavior for similar speed levels. The general model can be represented as –

$$LC = m\bar{v} + c + \varphi$$

- The slope and intercept in above equation vary for different vehicle types. For a car-car pair, the average LC varies from 1.173 m at 0 km/h to 1.581 m at 60 km/h. The average LC maintained by different vehicle pairs is mentioned in Table 4.4. In general, cars and three-wheelers maintain more LC with heavy vehicles and LCV's, whereas two-wheelers maintain the least LC among the vehicle types.
- Further, it is observed that vehicles maintain lesser LC between similar interacting vehicle types than dissimilar vehicle types. Due to this behavior, lateral clearance cannot be assumed as the sum of individual contribution of vehicles constituting the clearance.
- When a vehicle interacts with vehicles on both sides simultaneously, there is a compromise in maintaining lateral clearance at higher speeds for 3W-2W, car-2W and car-3W pairs. At 50 km/h average speed, the average LC decreases from 1.503 m to 1.347 m, 1.590 m to 1.481 m and 1.696 m to 1.455 m for car-3W, 3W-2W and car-2W pairs, respectively.

6.2.2 Analysis and modeling of longitudinal interactions

Longitudinal gaps are evaluated between a pair of leading and following vehicle (LV and FV) when the FV has stabilized behind LV and the relative speed between them is negligible (<5 km/h). Their variations with amount of staggering (lateral centerline separation or CS of LV and FV) and average speeds ($\bar{v}$) are studied. The data are extracted from video data recorded for various traffic sections across different cities. They key observations from this study are-

- Longitudinal gaps (LG) increase with $\bar{v}$ and decrease with CS. The variation can be represented by a deterministic part and stochastic part. The deterministic part consists of equation of a plane, having positive slope (a) with $\bar{v}$, negative slope (b) with CS, and intercept (c). The stochastic part consists of Burr-distributed residuals (φ) which are heteroskedastic (fan-shaped nature) with LG and can be transformed appropriately to make them homoscedastic. The residuals address the driver variability for same speed or CS levels. The general model can be represented as –

$$LG = a(\bar{v}) + b(CS) + c + \varphi$$

- The slopes and intercept in above equation vary for different vehicle types. For car-car pair, the average LG varies from 3.38 m at 0 km/h to 9.98 m at 60 km/h for CS=0 m, and from 2.13 m at 0 km/h to 8.73 m at 60 km/h for CS=1 m. The coefficients of above equation for different vehicle pairs are presented in Table 4.11. It is observed that LG increases with the size of LV. For instance, at 30 km/h, and *CS*=0 m, *LG* for 2W-car, car-car, LCV-car and heavy vehicle-car pairs are 5.18 m, 6.67 m, 6.68 m and 6.88 m, respectively.

- If vehicle follows two vehicles simultaneously, then it compromises significantly on maintenance of longitudinal gap. This compromise is higher if a smaller vehicle is following a larger vehicle. The percentage change of *LG* with the introduction of a second leading vehicle is mentioned in Fig. 4.19, for different vehicle pairs, speeds and centerline separations. Further, the compromise is higher with increase of *CS* and decrease of $\bar{v}$. As lateral clearance between two leading vehicles decreases, average longitudinal gap increases.

6.2.3 Overtaking decision-making criteria

Based on lateral veering of the approaching FV in collected video data of traffic streams, the categorical variable of overtaking decision of the following driver is determined. A logistic regression model is developed between the explanatory variables longitudinal gaps (*LG*), centerline separation (*CS*), relative speed ($v_{LV|FV}$), average speeds ($\bar{v}$) and presence of hindrance to overtake (*H*); and the categorical variable decision to overtake. Predicted probability (*p*) of overtake occurring can be calculated by

$$p = 1 - [\frac{1}{1 + e^{-z}}]$$

where, z is log-odds to overtake and given by,

$$z = \ln\left(\frac{probability\ to\ follow}{probability\ to\ overtake}\right) = \beta_0 + \beta_1\bar{v} + \beta_2 v_{LV|FV} + \beta_3 LG + \beta_4 CS + \beta_5 H.$$

This equation calculates the probability to overtake a particular vehicle for different combinations of LV and FV. From the development of this model, it is observed that-

- Probability to overtake increases with relative speed and centerline separation, and decreases with longitudinal gap and average speed between LV and FV. Further, this probability also decreases if there is a presence of hindering traffic or road edges to overtake.
- Probability to overtake a car by another car is more sensitive to change in centerline separation and average speed. Further, it is observed that smaller sized vehicles like two-wheelers have higher tendency to overtake.
- For a car-car pair, there is 8.9% decrease, 3.2% increase, 1.9% decrease, and 23% increase in probability to overtake on 5% increase of average speed, relative speed, longitudinal gap and centerline separation, respectively. Similar relationships are obtained for other pairs mentioned in Table 4.18.

6.2.4 Developed simulation model based on inter-vehicular gaps

A simulation model is developed based on lateral and longitudinal gap-maintaining behavior and overtaking decision modeling. Separate algorithms are devised for the reaction of drivers during following (maintaining a longitudinal gap), and during overtaking (allowable speed of vehicle while maintaining lateral clearances during overtaking). Field input parameters include desired and lateral speeds, acceleration-deceleration values from previous studies, traffic composition and average flow levels. The developed model is well-calibrated with field conditions by using genetic algorithms. Its performance is also compared with a commercial software VISSIM, by validating both these models with field data. The validation is conducted for the following-

- Macroscopic properties (speed-flow relationship), and
- Microscopic properties (time headway distribution, speed distribution, average lateral shifts, lateral and longitudinal gap-maintaining behavior, etc).

It was observed that the developed model can replicate real traffic stream behavior at both macroscopic and microscopic levels. The developed model is also used for generating specific cases useful for a traffic engineer. They are mentioned below-

- The model was calibrated for an 11.5 m wide section in Bengaluru city. The capacity of this section is estimated by fitting of a generalized model for speed-density curves. The estimated capacity from developed model is observed as 6,400 veh/h.
- The capacity is observed to increase linearly with desired speed from 4,940 cars/h at 50 km/h to 8,140 cars/h at 120 km/h desired speeds, by generating a hypothetical car-only traffic stream in the simulation model.
- Further, the capacity increases with an increase of road width, but it does not get doubled by doubling the road width as observed in lane disciplined traffic. With the addition of more lanes, capacity per lane decreases.
- The simulation model is also used to segregate bus traffic from other vehicles in the stream, and model the two segregated streams. It is observed that the capacity improves from 6,400 to 7,500 veh/h by segregating bus traffic from other vehicles.

6.3 Contribution of this research

Developed models for lateral and longitudinal gaps and a driver behavior model devised based on these models are the major contributions of this work. The detailed contribution of this work is presented below.

1. The traffic streams of developing countries have the key characteristics of weak lane discipline and heterogeneous vehicle types. Weak lane discipline behavior is addressed by developing a model for lateral clearance with speeds of the vehicles, and the introduction of centerline separation – an independent variable which takes into account the staggering of LV and FV in weak lane discipline traffic. The heterogeneous traffic characteristic is addressed by developing separate vehicle pairwise models.
2. An innovative method is developed for measuring the lateral clearance between vehicles accurately, by means of sensors attached to the vehicle's sides, in addition to GPS device to measure vehicle speeds. There were 6,016 lateral interactions observed across six cities with 32 different instrumented vehicles, making it one of the largest known data collection exercises for the study of lateral interactions in this traffic condition. To measure longitudinal gaps, a semi-manual, video image-based camera calibration program is

developed, which is used to extract trajectories of LV and FV in a mixed traffic stream. Based on trajectories, the longitudinal gaps, staggering and vehicle speeds were obtained. A total 14,056 interactions were observed for mixed traffic stream across 12 different sections having geographical and traffic variations.

3. The models developed for gap-maintaining behaviors consists of a deterministic and stochastic part. The stochastic part addresses the variability in driver behavior. It is observed that gap-maintaining behaviors cannot be developed for an individual vehicle type, but pairwise relationships need to be developed.
4. Further, when vehicle interacts (either laterally or longitudinally) with multiple vehicles simultaneously, it is observed that there is a significant compromise in gap-maintaining behavior, especially at higher speeds. This novelty has a significant contribution for the development of simulation model.
5. A categorical model for predicting decision of overtaking in mixed traffic conditions by means of inter-vehicular gaps and speeds is also developed for the first time.
6. The developed simulation model consists of separate modules for vehicle-following, free-flow and overtaking, depending on developed models for inter-vehicular gaps with speed and staggering. Every generated vehicle in the simulated traffic stream is assigned a random risk factor (a measure of aggressiveness) which addresses the driver heterogeneity. This risk factor governs the stochastic part of gap-maintaining models. Further, it also governs the overtaking decision-making of a vehicle in the simulation model, depending upon calculated probability to overtake and a driver's assigned risk factor. This unique approach addresses the driver variability in addition to mixed traffic and weak lane discipline.
7. The simulation model is validated with the field data using Genetic algorithms and also compared with commercial VISSIM software. The validation is conducted for both-macroscopic and microscopic stream properties. The model applicability is also tested, and the results are found to be consistent with previous researches.
8. Developed model can have several immediate applications, including traffic management strategies such as (i) Effect of widening of carriageway on capacity and stream speed; (ii) Effect of allowing or disallowing certain vehicles on the traffic stream behavior; (iii) Effect of design speed on capacity; (iv) Effect of segregation of certain vehicles on the traffic behavior.

6.4 Future scope

A list of motivations for future work using the outcome of this thesis is presented below.

1. *Development of gap-maintaining behavior for traffic in rural/semi urban areas:* This thesis has primarily focused on traffic in urban areas and the traffic locations are in million-plus population cities. Driver behavior in rural or semi-urban area maybe different, due to difference in road function (and thus road widths), difference in vehicle types (a higher percentage of non-motorized vehicles and agricultural tractors are observed), and due to

difference in trip purpose. A detailed study of similar gap-maintaining behavior can be conducted as a future extension to the work in this thesis.

2. *Development of simulation model for bidirectional roads*: Developed simulation model can be used with further additional models (such as vehicle interactions with opposing vehicles, acceleration when overtaking from the wrong side, etc.,) to develop a simulation model for bidirectional traffic.
3. *Development of driving simulators in mixed traffic:* The developed simulation model can be used to generate a traffic stream with desired flow and traffic composition in a driving simulator, and the performance of a driver can be evaluated based on his/her maneuvering abilities in this traffic stream.
4. *Development of automated vehicles in weak lane disciplined mixed traffic:* The maneuvering of an automated vehicle in mixed, no lane disciplined traffic can be programmed based on (i) inter-vehicular gap-maintaining risks of drivers surrounding automated vehicle; (ii) Comfortable driving requirement of vehicle user or passenger (i.e., comfortable acceleration and deceleration rates, safe perception of desired speeds, lateral clearances, etc.), and (iii) developed algorithm for vehicle-maneuvering in the simulation model.
5. *Development of road ecology models in mixed traffic stream:* The road ecology models (i.e., the environmental effect of traffic) could be developed by combination of this simulation model with added inputs from emission modeling of pollutants from different vehicle types.

Bibliography

Conference/ Journal publications

1. Ahmed, K. I., Ben-Akiva, M. E., Koutsopoulos, H. N., and Mishalani, R. G. (1996). Models of freeway lane changing and gap acceptance behavior. In: Proceedings of 13th International Symposium on the Theory of Traffic Flow and Transportation, Jul 1996, Lyon, France.
2. Alonso, L., Milanes, V., Torre-Ferrero, C., Godoy, J., Oria, J., and Pedro, T. (2011). Ultrasonic Sensors in Urban Traffic Driving-Aid Systems. Sensors, 11(1):661-673.
3. Ambarwati, L., Pel, A. J., Verhaeghe, R., and van Arem, B. (2014). Empirical analysis of heterogeneous traffic flow and calibration of porous flow model. Transportation Research Part C: Emerging technologies, 48:418-436
4. Anjaneyalu, M., and Nagaraj, B. Modelling congestion on urban roads using speed profile data. Journal of the Indian Roads Congress, 549.
5. Antoniou, C., Barcelo, J., Brackstone, M., Celikoglu, H.B., Ciuffo, B., Punzo, V., Sykes, P., Toledo, T., Vortisch, P., and Wagner, P. (2014). Traffic Simulation: Case for guidelines, European Commission. Joint Research Centre Institute for Energy and Transport, Science and Policy Report. doi: 10.2788/11382.
6. Arasan, V. and Koshy, R. (2005). Methodology for modeling highly heterogeneous traffic flow. Journal of Transportation Engineering, 131(7):544–551.
7. Arasan, V. T., and Vedagiri, P. (2009). Microsimulation Study of the Effect of Exclusive Bus Lanes on Heterogeneous Traffic Flow. Journal of Urban Planning and Development. 136(1):50-58. DOI:10.1061/(ASCE)0733-9488(2010)136:1(50)
8. Aycin, M. F., and Benekohal, R. F. (2000). Analysis of Stability and Performance of Car Following Models in Congested Traffic. In: Proceedings of the 79th Annual meeting of the Transportation Research Board, Jan 2000, Washington D.C., USA.
9. Bar-Gera, H., Shinar, D. (2005). The tendency of drivers to pass other vehicles. Transportation Research Part F: Traffic Psychology and behavior, 8(6):429–439.
10. Barmpounakis, E. N., Vlahogianni, E. I., and Golias, J. C. (2016). Extracting Kinematic Characteristics from Unmanned Aerial Vehicles. In: Proceedings of the 95th Annual meeting of the Transportation Research Board, Jan 2016, Washington D.C., USA.
11. Bas, E. K., and J. D. Crisman (1997). An easy to install camera calibration for traffic monitoring. In: Proceedings of IEEE Conference on Intelligent Transportation Systems, pp. 362–366 (1997).
12. Bekey, G. A., Burnham, G. O., and Seo, J. (1977). Control theoretic models of human drivers in car following. Human Factors, 19(4):399–413.
13. Benekohal, R. F., and Treiterer, J. (1989). CARSIM: car following model for simulation of traffic in normal and stop and go conditions. Transportation Research Record, 1194 (1989): 99–111

14. Bevrani, K., Chung, E., and Miska, M. (2012). Evaluation of the GHR car-following model for traffic safety studies. In: Proceedings of 25th ARRB Conference, Sep 2012, Perth, Australia.
15. Brackstone, M., and McDonald, M. (1999). Car-following: a historical review. Transportation Research Part F, 2:181–196.
16. Chakroborty P., Agrawal S., and Vasishtha K. (2004). Microscopic Modeling of Driver Behavior in Uninterrupted Traffic Flow. ASCE Journal of Transportation Engineering, 130:438-451.
17. Chandler, R. E., Herman, R., and Montroll, E. W. (1958). Traffic dynamics: studies in car following. Operations Research, 6:165–184.
18. Chandra, S., and Kumar, U. (2003). Effect of lane width on capacity under mixed traffic conditions in India. Journal of transportation engineering, 129 (2):155-160.
19. Chen, G., Meng, F., Fu, G., Deng, M., and Li, L. (2013). A cell automation traffic flow model for mixed traffic. In: Proceedings of the 13th COTA International Conference of Transportation Professionals (CICTP 2013), Jul 2013, Shenzen, China.
20. Chmura, T., Herz, B., Knorr, F., Pitz, T., and Schreckenberg, M. (2014). A simple stochastic cellular automaton for synchronized traffic flow. Journal of Physica A: Statistical Mechanics and its Applications, 405:332-337.
21. Chong, Y., Chen, Z, Li, Z., Lam, W, Zheng, C., and Li, Q. (2013). Integrated real-time vision-based preceding vehicle detection in urban roads. Journal of Neurocomputing, 116:114-149.
22. Choudhury, C. F., and Ben-Akiva, M. E. (2008). A lane selection model for urban intersections. Journal of the Transportation Research Board, 2088:167-176.
23. Choudhury, C. F., Ben-Akiva, M. E. (2013). Modelling driving decisions: a latent plan approach. Transportmetrica A: Transport Science, 9 (6):546-566.
24. Choudhury, C. F., Islam, M. M. (2016). Modelling acceleration decisions in traffic streams with weak lane discipline: A latent leader approach. Transportation Research Part C: Emerging Technologies, 67:214–226.
25. Comert, G. (2013). Simple analytical models for estimating the queue lengths from probe vehicles at traffic signals. Transportation Research Part B: Methodological. 55: 59–74.
26. Courtney, J. W., Magee, M. J., and Aggarwal, J. K. (1984). Robot guidance using computer vision, Pattern Recognition, 17(6), 585–592.
27. Das, S., and Bowles, B. A. (1999). Simulations of highway chaos using fuzzy logic. In: Proceedings of 18th International Conference of North American Fuzzy Information Processing Society (NAFIPS), Jun 1999, New York, USA.
28. Delpiano, R., Herrera M. J. C, and Coeymans A. J. E. (2015). Characteristics of lateral vehicle interaction. Transportmetrica A: Transport Science, 11:7, 636-647, DOI:10.1080/23249935.2015.1059377

29. Dhamaniya, A., and Chandra, S. (2017). Influence of Operating Speed on Capacity of Urban Arterial Midblock Sections. International Journal of Civil Engineering, 1-10. doi:10.1007/s40999-017-0206-7
30. Dimayacyac, E., and Palmiano, H. (2016). Calibrating Relative Velocity and Lateral Clearance Parameters of a Lane Changing Model for Traffic Microsimulation. In: Proceedings of 23rd Annual Conference of the Transportation Science Society of the Philippines, Aug 2016, Quezon City, Philippines.
31. Evans, L., and Rothery, R. (1973). Experimental Measurements of Perceptual Thresholds in Car Following. Highway Research Record 454, Transportation Research Board, Washington, DC.
32. Fambro, D., Koppa, R., Picha, D., and Fitzpatrick, K. (2000). Driver Braking Performance in Stopping Sight Distance Situations. Transportation Research Record: Journal of the Transportation Research Board 1701(02):9-16.
33. Farah, H., and Toledo, T. (2010). Passing behavior on two-lane highways. Transportation Research Part F, 13:355–364.
34. Feng, Y., Hourdos, J., and Davis, G. A. (2014). Probe vehicle based real-time traffic monitoring on urban roadways. Transportation Research Part C: Emerging Technologies 40:160–178.
35. Ferrari, P. (1989). The effect of driver behavior on motorway reliability. Transportation Research Part B, 23(2):139–150. doi: 10.1016/0191-2615(89)90037-4
36. Fukui, I. (1981). TV image processing to determine the position of a robot vehicle, Pattern Recognition, 14(1–6):101–109.
37. Fukui, M., and Ishibashi, Y. (1996). Traffic Flow in 1D Cellular Automaton Model including Cars Moving with High Speed. Journal of the Physical Society of Japan, 65:1868-1870. DOI: 10.1143/JPSJ.65.1868
38. Fung, G. S. K., Yung, N. H. C., and Pang, G. K. H. (2003). Camera calibration from road markings. Optical Engineering, 42 (10):2967-2977.
39. Gazis, D., Herman, R., and Rothery, R. (1960). Non-linear follow-the-leader models of traffic flow Operations Research, 9(4):545-567.
40. Gipps, P. (1981). A behavioural car following model for computer simulation. Transportation Research Part B: Methodological, 15:105–111.
41. Gipps, P. G. (1986). A model for the structure of lane-changing decisions. Transportation Research Part B: Methodological, 20 (5), 403-414.
42. Grabner, H., Nguyen, T. T., Gruber, B., H. Bischof, H. (2008). On-line boosting-based car detection from aerial images. ISPRS Journal of Photogrammetry and Remote Sensing, 63:382-396.
43. Gunay, B. (2003). Methods to quantify the discipline of lane-based-driving. Journal of Traffic Engineering and Control, 44(1):22-27.
44. Gunay, B. (2007). Car-following theory with lateral discomfort. Transportation Research Part B: Methodological, 41 (7):722–735.

45. Gunay, B. (2009). Rationality of a non-lane-based car following-theory. Proceedings of the Institution of Civil Engineers, Transport, 162 TR1:27–37.
46. Gunay, B., and Erdemir, G. (2011). Lateral Analysis of Longitudinal Headways in Traffic Flow. International Journal of Engineering and Applied Sciences (IJEAS). 3(2):90-100.
47. Gundaliya, P. J., Mathew, T. V., and Dhingra, S. L. (2010). Heterogeneous traffic flow modelling for an arterial using grid based approach. Journal of Advanced Transportation, 42(4):467-491.
48. Gupta, S., Chakroborty, P., and Mukherjee, A. (1998). Microscopic Simulation of Vehicular Traffic On Congested Roads. In: Proceedings of International Symposium on Industrial Robotic System - 98, Bangalore, India.
49. Gurumurthy, K. M., Singh, V., and Asaithambi, G. (2016). Microscopic Analysis of Lateral and Longitudinal Gaps in Mixed Traffic Conditions with Weak Lane Discipline. In: Proceedings of Transportation Planning and Methodologies in Developing Countries (TPMDC 2016), Dec 2016, Mumbai, India.
50. Helander, M., and Hagvall, B. (1976). An instrumented vehicle for studies of driver behavior. Accident Analysis and Prevention, 8(4):271–277.
51. Helly, W. (1959). Simulation of Bottlenecks in Single Lane Traffic Flow. In Proceedings of the Symposium on Theory of Traffic Flow, Research Laboratories, General Motors:207–238.
52. Hugemann, W. (2002). Driver reaction times in Road Traffic. In: Proceedings of EVU, Sep 2002, Portoroz, Slovenia.
53. Jia, B., and Gao, Z. (2007). Models and Simulations of Traffic System Based on the Theory of Cellular Automaton. Science Press, Beijing.
54. Jin, S., Wang, D., Tao, P., and Li, P. (2010). Non-lane-based Full Velocity Difference Car Following Model. Physica A 389(21):4654–4662.
55. Jin, S., Huang, Z., Tao, P., and Wang, D. (2011). Car-following theory of steady-state traffic flow using time-to-collision. Journal of Zhejiang University-SCIENCE A (Applied Physics and Engineering), 645-654.
56. Kala, R., and Warwick, K. (2013). Heuristic based evolution for the coordination of autonomous vehicles in the absence of speed lanes, Journal of Applied Soft Computing, 19:387-402.
57. Kanagaraj, V., Asaithambi, G., Srinivasan, K., and Sivanandan, R. (2011). Vehicle Classwise Analysis of Time Gaps and Headways under Heterogeneous Traffic. In: Proceedings of Transportation Research Board 90th Annual Meeting, 11-4249, Jan 2011, Washington D.C., USA.
58. Kato S., and S. Tsugawa. (2001). Cooperative driving of autonomous vehicles based on localization, Inter-vehicle communications and vision systems. JSAE Review, 22(4):503–509
59. Kerner, B. S., Klenov, S. L., and Wolf, D. E. (2002). Cellular automata approach to three-phase traffic theory. Journal of Physics A, 35:9971-10013.

60. Khan, S. I., and Maini, P. (2000). Modeling heterogeneous traffic flow. In: Proceedings of Transportation Research Board 79th Annual Meeting Transportation Research Record, 1678, Jan 2000, Washington, D.C., USA.
61. Kikuchi, S., and Chakroborty, P. (1992). Car-following model based on fuzzy inference system. Transportation Research Record 1365, Transportation Research Board, National Research Council, Washington D. C., 82–91.
62. Kim, S.W.E. (1998). Performance comparison of loop/piezo and ultrasonic sensor-based traffic detection systems for collecting individual vehicle information. In: Proceedings of the 5th World Congress on Intelligent Transport Systems, Oct 1998, Seoul, South Korea.
63. Krauss, S., Nagel, K., and Wagner, P. (1999). The mechanism of flow breakdown in traffic flow models. In: Proceedings of the 14th international symposium of transportation and traffic theory, Jul 1999, Jerusalem, Israel.
64. Kudarauskas, N. (2007). Analysis of emergency braking of a vehicle. Transport, 22(3):154-159.
65. Kwong, K., Kavaler, R., Rajagopal, R., and Varaiya, P. (2009). Arterial travel time estimation based on vehicle re-identification using wireless magnetic sensors. Transportation Research Part C: Emerging Technologies, 17(6):586-606.
66. Lan, J., Ziang, Y., Wang, L., and Shi, Y. (2011). Vehicle detection and classification by measuring and processing magnetic signal. Journal of Measurement, 44(1):174-180.
67. Lan, L., and Chang, C. (2005). Inhomogeneous cellular automata modeling for mixed traffic with cars and motorcycles. Journal of Advanced Transportation, 39(3):323-349.
68. Lee, D. N. (1976). A theory of visual control of braking based on information about time to collision. Perception, 5(4), 437–459. doi: 10.1068/p050437
69. Li, L., Jiang, R., Jia, B., and Zhao, X. (2010). Cellular automaton model of Road traffic flow. Modern Traffic Flow Theory and Applications, Vol. I, Highway Traffic, Tsinghua University Press, Beijing, China, 2010. ISBN 978-7-302-23807-2.
70. Li, Z. X., Yang, X., and Li, Z. (2006). Application of Cement-Based Piezoelectric Sensors for Monitoring Traffic Flows. Journal of Transportation Engineering, 132(7):565-573.
71. Mahalel, D., and Hakkert, A. (1983). Traffic arrival patterns on a cross Section of a multilane highway. Transportation Research Part A: General, 17(4):263-270.
72. Mallikarjuna C., and Rao, K. V. R. (2009). Cellular Automata model for heterogeneous traffic. Journal of Advanced Transportation, 43(3):321-345.
73. Mallikarjuna, C., Tharun, B., and Pal, D. Analysis of the Lateral Gap Maintaining Behavior of Vehicles in Heterogeneous Traffic Stream. In: Proceedings of 2nd Conference of Transportation Research Group of India (2nd CTRG), Dec 2013, Agra, India.
74. Mallikarjuna, C., and Rao, K. V. R. (2006). Area occupancy characteristics of Heterogeneous Traffic. Transportmetrica, 2(3):223 – 236.
75. Manjunatha, P., Vortisch, P., Mathew, T. V. (2013). Methodology for the Calibration of VISSIM in Mixed Traffic. In: Proceedings of Transportation Research Board 92nd Annual Meeting Jan 2013, Washington, D.C., USA.

76. Marwah, B. R., and Singh, B. (2000). Level of service classification for urban heterogeneous traffic: A case study of Kanpur metropolis. Transportation Research Circular E-C018: Proceedings of 4th International Symposium on Highway Capacity, Maui, Hawaii, 271–286.
77. Mathew, T. V., and Radhakrishnan, P. (2010) Calibration of microsimulation models for nonlane-based heterogeneous traffic at signalized intersections. Journal of Urban Planning and Development, 136(1):59-66
78. Mathew, T., Munigety, C., and Bajpai, A. (2013). A Strip-based Approach for Simulation of Mixed Traffic Conditions. ASCE Journal of Computations in Civil Engineering,29(5):1-1. DOI:10.1061/(ASCE)CP.1943-5487.0000378.
79. Maurya, A. K., and Chakroborty, P. (2007). CASIM: A realistic CA based traffic flow model. In: Proceedings of 11th World Conference on Transportation Research, Berkeley, USA.
80. Metkari, M., Budhkar, A., and Maurya, A. (2013). Development of Simulation Model for Heterogeneous Traffic with no Lane Discipline. In: Proceedings of the 2nd CTRG, Agra, India, 360-369.
81. Michaels, R. M. (1963). Perceptual factors in car following. In: Proceedings of the second international symposium on the theory of road traffic flow, Paris, France, 44–59.
82. Munigety, C. R., and Mathew, T. V. (2016). Towards Behavioral Modeling of Drivers in Mixed Traffic Conditions. Transportation in Developing Economies, 2(1).
83. Munigety, C. R., Vicraman, V., Mathew, T.V. (2014). Semiautomated Tool for Extraction of Microlevel Traffic Data from Videographic Survey. Journal of the Transportation Research Board, 2443, 88–95.
84. Nagel, K., and Schreckenberg, M. (1992). A cellular automation model for freeway traffic. Journal of Physics I, France 2, pages 2221–2229.
85. Nagraj, B. N., George, K. J., and John, P. K. (1990). A study of linear and lateral placement of vehicles in mixed traffic environment through video-recording. Highway Research. Bulletin, Indian Roads Congress, New Delhi, India, (42):105-136.
86. Nakayama, A. and Sugiyama, Y. (2003). Two-Dimensional Optimal Velocity Model for Pedestrians and Biological Motion. Modeling of Complex Systems: Seventh Granada Lectures, AIP, 661(1):107-110.
87. Niar, R., Mahmassani, H. S., Miller-Hooks, E. (2011). “A porous flow approach to modeling heterogeneous traffic in disordered systems”. 19th International Symposium on Transportation and Traffic Theory, 17:611-627.
88. NSour, S., and A. Santiago (1994). Comprehensive Plan Development for Testing, Calibration And Validation Of CORSIM. In: Proceedings of the 64th ITE Annual Transportation Engineers, Dallas, USA, 486-490.
89. Pal, D., and Mallikarjuna, C. (2016). Analysis of the effect of variable lateral gap maintaining behavior of vehicles on traffic flow modeling. In: Procedia Engineering 142 (2016):198-204. Presented at Sustainable Development of Civil, Urban and Transportation Engineering Conference (CUTE-2016), Apr 2016, Ho Chi Minh City, Vietnam.

90. Pal, D., and Mallikarjuna, C. (2010). Cellular Automata Cell Structure for Modeling Heterogenous Traffic. Transporti Europei, 45:50-63.
91. Pipes, L. A. (1953). An operational analysis of traffic dynamics. Journal of Applied Physics, 24:274–281
92. Pollard, E., Morignot, P. and Nashashibi, F. (2013). An ontology-based model to determine the automation level of an automated vehicle for co-driving. In: IEEE Proceedings of the 16th International Conference on Information Fusion, Jul 2013, Istanbul, Turkey. ISBN 978-1-4799-0284-2.
93. Pytka, J. A., Piotr, T., Fijalkowski, S., Budzynski, P., Dabrowski, J., Kupicz, W., and Pytkac, P. (2011). An instrumented vehicle for offroad dynamics testing. Journal of Terramechanics, 48:384–395.
94. Qingyi, A. I., Zhuo, Y. A. O., Heng, W. E. I., and Zhixia, L. I. (2010). Identifying characteristics of freeway traffic headway by vehicle types using video trajectory data. In: Proceedings of Tenth International Conference of Chinese Transportation Professionals (ICCTP), American Society of Civil Engineers. doi:10.1061/41127(382)214.
95. Rahman, M., Chowdhury, M., Xie, Y., He, Y. (2013). Review of Microscopic Lane-Changing Models and Future Research Opportunities. IEEE Transactions on Intelligent Transportation Systems, 14 (4):1942-1956.
96. Rakha, H., and Crowther, B. (2003). Comparison and calibration of FRESIM and INTEGRATION steady- state car-following behavior. Transportation Research Part A, 37:1-27.
97. Ramanayya, T. V. (1988). Highway capacity under mixed traffic conditions. Traffic Engineering and Control, 29:284–87.
98. Ravishankar, K. V. R., and Mathew, T. V. (2011). Vehicle-type dependent car-following model for heterogeneous traffic conditions. Journal of Transportation Engineering, ASCE, 137 (11):775–781
99. Reiter, U. (1994). Empirical studies as basis for traffic flow models. Proceedings of the second international symposium on highway capacity, 2:493–502.
100. Sayer, J. R., Mefford, M. L., and Huang, R. (2003). The effect of lead vehicle size on driver following behavior: Is ignorance truly bliss? In: Proceedings of the 2nd international driving symposium on human factors in driver assessment, training and vehicle design, University of Iowa, USA.
101. Siddharth, S. M. P., and Ramadurai, G. (2013). Calibration of VISSIM for Indian Heterogeneous Traffic Conditions. Procedia - Social and Behavioral Sciences, 104(0):380-389.
102. Simon P. M., and Gutowitz H. A. (1998). A Cellular Automaton Model for Bi-Directional Traffic. Physics Review E, 57:2441-2444.
103. Sreekumar, M., and Maurya, A. (2012), Need for a Comprehensive Traffic Simulation Model in Indian Context. In: Proceedings of EFITRA-2012, Mar 2012, Wardha, India, published in International Journal of Computer Applications, 2012.

104. Sun, Z., Bebis, G., Miller, R. (2004). On-Road Vehicle Detection Using Optical Sensors: A Review. In: Proceedings of the 7th International IEEE Conference on Intelligent Transportation Systems, Oct 2004, Washington D.C., USA.
105. Tiwari, G., Fazio, J., and Gaurav, S. (2007). Traffic planning for non-homogeneous traffic. Sadhana, 32(4):309–328.
106. Toledo, T. (2002). Integrated driving behavior models. Ph.D. dissertation, Department of Civil and Environmental Engineering, Massachusetts Institute of Technology, Massachussetts, USA.
107. Toledo, T., and Farah, H. (2011). Alternative Definitions of Passing Critical gaps. Journal of the Transportation Research Board, 2260:76–82.
108. Toledo, T., Koutsopoulos, H. N., and Ben-Akiva, M. E. (2003). Modeling Integrated Lane-Changing Behavior. Journal of the Transportation Research Board, 1857:30-38.
109. Treiber, M., and Helbing, D. (2002). Realistische Mikrosimulation von Straßenverkehr mit einem einfachen modell. In: Proceedings of 16th Symposium Simulationstechnik ASIM, Sept 2013, Rostock, Germany.
110. Venter, C., and Knoetze, H. (2013). Lateral clearance between vehicles and bicycles on urban roads. In: Proceedings of 32nd South African Transport Conference (SATC 2013), Prertoria, South Africa.
111. Wang H., Wang ,W., and Chen, J. (2011). General Newell Model and Related Second-Order Expressions. Transportation Research Record: Journal of the Transportation Research Board, 2260:42–49.
112. Wang, L. L., and W. H. Tsai (1991). Camera calibration by vanishing lines for 3-D computer vision, IEEE Transactions on Pattern Analysis and Machine Intelligence, 13(4):370–376.
113. Wiedemann, R. (1974). Simulation des Strassenverkehrsflusses. Technical report, Institut fur Verkehrswesen, Universitat Karlsruhe, Karlsruhe, Germany, In German.
114. Wiedemann, R., and Schwerdtfeger, T. (1987). Makroskopisches simulations-modell fur schnellstrassennetze mit berucksichtigung von einzelfahrzeugen. Technical report, Bundesministerium fur Verkehr, Abt. Strassenbau, Bonn, Germany, In German.
115. Wong, C., Qidwai, U., 2004. Vehicle collision avoidance system [VCAS] Sensors. In Proceedings of IEEE, 316–319.
116. Xie, D. F., Gao, Z. Y., Zhao, X. M. (2008). Stabilization of traffic flow based on the multiple information of preceding cars. Communications in Computational Physics, 3:899-912.
117. Yang, Q., Koutsopoulos, H. N. (1996). A microscopic traffic simulator for evaluation of dynamic traffic management systems. Transportation Research Part C: Emerging Technologies, 4 (3):113-129.
118. Ye, F., and Zhang, Y. (2009). Vehicle type-specific headway analysis using freeway traffic data. Transportation Research Record: Journal of the Transportation Research Board, 2124:222-230.

119. Zhang, X., and Bham, G. H. (2007). Estimation of driver reaction time from detailed vehicle trajectory data. In: Proceeding of the 18th IASTED international conference, May-Jun 2007, Montreal, Canada, 574–579.
120. Zheng, Z. (2014). Recent developments and research needs in modeling lane changing. Transportation Research Part B: Methodological, 60:16–32.
121. Zwahlen, H. T., Russ, A., Oner, E., Parthasarathy, M. (2005). Evaluation of microwave radar trailers for nonintrusive traffic measurements. Transportation Research Record: Journal of the Transportation Research Board, 1917(1):127–140.

Theses

1. Ahmed, K. I. (1999). Modeling drivers' acceleration and lane changing behavior. PhD Dissertation, Department of Civil and Environmental Engineering, Massachusetts Institute of Technology, Massachusetts, USA.
2. Bokare, P. S. (2013). Modeling of acceleration and deceleration behavior of vehicles. PhD dissertation, Indian Institute of Technology, Guwahati, India.
3. Iqbal, M. S. (1994). Analytical and Simulation Model of Weaving Area Operations Under Non-Freeway Conditions. PhD dissertation, New Jersey Institute of Technology, USA.
4. Maurya, A. K. (2007). Development of a Comprehensive Microscopic Model for Simulation of Large Uninterrupted Traffic streams without Lane Discipline. PhD dissertation, Indian Institute of Technology, Kanpur, India.
5. Siddiqui, A. M. (2012). Modeling Drivers Lateral Movement Behavior under Weak-Lane disciplined Traffic Conditions. Masters' thesis, Department of Civil Engineering, Bangladesh University of Engineering and Technology, Dhaka, Bangladesh, Dec. 2012.
6. Zarean, M. (1987). Development of a Simulation Model for Freeway Weaving Sections. PhD dissertation, Ohio State University, USA.

Books/ manuals

1. CORSIM (1.04) User Manual (1998). Office of Safety and Traffic Operations RandD, Intelligent Systems and Technology Division (HSR-10), US Department of Transportation, Virginia, USA.
2. AASHTO (2011). A Policy on Geometric Design of Highways and Streets, Green Book. American Association of State Highway and Transportation Officials
3. FRESIM User Guide. Turner-Fairbank Highway Research Center. FHWA, U.S. Department of Transportation, April 1994.
4. Highway Capacity Manual (2000). Transportation Research Board, National Research Council, Washington D.C., USA.
5. IRC 106:1990. Guidelines for capacity of urban roads in plain areas. Indian Roads Congress, 1990, Ministry of Road Transport and Highways, New Delhi, India.
6. Manual on Uniform Traffic Control Devices. Federal Highway Administration, U.S. Department of Transportation, Washington, D.C., 2010.

7. Microscopic traffic simulation: The simulation system MISSION. By Wiedemann, R., and Reiter, U. (1992). In: CEC Project ICARUS (V1052), Final Report.
8. PTV VISSIM 6 64-bit. User manual (2013). PTV group, PTV UK Ltd.
9. Racelogic Video VBOX lite with cameras- User Manual (2011). VBOX motorsport, Racelogic Ltd.

Websites

1. AIMSUN. Transport Simulation Systems (TSS). Website: https://www.aimsun.com/aimsun/free-trial/. *Accessed on 13th June 2016*.
2. TRAZER (Traffic extractor and ennumerator). Kritikal solutions. Website: http://its.kritikalsolutions.com/index.php/component/product/view=productandid=2. *Accessed on 14th May 2017*.

List of Publications

International Journals

1. **Budhkar, A. K.** and Maurya, A. K. (2017). Characteristics of Lateral Vehicular Interactions in Heterogeneous Traffic with Weak Lane Discipline. *Published in* Journal of Modern Transportation, Vol. 25, Issue 2, pp.74-89. DOI: 10.1007/s40534-017-0130-1.
2. **Budhkar, A. K.** and Maurya, A. K. (2017). Multiple-leader vehicle-following behavior in heterogeneous, weak lane discipline traffic. *Published in* Journal of Transportation in Developing Economies (TiDE)., Vol. 3, Issue 20, pp.1-17. DOI: 10.1007/s40890-017-0049-6.
3. **Budhkar, A. K.** and Maurya, A. K. (2017). Overtaking decision modeling in heterogeneous, weak lane discipline traffic. *Accepted for publication* in Journal of the Eastern Asia Society for Transportation Studies.
4. Das, S., Maurya, A. K. and **Budhkar, A. K.** (2017). Determinants of Time-headway in staggered car-following conditions. *Accepted for publication*, in Transportation Letters.
5. **Budhkar, A. K.** and Maurya, A. K. (2017). Development of a comprehensive simulation model for mixed traffic conditions. *Communicated*, in Computer-Aided Civil and Infrastructure Engineering.

International Conferences

1. **Budhkar, A. K.** and Maurya, A. K. (2017). Analysis of lateral interaction time in mixed traffic conditions. Submitted for presentation at the 4th Conference of Transportation Research Group of India (4th CTRG), to be held in Mumbai, India during 17-20 December, 2017.
2. **Budhkar, A. K.** and Maurya, A. K. (2017). Overtaking decision modeling in heterogeneous, weak lane discipline traffic. *Presented* at the 12th Eastern Asia Society for Transportation Studies (EASTS) to be organized in Ho Chi Minh City (HCMC), Vietnam during 18-21 September, 2017.
3. Budhkar, A. K. and Maurya, A. K. (2016). Lateral Gap maintained by vehicles under constrained conditions. Presented in International Conference Transportation Planning and Implementation Methodologies for Developing Countries (TPMDC-2016) held in IIT-Bombay, Mumbai, India during 19-21 December, 2016.
4. Budhkar, A. K. and Maurya, A. K. (2016). Modeling Gap-Maintenance in Heterogeneous No Lane discipline Traffic. Presented in 1st International Conference of Transportation Infrastructure and Materials (ICTIM-2016) held in Chang’an University, Xi’an, China during 16-18 July 2016. ISBN: 978-1-60595-367-0.
5. Budhkar, A. K. and Maurya, A. K. (2016). Study of inter-vehicular lateral gaps in mixed traffic stream with weak lane discipline. Presented in 14th World Conference on Transportation Research (WCTRS-2016) held in Shanghai, China during 10-15 July 2016.
6. Budhkar, A. K. and Maurya, A. K. (2015). A methodology to calculate inter-vehicular

longitudinal distances in heterogeneous traffic. Presented in 3rd Conference of Transportation Research Group of India (3rd CTRG), held in Kolkata, India during 17-20 December, 2015.

7. Budhkar, A. K., Maurya, A. K. and Kothari, K. (2015). Development of methodology to study longitudinal gap-speed relationship of vehicles in heterogeneous traffic using laser sensor. National Conference and Workshop on Recent Advances in Traffic Engineering (RATE 15), held at SVNIT, Surat, India during 3-4 July, 2015.
8. Maurya, A. K., Mahapatra, G., Budhkar, A. K., Khandelwal, P., Kumar, M. and Panda, C. (2014). Sensor Based Measurement of Vehicle's Lateral Clearance with Road Edge. Conference of Transportation Planning and Implementation methodologies for Developing Countries (TPMDC 2014), held at Indian Institute of Technology, Bombay during 12-14 December 2014.
9. Budhkar, A. K. and Maurya, A.K. (2014). Modeling of Bidirectional Mixed Traffic Stream with Weak Lane Discipline. In: Proceedings of 93rd Annual Transportation Research Board (TRB) meeting during Jan 12-14, 2014, Washington D.C., USA.
10. Metkari, M., Budhkar, A. K. and Maurya, A. K. (2013). Development of Simulation Model for Heterogeneous Traffic with No Lane Discipline. Presented in 2nd Conference of Transportation Research Group (CTRG-India) held at Agra, India; and proceedings published in Procedia - Social and Behavioral Sciences, Volume 104, 2 December 2013, Pages 360-369.